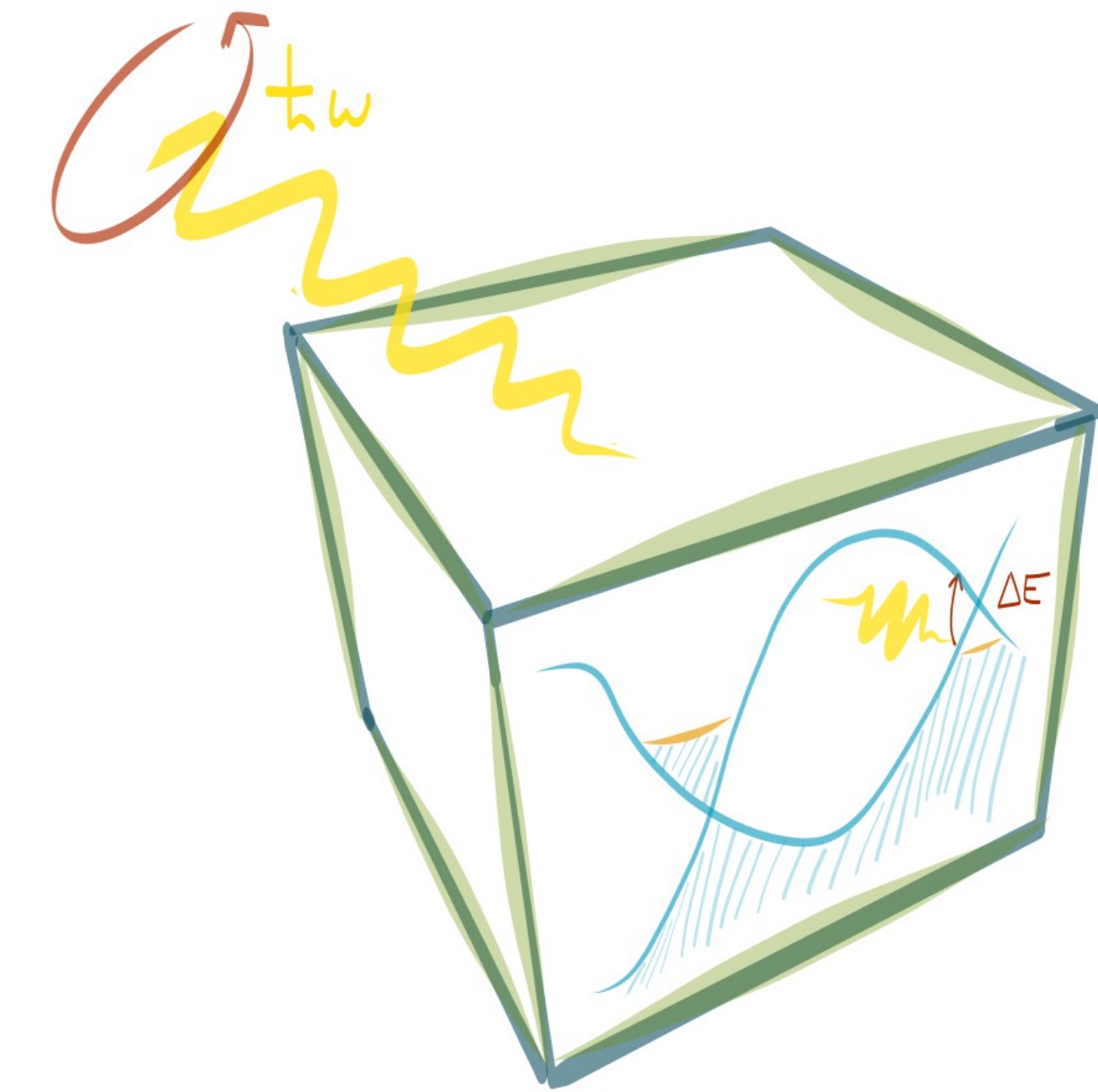


Quantized optical responses in chiral insulators and metals

Adolfo G. Grushin (Néel / CNRS) KITP 10/12/2019

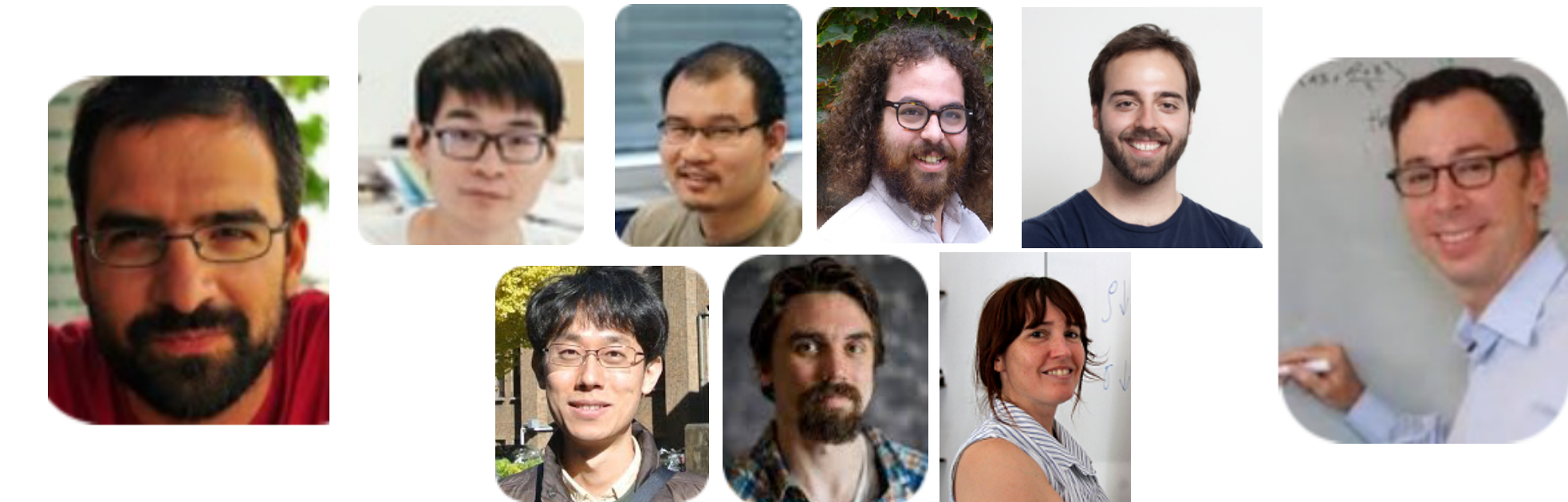
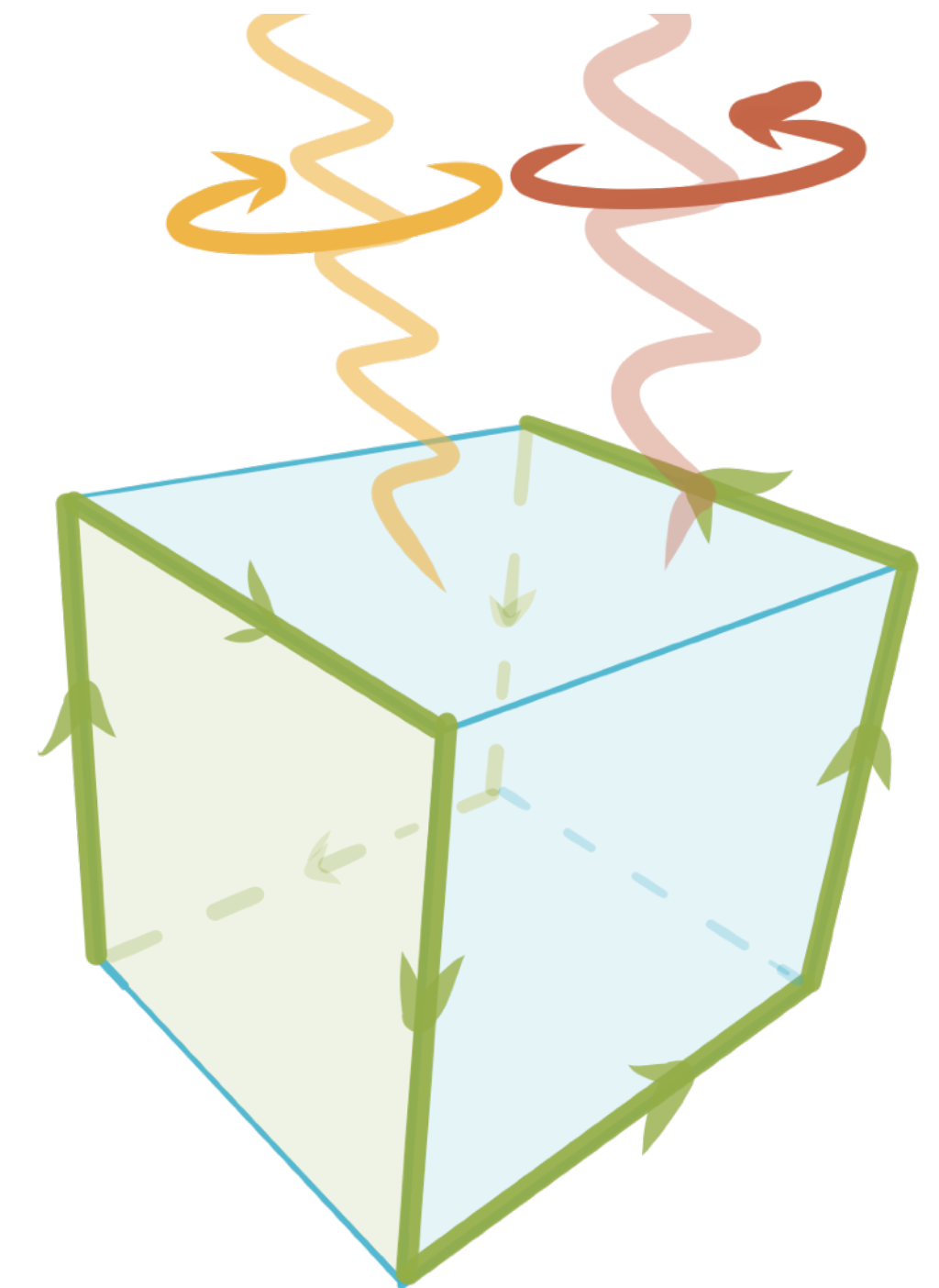


1907.02537
(to appear in PRR)

metallic

1906.05863
(to appear in PRL)

insulating



F. Flicker, F. de Juan, T. Morimoto, B. Bradlyn, M. Vergniory, AGG PRB (2018)

F. de Juan, AGG, T. Morimoto, J. E. Moore Nat. Comm (2017)

M.A. Sanchez-Martinez, F. de Juan, AGG PRB (2019)

FET-OPEN



Quantization

Quantization

...not so often experimentally observed

$$j_i = \sigma_{ij} E_j$$

Quantum Hall effect

von Klitzing, Tsui, Stormer (80's)

Rotation of plane of polarization

L. Wu, et al Science (2016)

Quantization

...not so often experimentally observed

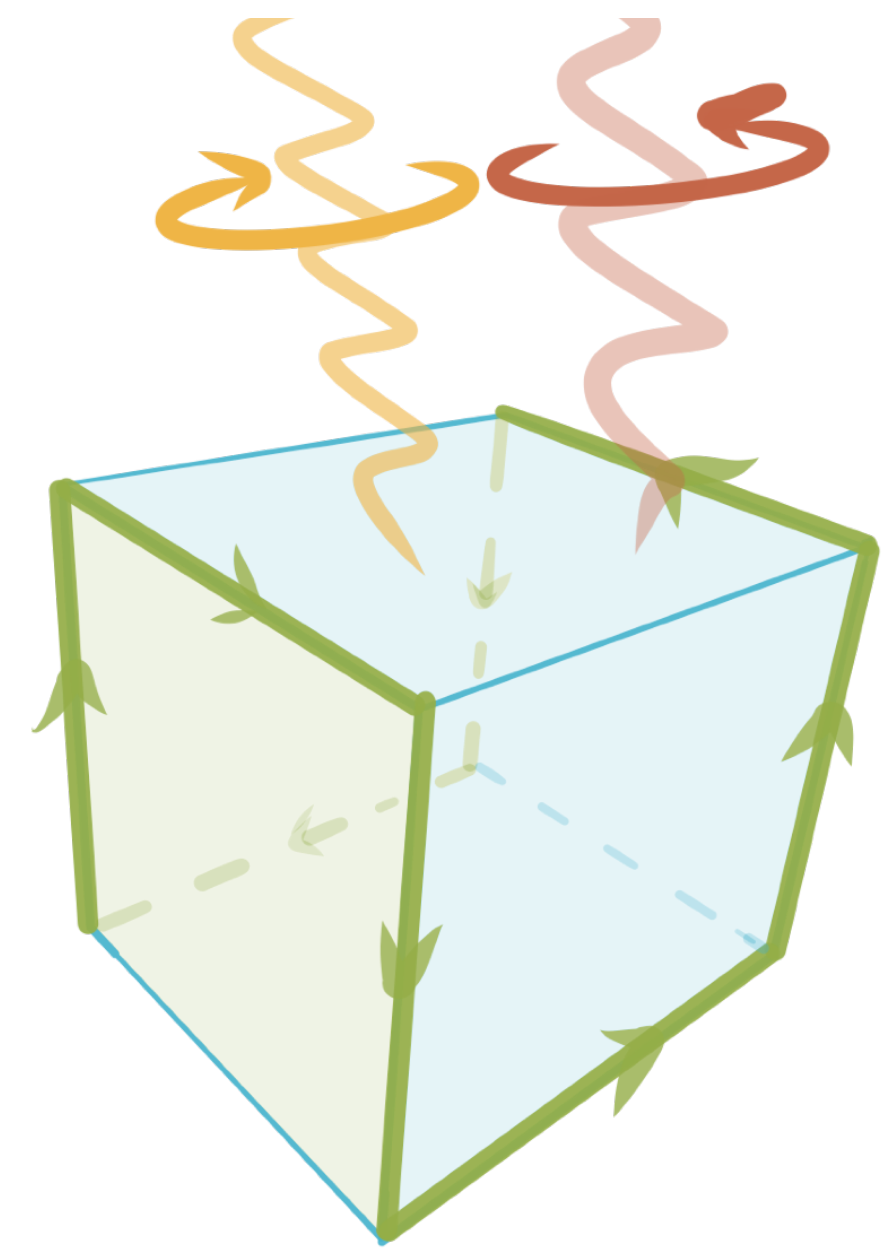
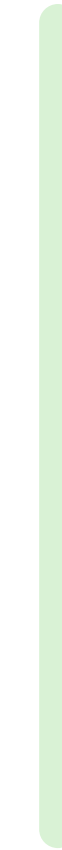
$$j_i = \sigma_{ij} E_j$$

Quantum Hall effect

von Klitzing, Tsui, Stormer (80's)

Rotation of plane of polarization

L. Wu, et al Science (2016)



Quantization

...not so often experimentally observed

$$j_i = \sigma_{ij} E_j + \sigma_{ijkl} E_j E_l + \dots$$

Quantum Hall effect

von Klitzing, Tsui, Stormer (80's)

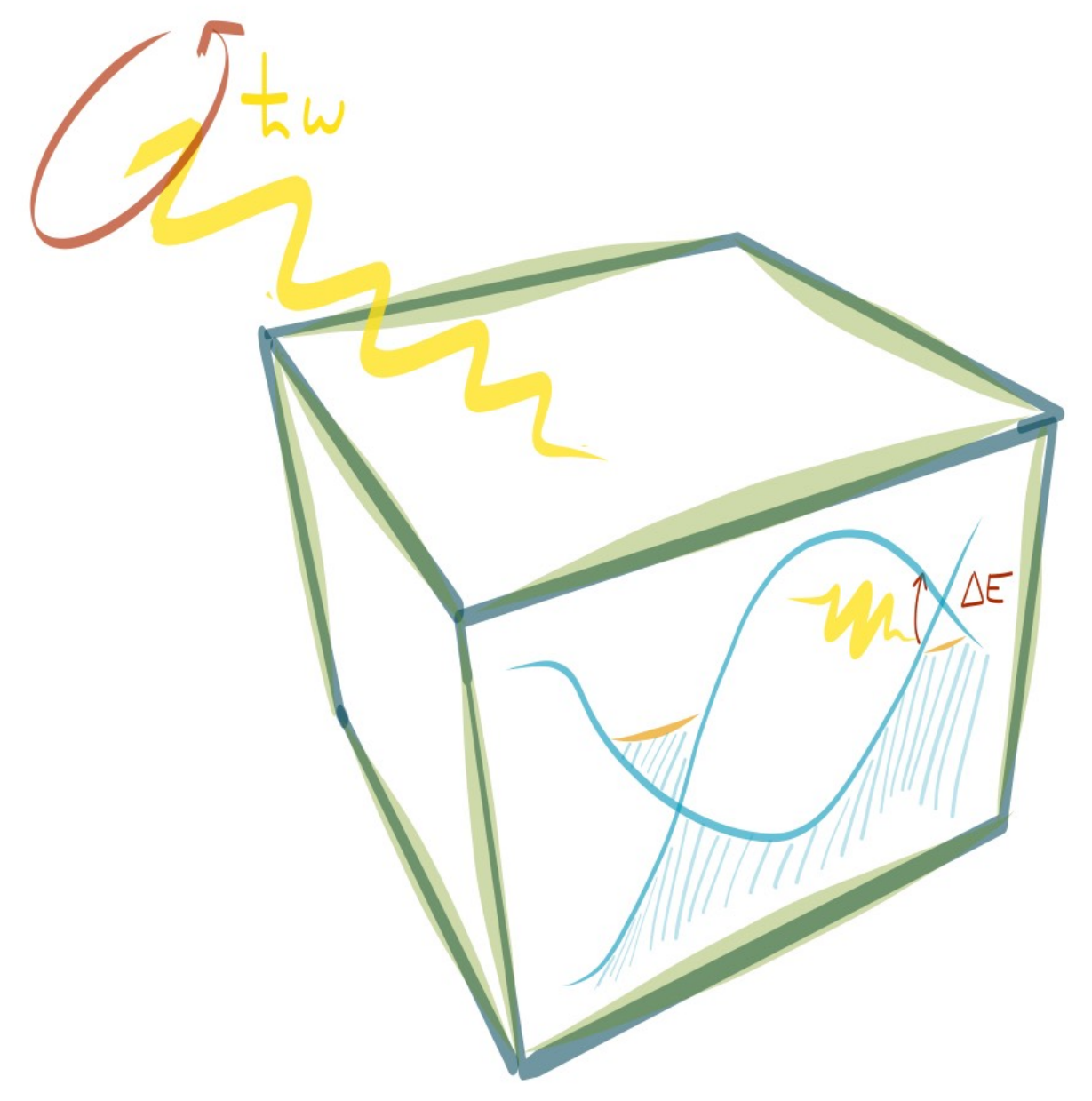
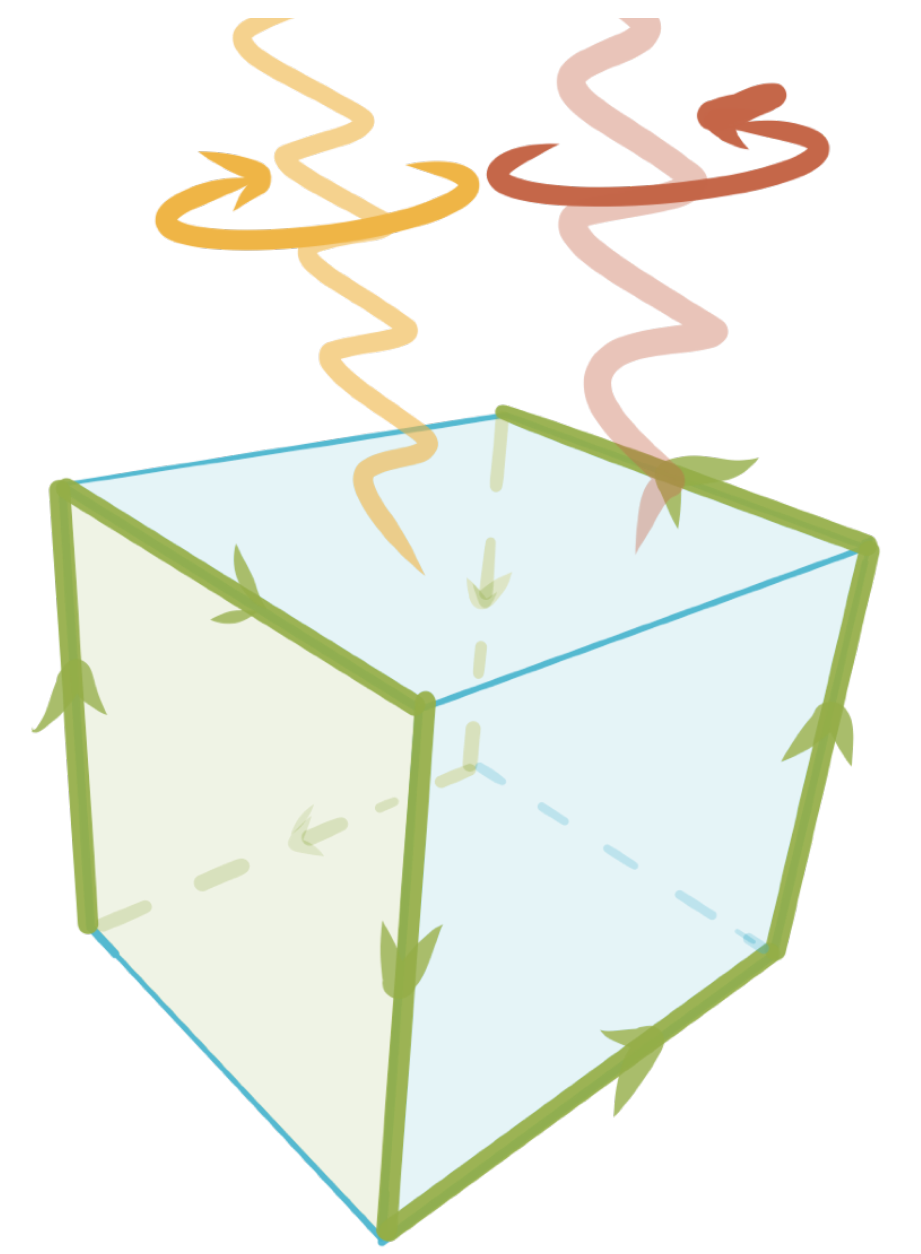
Rotation of plane of polarization

L. Wu, et al Science (2016)

Quantized photogalvanic effect

F. De Juan et al Nat. Comm (2017)

D. Rees et al arXiv: 1902.03230



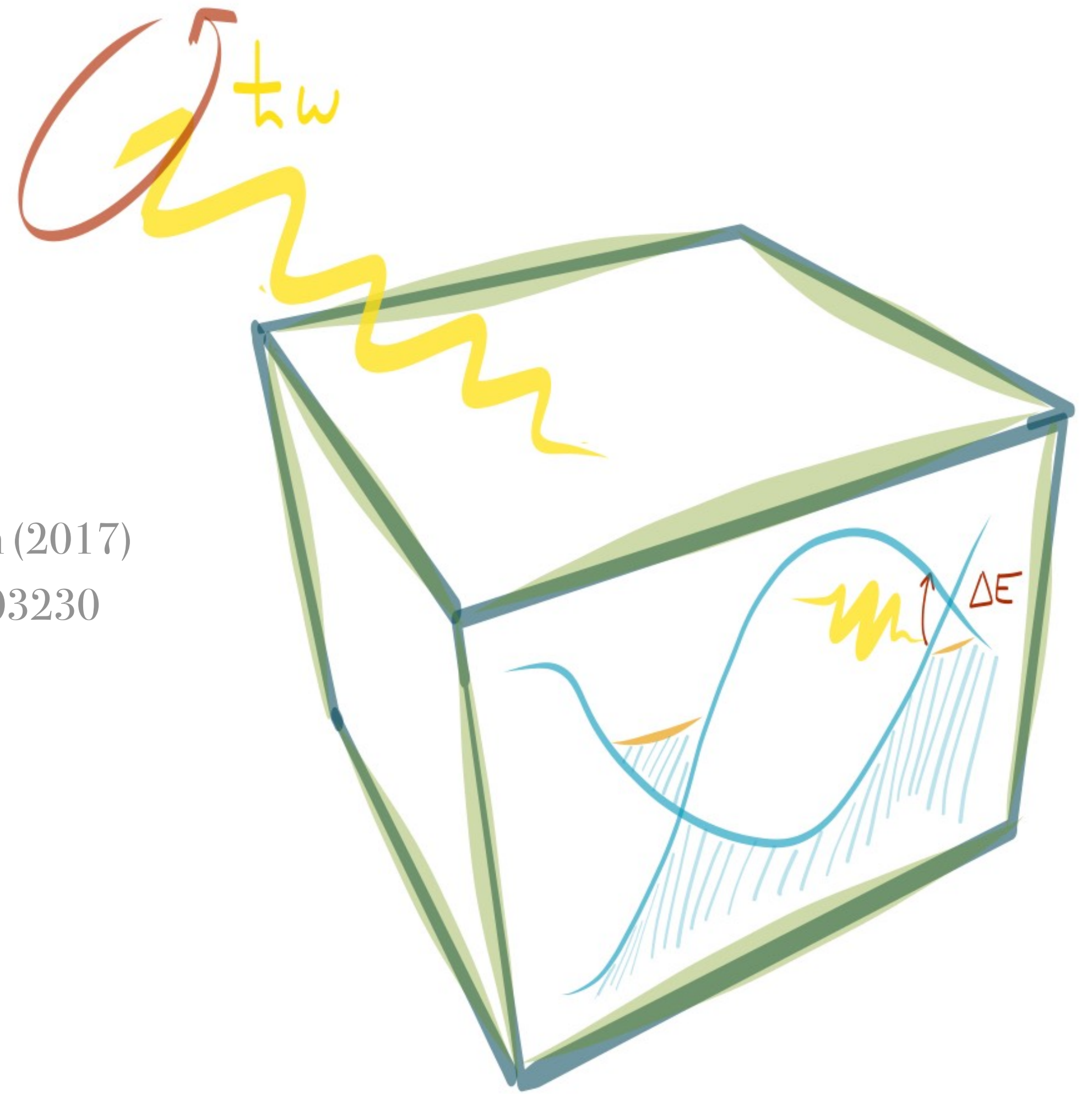
Quantization

$$j_i = \sigma_{ij} E_j + \sigma_{ijl} E_j E_l + \dots$$

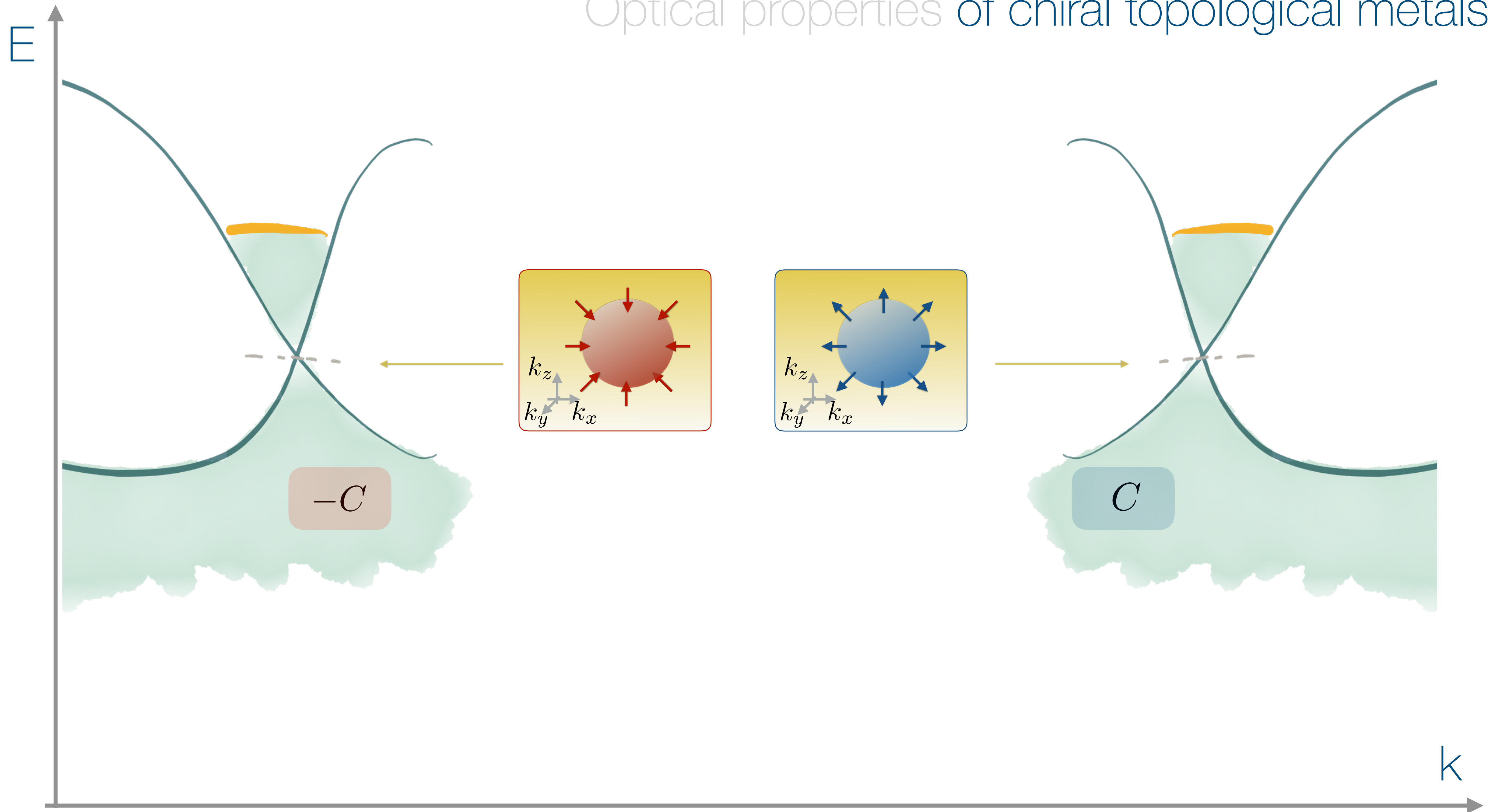
Quantized photogalvanic effect

F. De Juan et al Nat. Comm (2017)

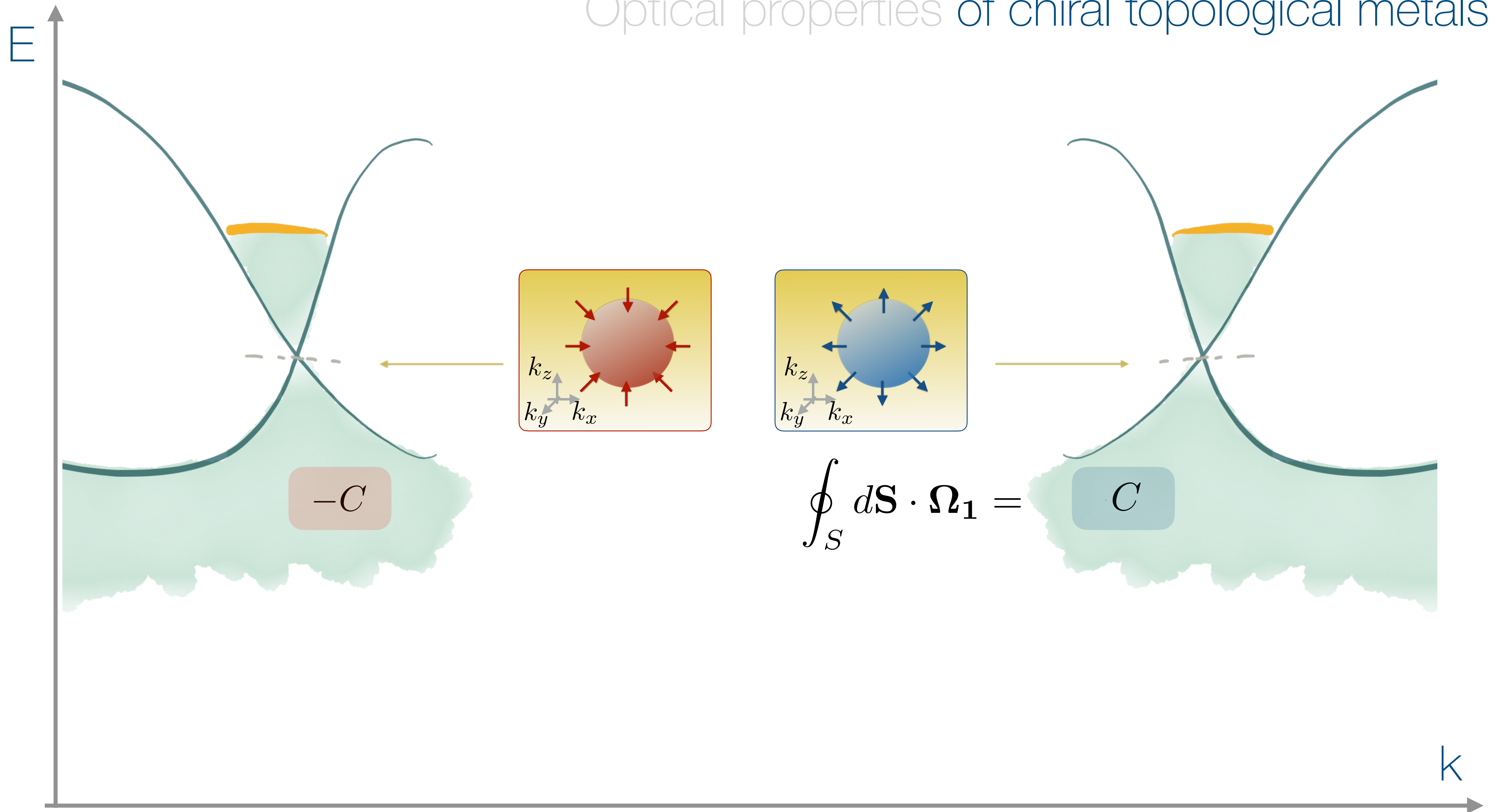
D. Rees et al arXiv: 1902.03230



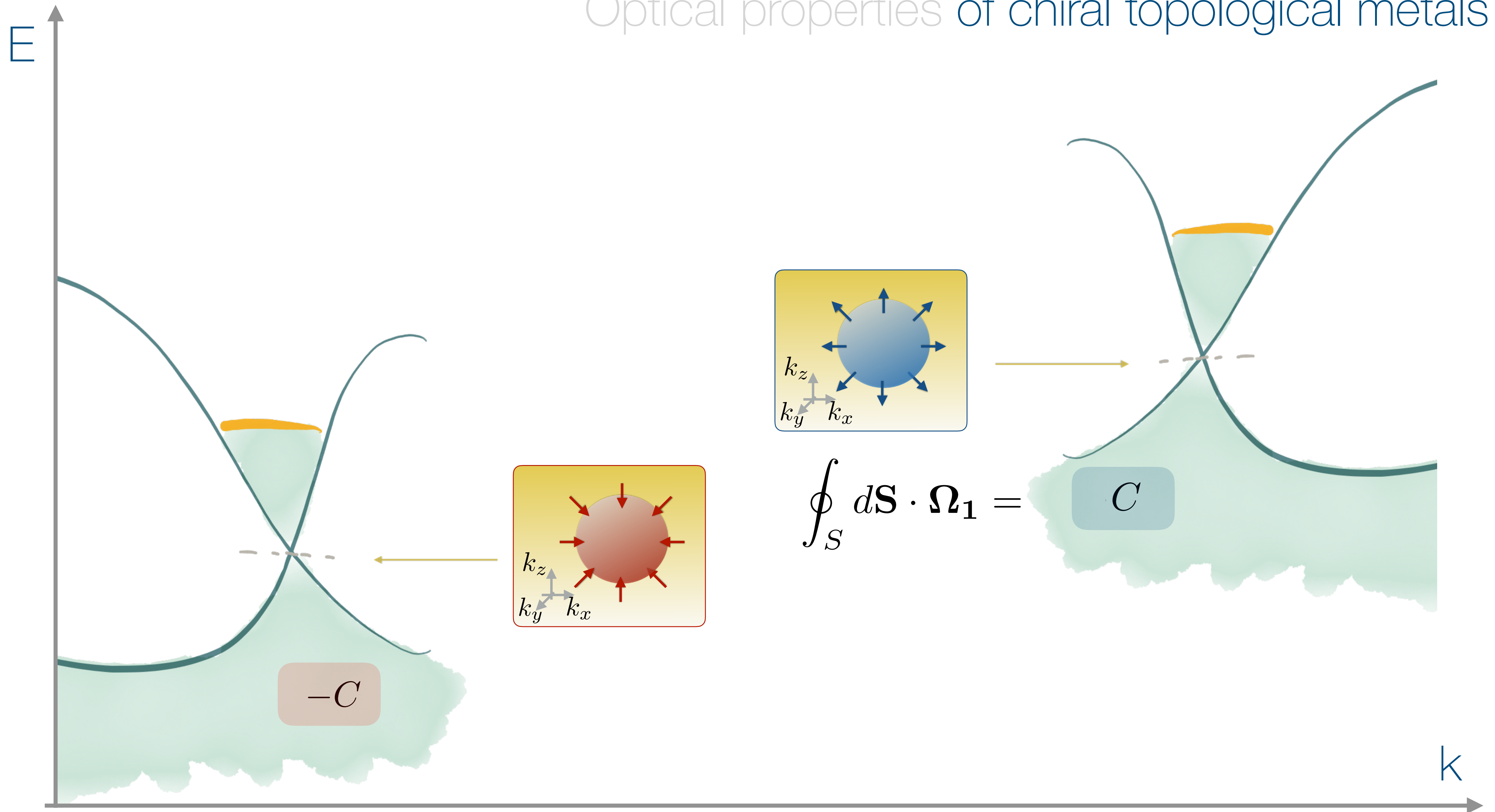
Optical properties of chiral topological metals



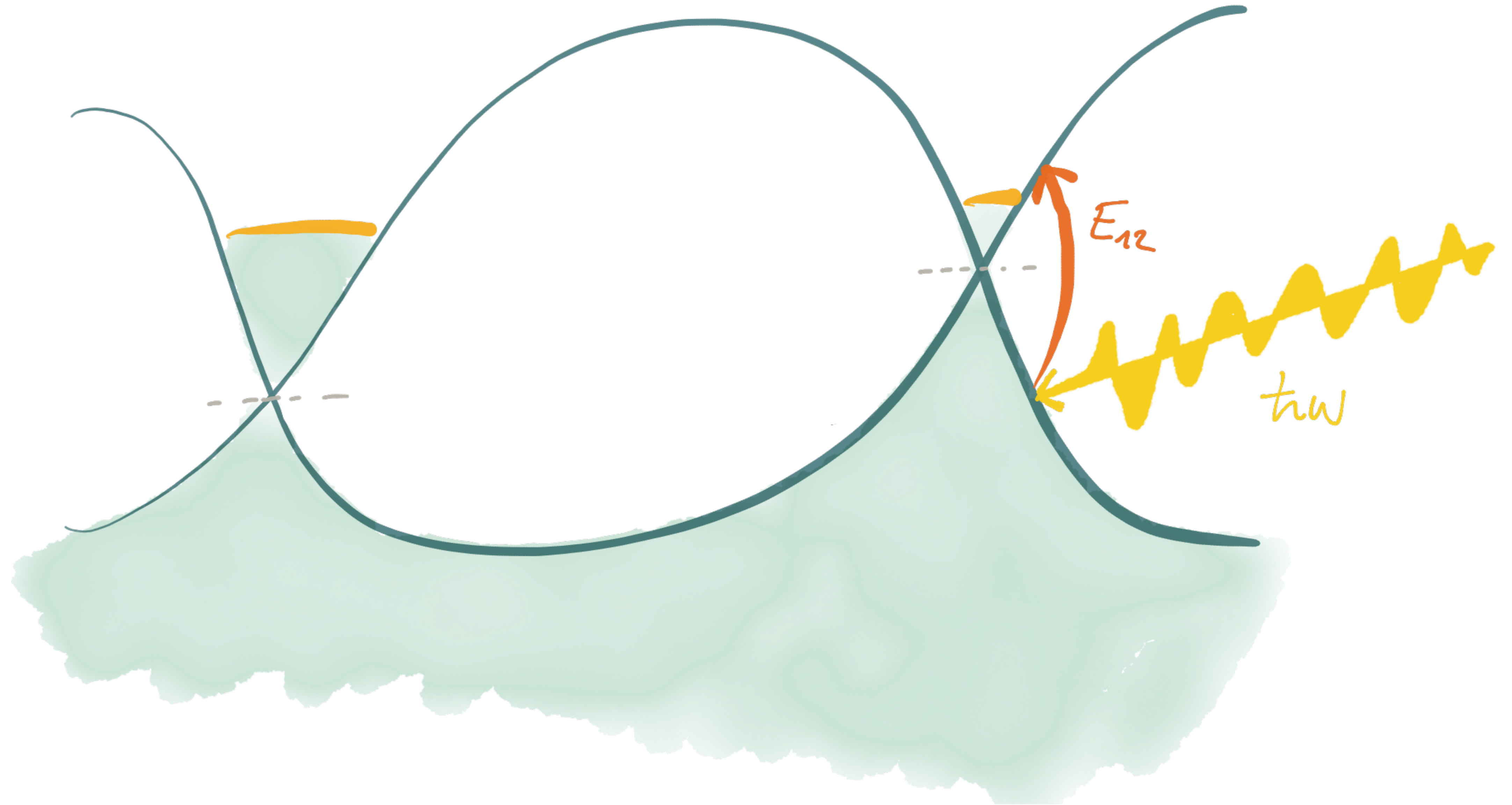
Optical properties of chiral topological metals



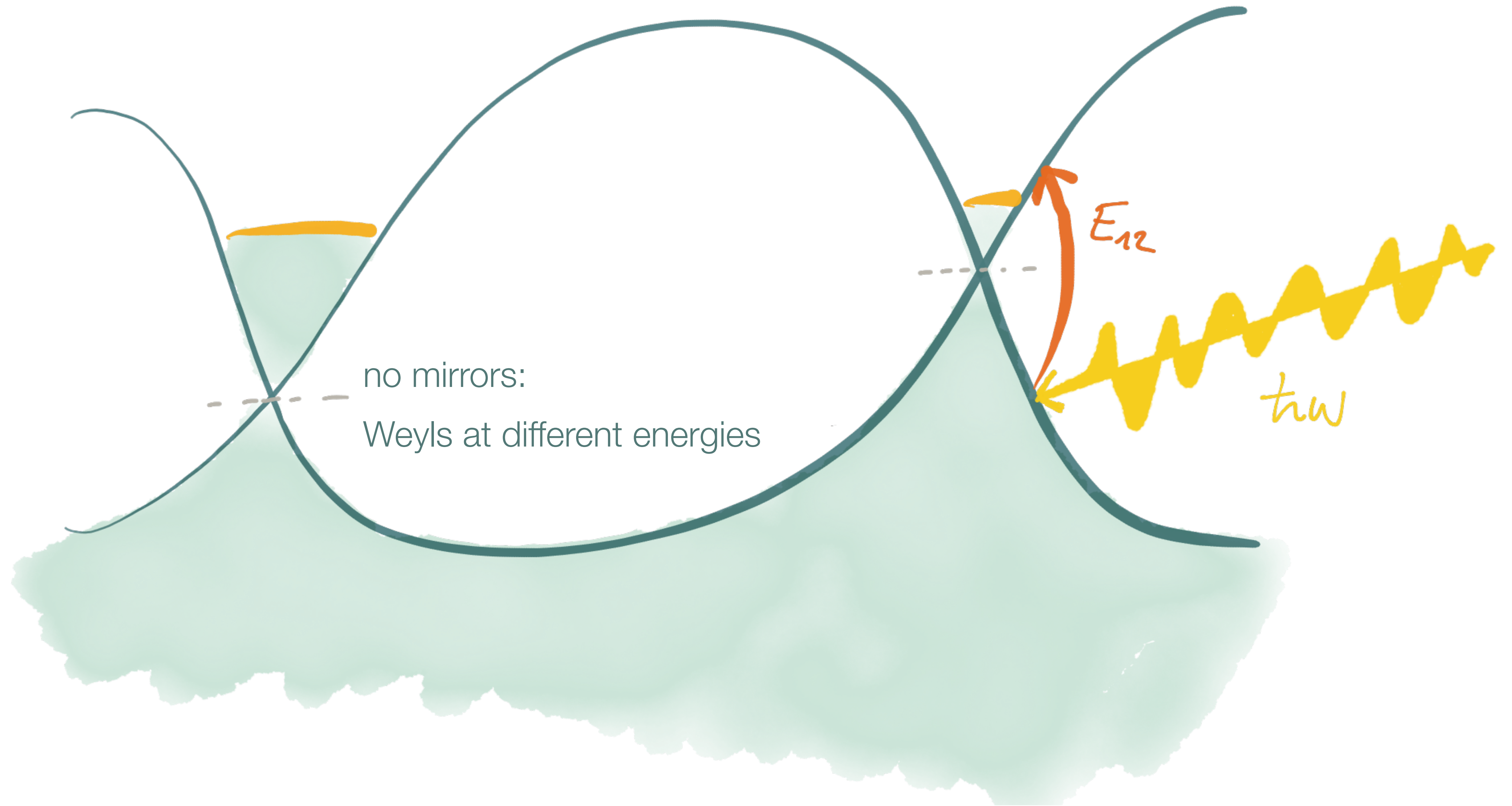
Optical properties of chiral topological metals



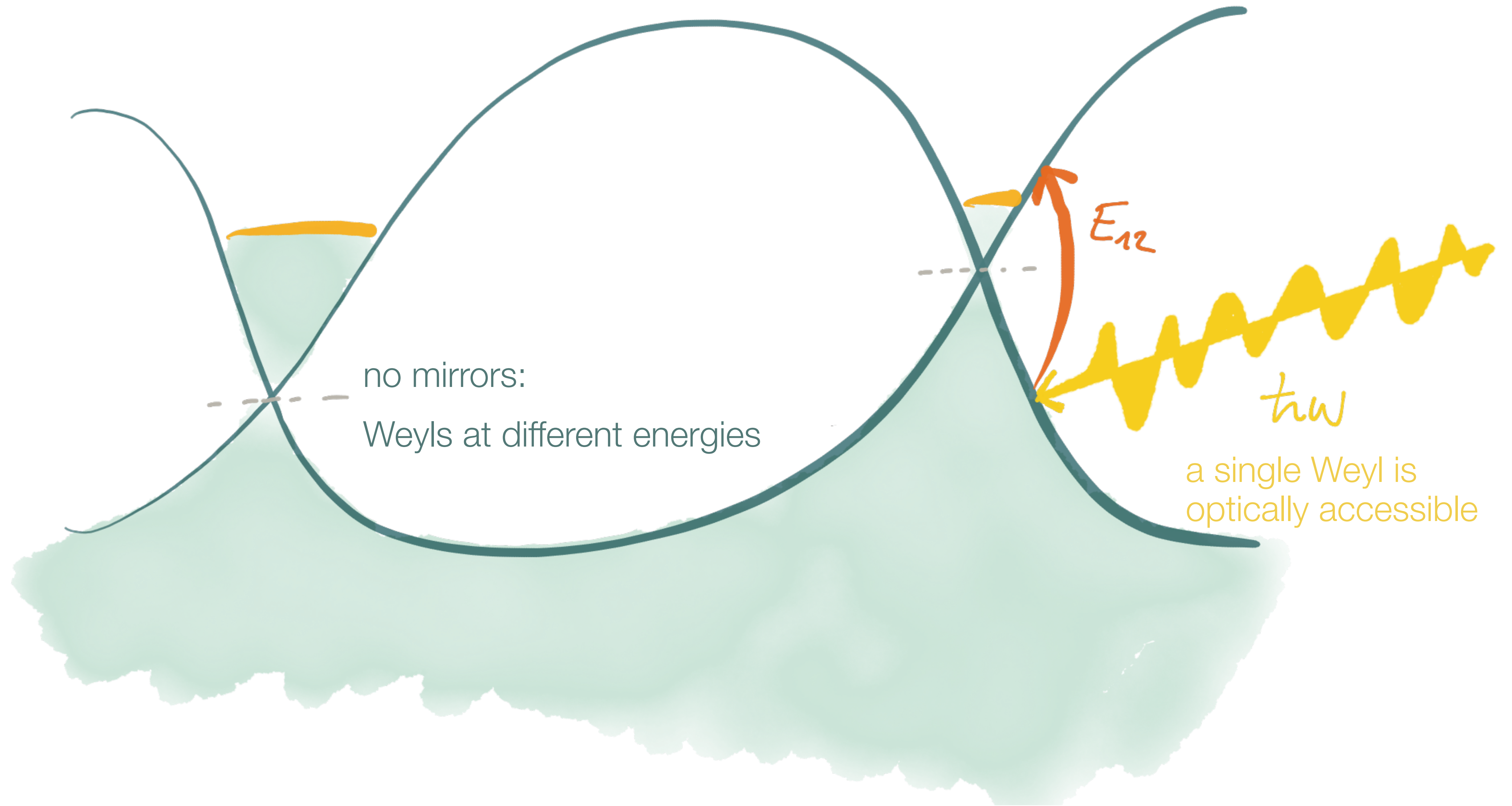
Optical properties of chiral topological metals



Optical properties of chiral topological metals



Optical properties of chiral topological metals

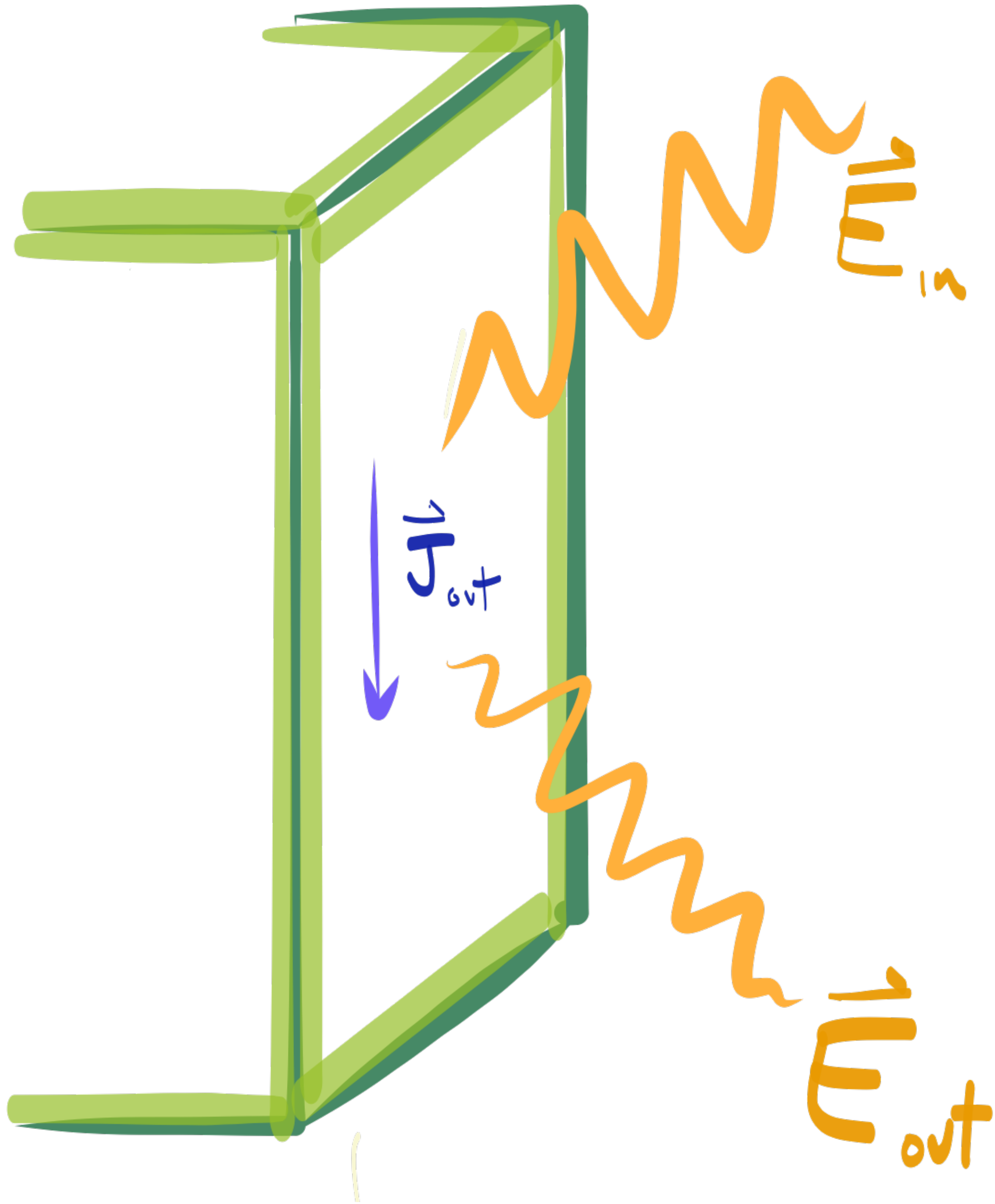


no mirrors:
Weyls at different energies

E_{12}

tw

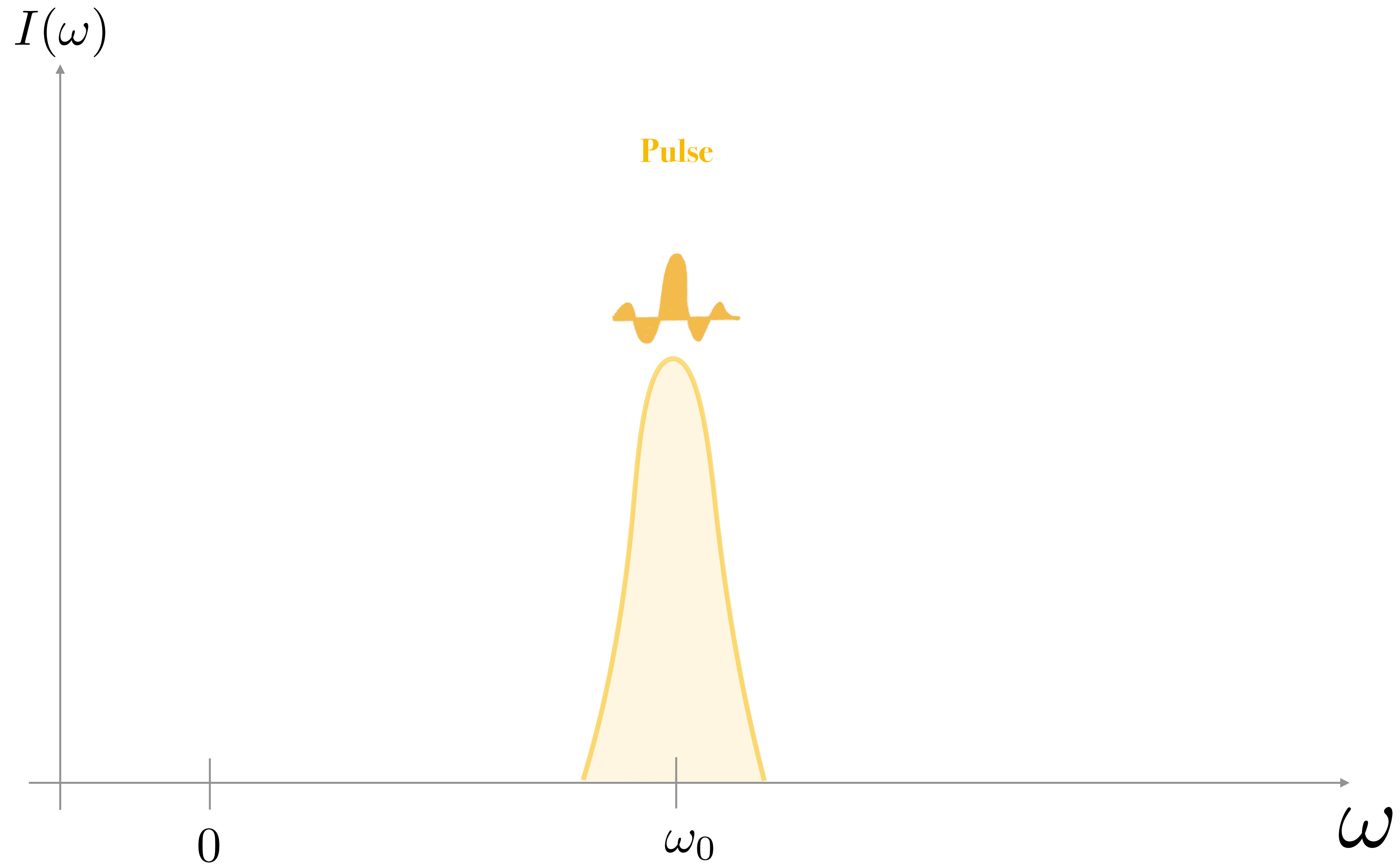
a single Weyl is
optically accessible



$$j_i \propto \sigma_{ijl} E_j E_l$$

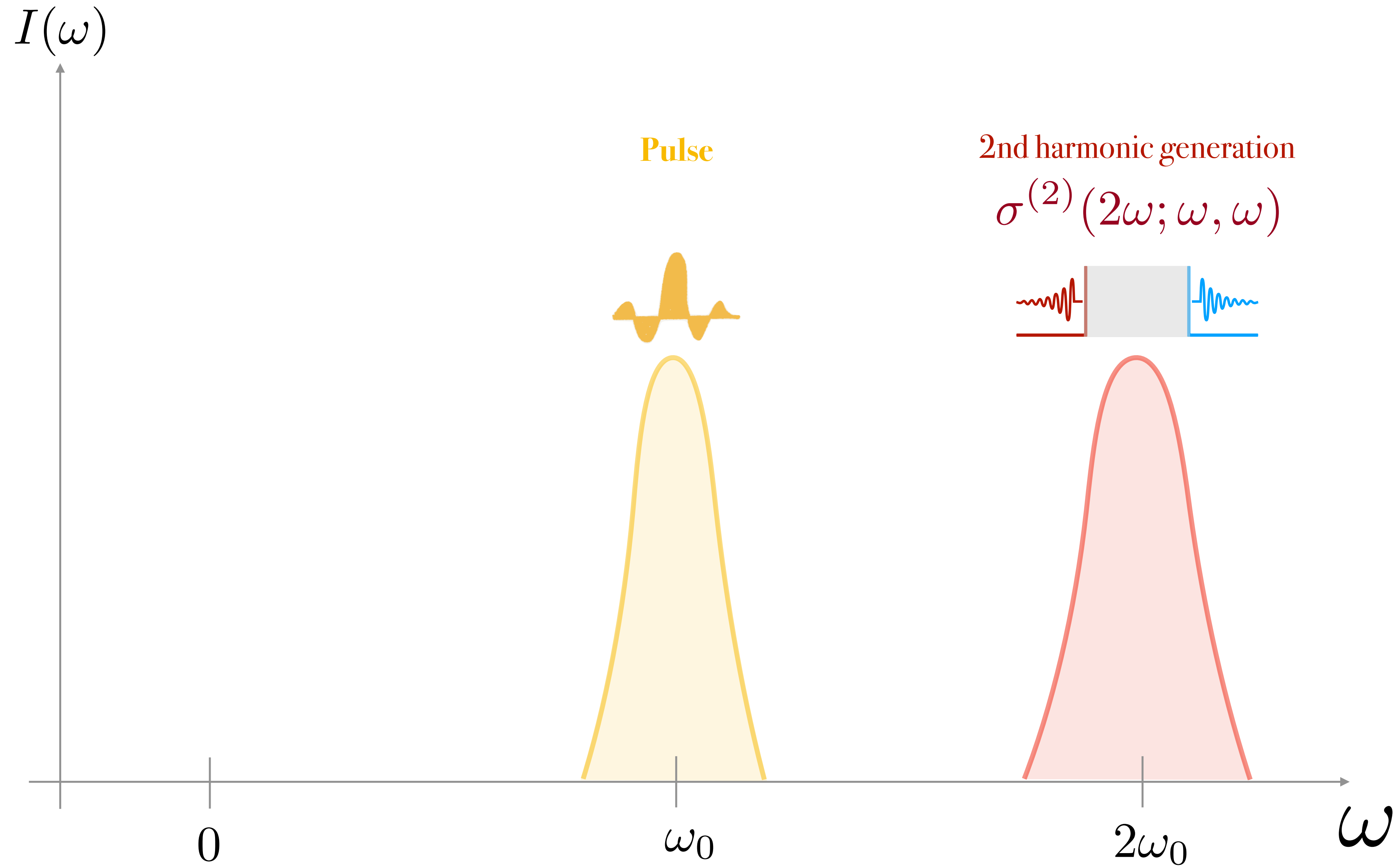
Second order zoo

$$\dot{j}_i \propto \sigma_{ijkl} E_j E_l$$



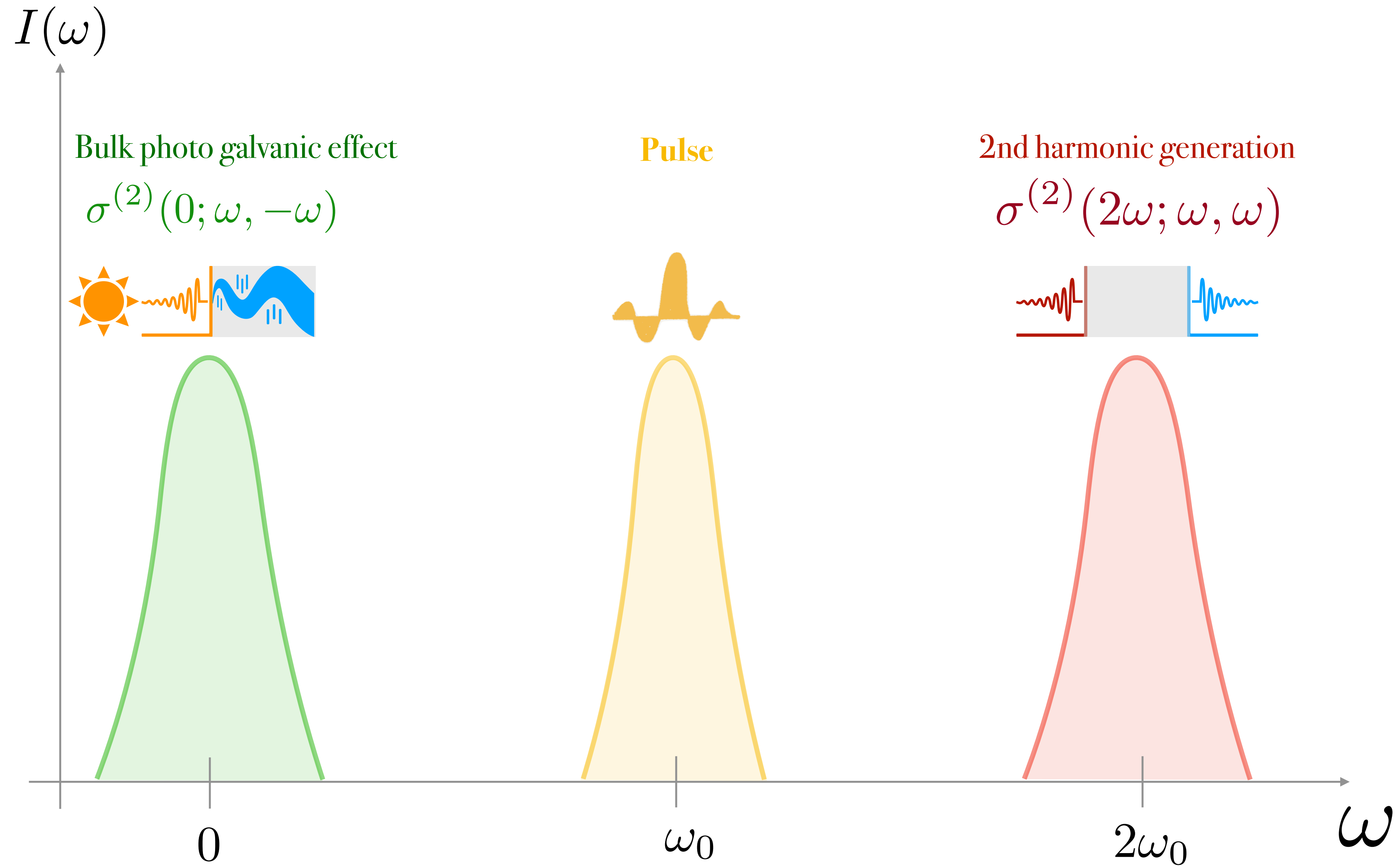
Second order zoo

$$j_i \propto \sigma_{ijkl} E_j E_l$$



Second order zoo

$$j_i \propto \sigma_{ijkl} E_j E_l$$



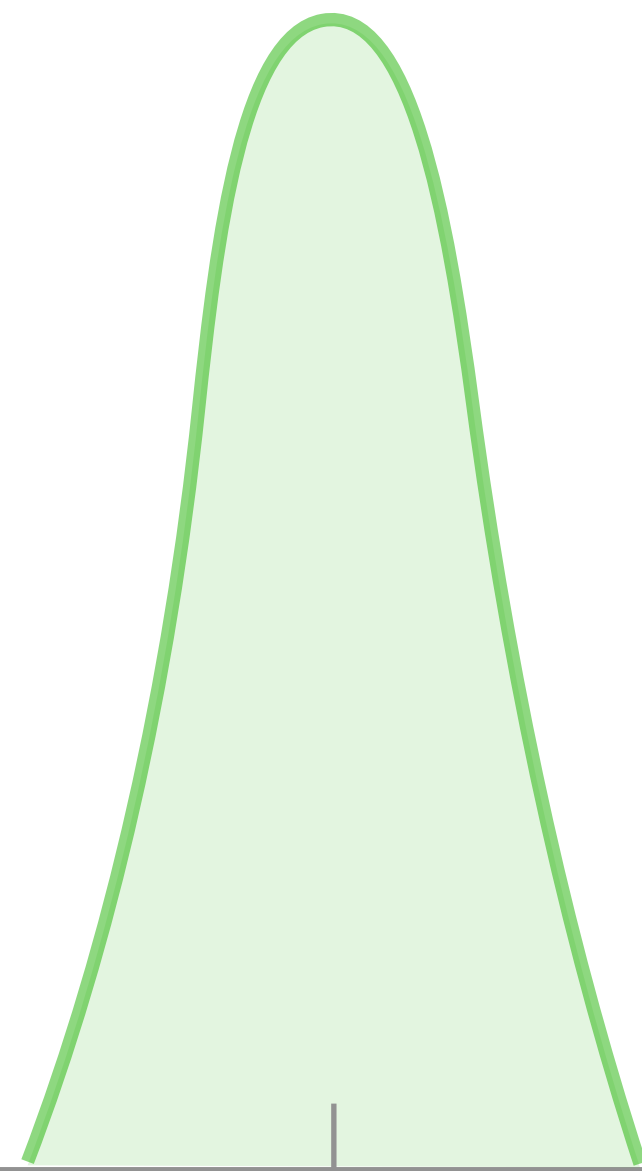
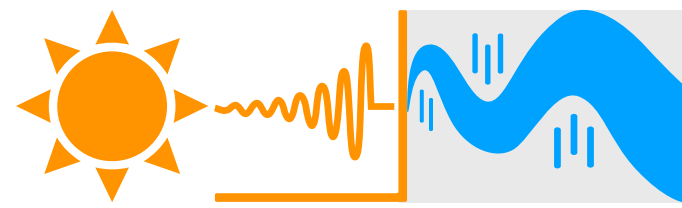
Second order zoo

$$j_i \propto \sigma_{ijkl} E_j E_l$$

$I(\omega)$

Bulk photo galvanic effect

$$\sigma^{(2)}(0; \omega, -\omega)$$



0

ω

Second order zoo

$$j_i \propto \sigma_{ijkl} E_j E_l$$

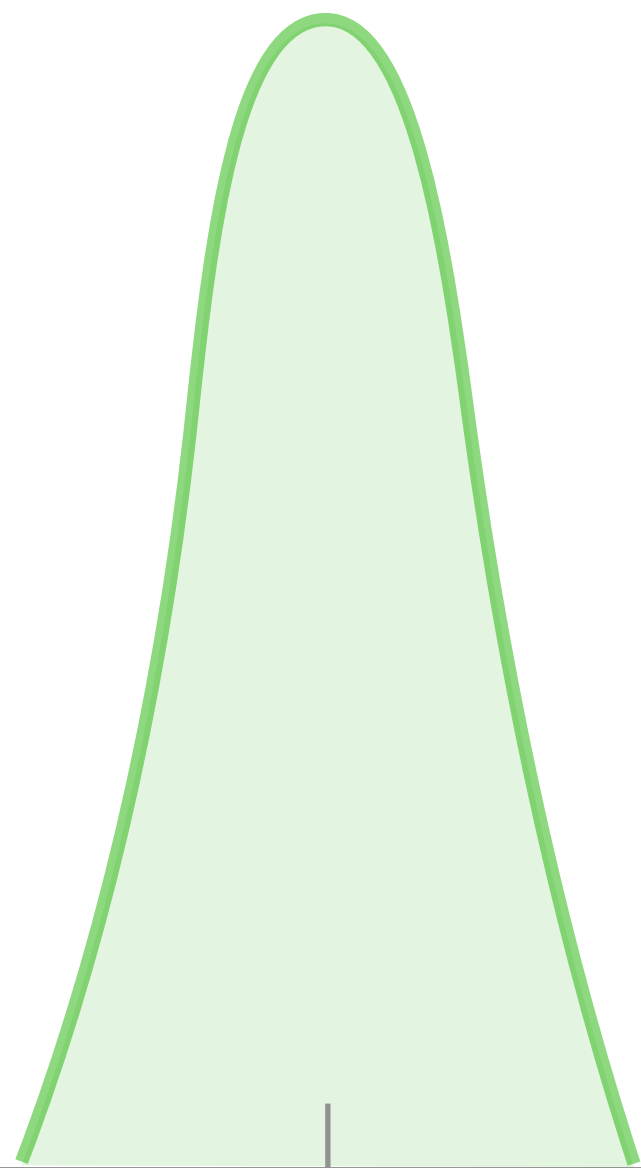
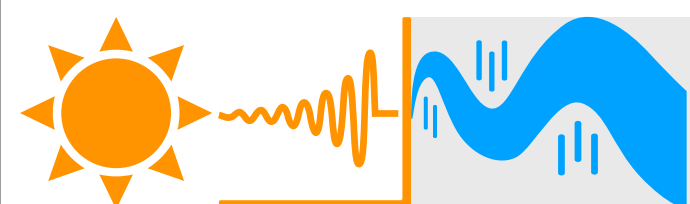
Shift current

Injection current

$I(\omega)$

Bulk photo galvanic effect

$$\sigma^{(2)}(0; \omega, -\omega)$$

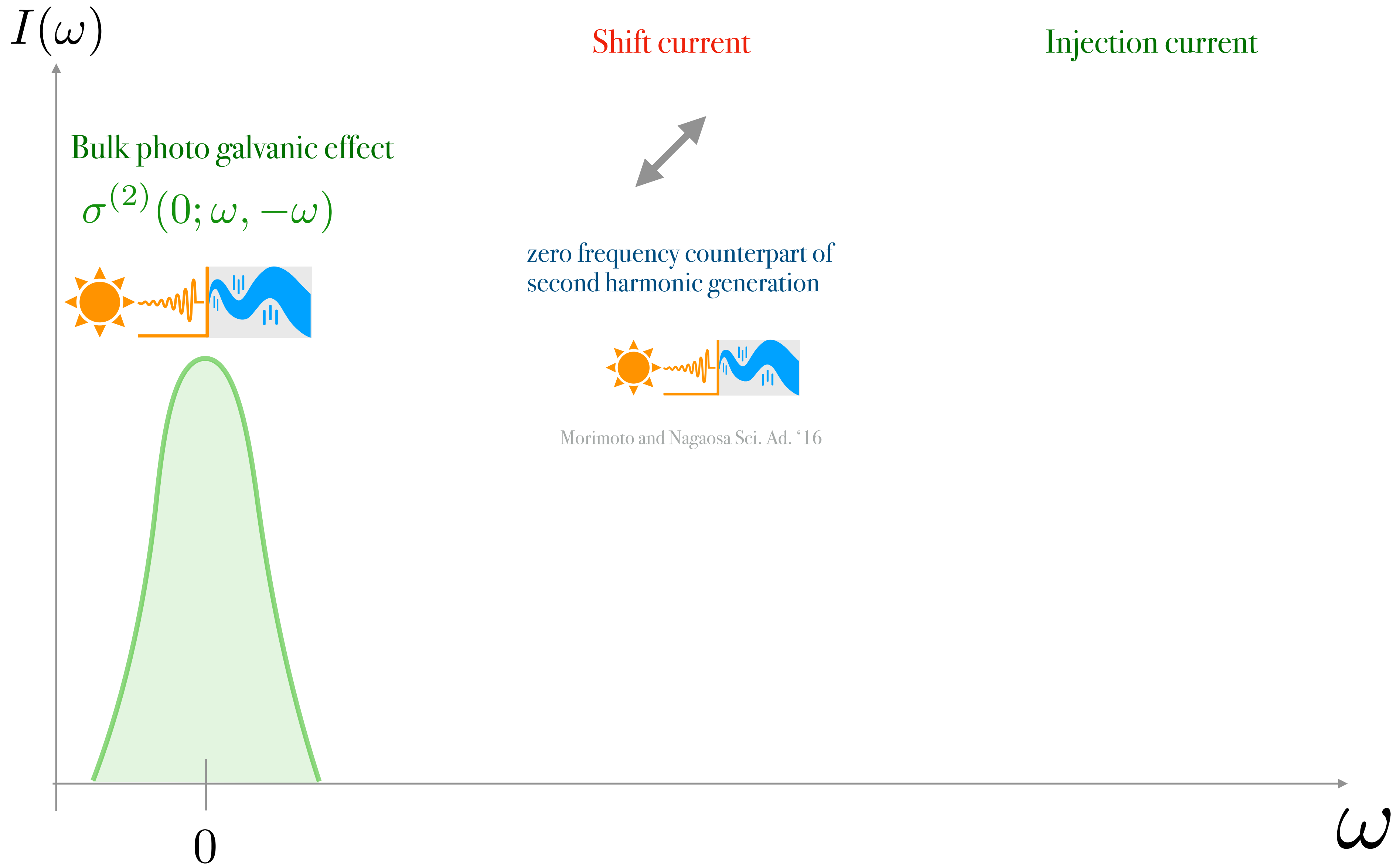


0

ω

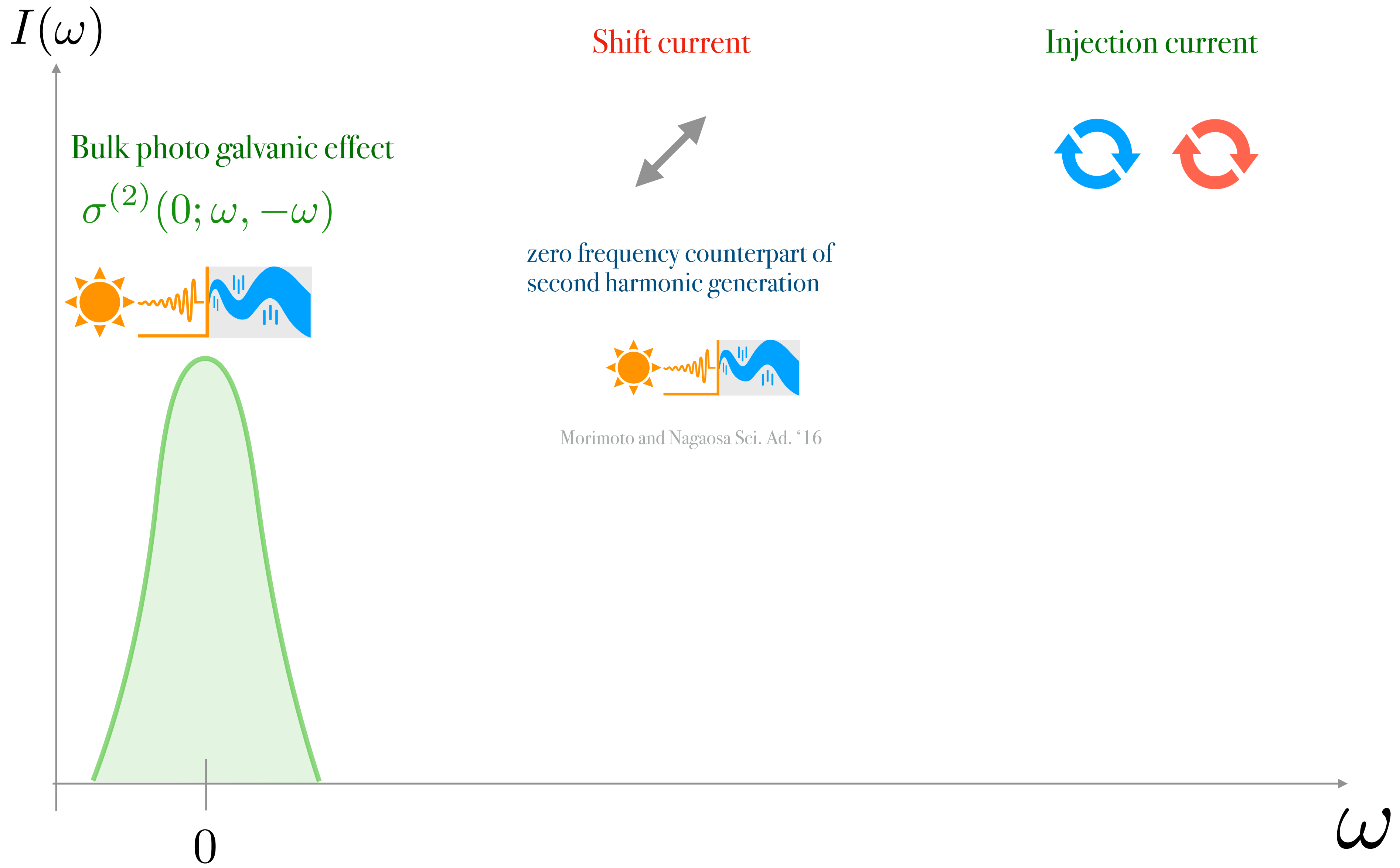
Second order zoo

$$j_i \propto \sigma_{ijkl} E_j E_l$$



Second order zoo

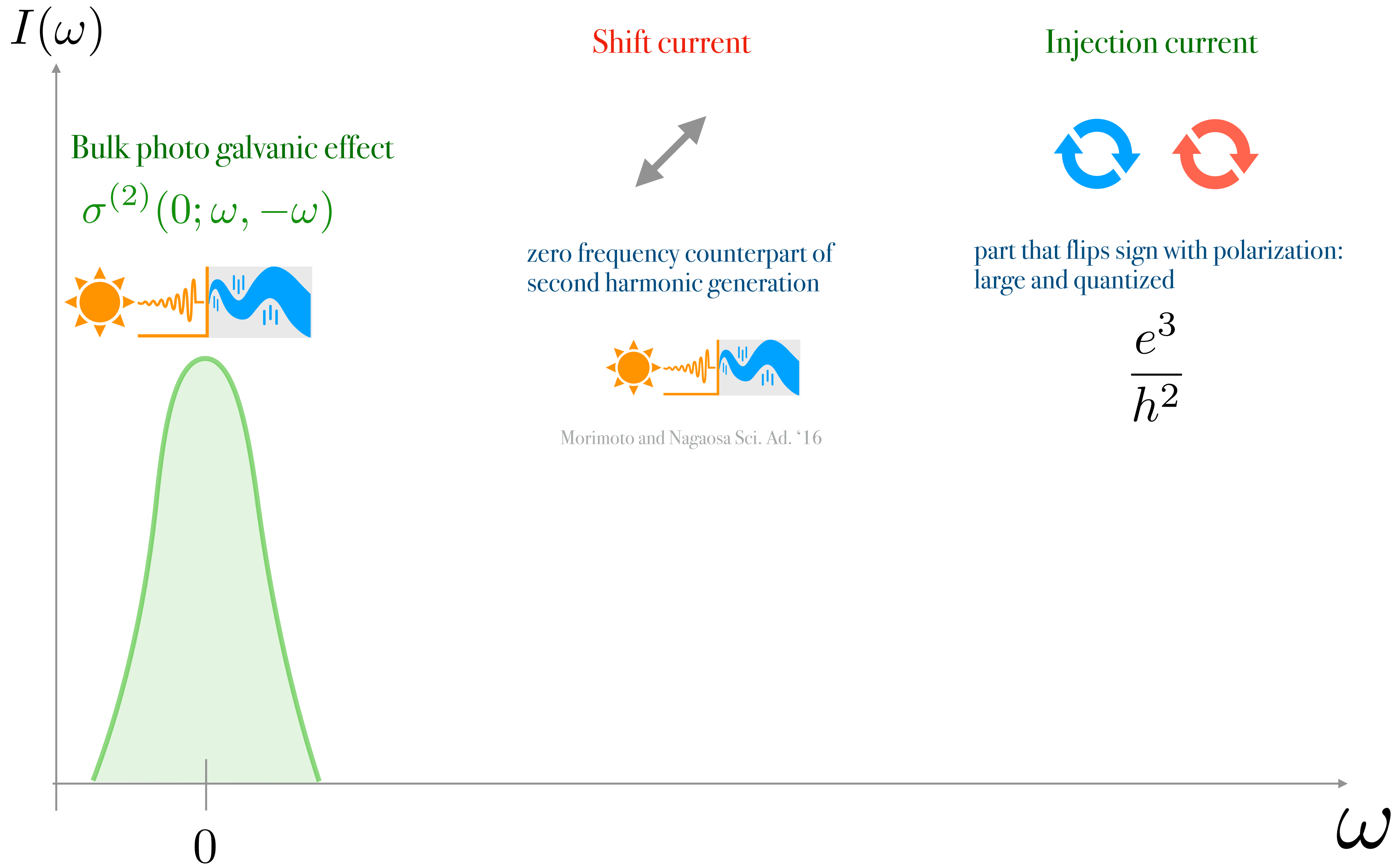
$$j_i \propto \sigma_{ijl} E_j E_l$$



Morimoto and Nagaosa Sci. Ad. '16

Second order zoo

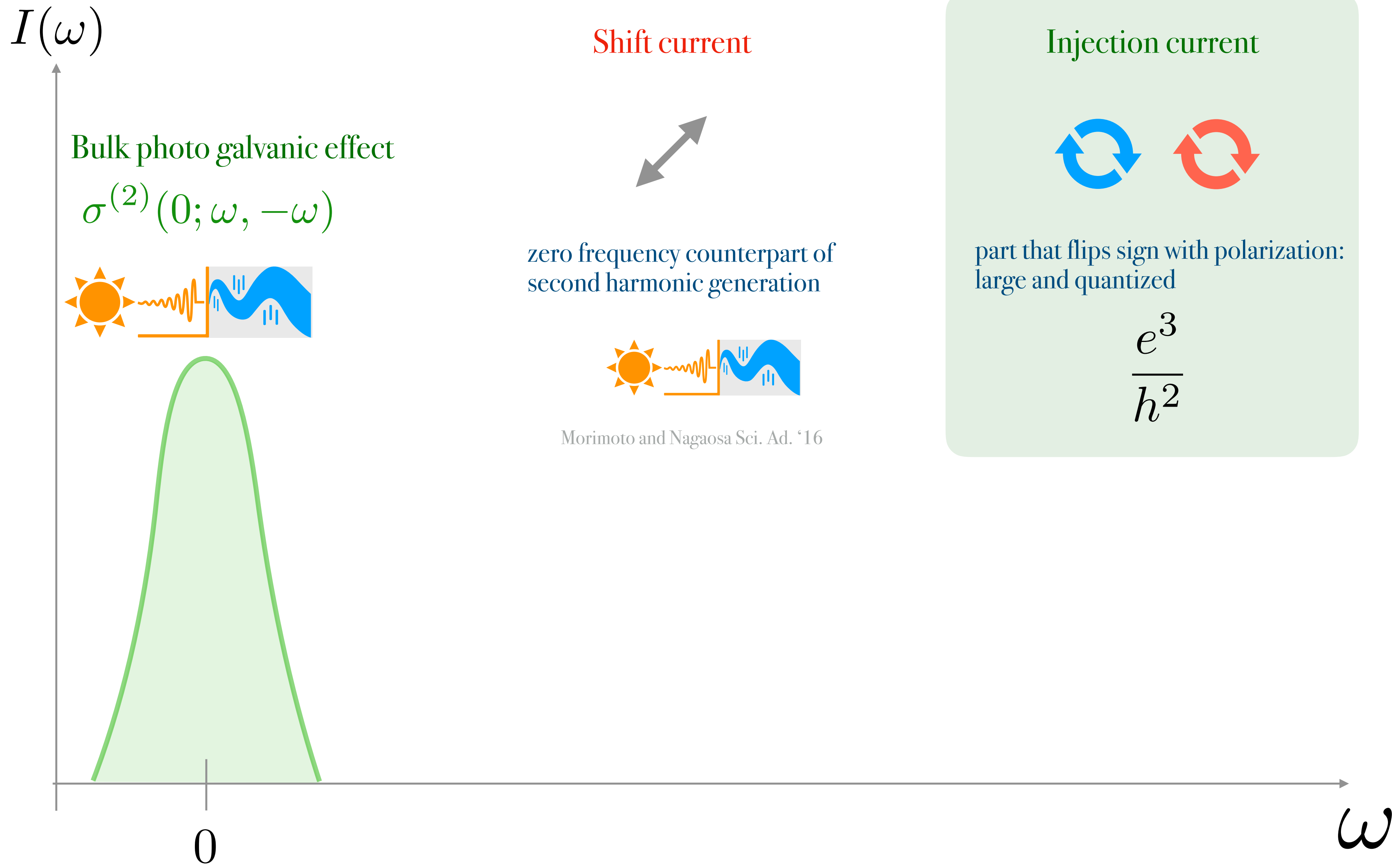
$$j_i \propto \sigma_{ijl} E_j E_l$$



Morimoto and Nagaosa Sci. Ad. '16

Second order zoo

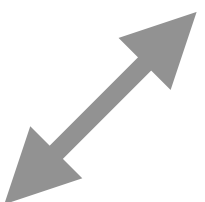
$$j_i \propto \sigma_{ijkl} E_j E_l$$



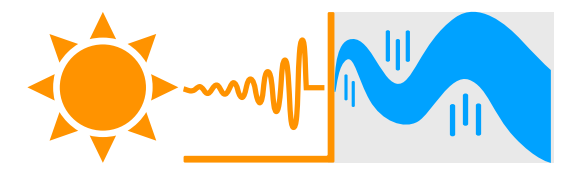
Bulk photo galvanic effect
 $\sigma^{(2)}(0; \omega, -\omega)$



Shift current

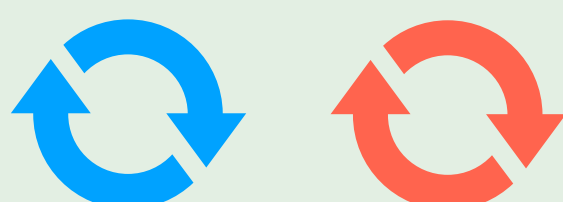


zero frequency counterpart of
 second harmonic generation



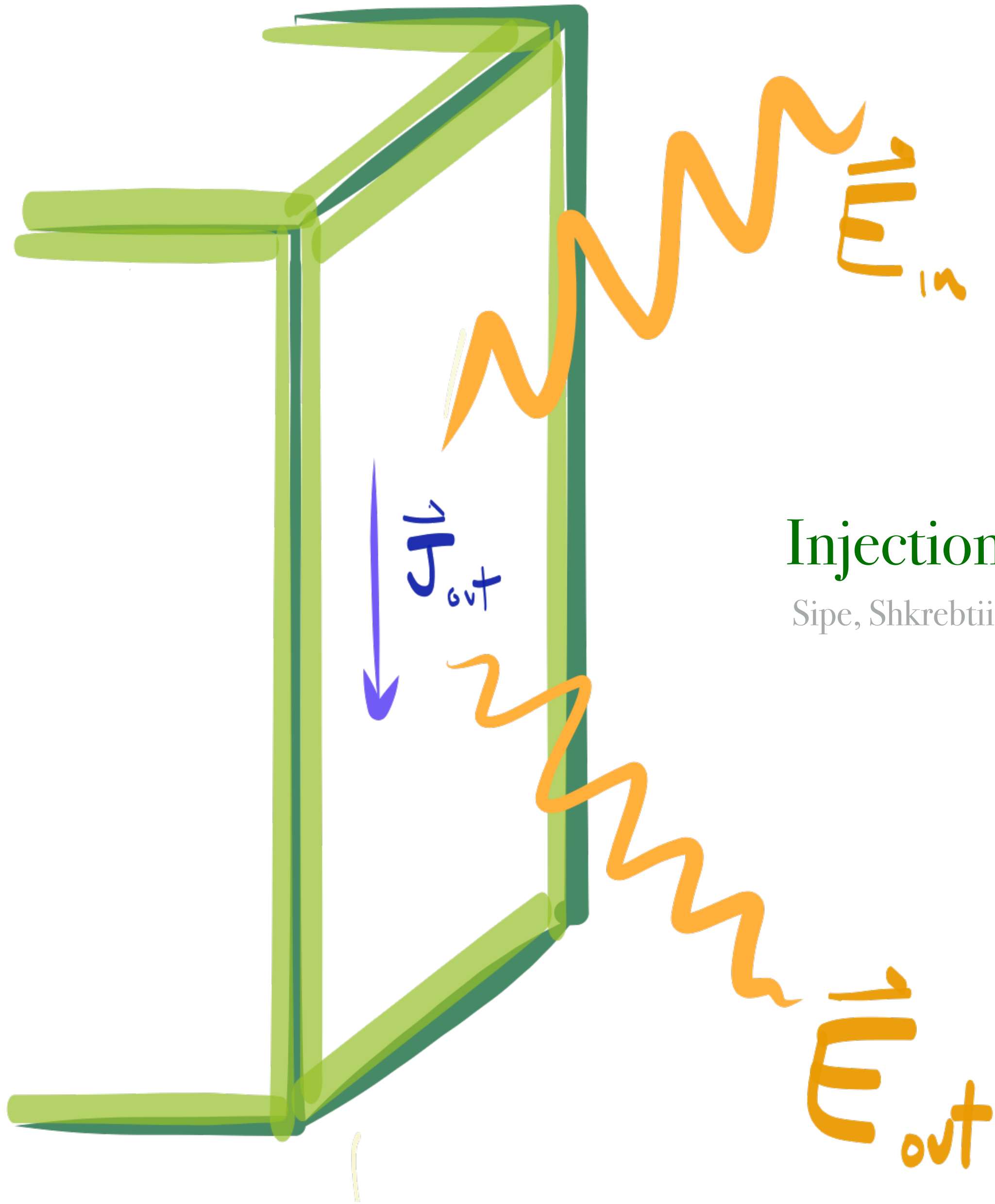
Morimoto and Nagaosa Sci. Ad. '16

Injection current



part that flips sign with polarization:
 large and quantized

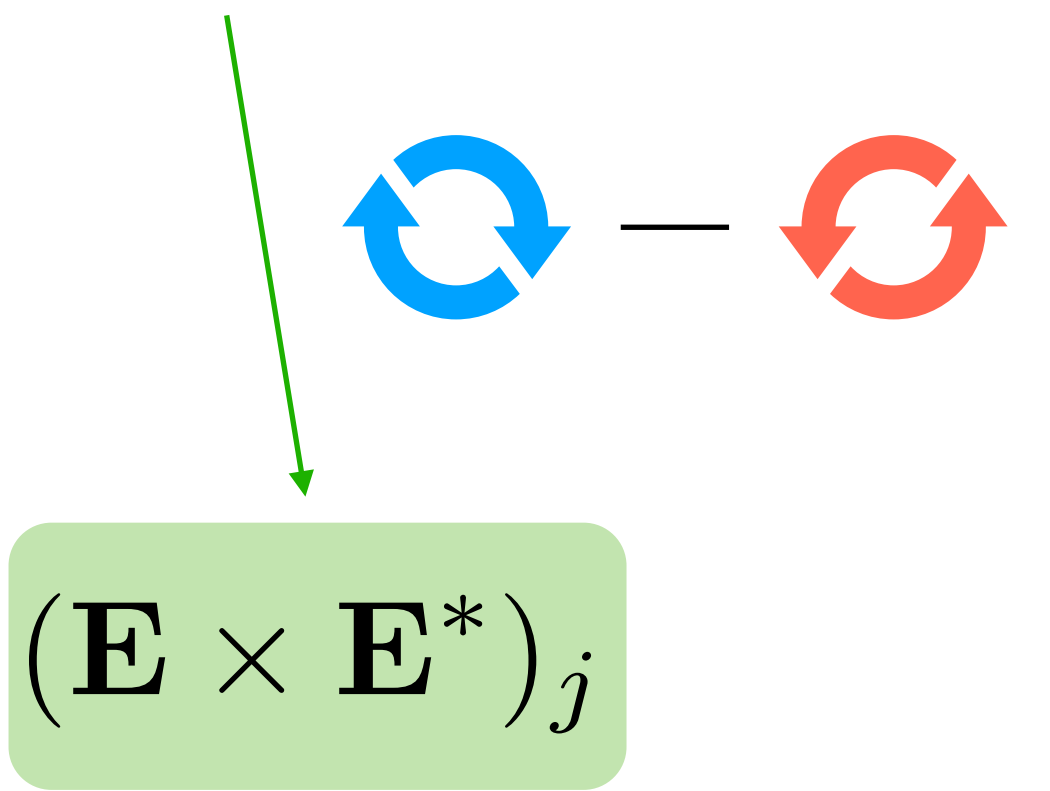
$$\frac{e^3}{h^2}$$



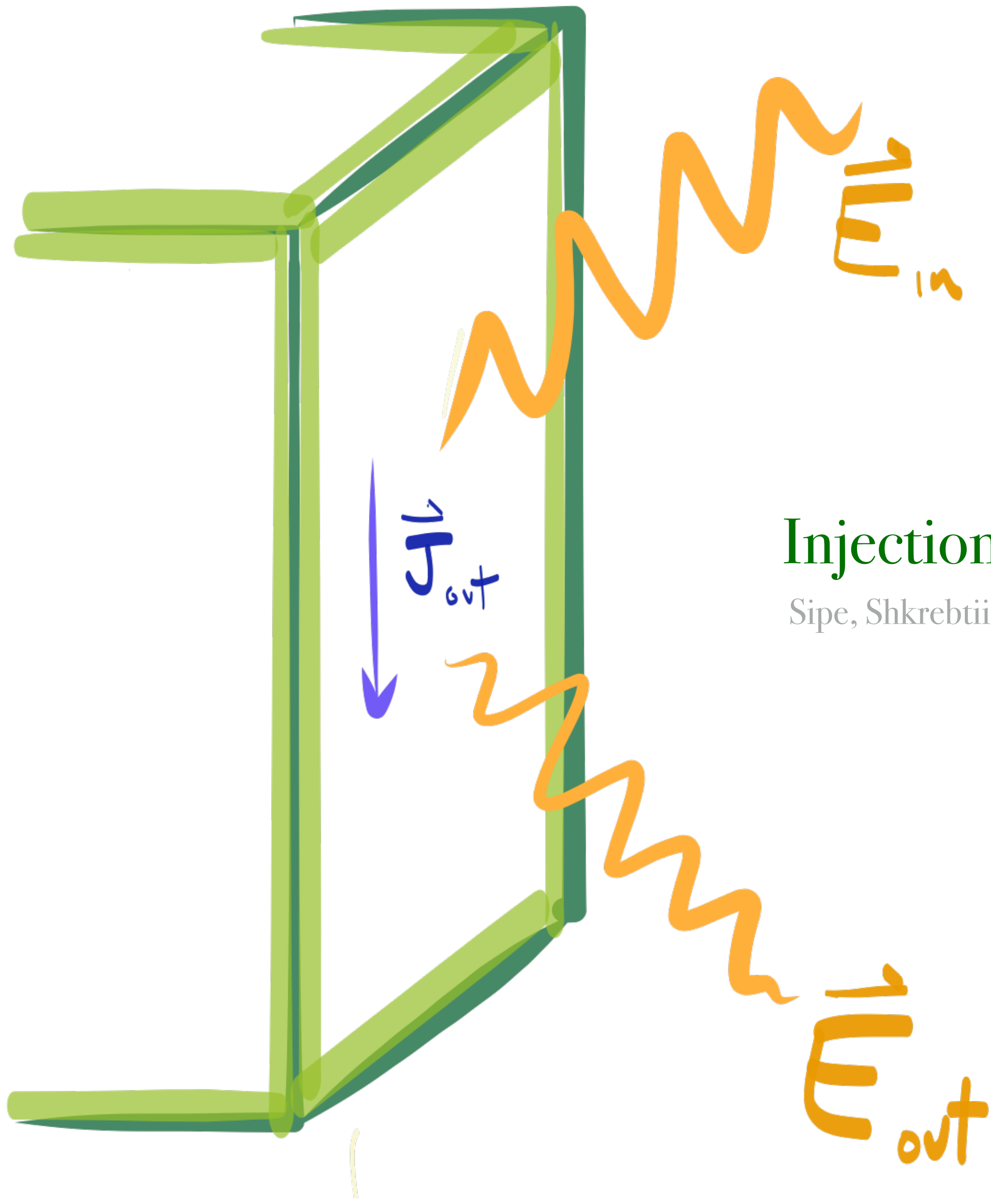
Injection current

Sipe, Shkrebtii, PRB (2000)

$$j_i \propto \sigma_{ijkl} E_j E_l$$



$$(\mathbf{E} \times \mathbf{E}^*)_j$$



Injection current

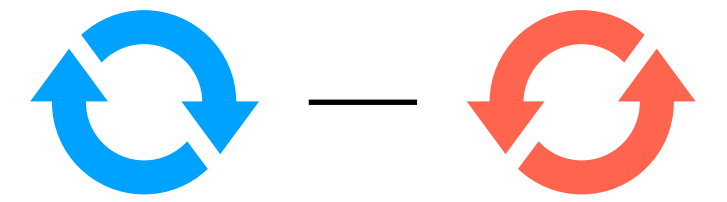
Sipe, Shkrebtii, PRB (2000)

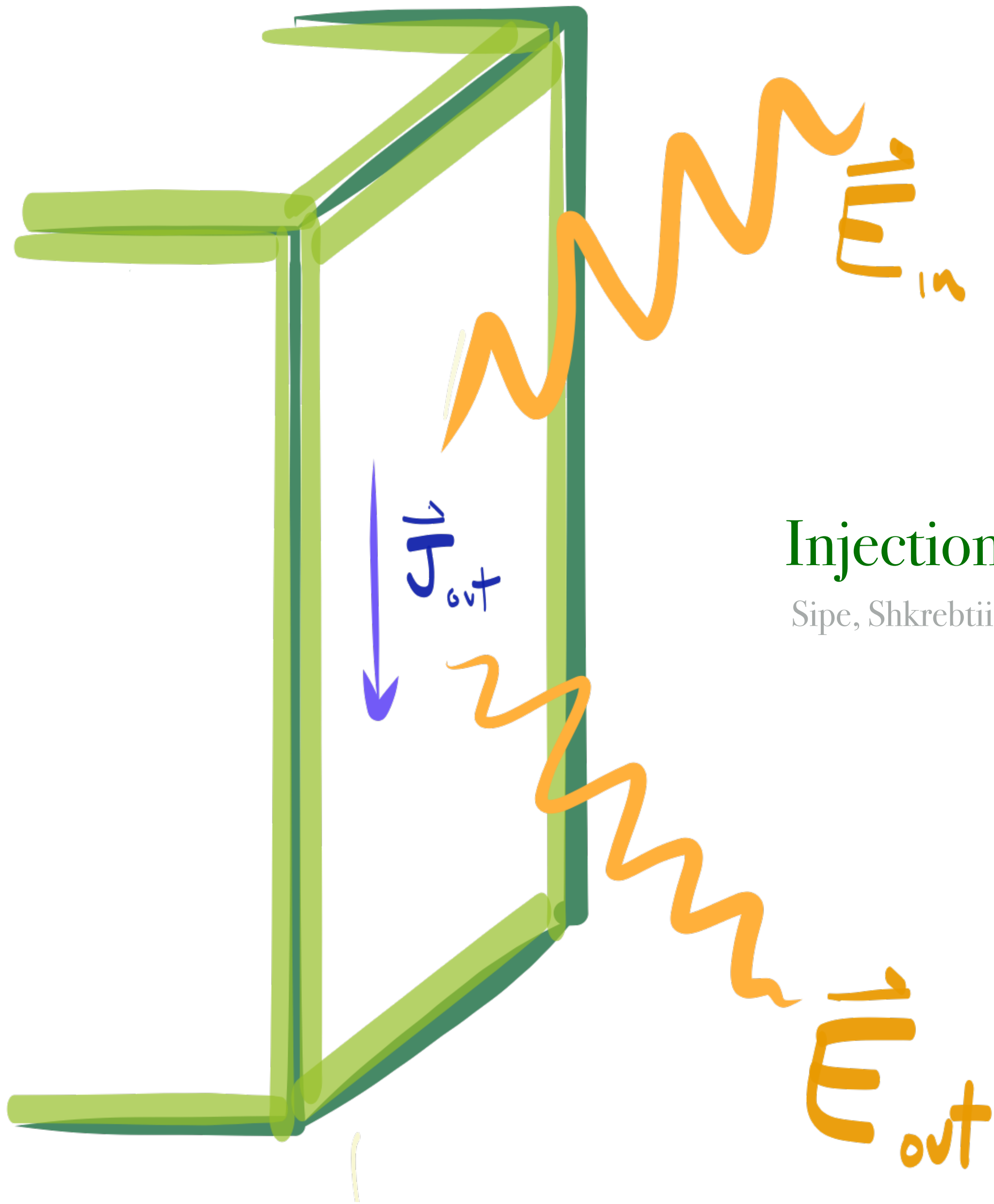
$$j_i \propto \sigma_{ijl} E_j E_l$$

$$\propto (i\omega)^{-1}$$

$$\frac{dj_i}{dt}$$

$$(\mathbf{E} \times \mathbf{E}^*)_j$$





Injection current

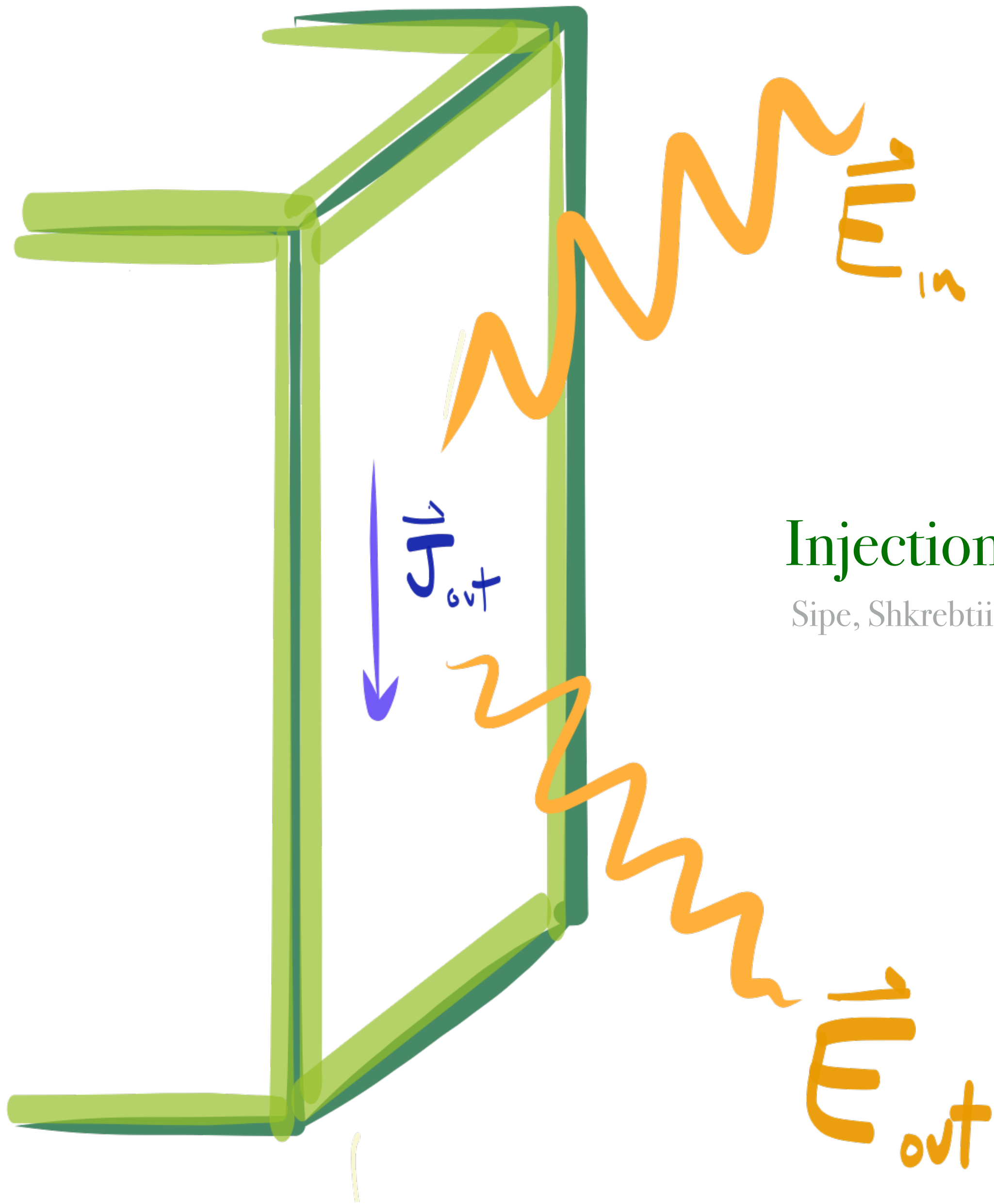
Sipe, Shkrebtti, PRB (2000)

$$j_i \propto \sigma_{ijl} E_j E_l$$

$$\propto (i\omega)^{-1}$$



$$\frac{dj_i}{dt} = \beta_{ij}(\omega) (\mathbf{E} \times \mathbf{E}^*)_j$$

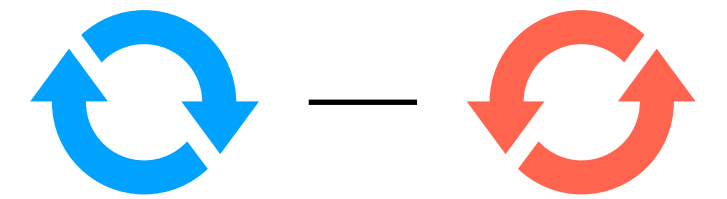


Injection current

Sipe, Shkrebtti, PRB (2000)

$$j_i \propto \sigma_{ijl} E_j E_l$$

$$\propto (i\omega)^{-1}$$



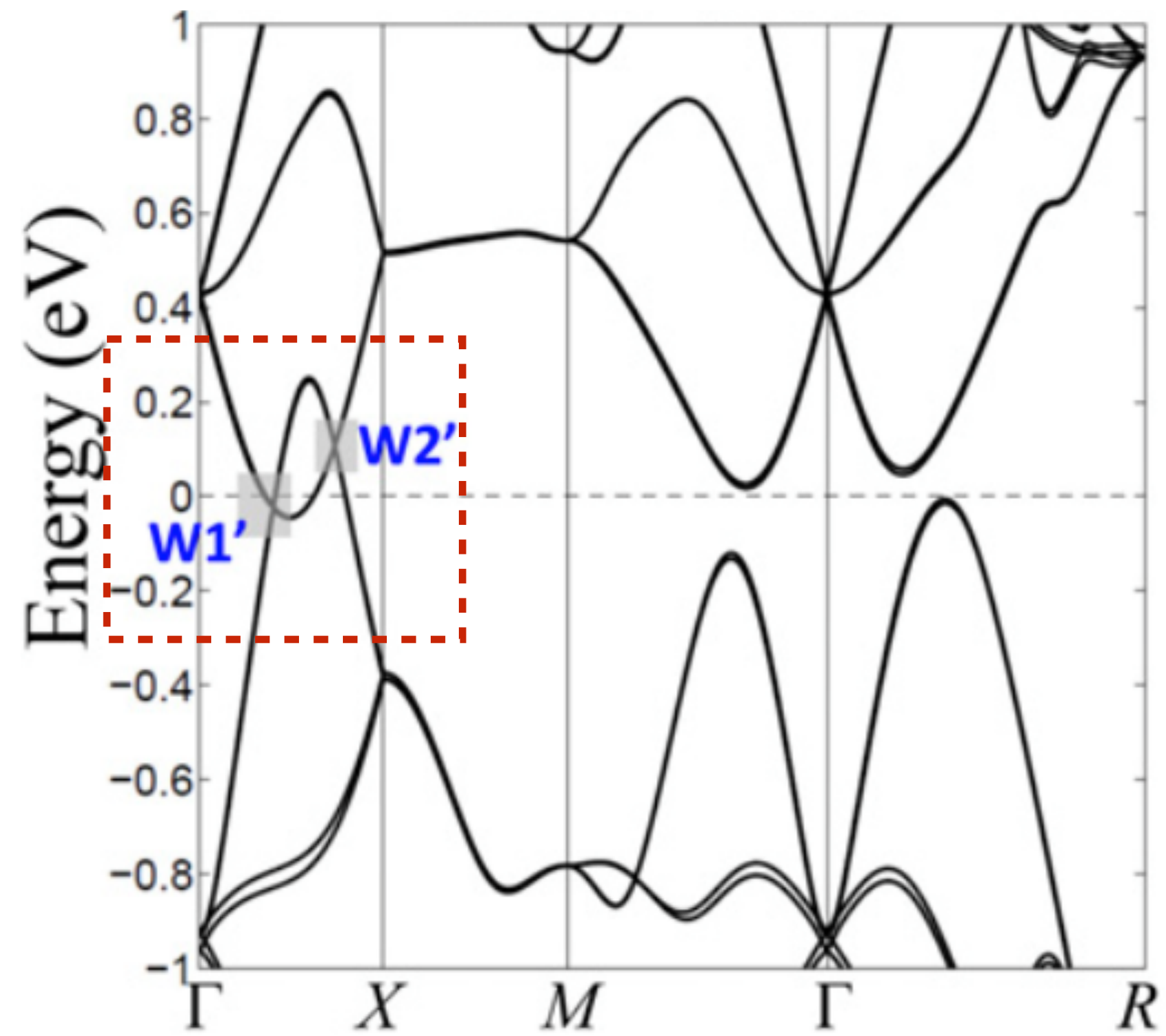
$$\frac{dj_i}{dt} = \beta_{ij}(\omega) (\mathbf{E} \times \mathbf{E}^*)_j$$

$$\text{Tr}[\beta] = i \frac{e^3}{2h^2} \oint_S d\mathbf{S} \cdot \boldsymbol{\Omega}_1$$

F. de Juan, AGG, T. Morimoto, J. E. Moore Nat. Comm (2017)

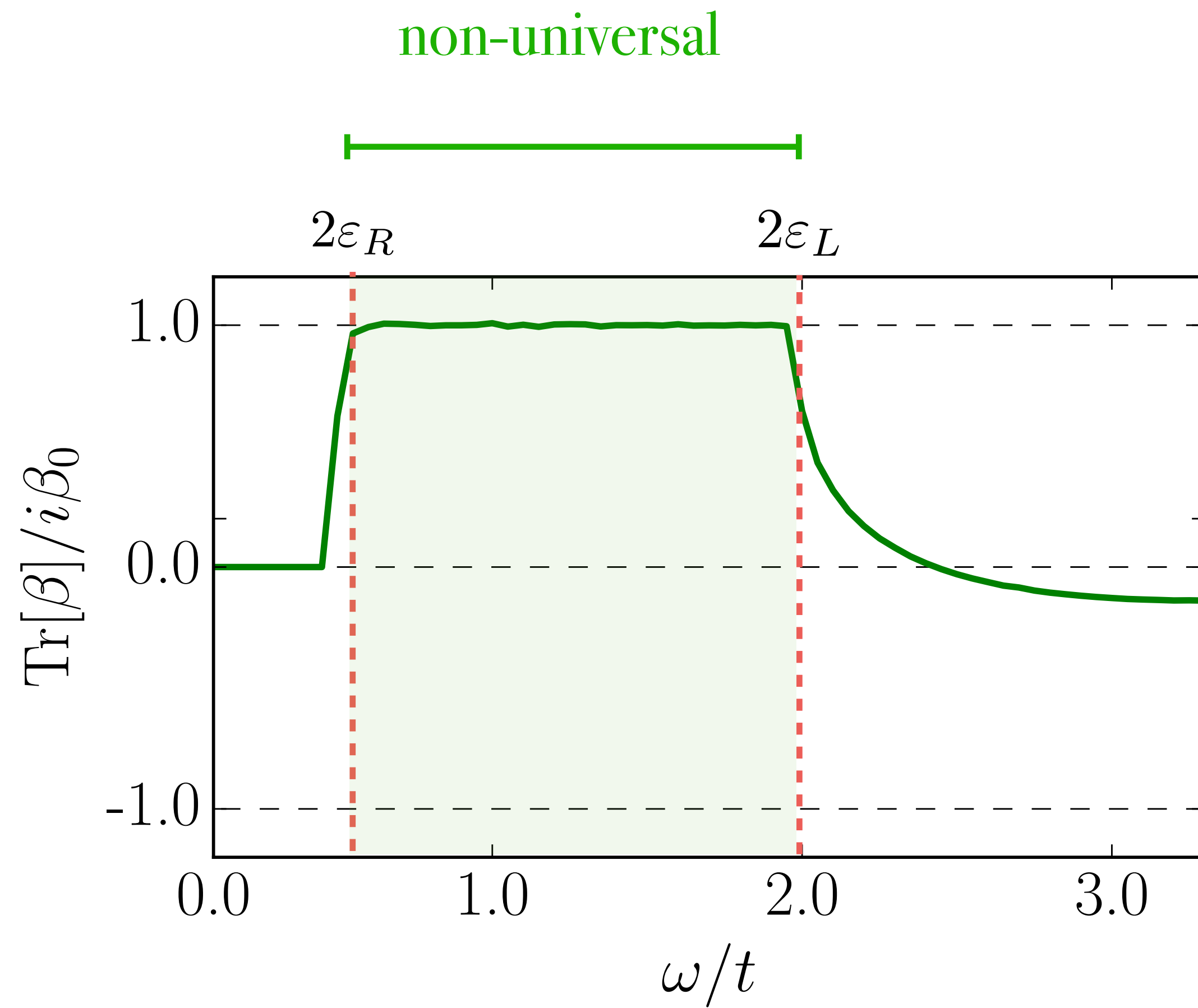
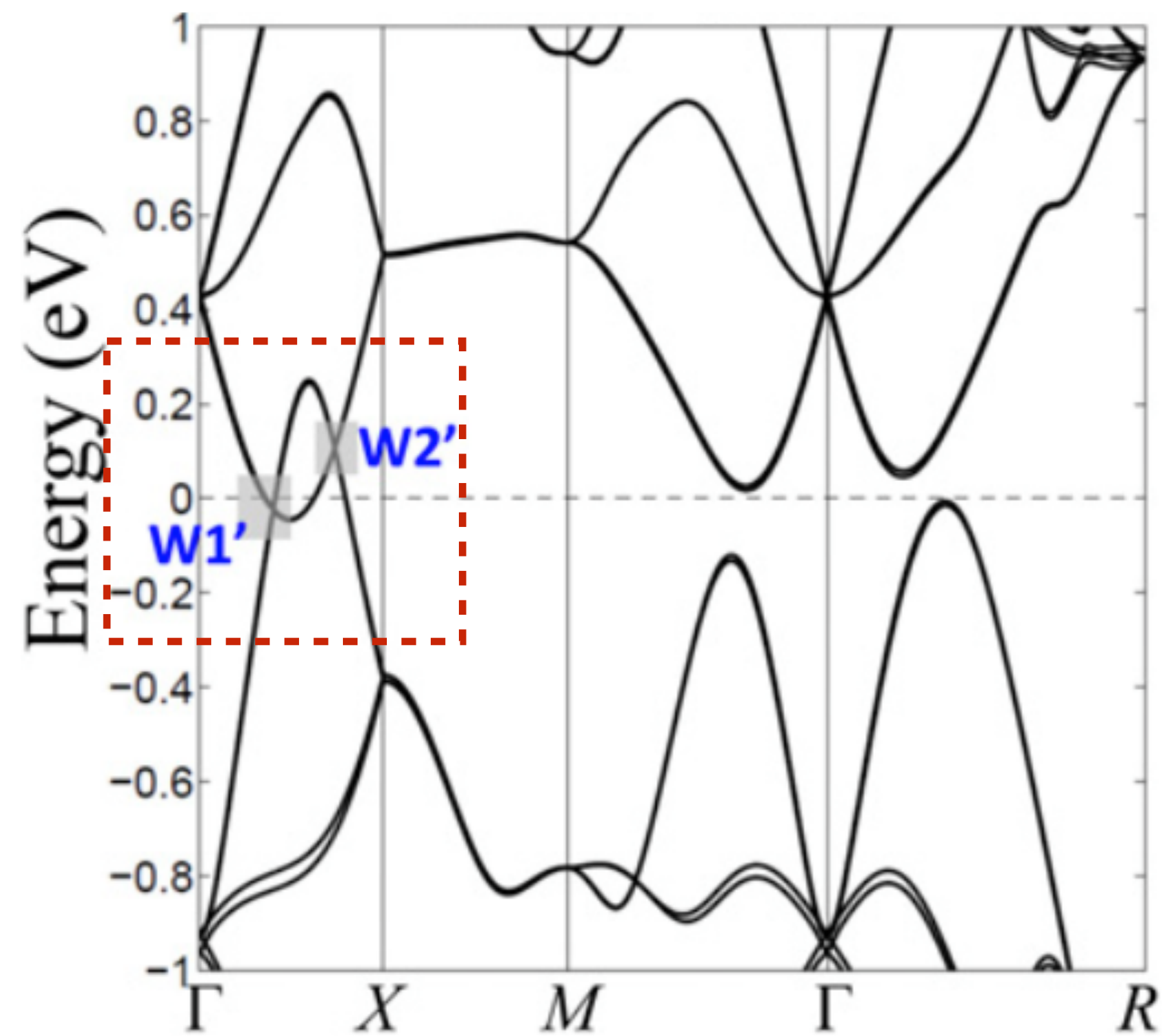
SrSi₂

Huang, et al. PNAS 113 1180 (2015)



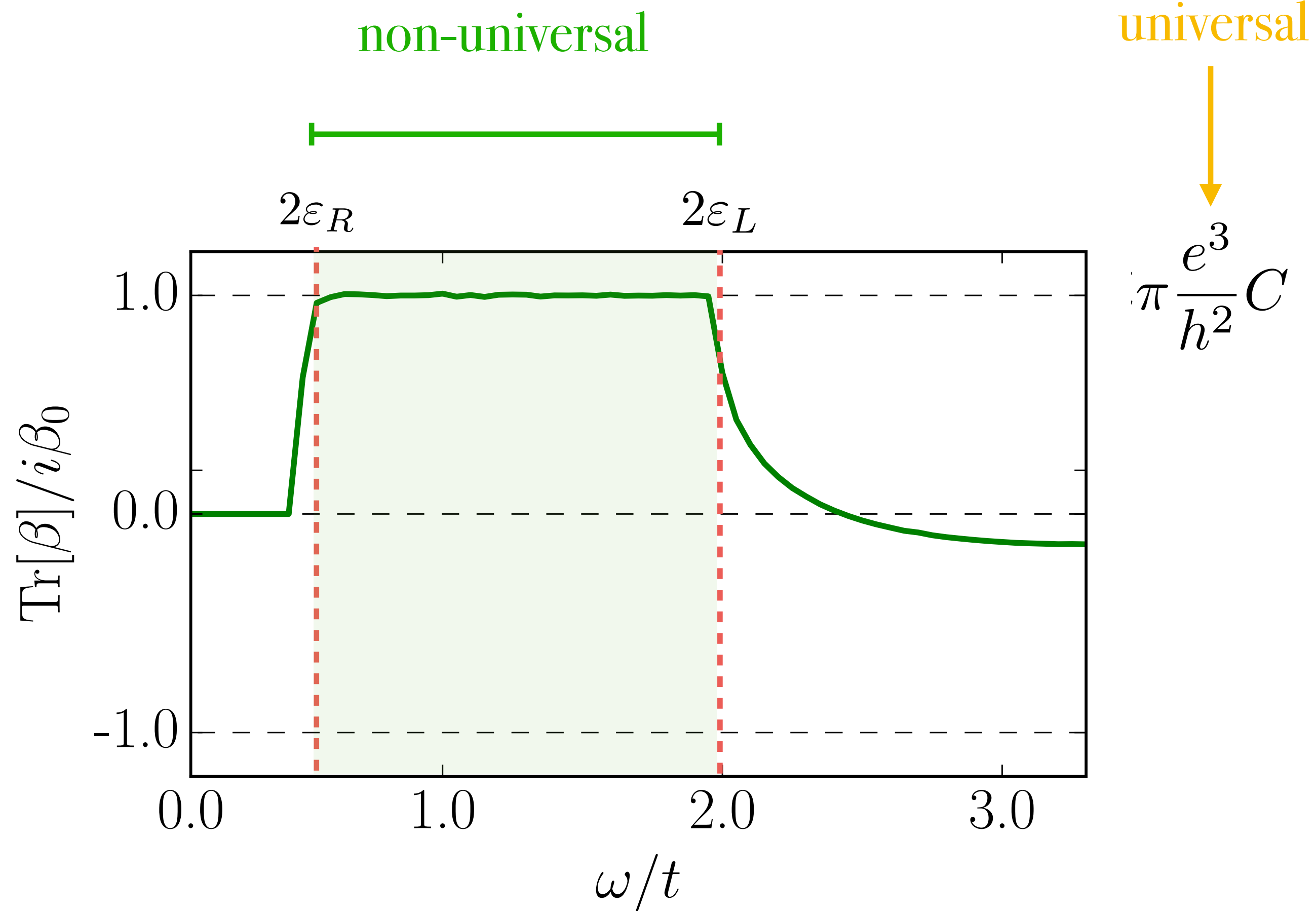
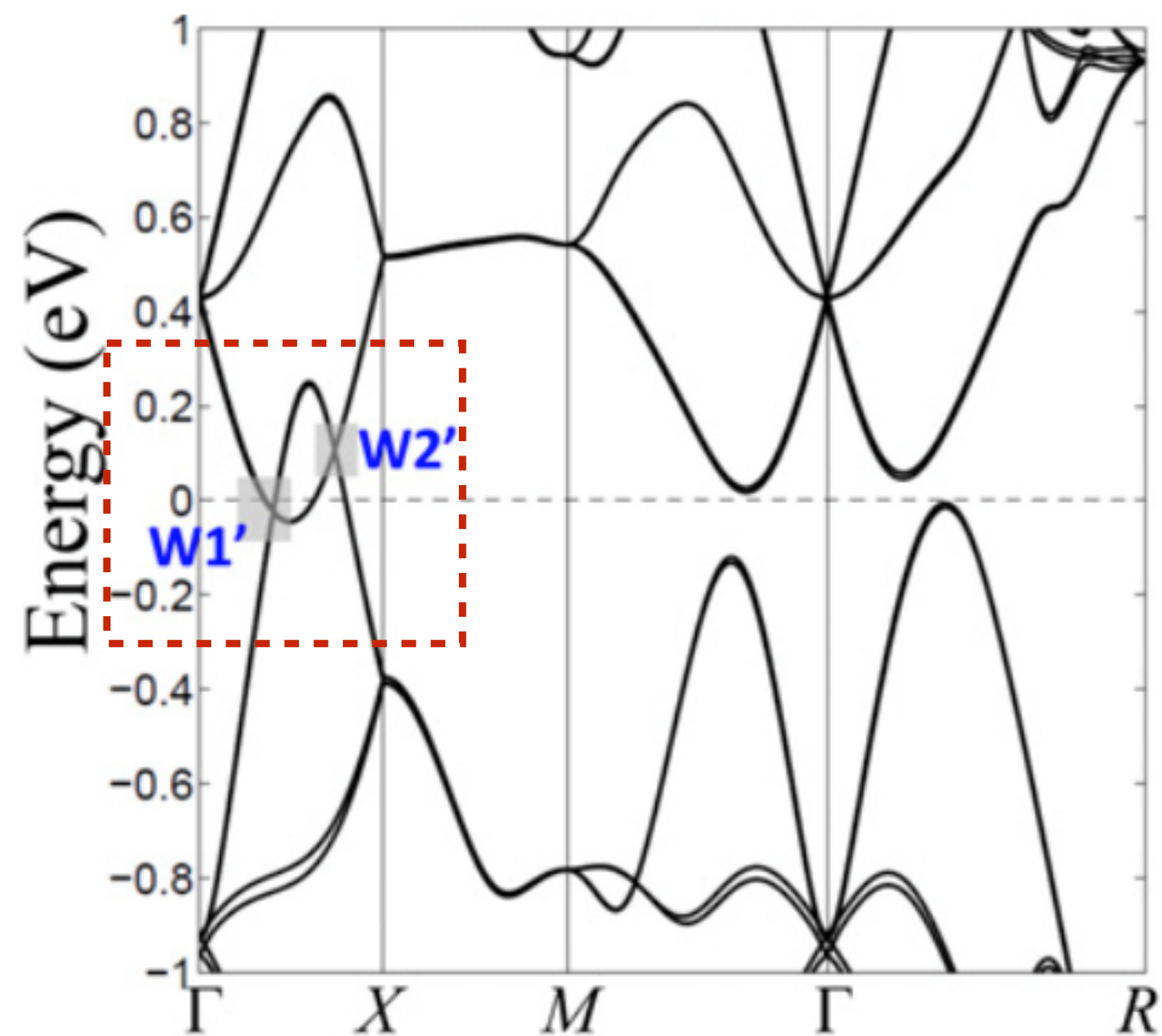
SrSi₂

Huang, et al. PNAS 113 1180 (2015)



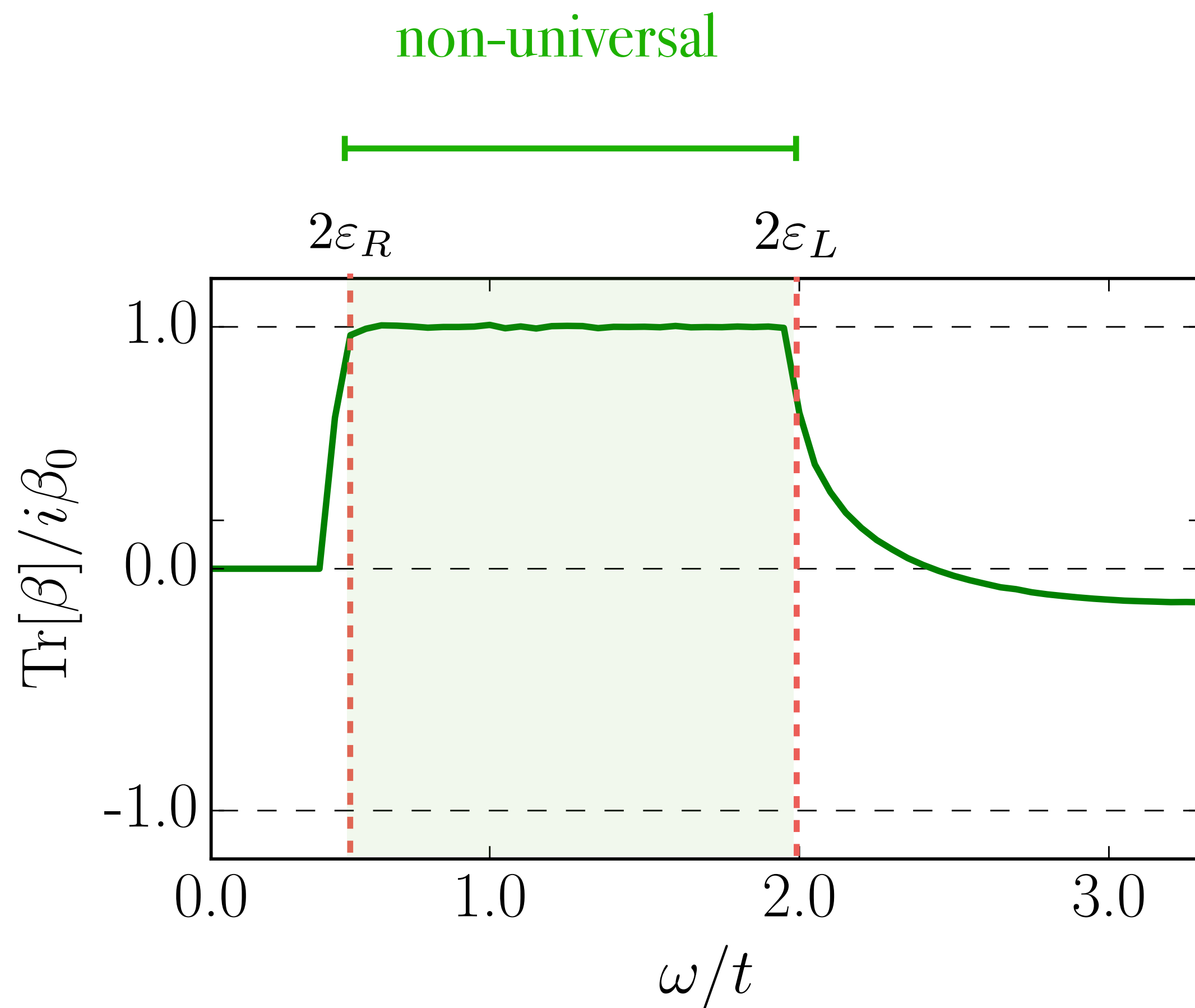
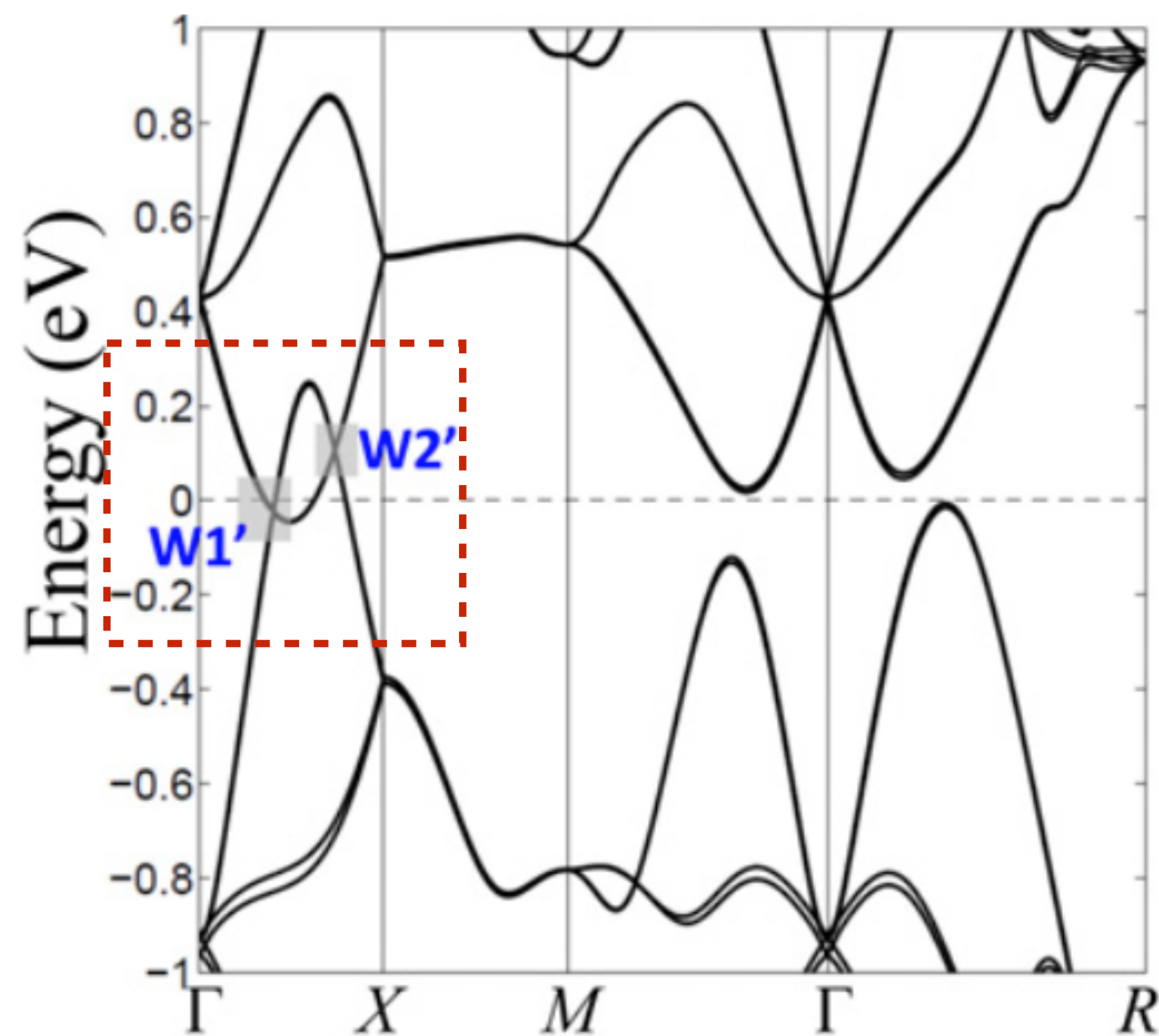
SrSi₂

Huang, et al. PNAS 113 1180 (2015)



SrSi₂

Huang, et al. PNAS 113 1180 (2015)



universal

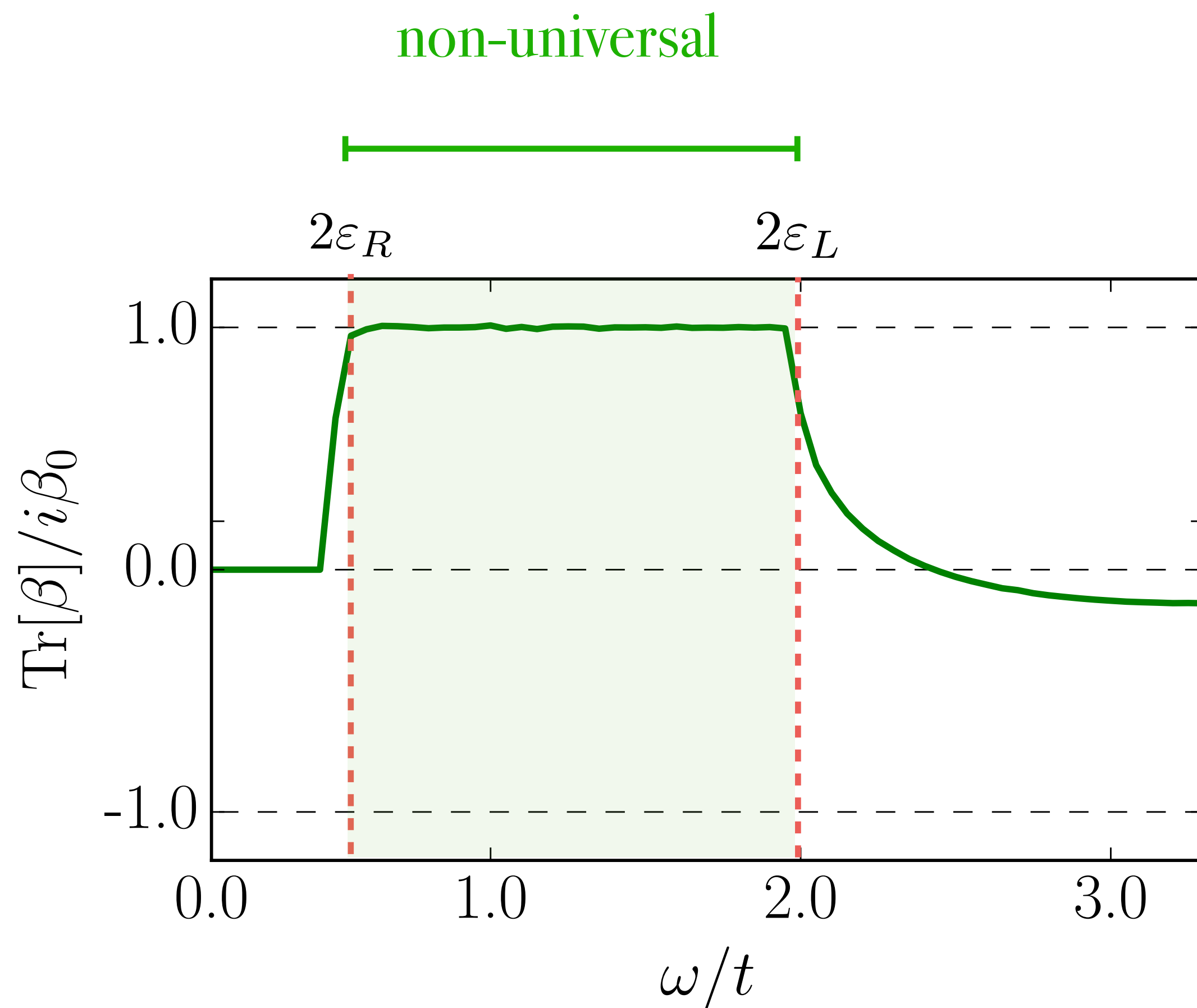
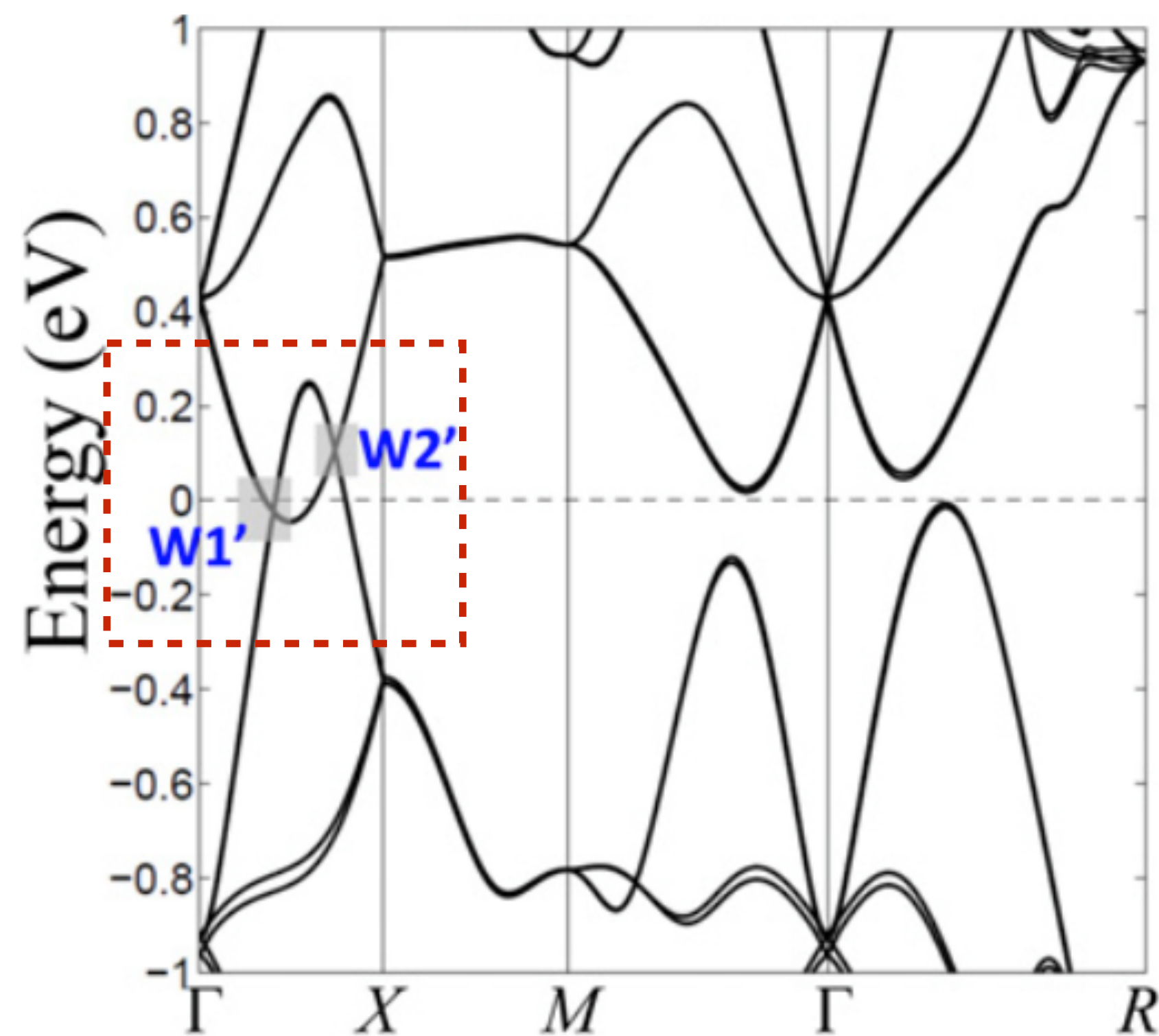
$$\pi \frac{e^3}{h^2} C$$

$$+ \mathcal{O}\left(\frac{\omega^2}{\Delta E^2}\right)$$

multi-band correction

SrSi₂

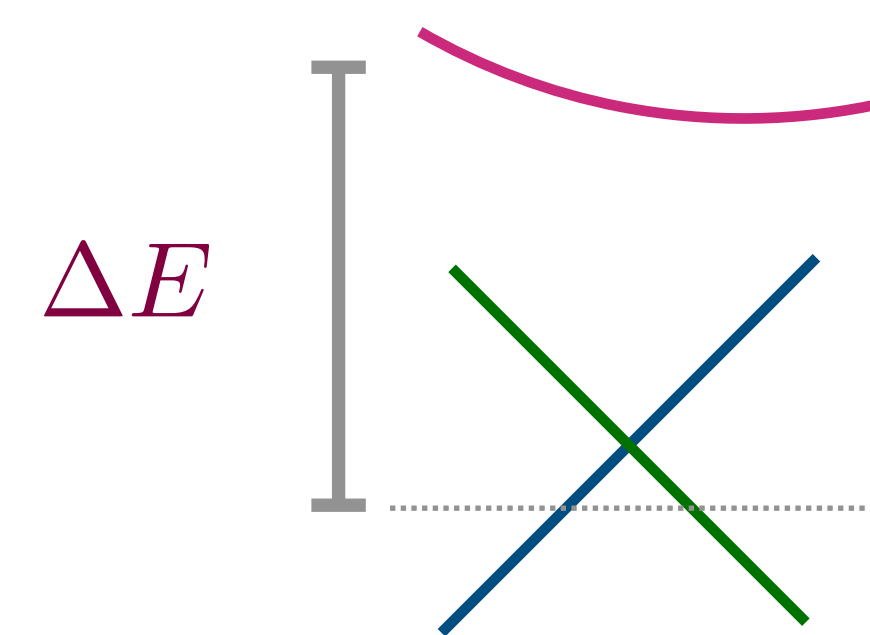
Huang, et al. PNAS 113 1180 (2015)



universal

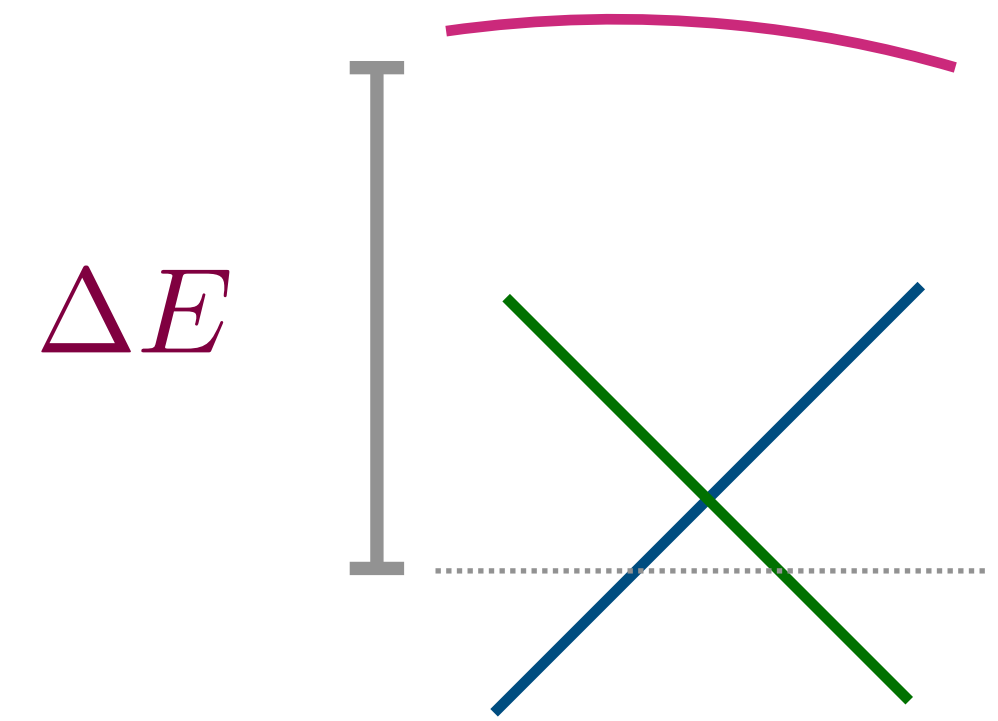
$$\pi \frac{e^3}{h^2} C + \mathcal{O}\left(\frac{\omega^2}{\Delta E^2}\right)$$

multi-band correction



Reality

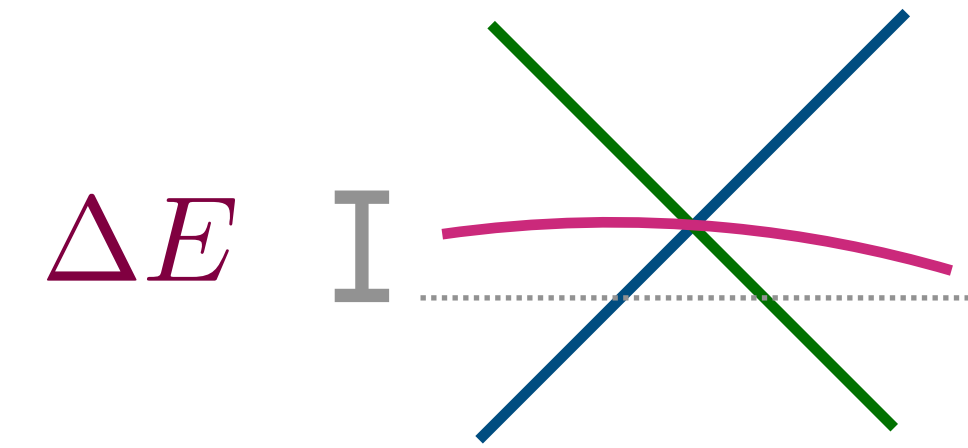
Many bands



$$\delta\beta = M_{13} \frac{\omega^2}{\Delta E_{13}^2}$$

Reality

Many bands



$$\delta\beta = M_{13} \frac{\omega^2}{\Delta E_{13}^2}$$

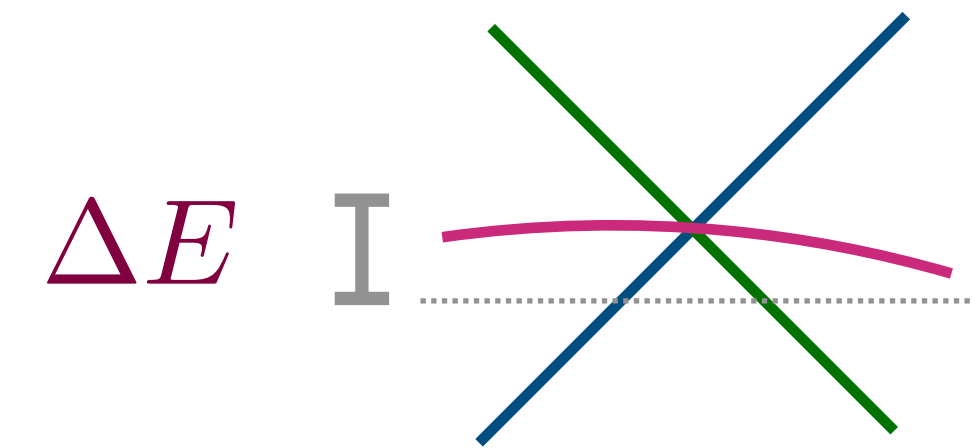
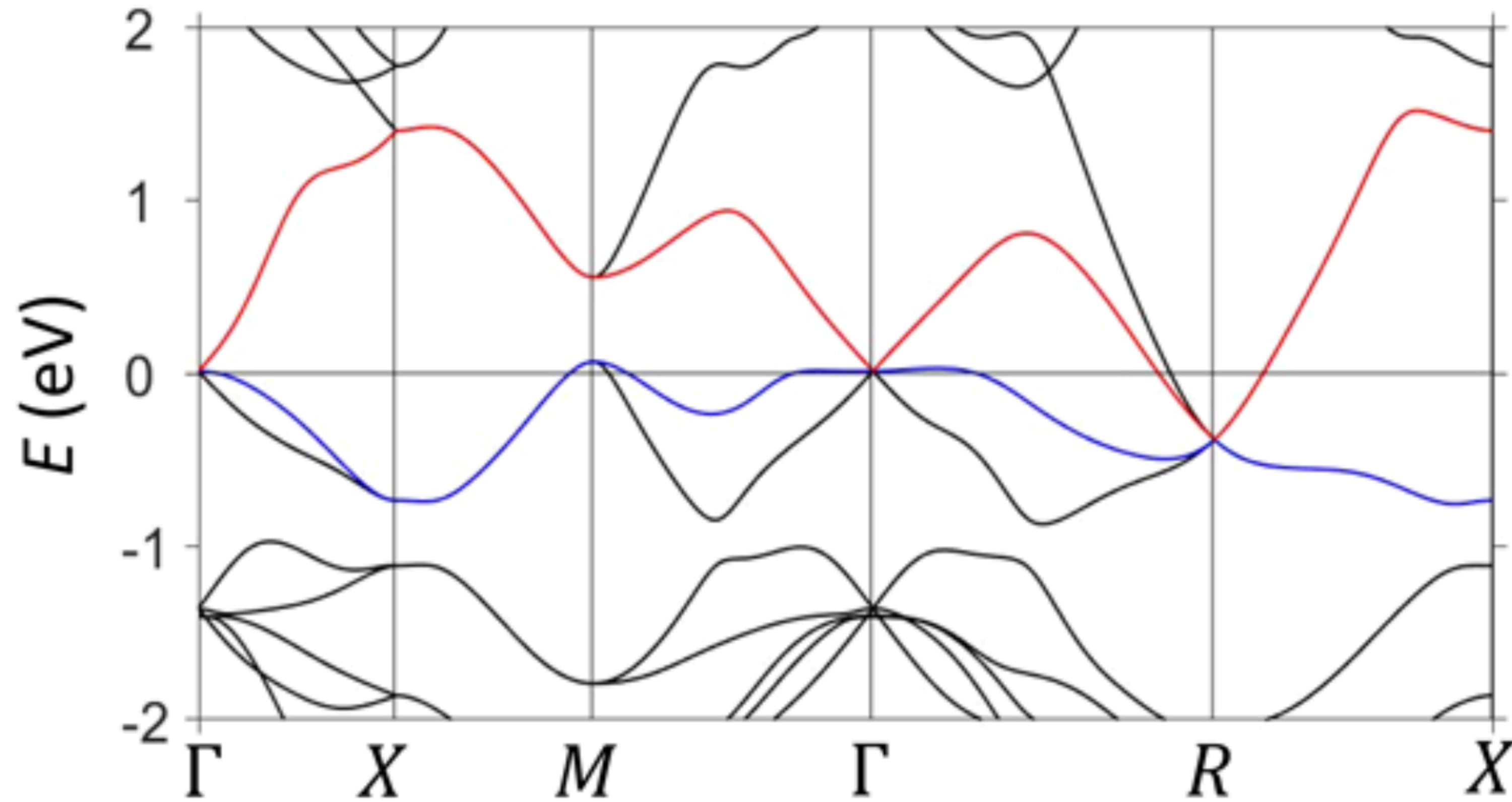
Nodal crossings with three or more bands⁵¹, however, are not expected to display quantization of this type as the corrections from equation (8) cannot be made small.

Reality

RhSi

Chang et. al PRL '17

Many bands



$$\delta\beta = M_{13} \frac{\omega^2}{\Delta E_{13}^2}$$

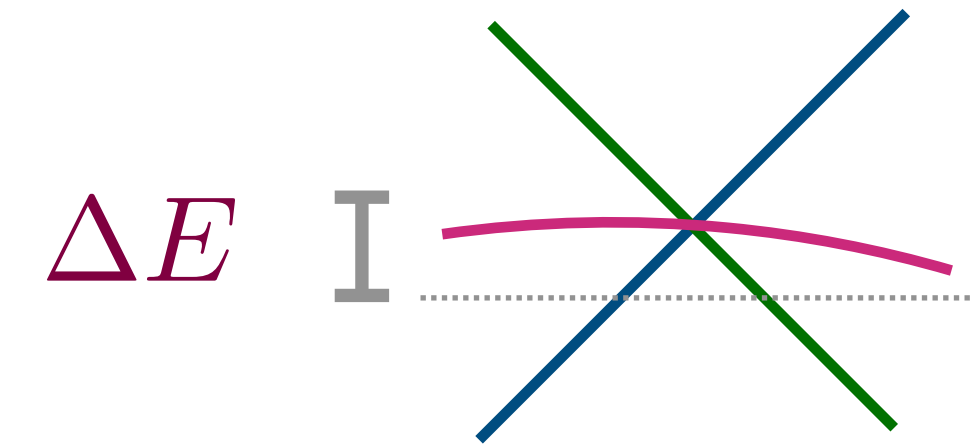
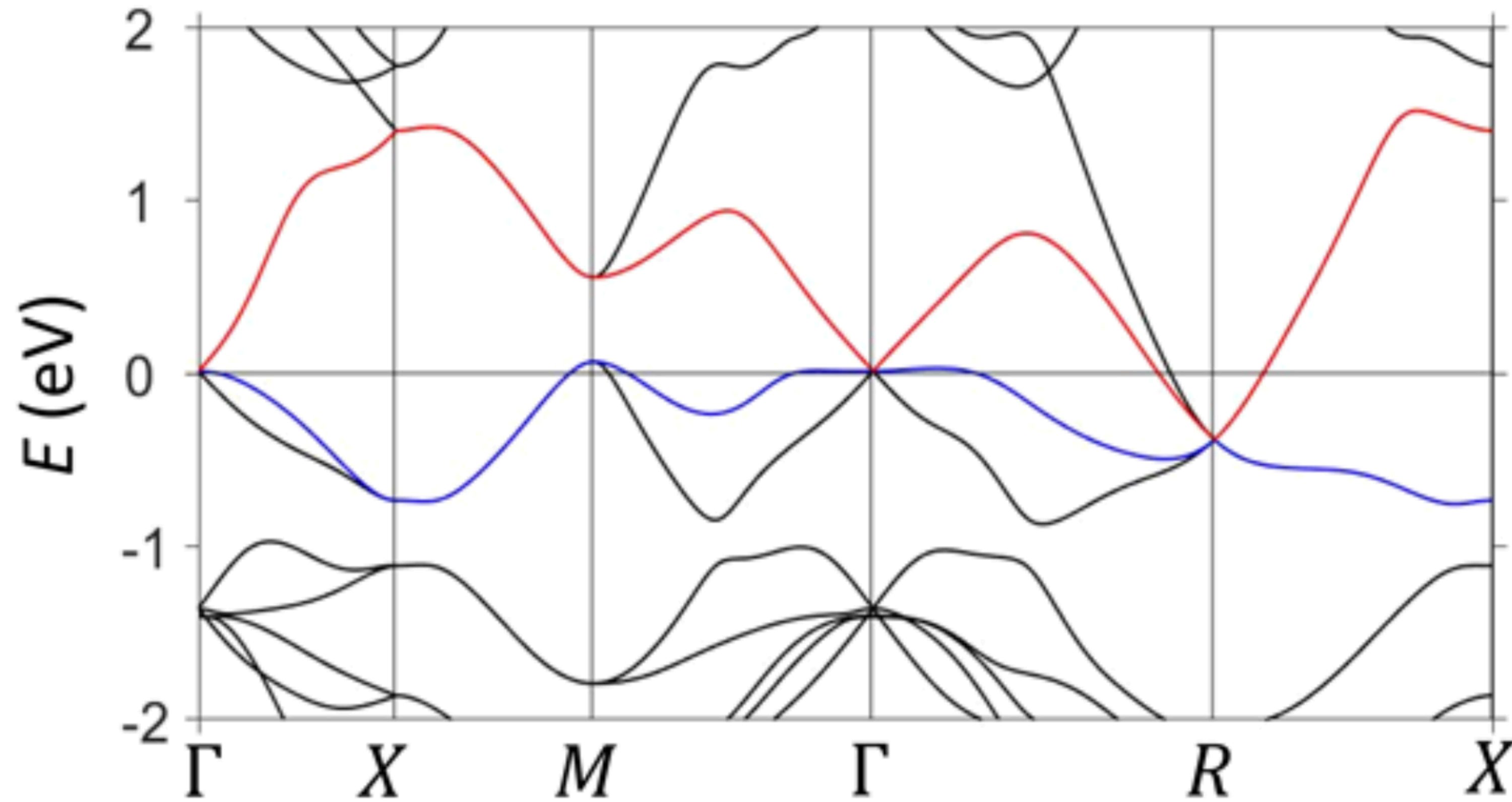
Nodal crossings with three or more bands⁵¹, however, are not expected to display quantization of this type as the corrections from equation (8) cannot be made small.

Reality

RhSi

Chang et. al PRL '17

Many bands



$$\delta\beta = M_{13} \frac{\omega^2}{\Delta E_{13}^2}$$

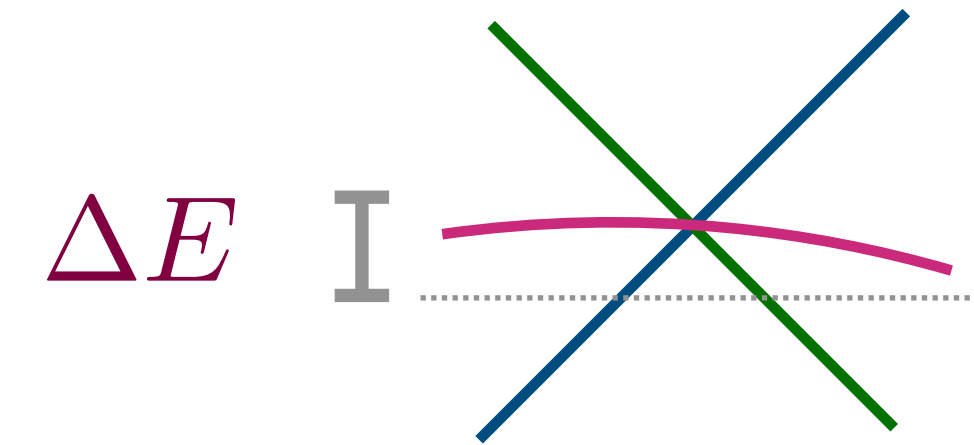
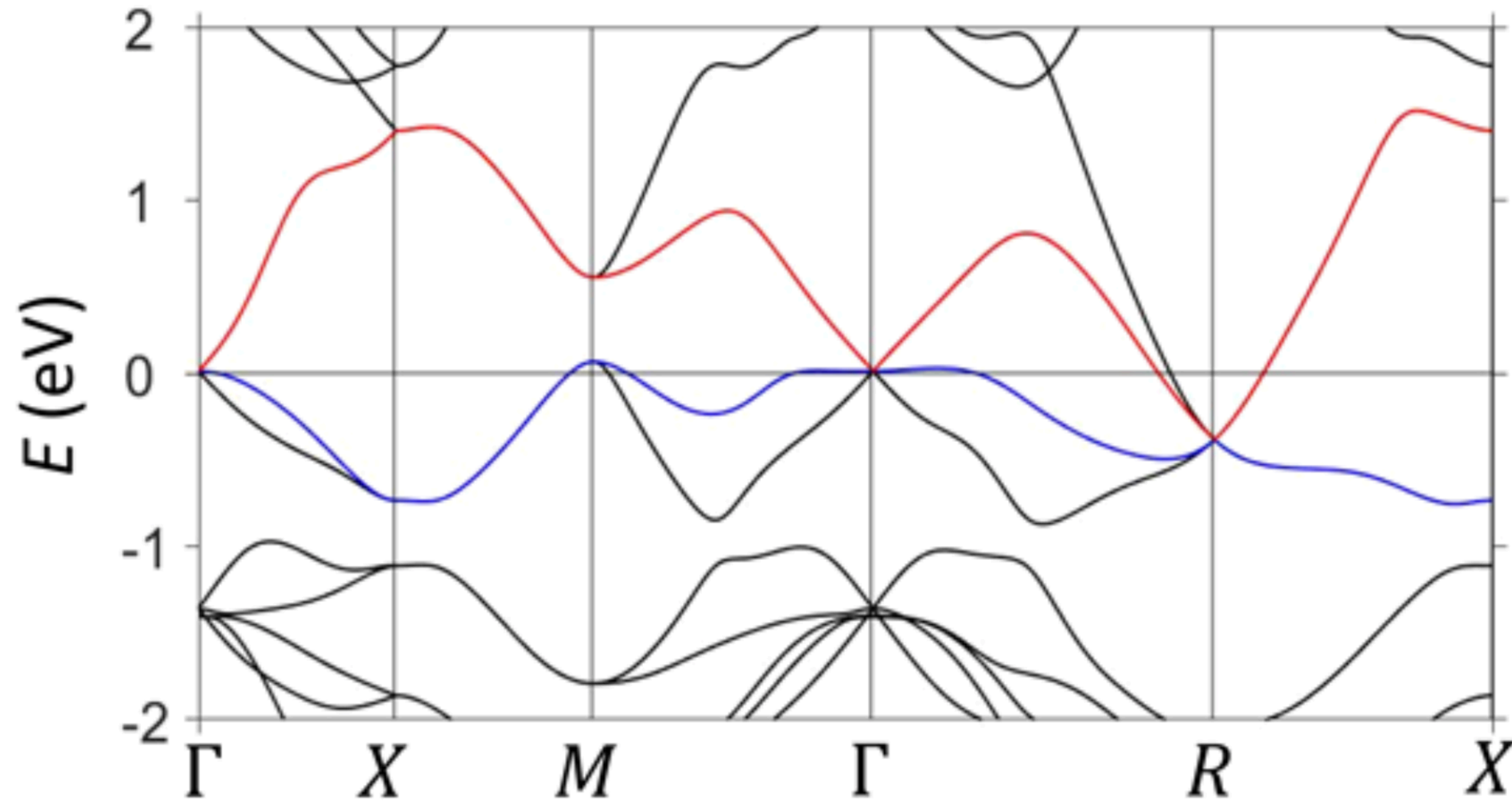
Nodal crossings with three or more bands⁵¹, however, are not expected to display quantization of this type as the corrections from equation (8) cannot be made small.

Reality

RhSi

Chang et. al PRL '17

Many bands



$$\delta\beta = M_{13} \frac{\omega^2}{\Delta E_{13}^2}$$

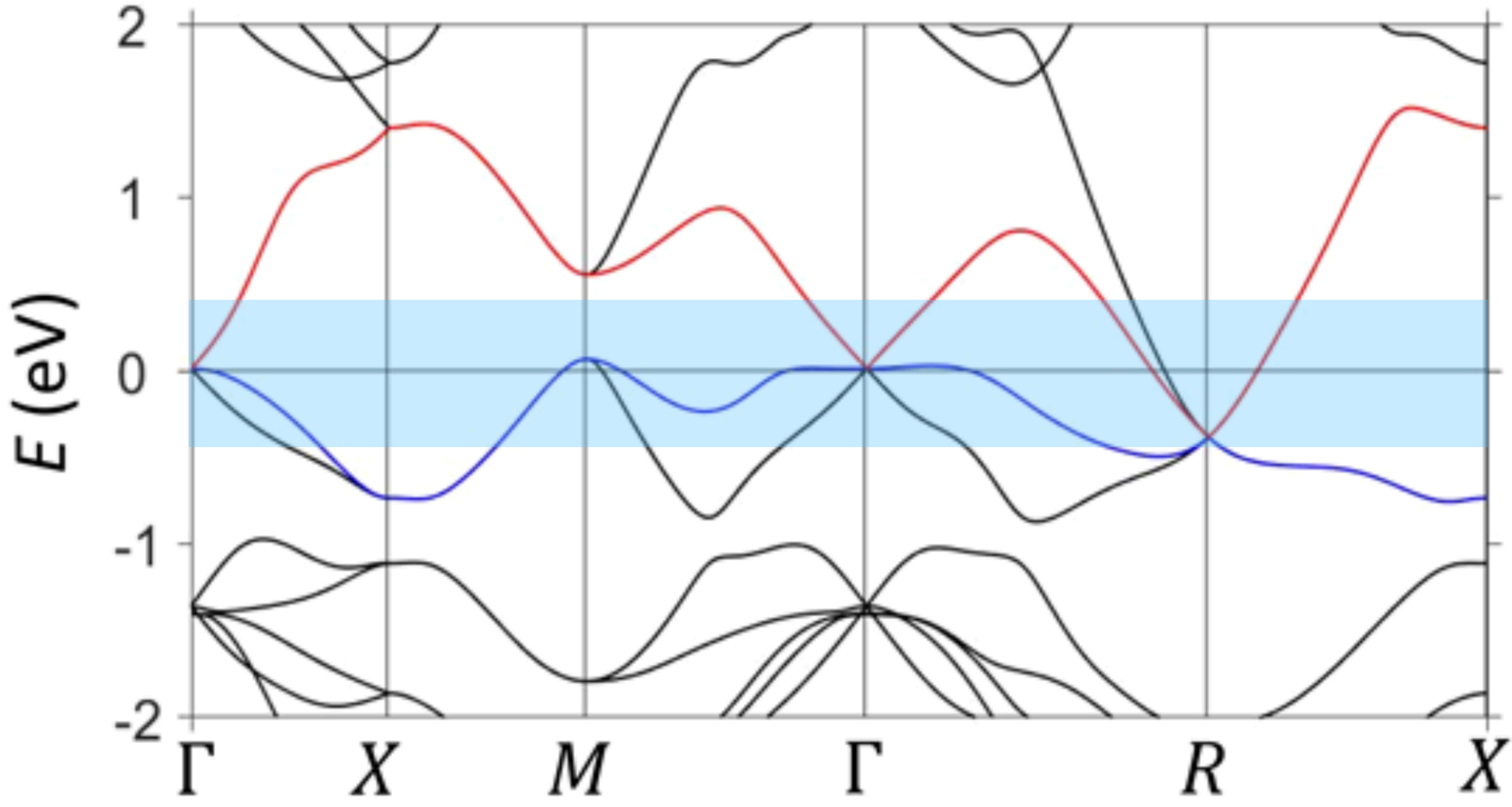
$$H(\phi, \vec{k}) = \vec{S}(\phi) \cdot \vec{k}$$

Nodal crossings with three or more bands⁵¹, however, are not expected to display quantization of this type as the corrections from equation (8) cannot be made small.

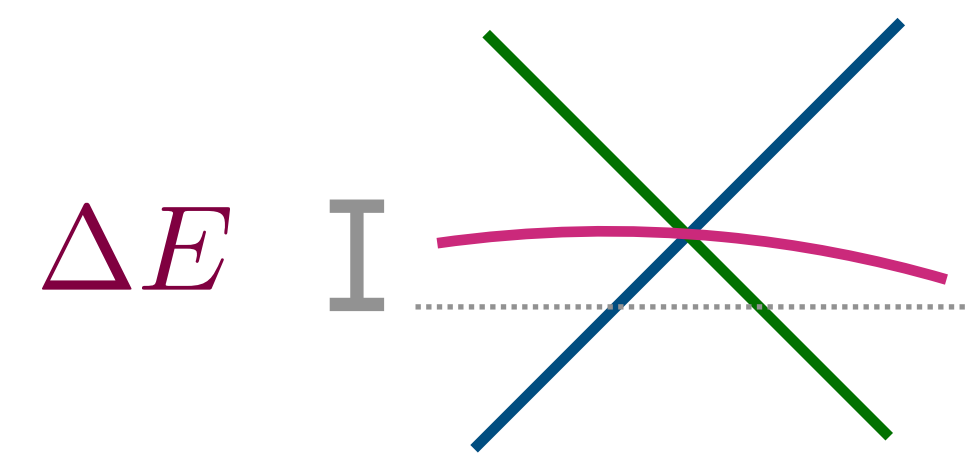
Reality

RhSi

Chang et. al PRL '17



Many bands



$$\delta\beta = M_{13} \frac{\omega^2}{\Delta E_{13}^2}$$

Nodal crossings with three or more bands⁵¹, however, are not expected to display quantization of this type as the corrections from equation (8) cannot be made small.

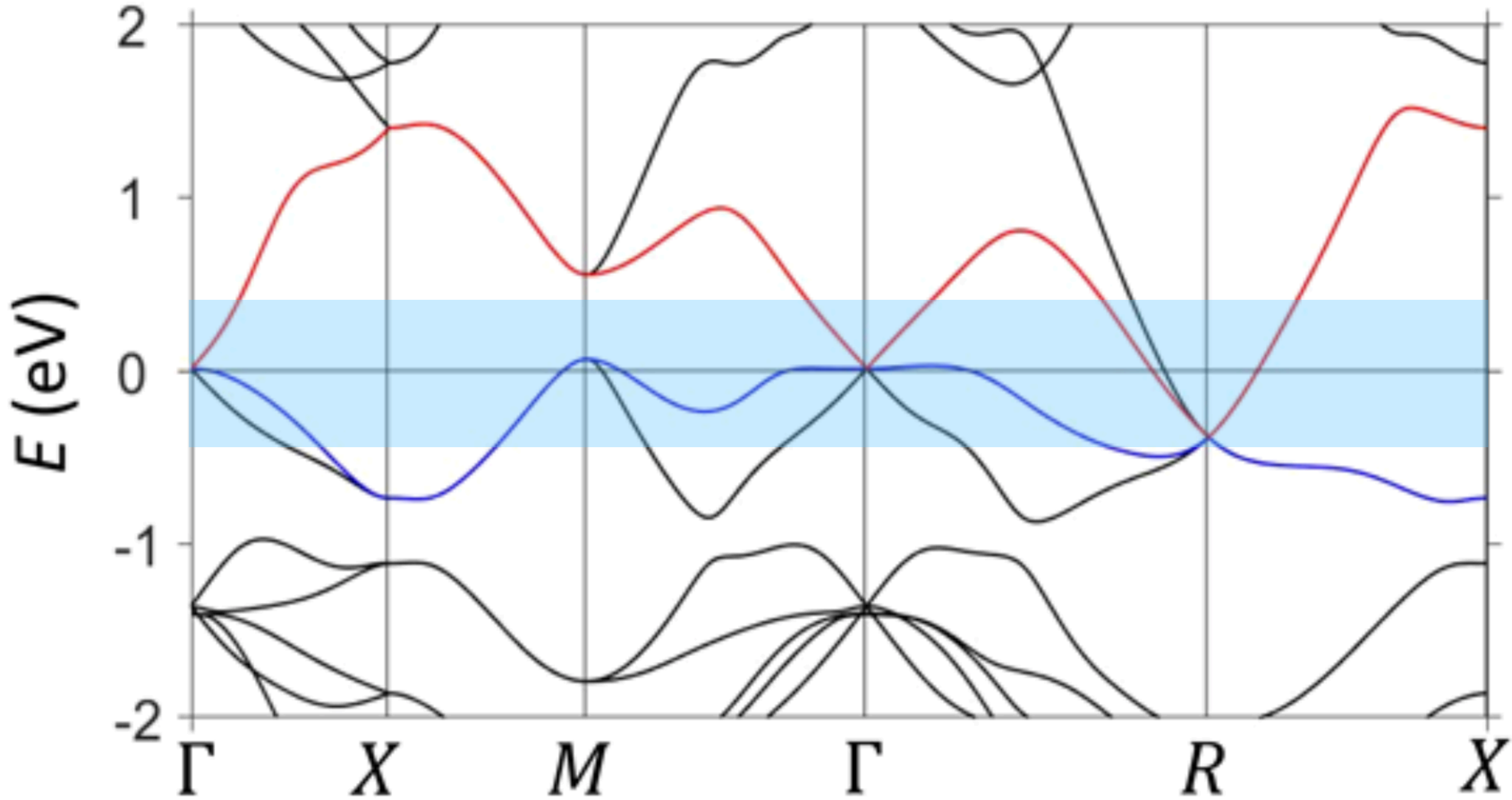
$$H(\phi, \vec{k}) = \vec{S}(\phi) \cdot \vec{k}$$

$$\beta(\omega) = 4\pi^2 \beta_0 C_\Sigma$$

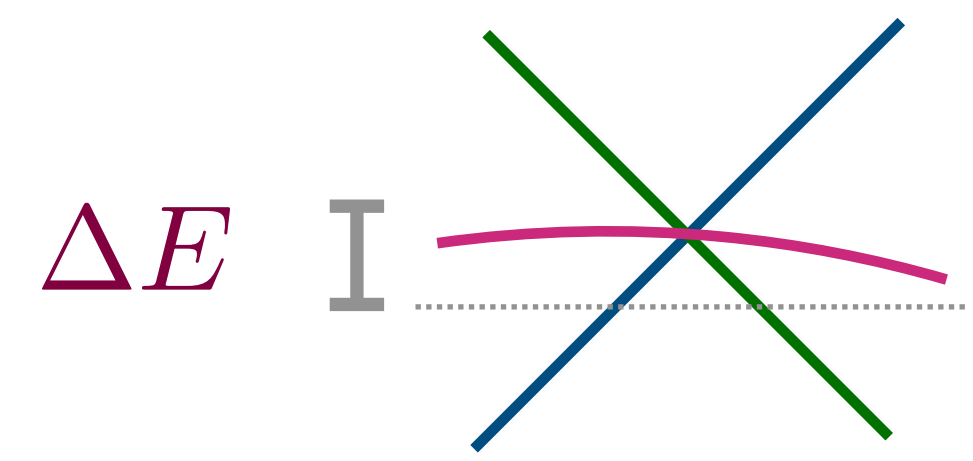
Reality

RhSi

Chang et. al PRL '17



Many bands



$$\delta\beta = M_{13} \frac{\omega^2}{\Delta E_{13}^2}$$

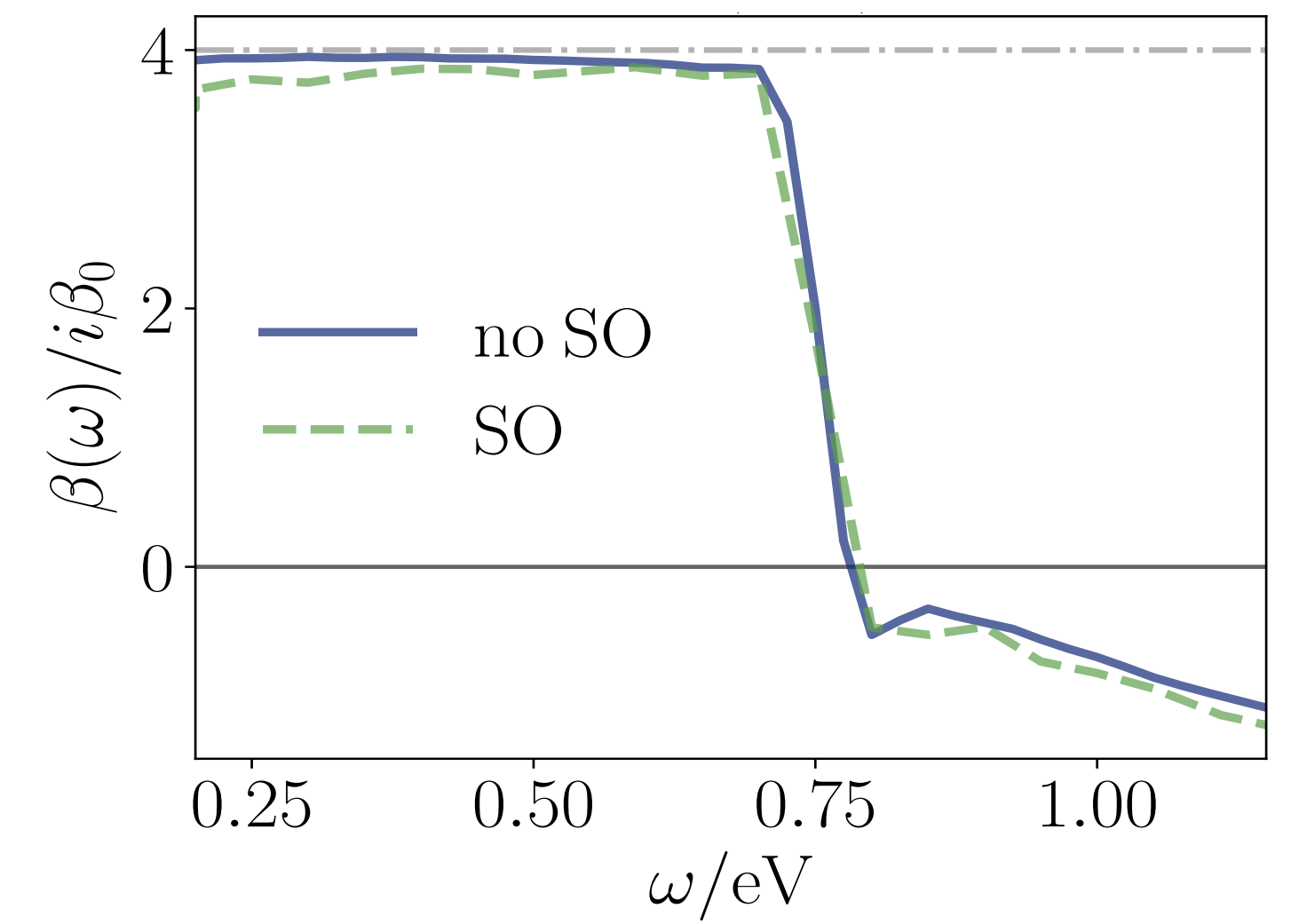
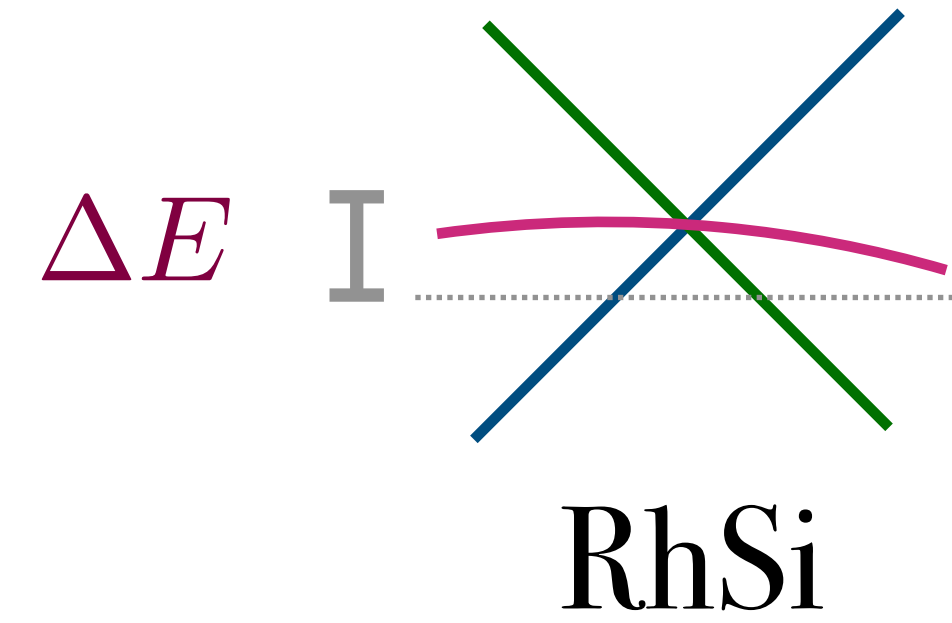
$$H(\phi, \vec{k}) = \vec{S}(\phi) \cdot \vec{k}$$

$$\beta(\omega) = 4\pi^2 \beta_0 C_\Sigma$$

Nodal crossings with three or more bands⁵¹, however, are ~~not~~ expected to display quantization of this type as the corrections from equation (8) cannot be made small.

Reality

Many bands



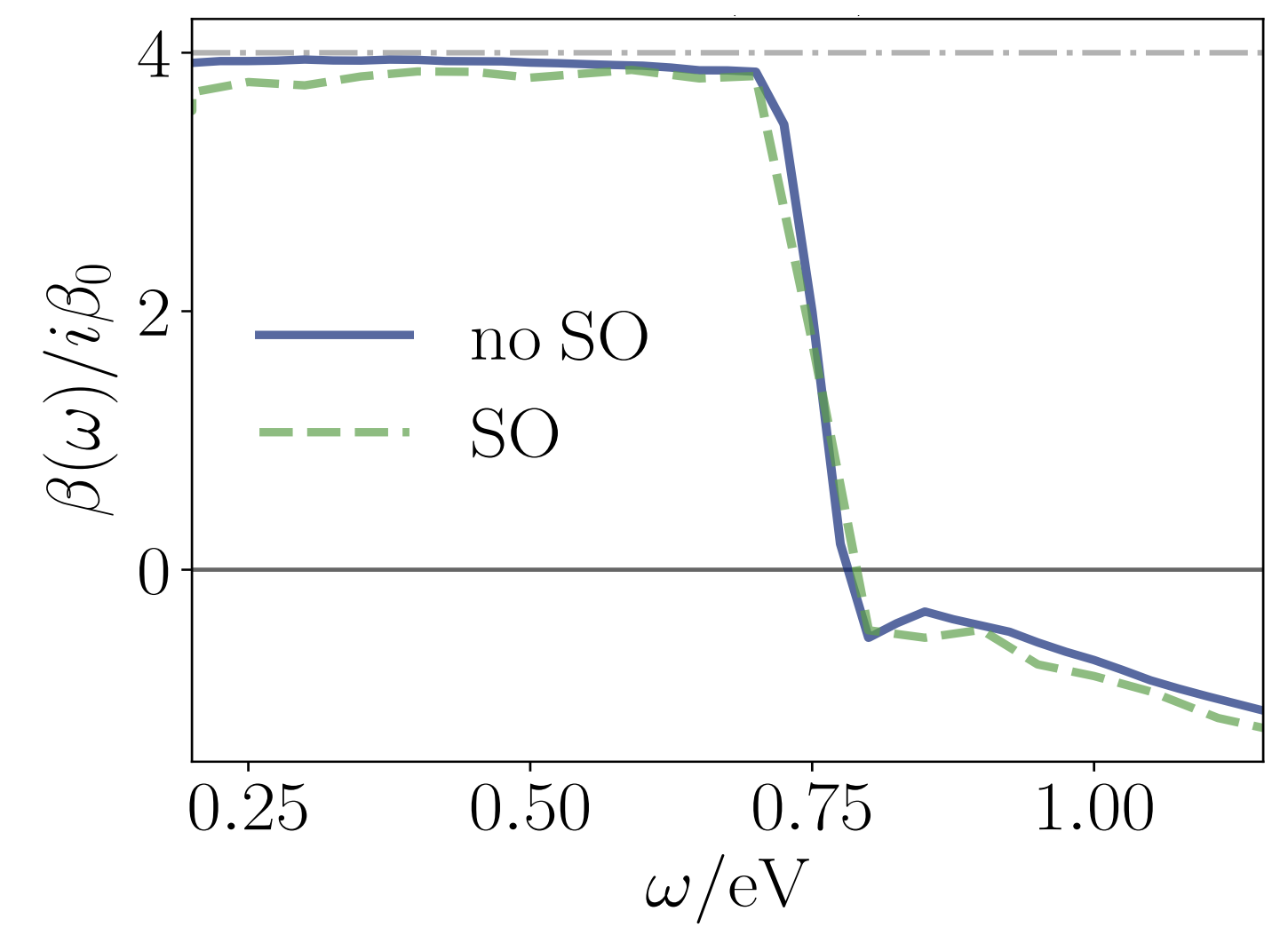
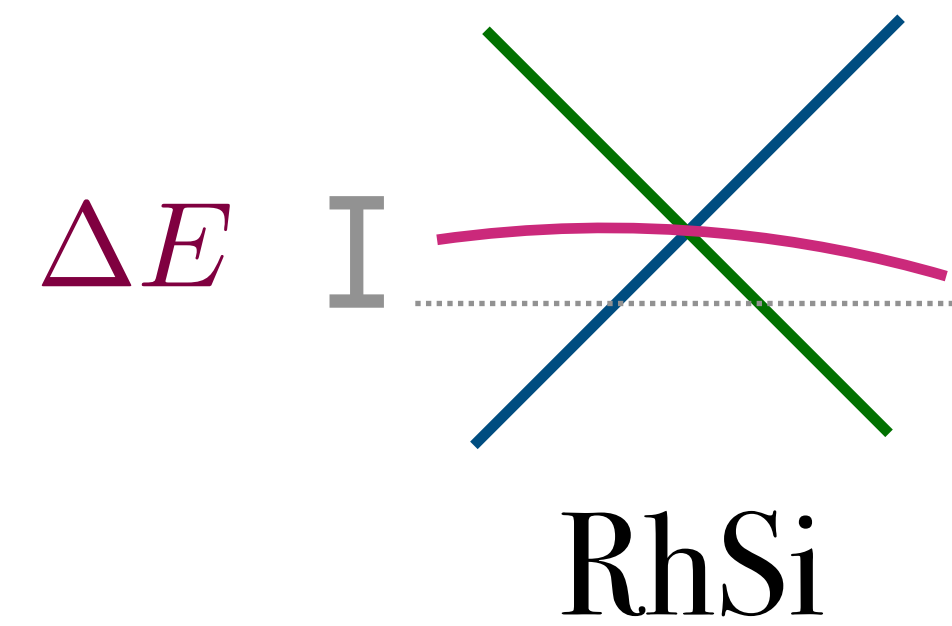
F. Flicker, F. de Juan, T. Morimoto, B. Bradlyn, M. Vergniory, AGG PRB (2018)

F. De Juan et al Nat. Comm (2017)

Reality

Disorder \mathcal{T}

Many bands



F. Flicker, F. de Juan, T. Morimoto, B. Bradlyn, M. Vergniory, AGG PRB (2018)

F. De Juan et al Nat. Comm (2017)

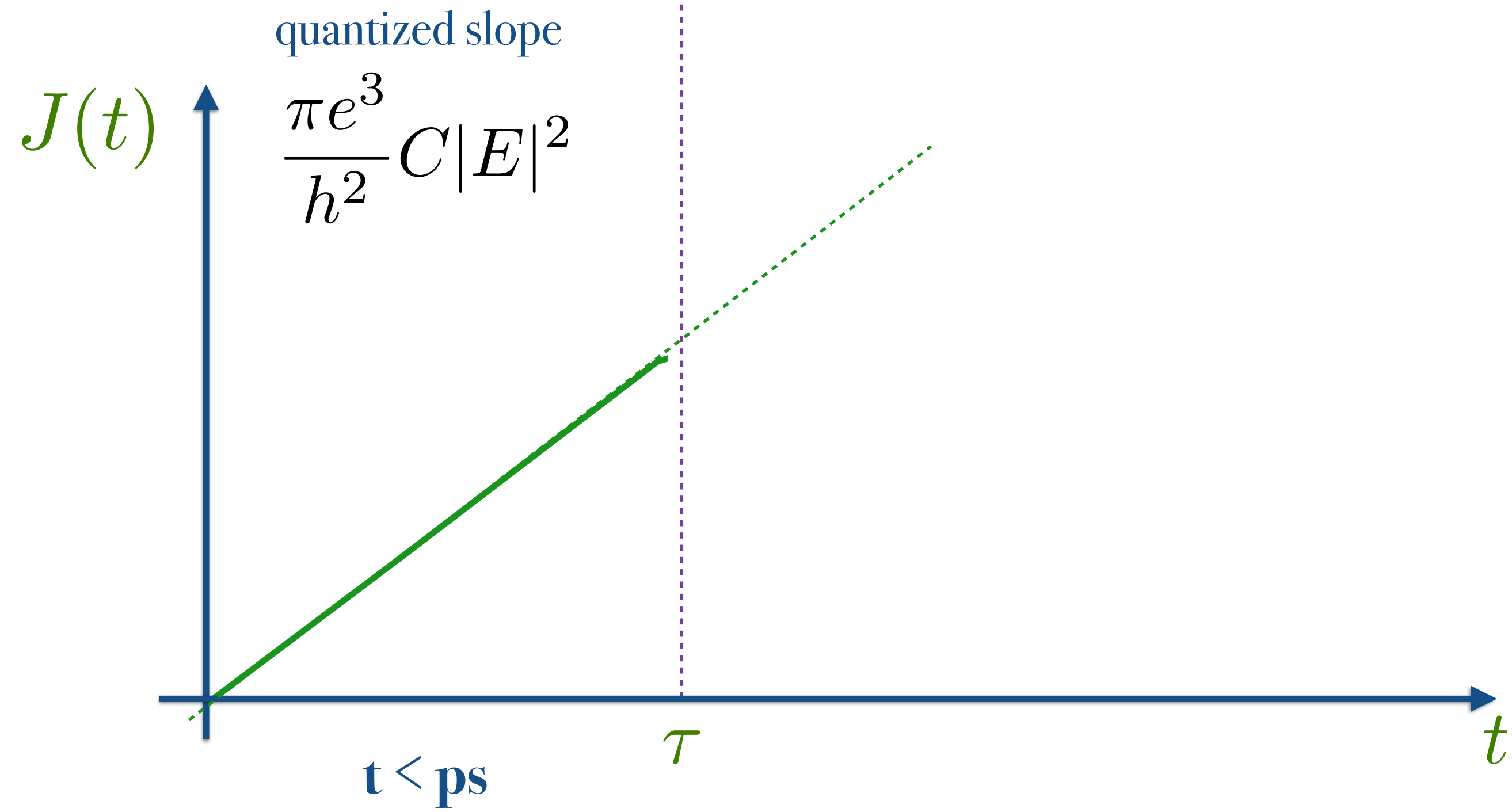
Disorder \mathcal{T}

$$\frac{dj_i}{dt} = \beta_{ij}(\omega)(\mathbf{E} \times \mathbf{E}^*)_j$$



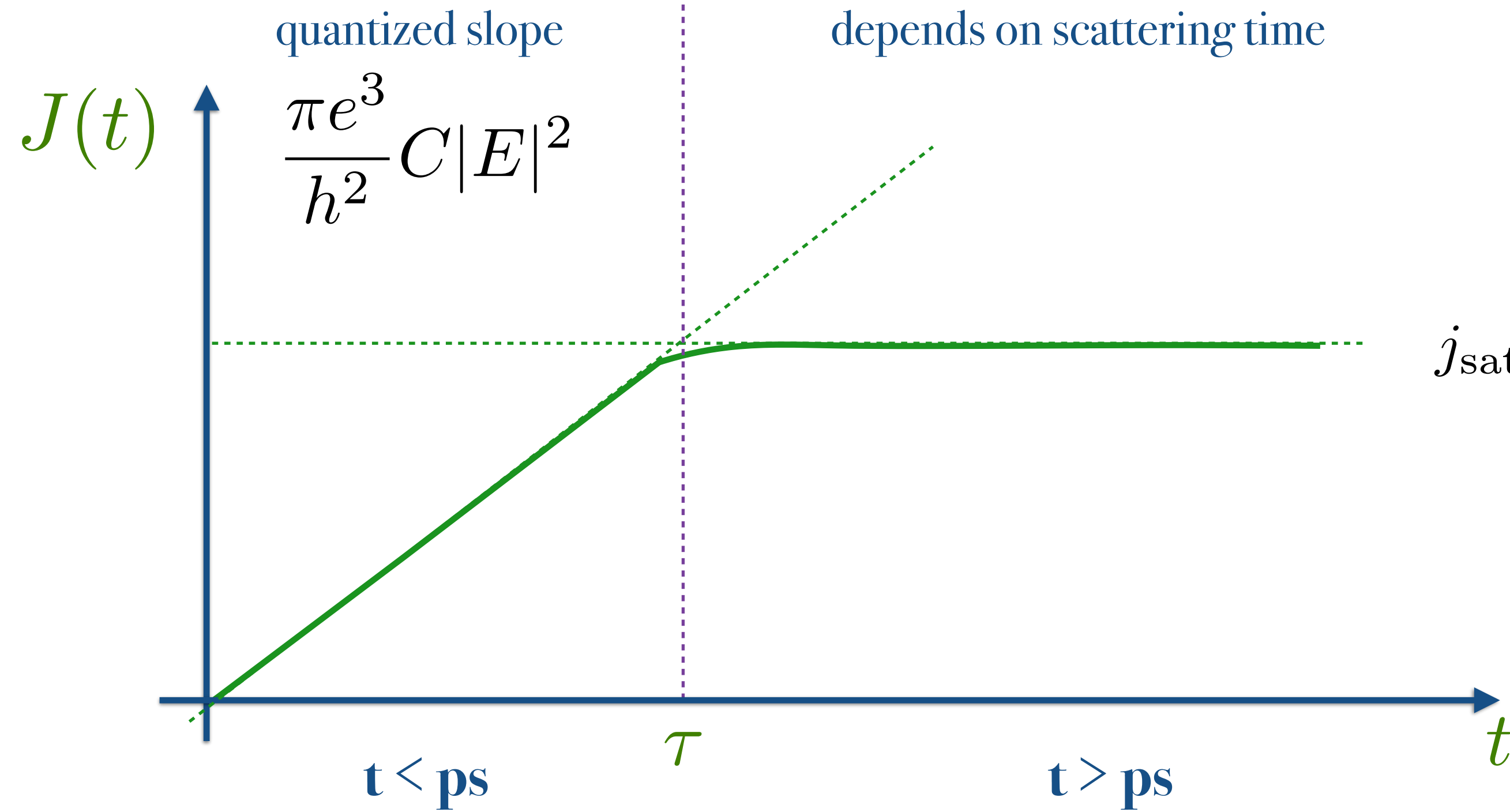
Disorder τ

$$\frac{dj_i}{dt} = \beta_{ij}(\omega)(\mathbf{E} \times \mathbf{E}^*)_j$$



Disorder τ

$$\frac{dj_i}{dt} = \beta_{ij}(\omega)(\mathbf{E} \times \mathbf{E}^*)_j$$



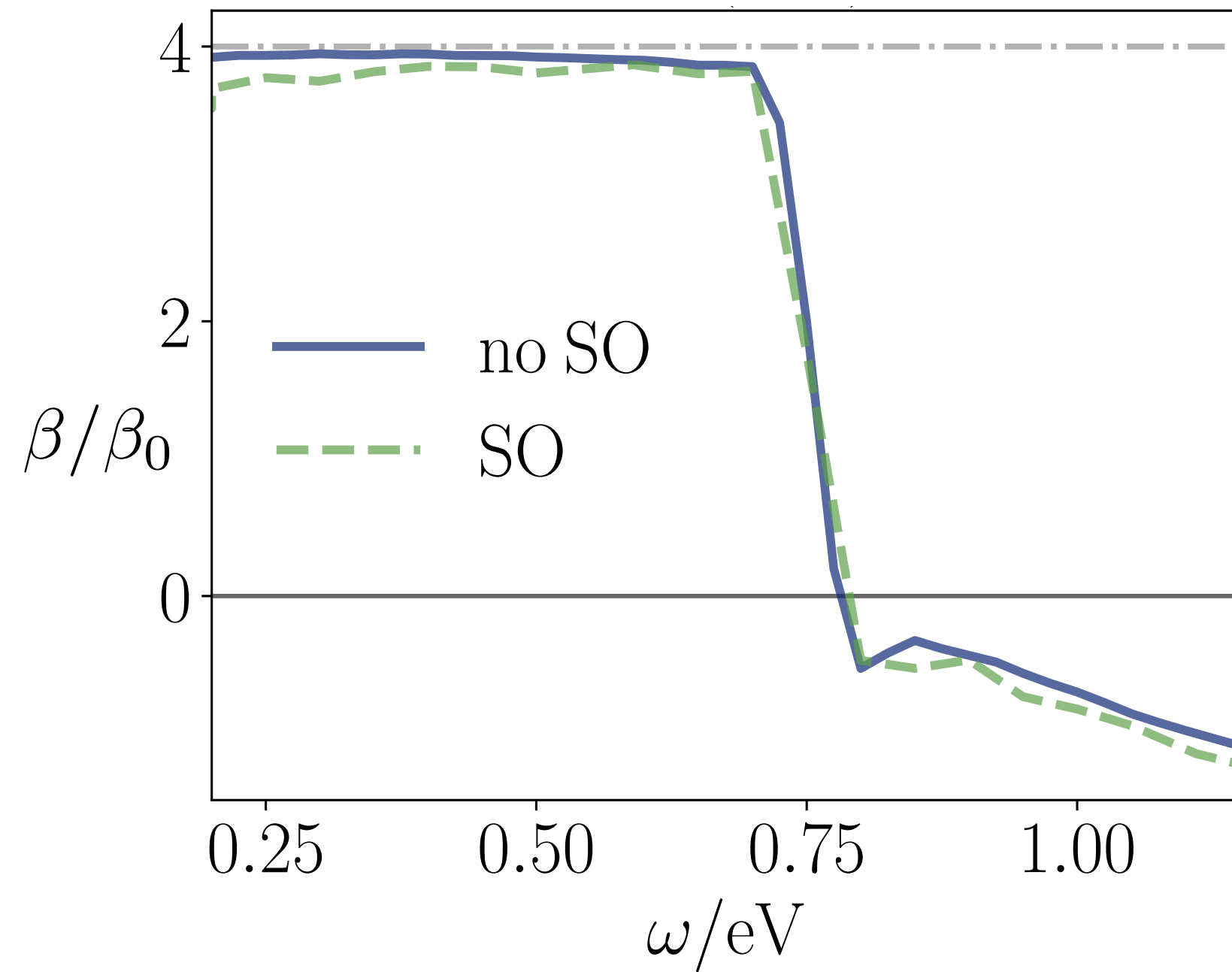
$$j_{\text{sat}} = \tau \frac{\pi e^3}{h^2} C |E|^2$$

E. J. König et al. PRB'17

Quantized non-linear response in RhSi

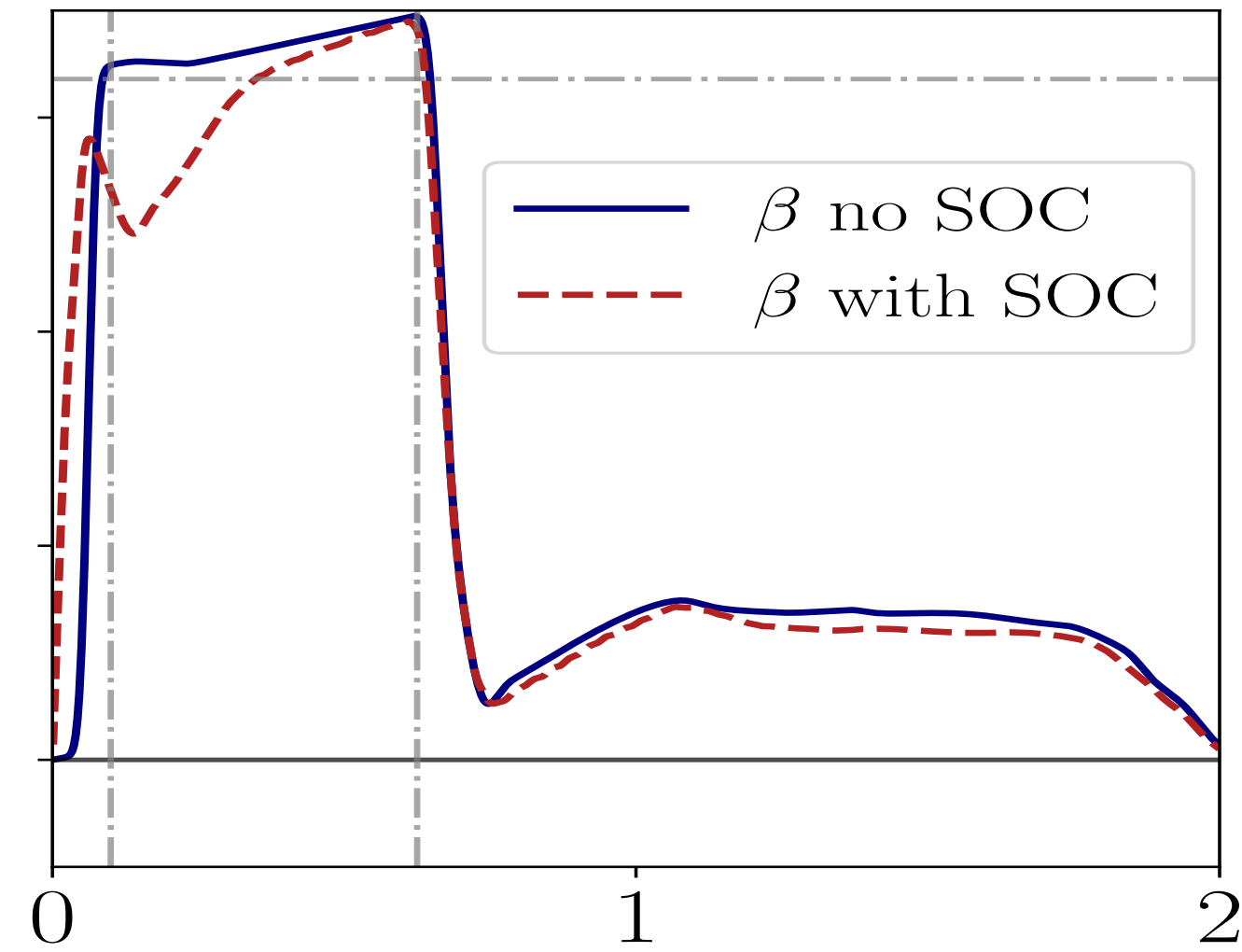
$$j_{\text{sat}} = \tau \frac{\pi e^3}{h^2} C |E|^2$$

Tight binding



F. Flicker et. al. PRB (2018)

DFT



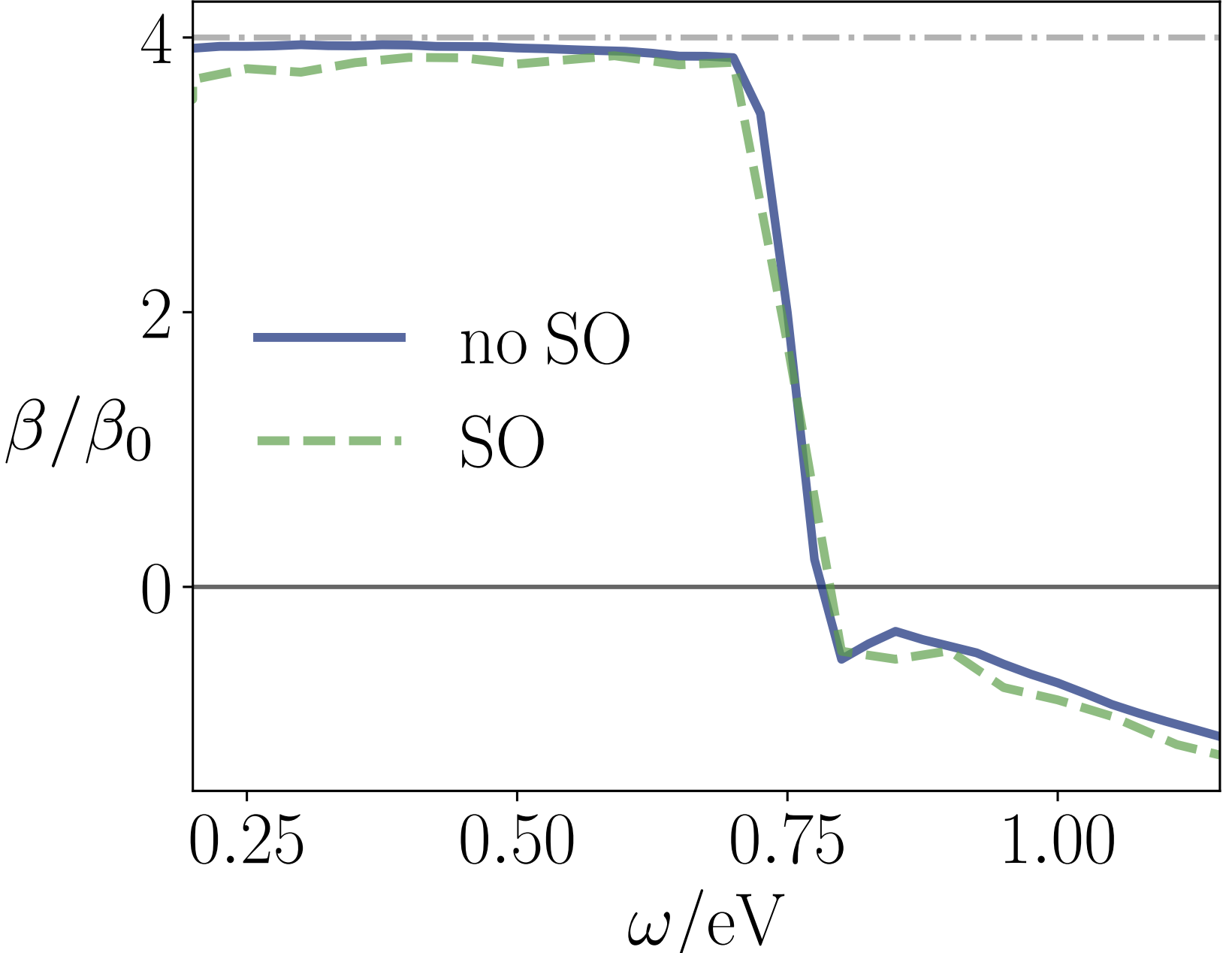
F. De Juan, Y. Zhang, et. al. arXiv: 1907.02537



Quantized non-linear response in RhSi

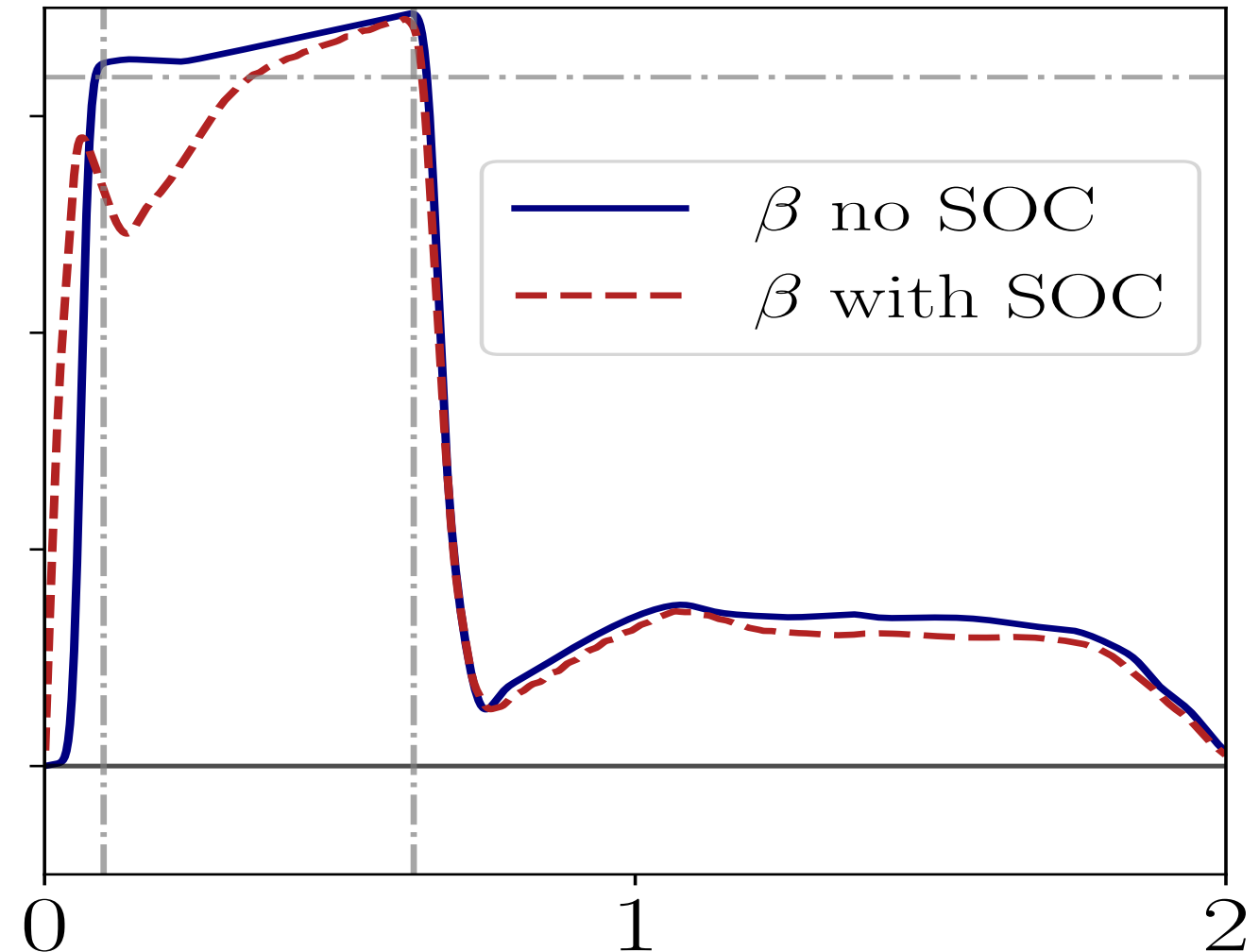
$$j_{\text{sat}} = \tau \frac{\pi e^3}{h^2} C |E|^2$$

Tight binding



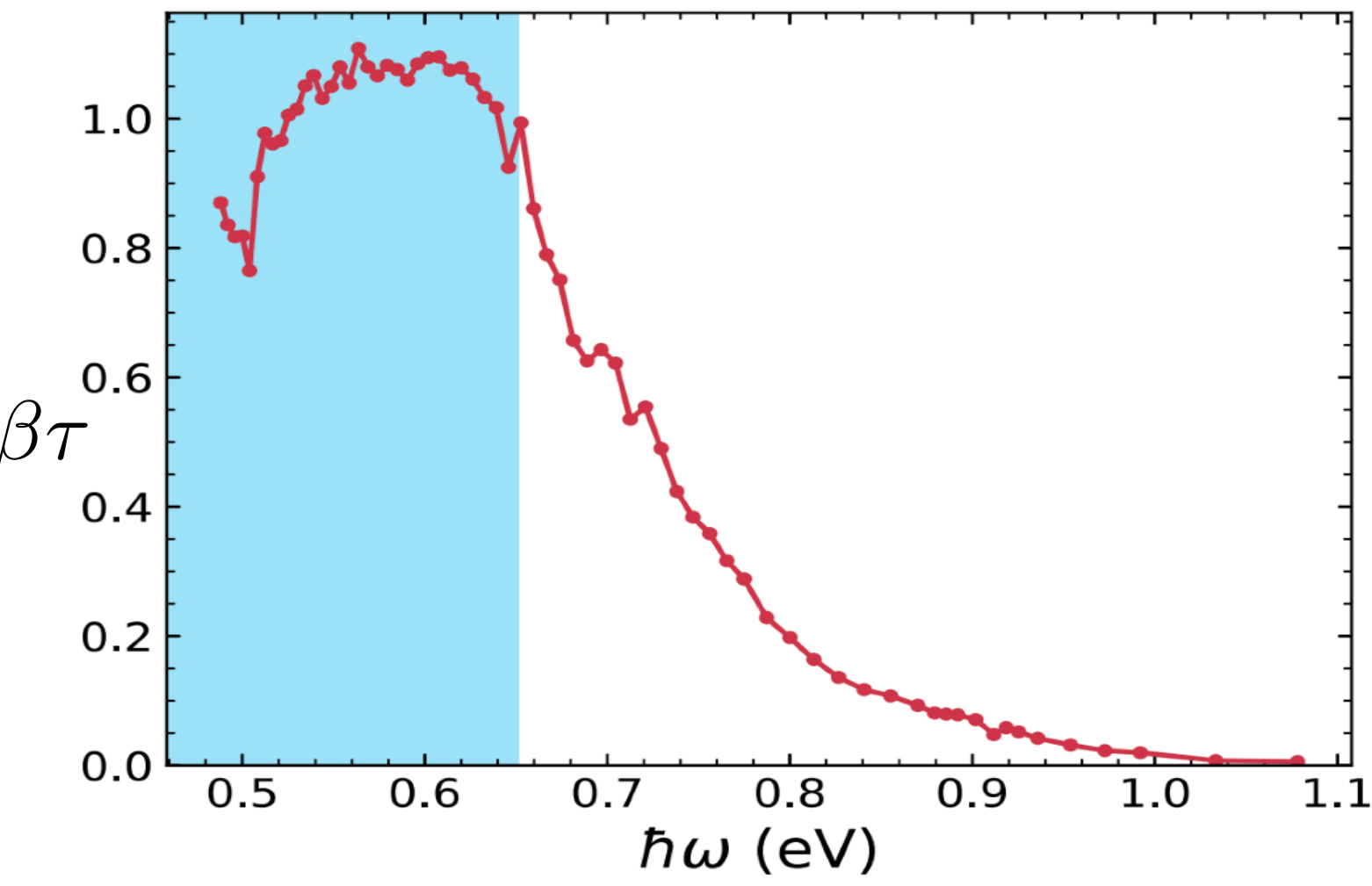
F. Flicker et. al. PRB (2018)

DFT



F. De Juan, Y. Zhang, et. al. arXiv: 1907.02537

Experiment

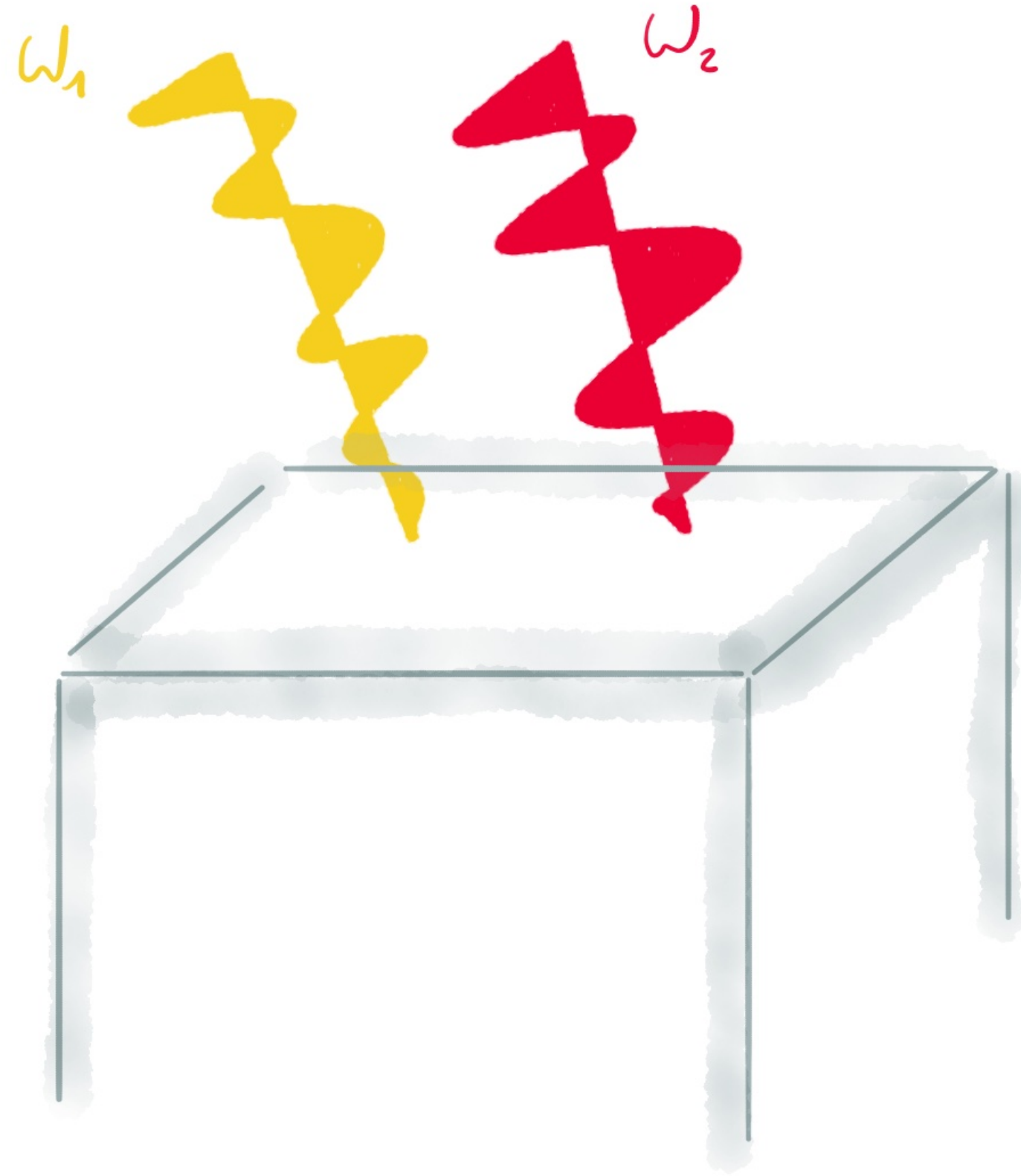


D. Rees. arXiv: 1902.03230



An alternative: difference frequency generation

signal that oscillates with the frequency difference $\Delta\omega = \omega_1 - \omega_2$



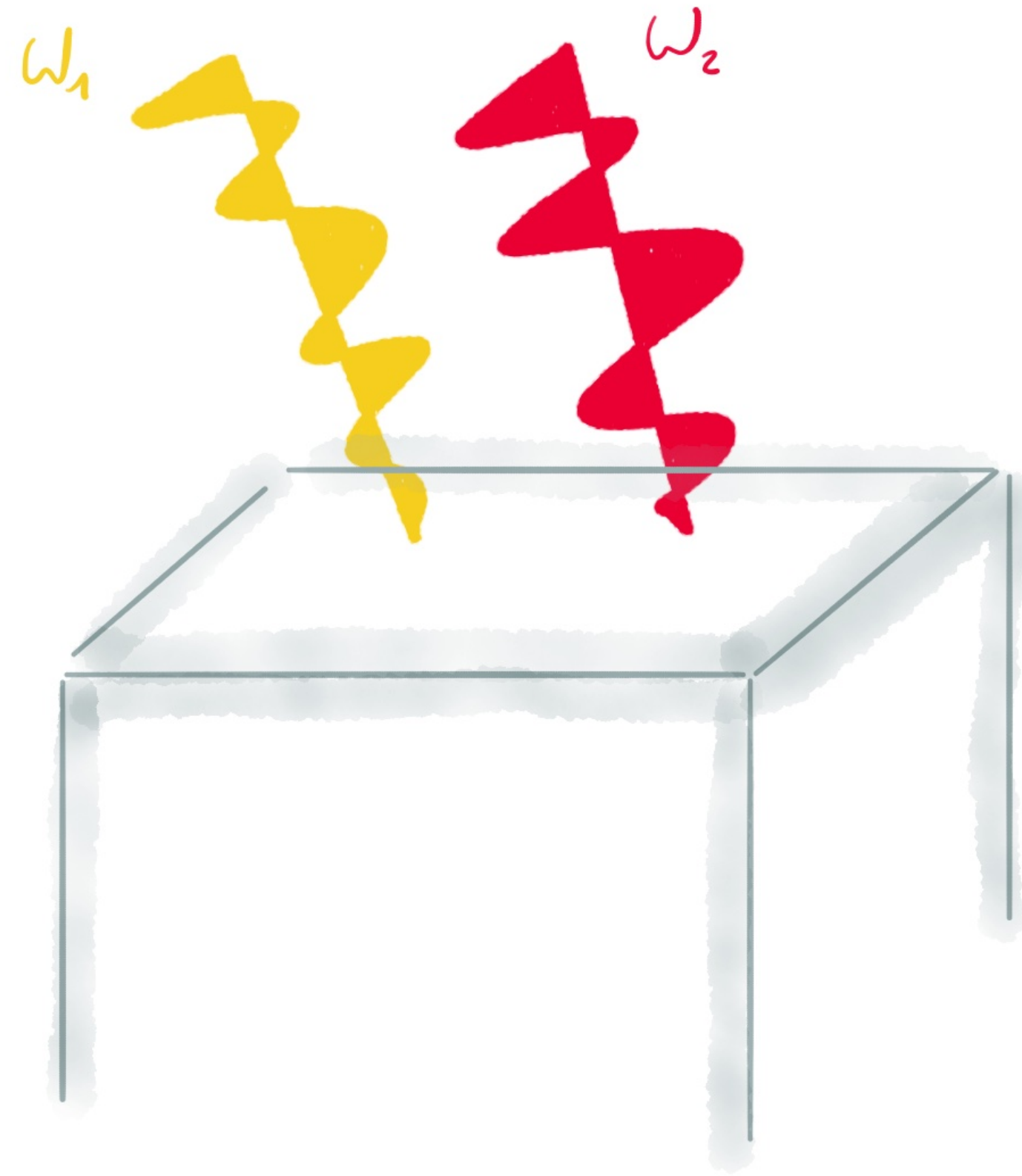
Genkin & Mednis , Sov. Phys. JETP **27**, 609 (1968)

Belinicher, Sov. Phys. Semicond. **20**, 558 (1986)

Pershan, Phys. Rev. **143**, 574 (1965)

An alternative: difference frequency generation

signal that oscillates with the frequency difference $\Delta\omega = \omega_1 - \omega_2$



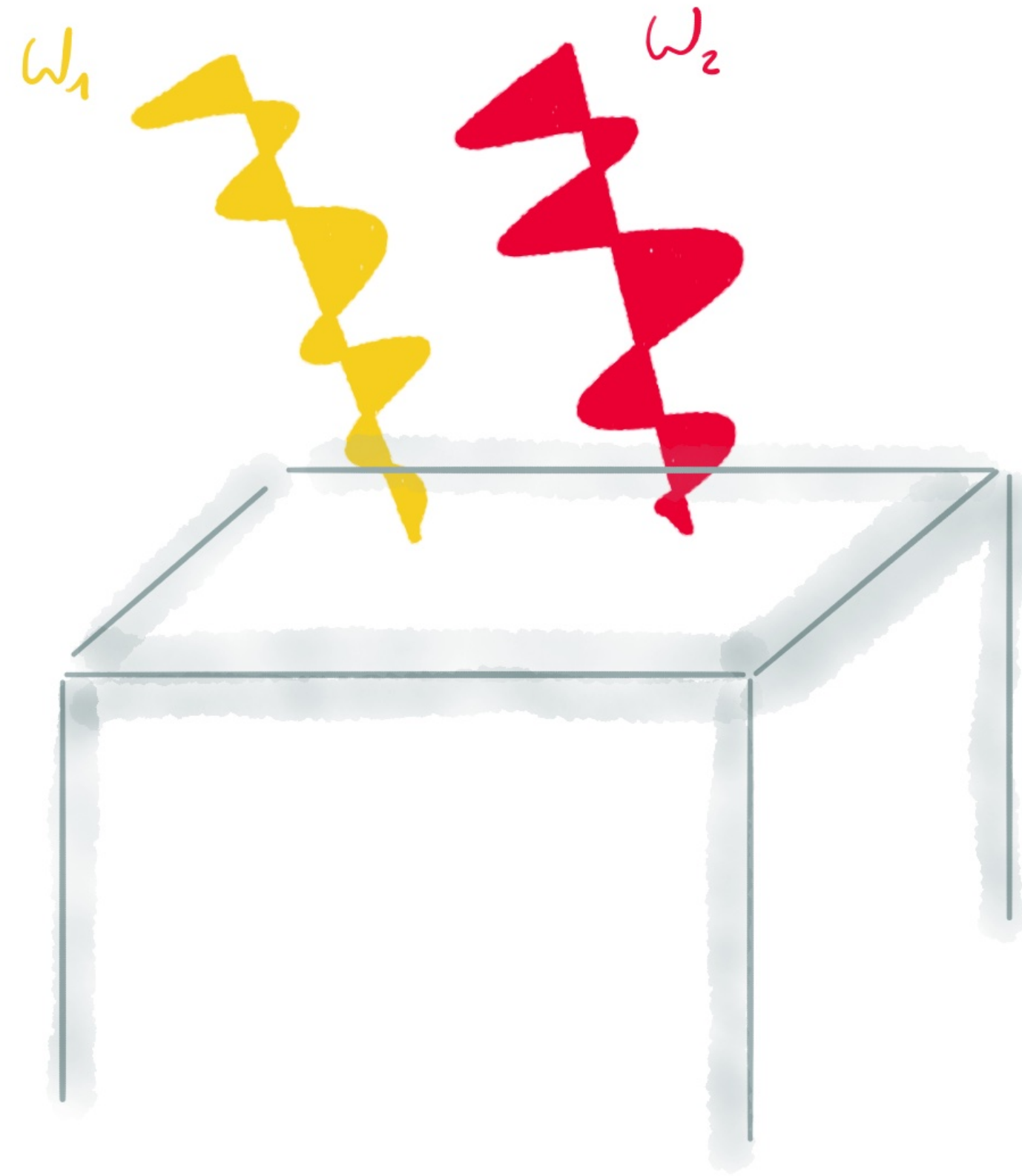
Genkin & Mednis , Sov. Phys. JETP **27**, 609 (1968)

Belinicher, Sov. Phys. Semicond. **20**, 558 (1986)

Pershan, Phys. Rev. **143**, 574 (1965)

An alternative: difference frequency generation

signal that oscillates with the frequency difference $\Delta\omega = \omega_1 - \omega_2$



if: $\omega \gg \Delta\omega \gg \tau^{-1}$ with $\omega = \omega_1 + \omega_2$

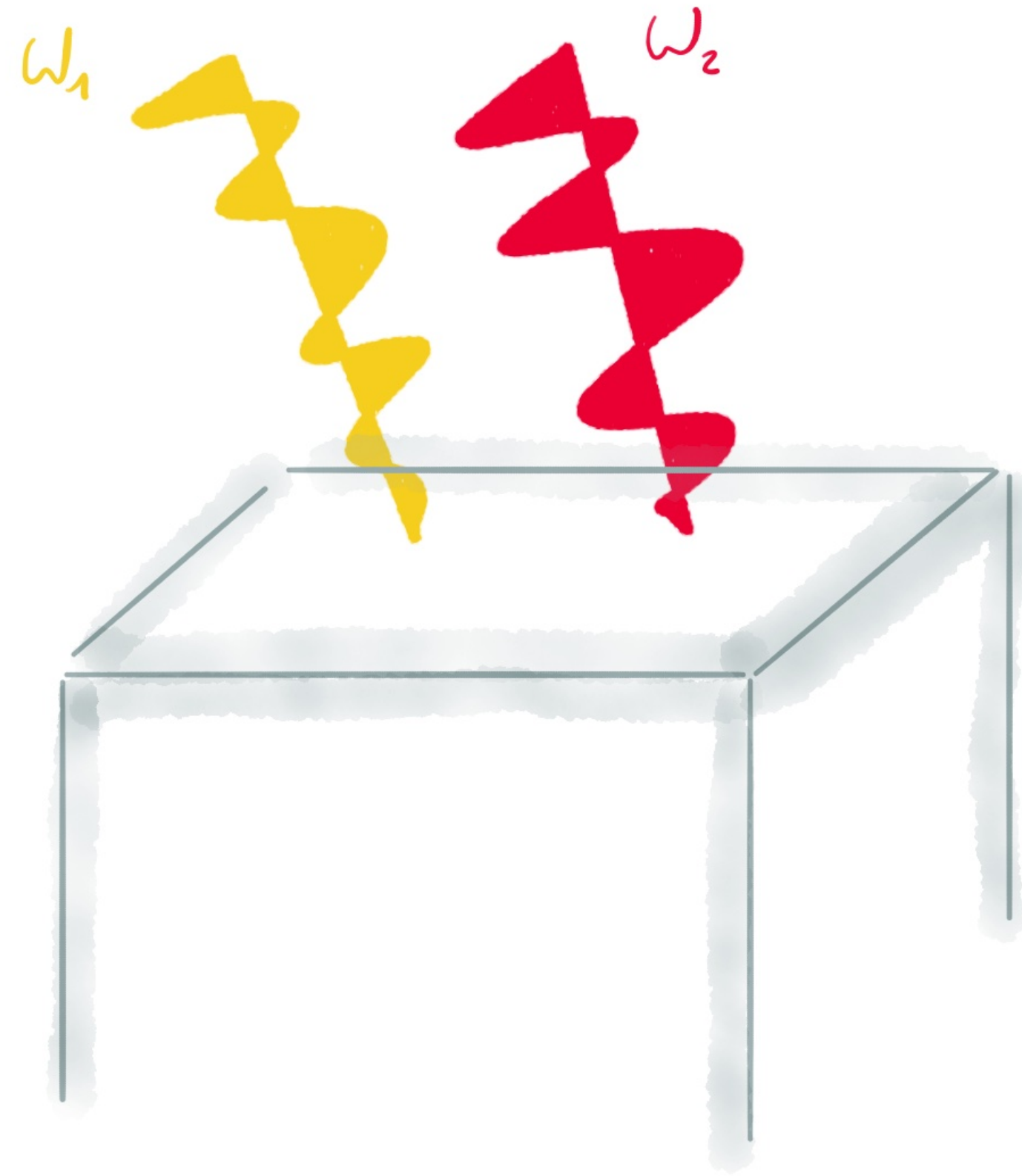
Genkin & Mednis , Sov. Phys. JETP **27**, 609 (1968)

Belinicher, Sov. Phys. Semicond. **20**, 558 (1986)

Pershan, Phys. Rev. **143**, 574 (1965)

An alternative: difference frequency generation

signal that oscillates with the frequency difference $\Delta\omega = \omega_1 - \omega_2$



if: $\omega \gg \Delta\omega \gg \tau^{-1}$ with $\omega = \omega_1 + \omega_2$

$$J^a(t) = 4 \left[\frac{\sin(\Delta\omega t)}{\Delta\omega} \beta^{ab}(\omega) + \cos(\Delta\omega t) \gamma^{ab}(\omega) \right] [\vec{E} \times \vec{E}^*]^b$$

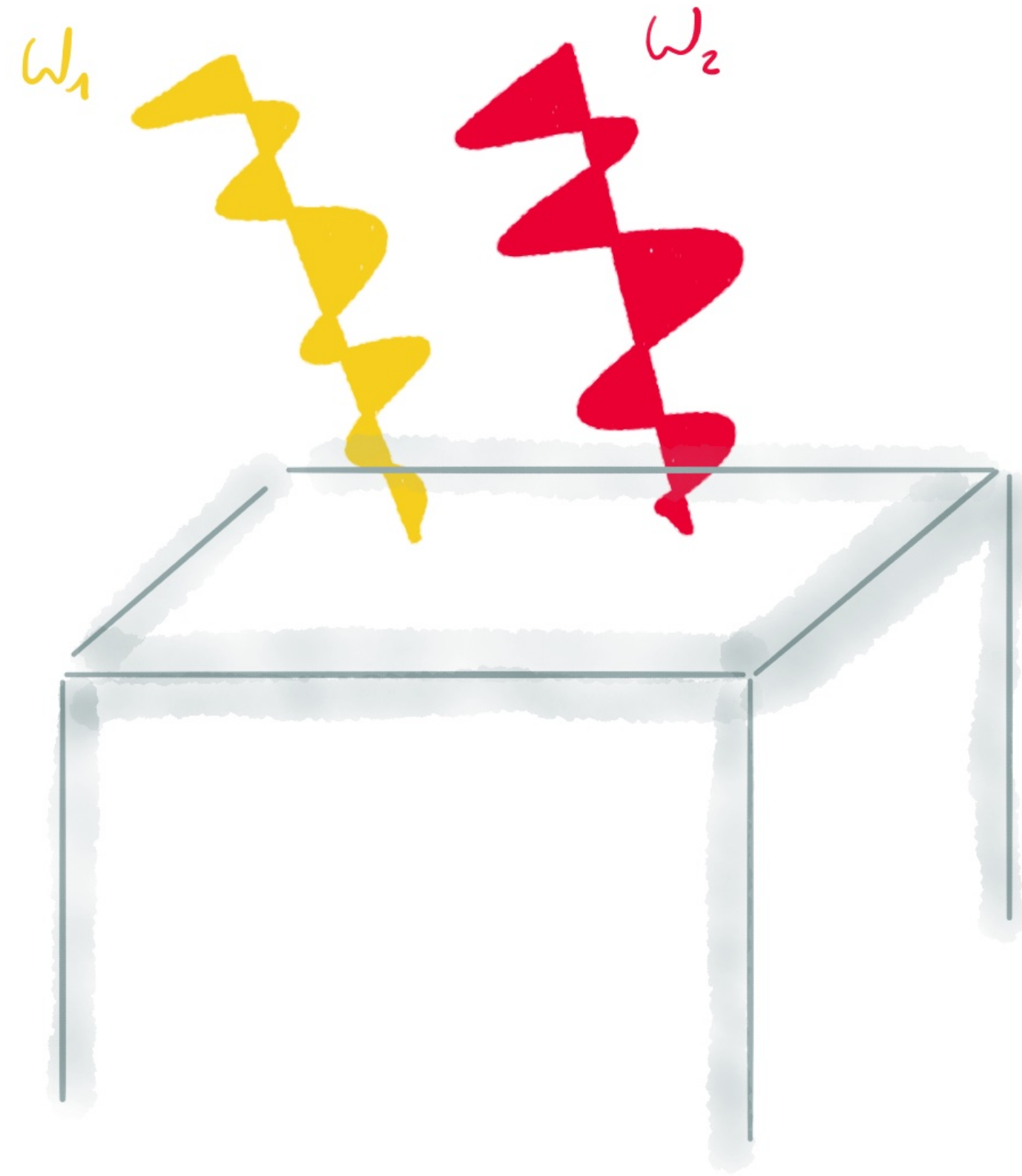
Genkin & Mednis , Sov. Phys. JETP **27**, 609 (1968)

Belinicher, Sov. Phys. Semicond. **20**, 558 (1986)

Pershan, Phys. Rev. **143**, 574 (1965)

An alternative: difference frequency generation

signal that oscillates with the frequency difference $\Delta\omega = \omega_1 - \omega_2$



if: $\omega \gg \Delta\omega \gg \tau^{-1}$ with $\omega = \omega_1 + \omega_2$

$$J^a(t) = 4 \left[\frac{\sin(\Delta\omega t)}{\Delta\omega} \beta^{ab}(\omega) + \cos(\Delta\omega t) \gamma^{ab}(\omega) \right] [\vec{E} \times \vec{E}^*]^b$$

$\beta^{ab}(\omega)$
CPGE

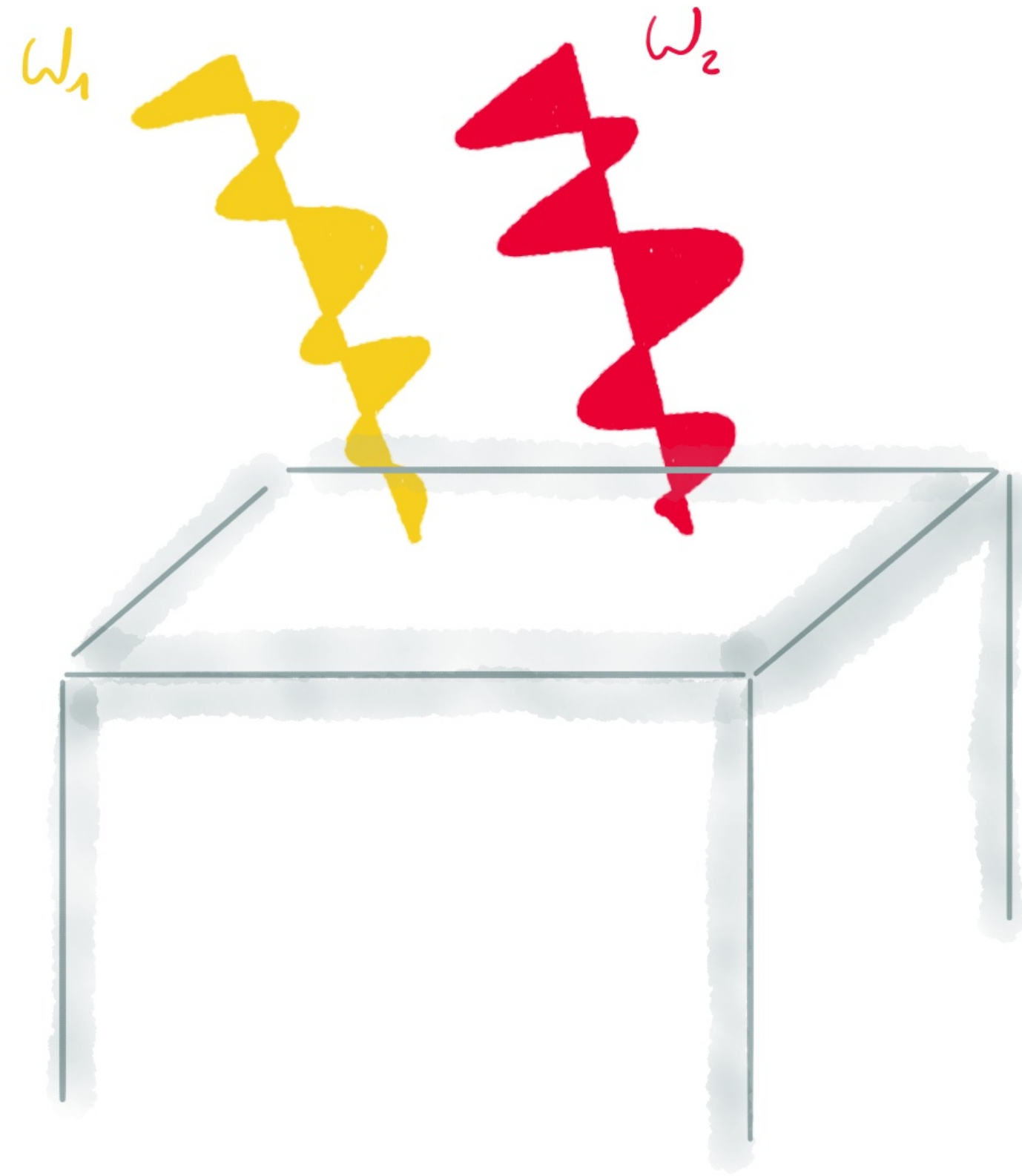
Genkin & Mednis , Sov. Phys. JETP **27**, 609 (1968)

Belinicher, Sov. Phys. Semicond. **20**, 558 (1986)

Pershan, Phys. Rev. **143**, 574 (1965)

An alternative: difference frequency generation

signal that oscillates with the frequency difference $\Delta\omega = \omega_1 - \omega_2$



if: $\omega \gg \Delta\omega \gg \tau^{-1}$ with $\omega = \omega_1 + \omega_2$

$$J^a(t) = 4 \left[\frac{\sin(\Delta\omega t)}{\Delta\omega} \beta^{ab}(\omega) + \cos(\Delta\omega t) \gamma^{ab}(\omega) \right] [\vec{E} \times \vec{E}^*]^b$$

CPGE Free carrier

Genkin & Mednis , Sov. Phys. JETP **27**, 609 (1968)

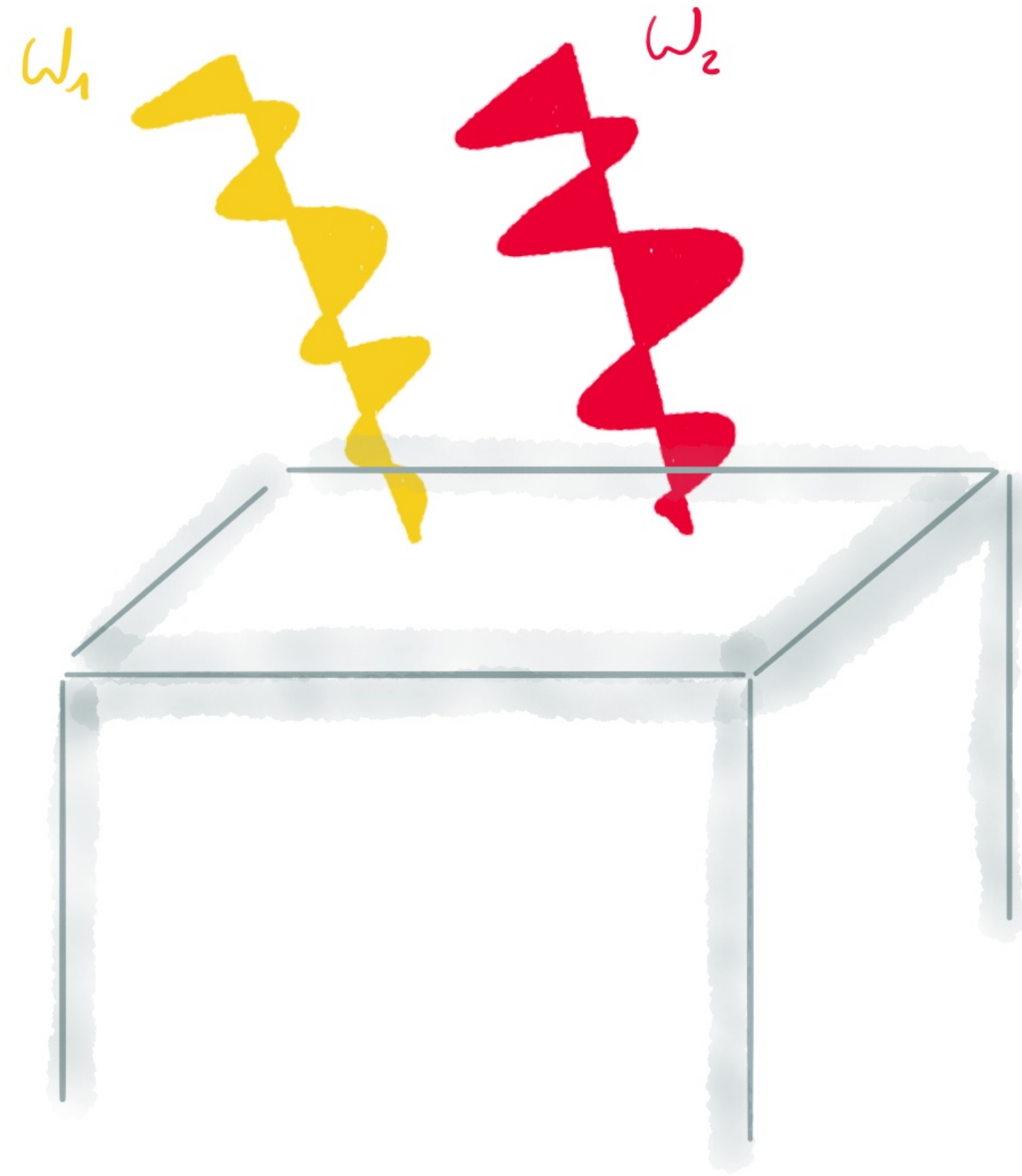
Belinicher, Sov. Phys. Semicond. **20**, 558 (1986)

Pershan, Phys. Rev. **143**, 574 (1965)

An alternative: difference frequency generation

signal that oscillates with the frequency difference

$$\Delta\omega = \omega_1 - \omega_2$$



if: $\omega \gg \Delta\omega \gg \tau^{-1}$ with $\omega = \omega_1 + \omega_2$

$$J^a(t) = 4 \left[\frac{\sin(\Delta\omega t)}{\Delta\omega} \beta^{ab}(\omega) + \cos(\Delta\omega t) \gamma^{ab}(\omega) \right] [\vec{E} \times \vec{E}^*]^b$$

CPGE

Free carrier

k derivative of the integrand of the reactive part of the linear conductivity

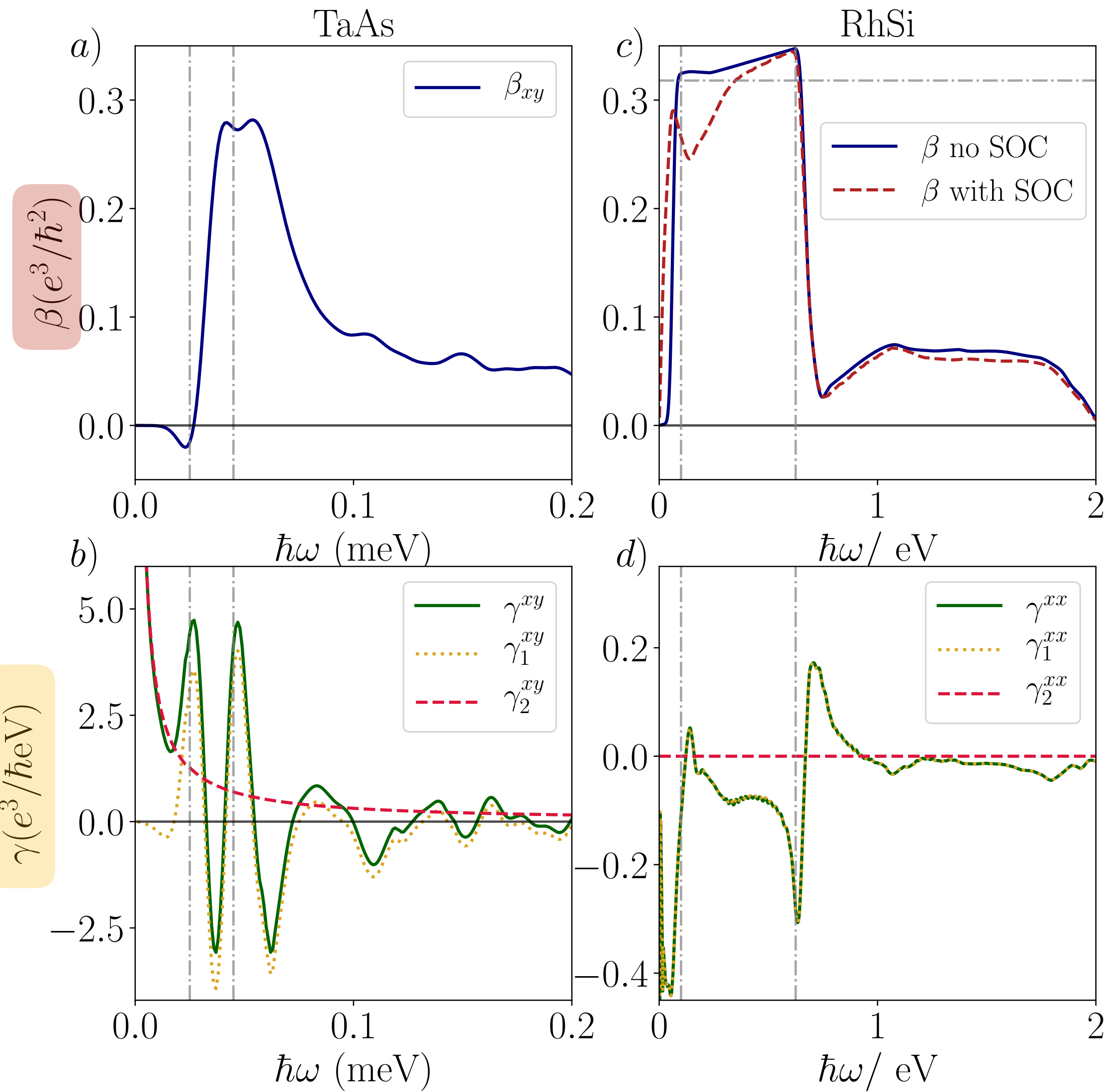
$$\sigma_{\text{rea}}^{ab} = \sigma^{ab} - (\sigma^{ba})^*$$

Genkin & Mednis, Sov. Phys. JETP **27**, 609 (1968)

Belinicher, Sov. Phys. Semicond. **20**, 558 (1986)

Pershan, Phys. Rev. **143**, 574 (1965)

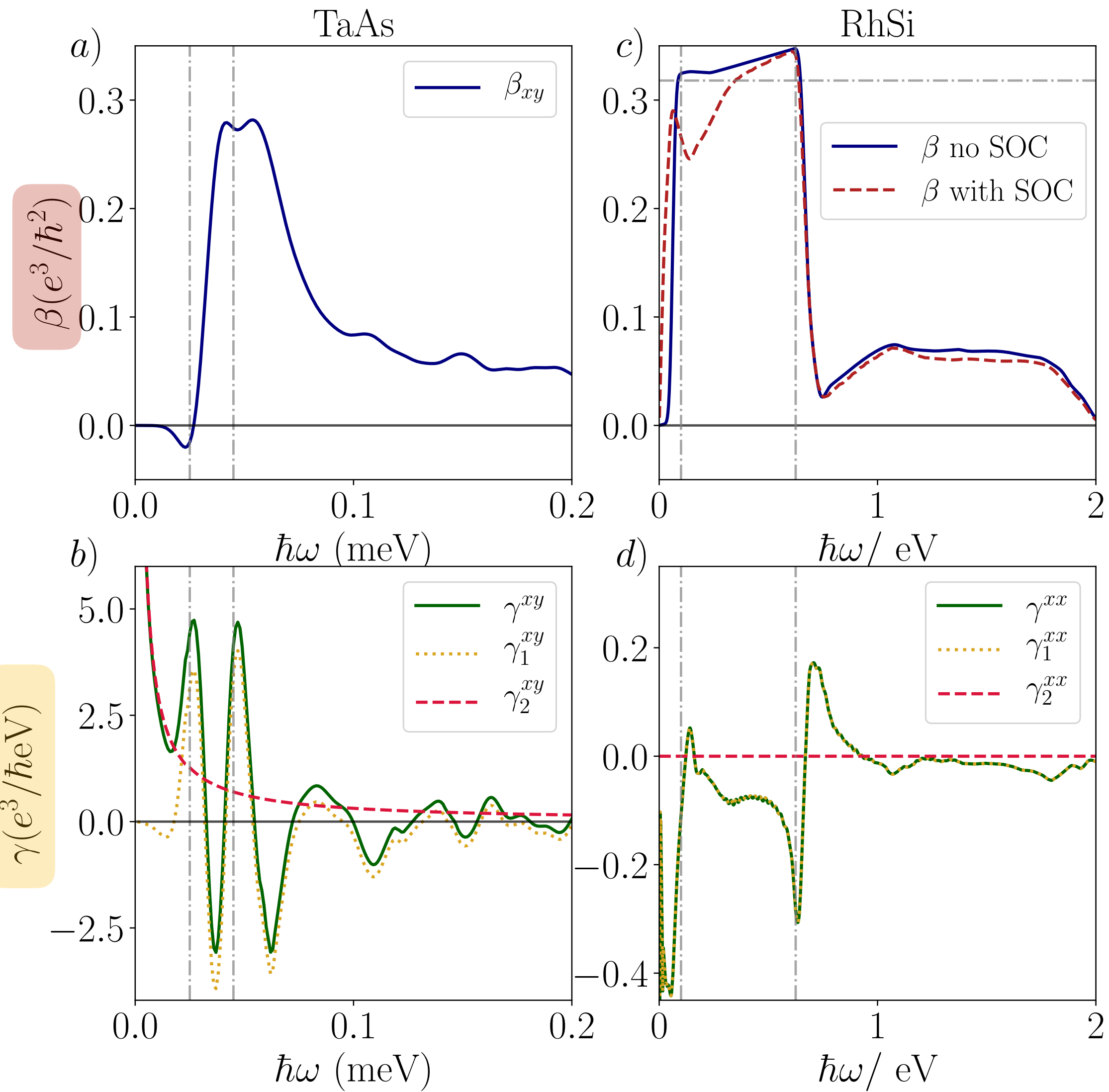
An alternative: difference frequency generation



$$J^a(t) = 4 \left[\frac{\sin(\Delta\omega t)}{\Delta\omega} \beta^{ab}(\omega) + \cos(\Delta\omega t) \gamma^{ab}(\omega) \right] [\vec{E} \times \vec{E}^*]^b$$

CPGE
Free carrier

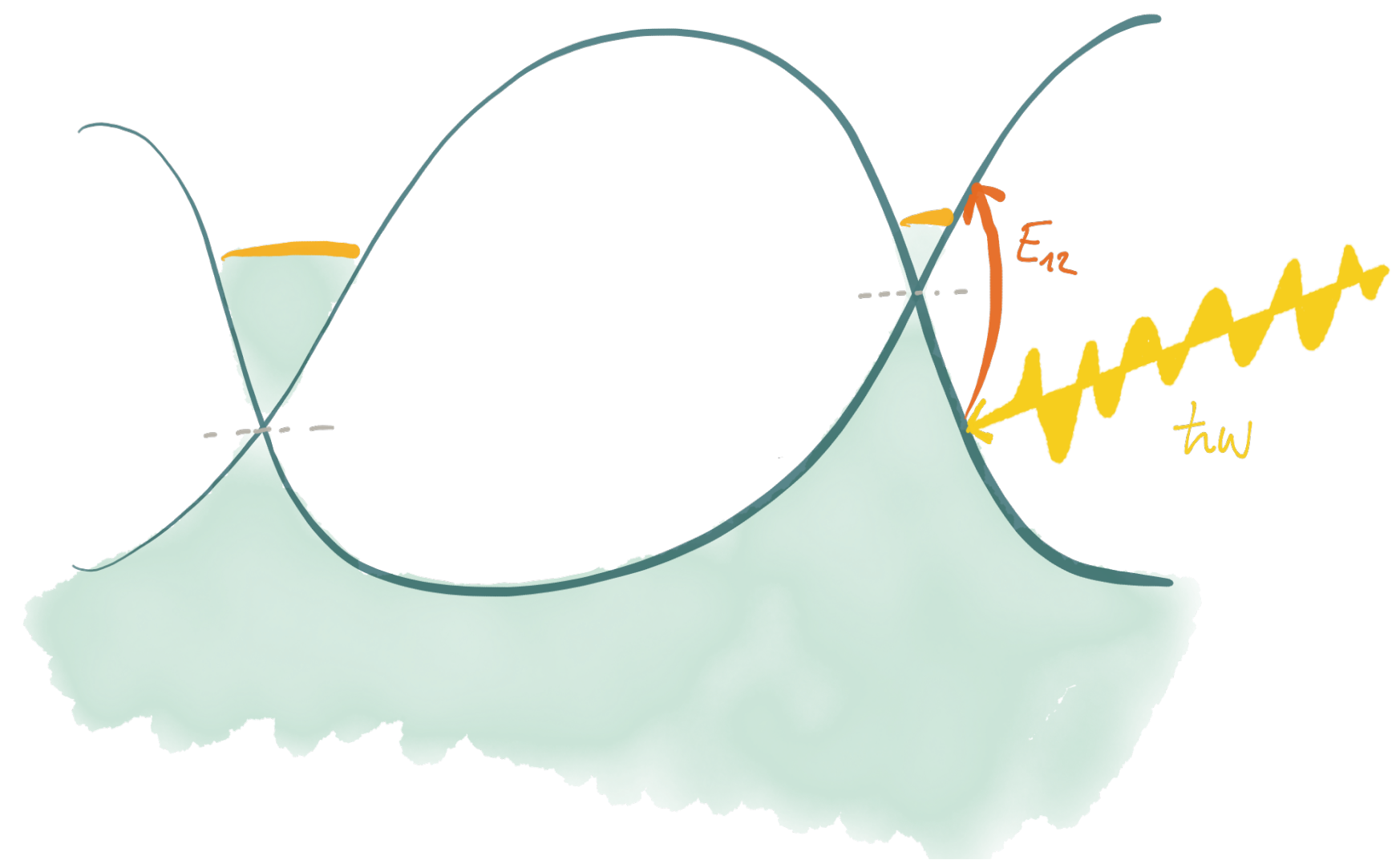
An alternative: difference frequency generation



$$J^a(t) = 4 \left[\frac{\sin(\Delta\omega t)}{\Delta\omega} \beta^{ab}(\omega) + \cos(\Delta\omega t) \gamma^{ab}(\omega) \right] [\vec{E} \times \vec{E}^*]^b$$

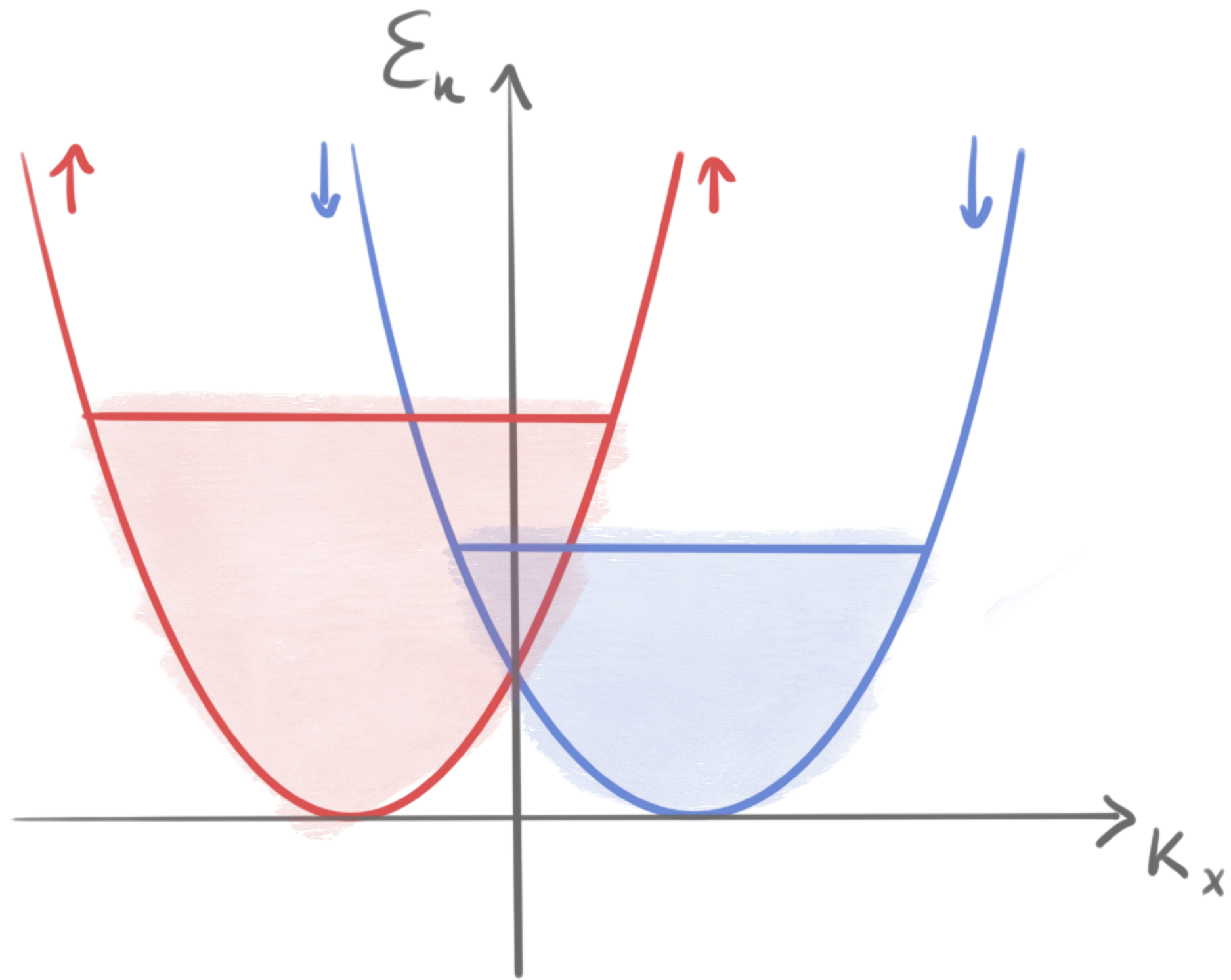
CPGE
Free carrier

Divergences and plateaus appear at node activation frequencies



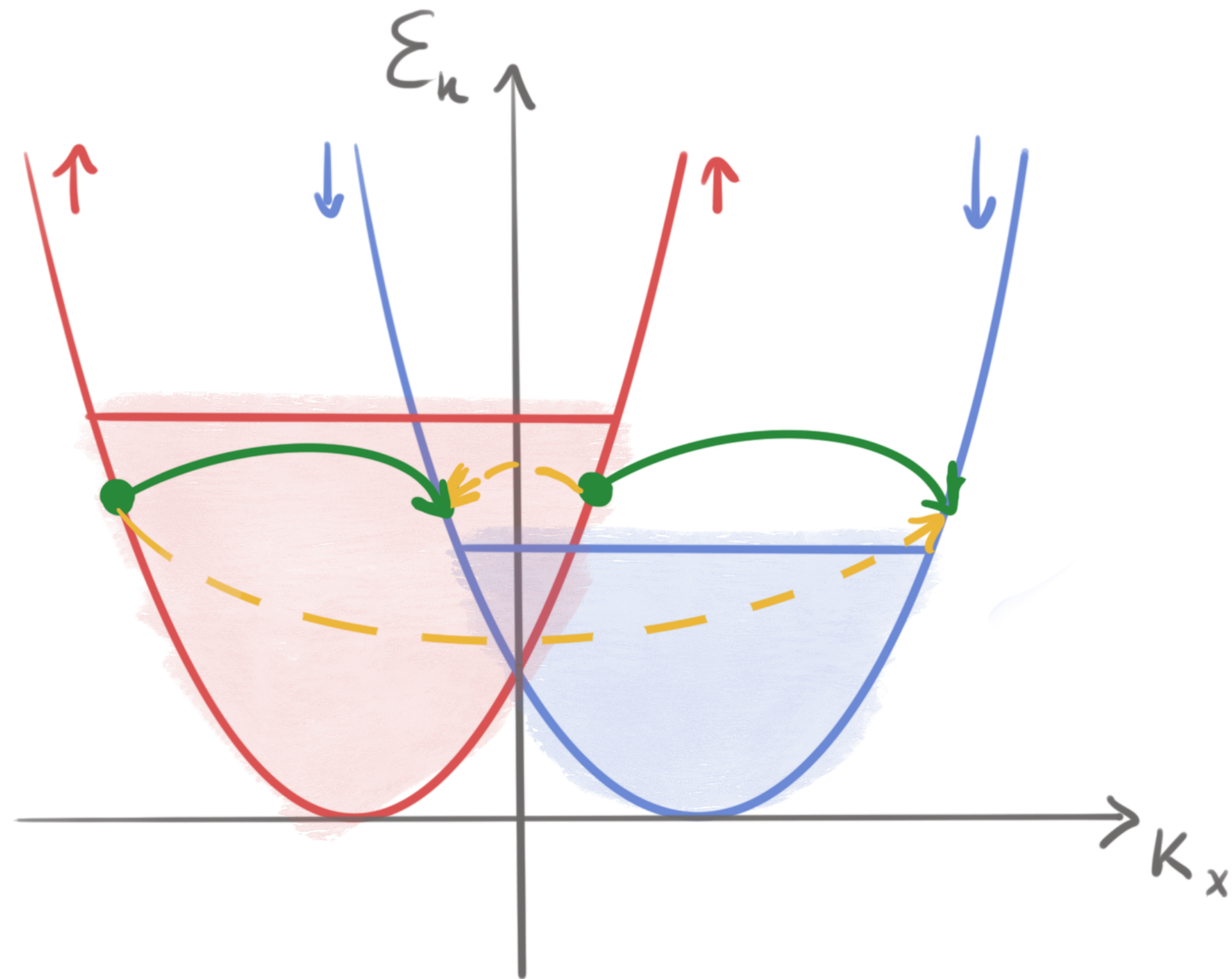
Food for spin-thought: Spin-galvanic effect

Asymmetric spin populations and scattering induces electric current



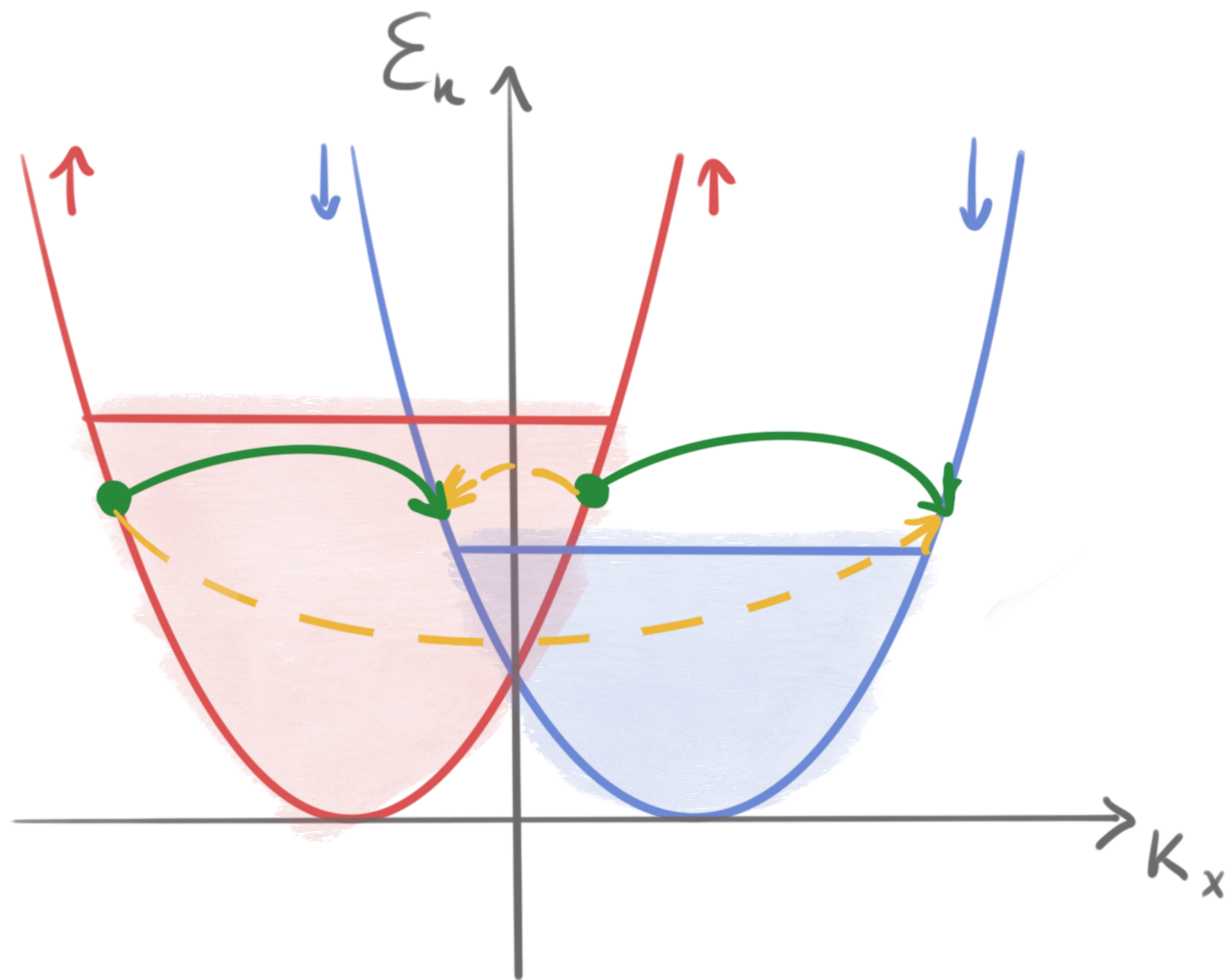
Food for spin-thought: Spin-galvanic effect

Asymmetric spin populations and scattering induces electric current



Food for spin-thought: Spin-galvanic effect

Asymmetric spin populations and scattering induces electric current



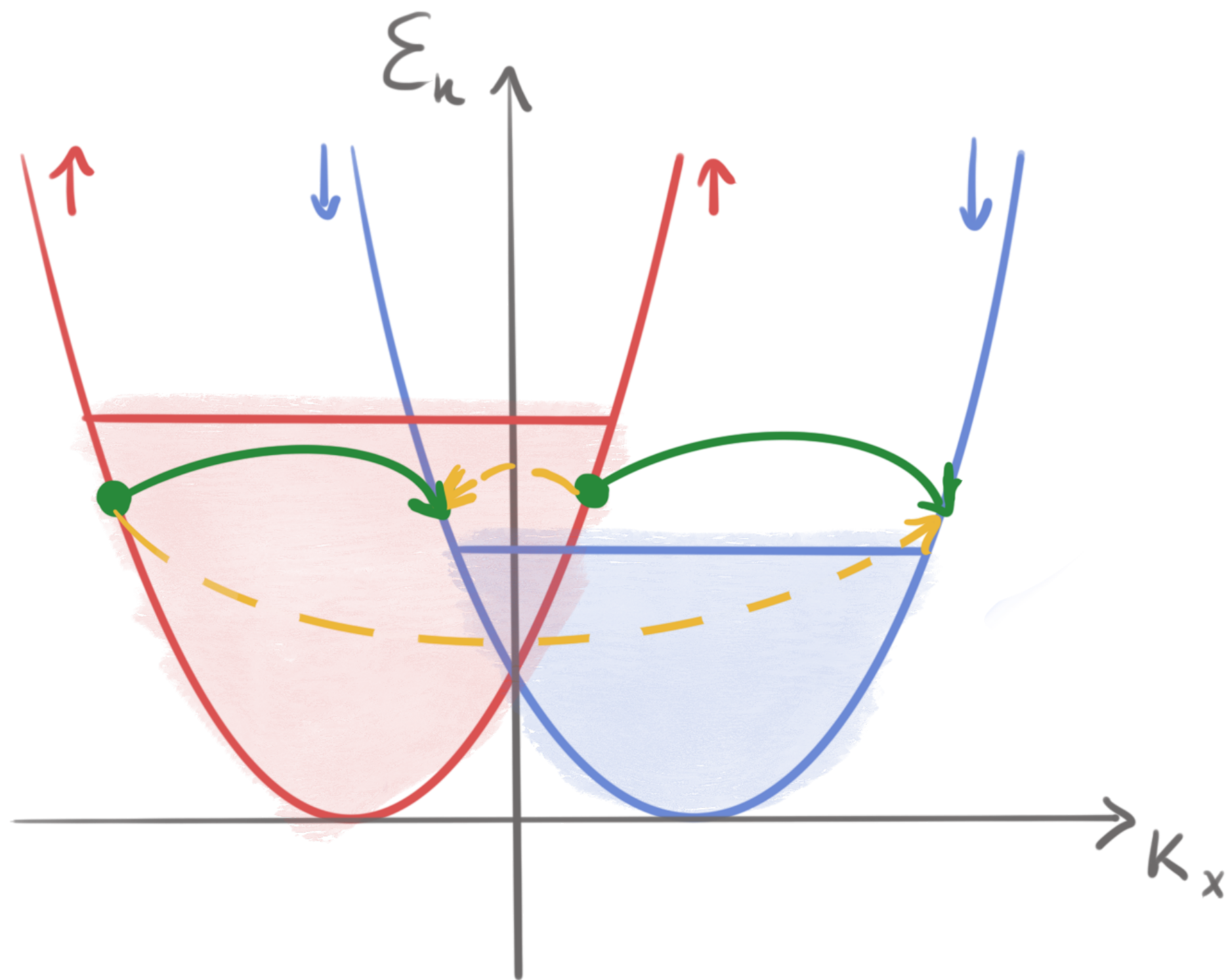
$$\dot{J}_i = \tau_s Q_{ij} S_j$$

electron spin

allowed in gyrotropic point groups

Food for spin-thought: Spin-galvanic effect

Asymmetric spin populations and scattering induces electric current



$$\dot{J}_i = \tau_s Q_{ij} S_j$$

electron spin

allowed in gyrotropic point groups

photon angular momentum

$$\dot{J}_i = \tau \beta_{ij} (\mathbf{E} \times \mathbf{E}^*)_j$$

Quantization

...not so often experimentally observed

$$j_i = \sigma_{ij} E_j + \sigma_{ijl} E_j E_l + \dots$$

Quantum Hall effect

von Klitzing, Tsui, Stormer (80's)

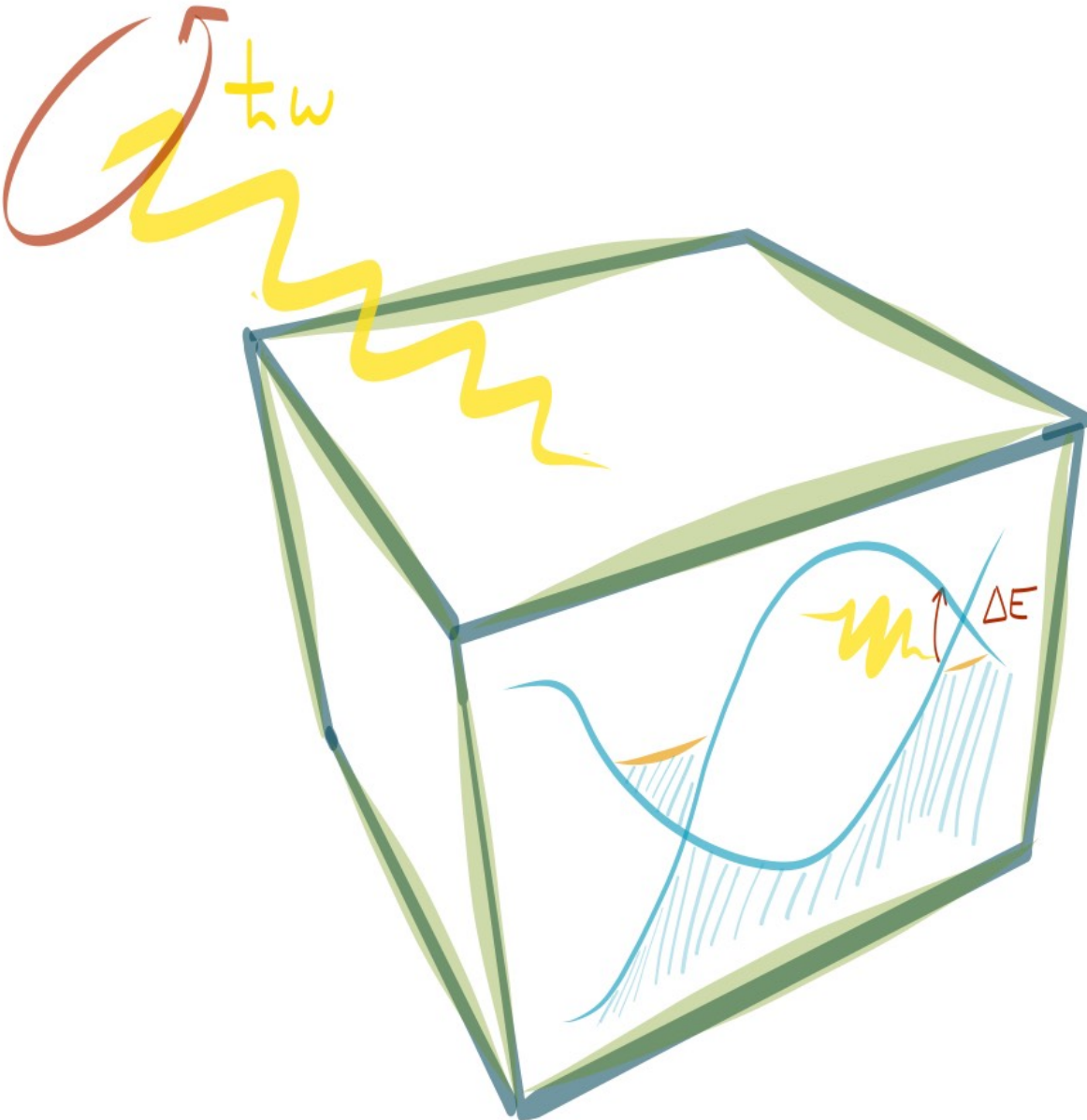
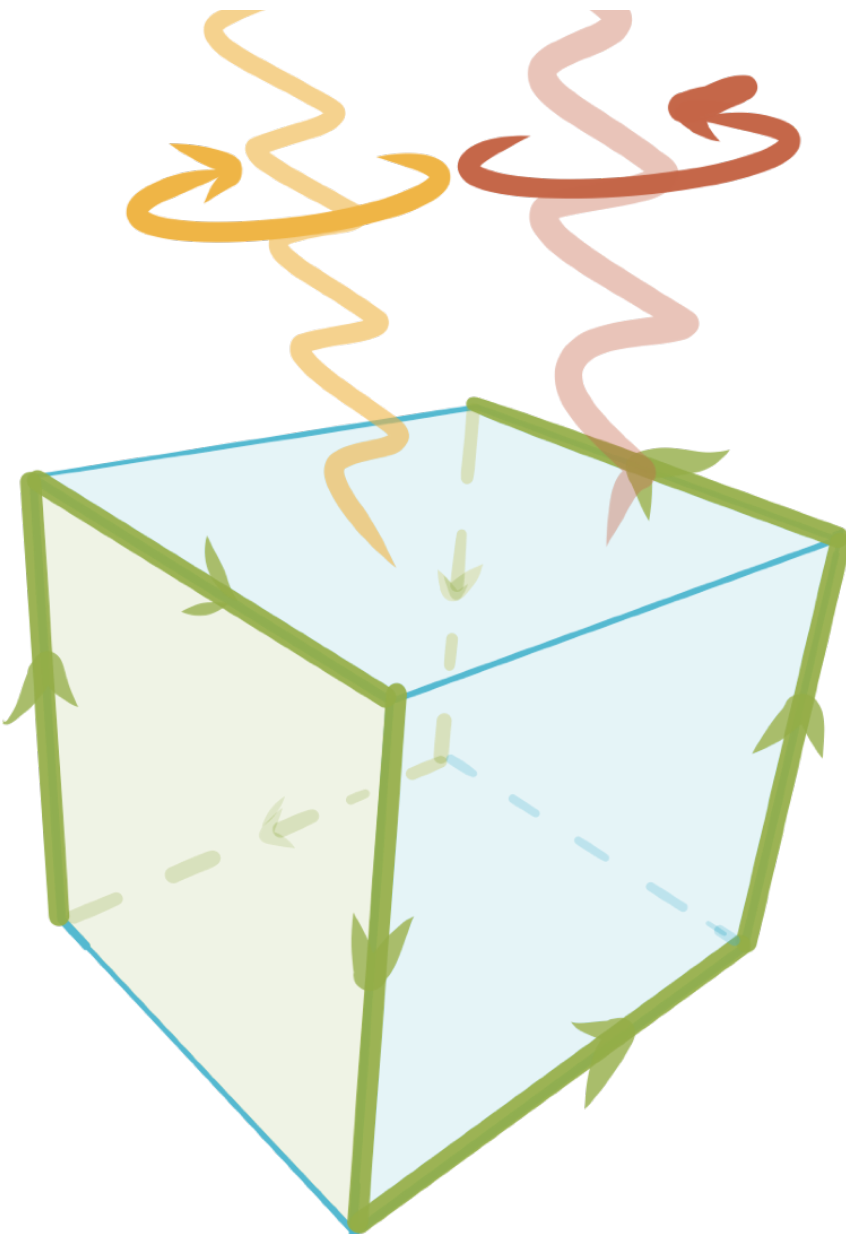
Rotation of plane of polarization

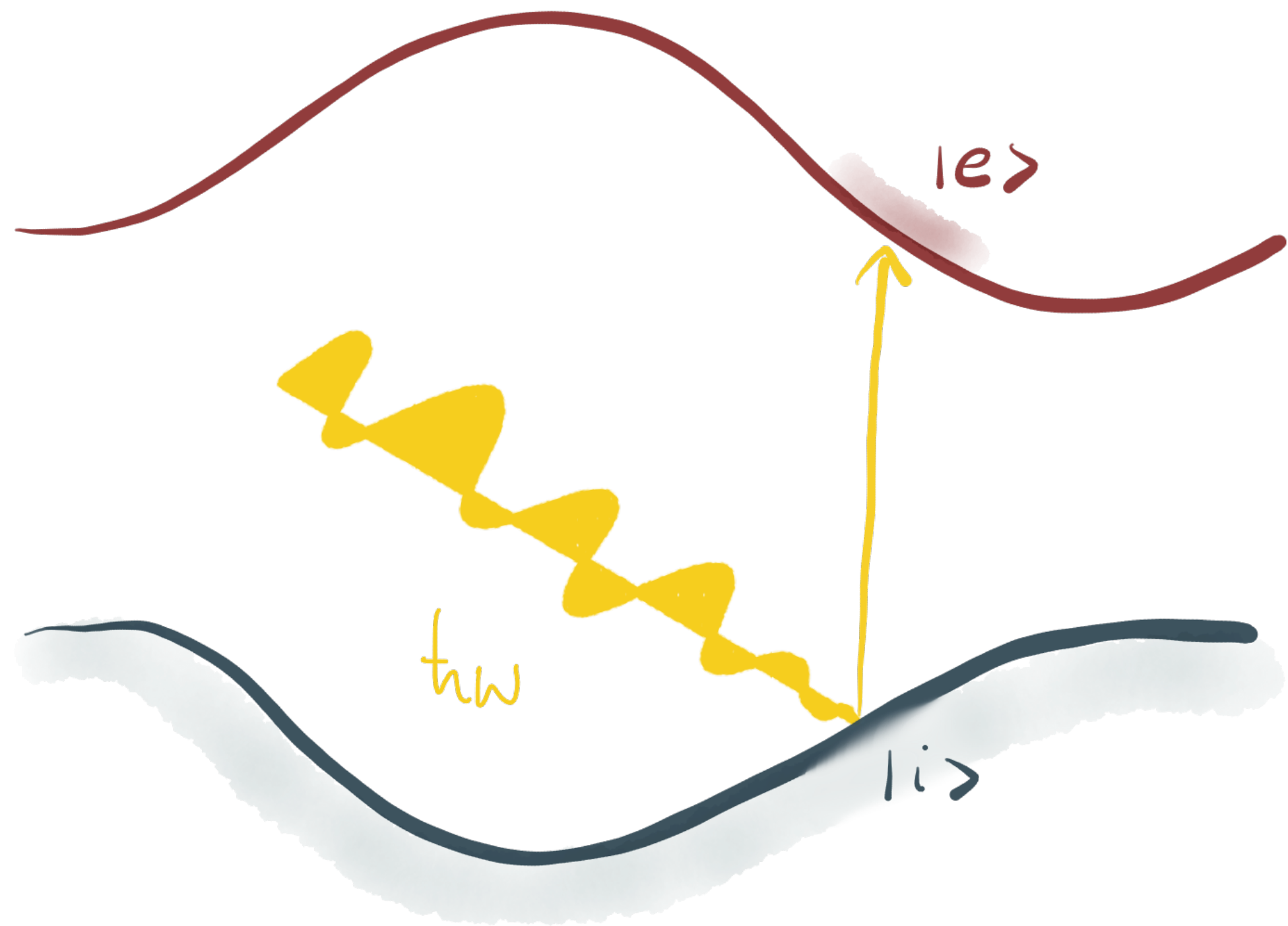
L. Wu, et al Science (2016)

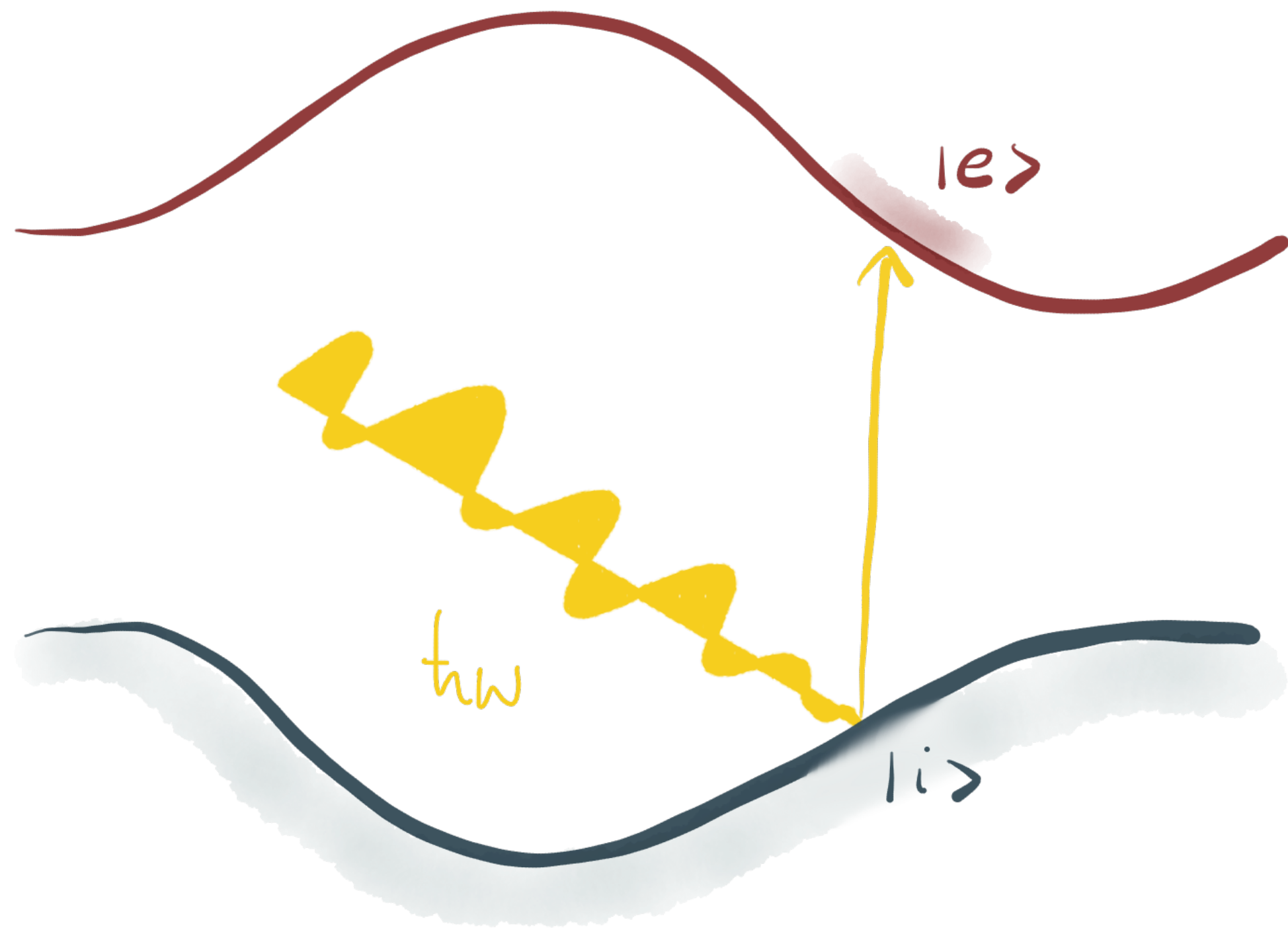
Quantized photogalvanic effect

F. De Juan et al Nat. Comm (2017)

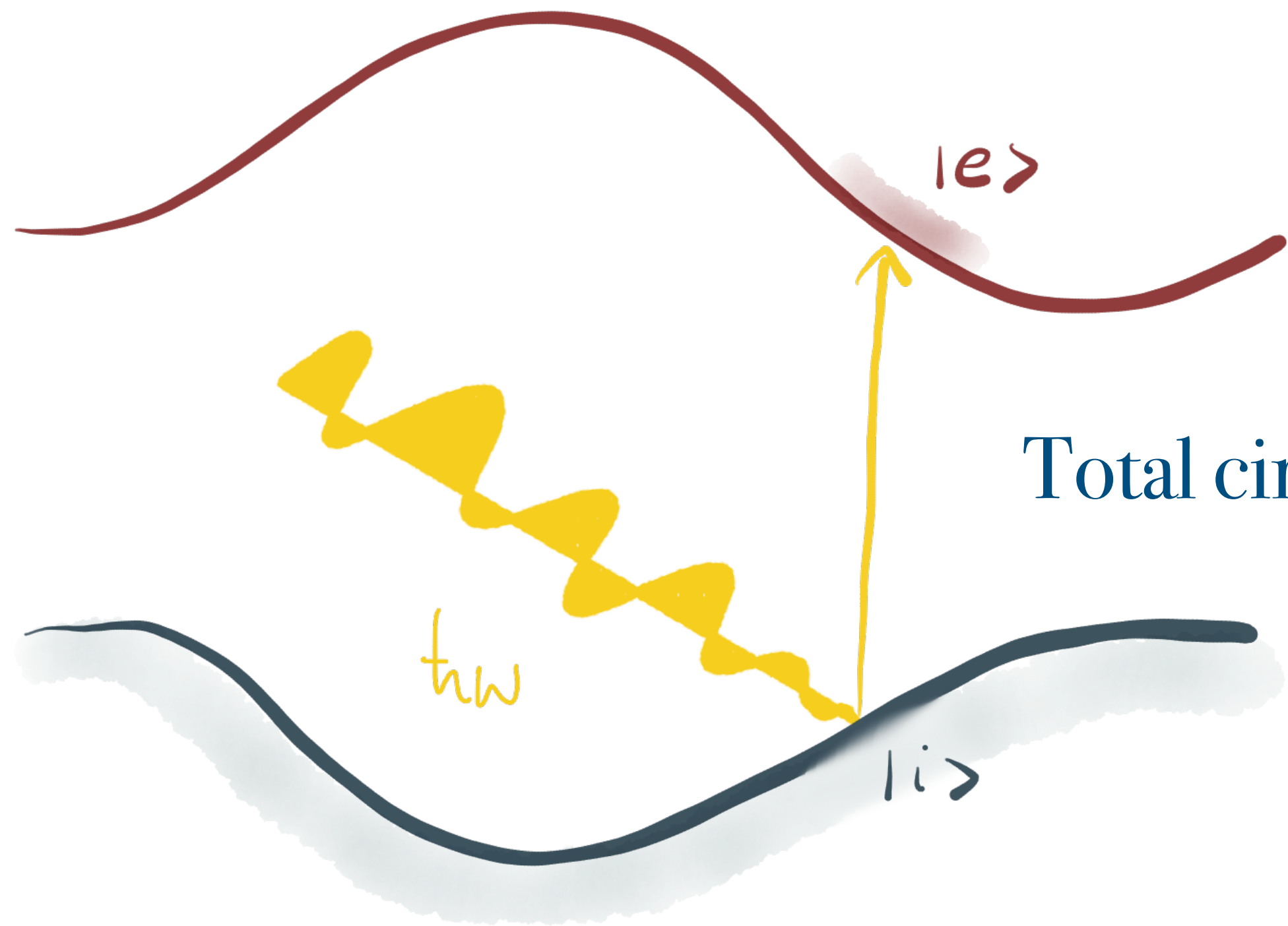
D. Rees et al arXiv: 1902.03230





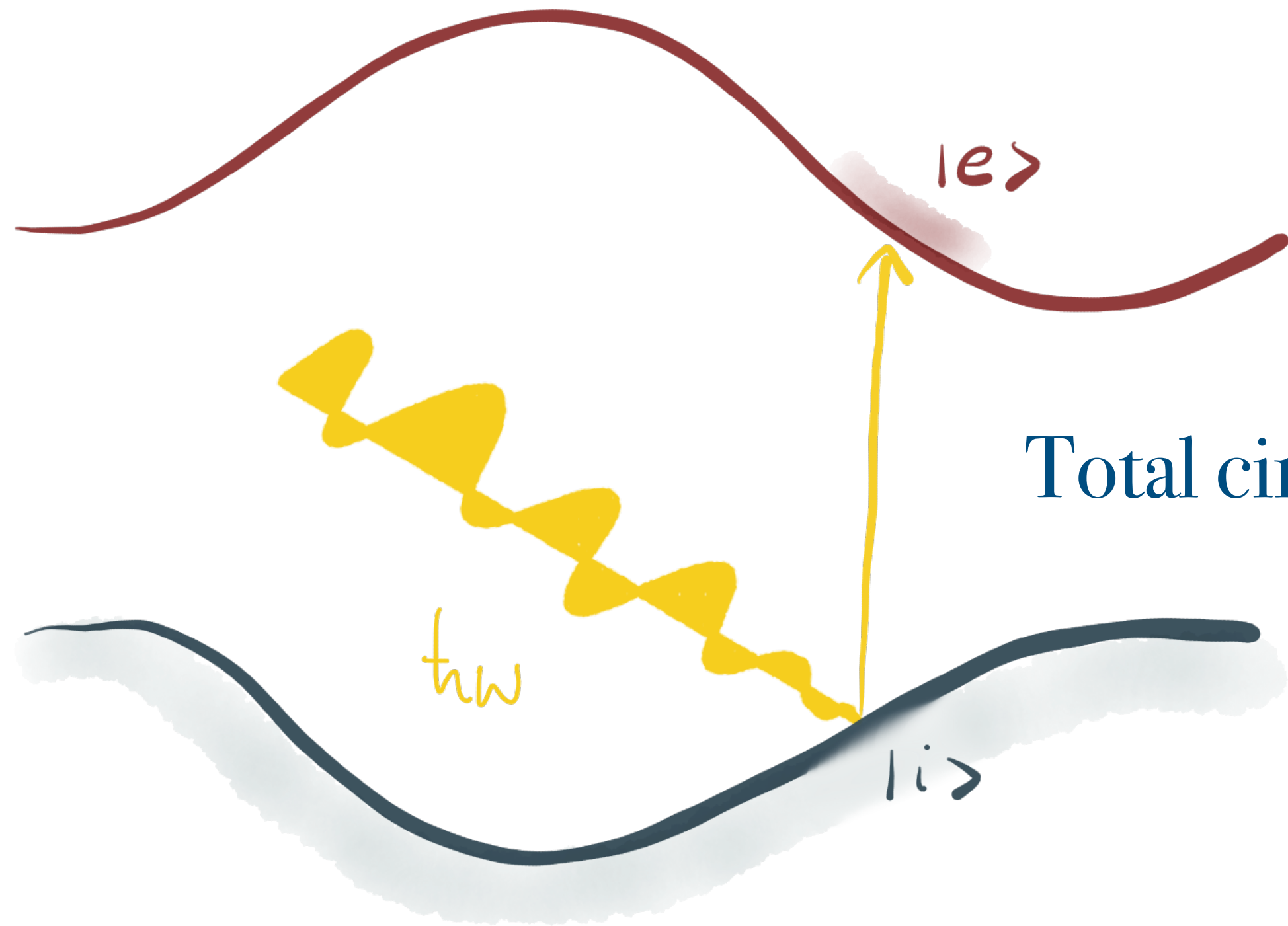


Circular dichroism of chiral 3D-HOTIs
is quantized to integers, and
distinguishes different HOTIs



Total circular dichroism measures the DC Hall conductivity

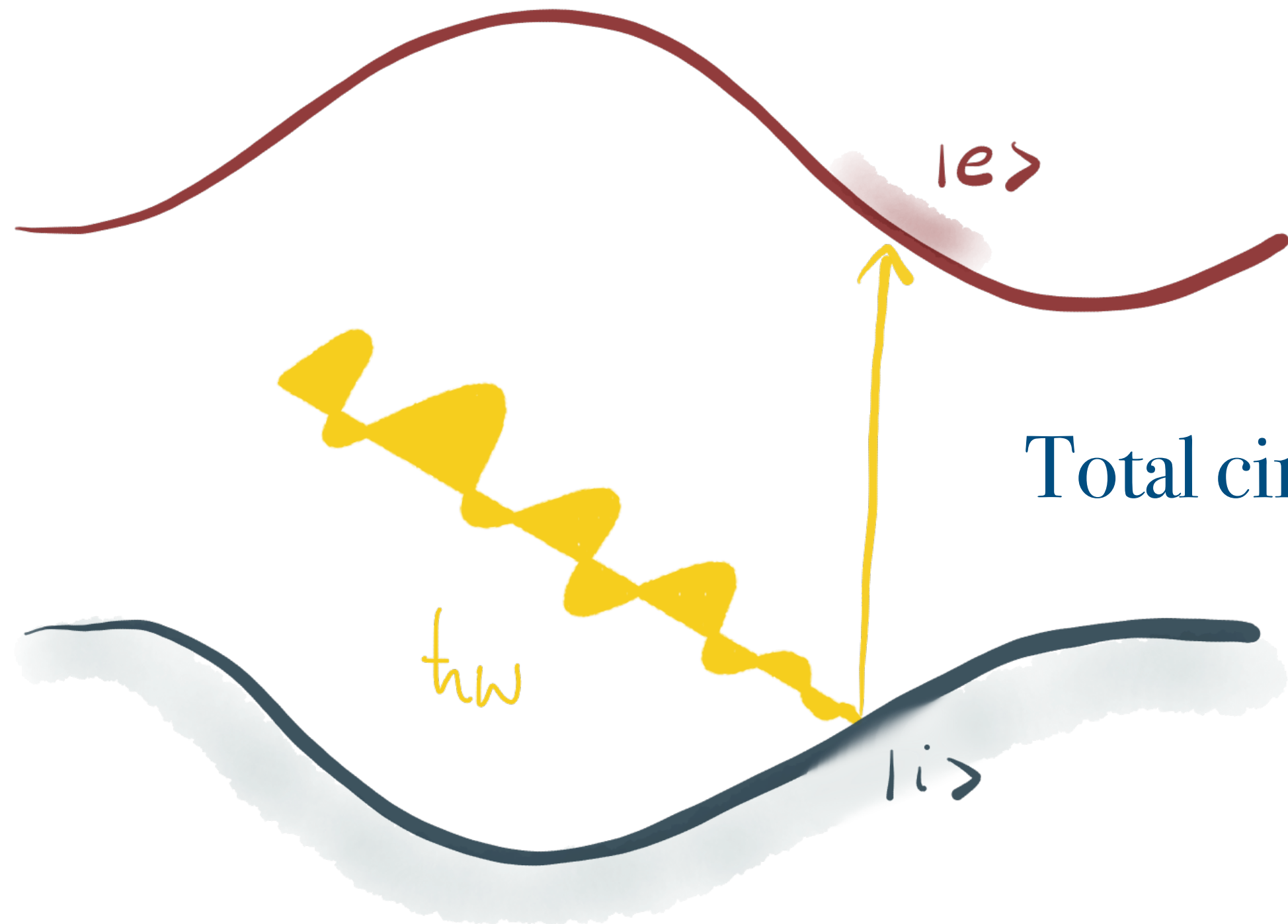
Absorbed power $\frac{P}{A} = \text{Re} \langle J_i^* E_i \rangle$



Total circular dichroism measures the DC Hall conductivity

Absorbed power $\frac{P}{A} = \text{Re} \langle J_i^* E_i \rangle$

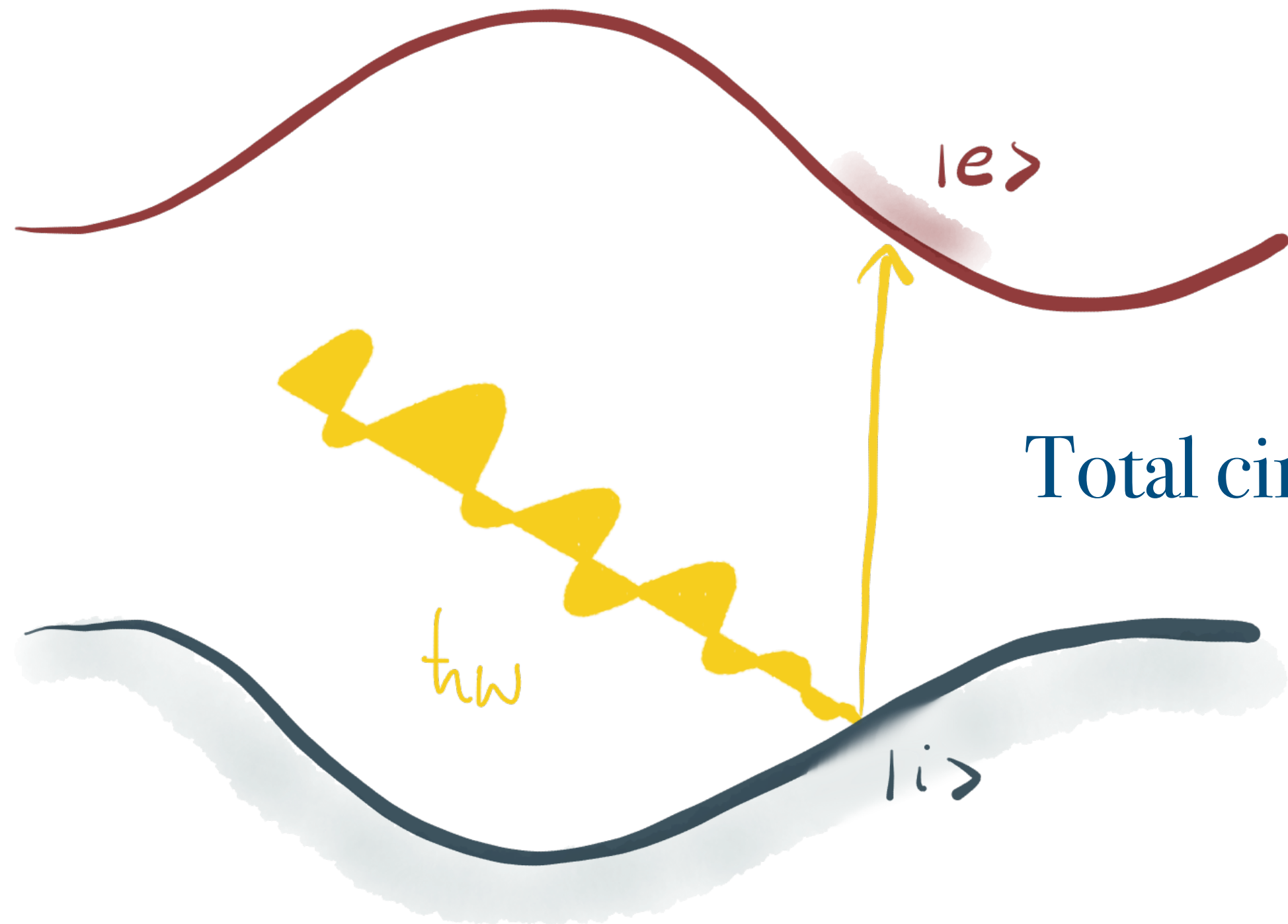
↑ current
 $J_i = \sigma_{ij} E_j$



Total circular dichroism measures the DC Hall conductivity

Absorbed power $\frac{P}{A} = \text{Re} \langle J_i^* E_i \rangle = \text{Re} [\sigma_{ij}^* E_i^* E_j]$

\uparrow current
 $J_i = \sigma_{ij} E_j$

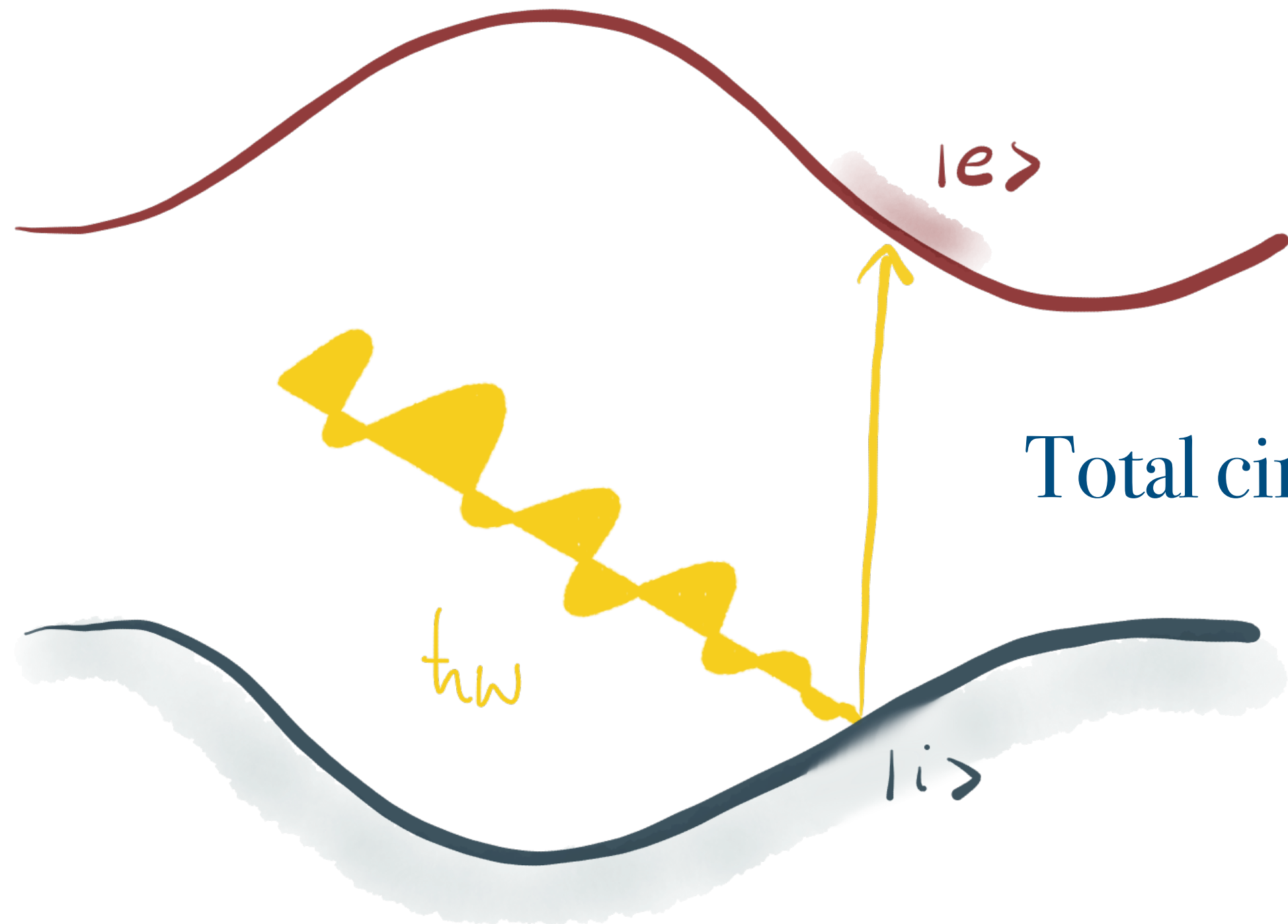


Total circular dichroism measures the DC Hall conductivity

Absorbed power $\frac{P}{A} = \text{Re} \langle J_i^* E_i \rangle = \text{Re} [\sigma_{ij}^* E_i^* E_j]$

↑ current $J_i = \sigma_{ij} E_j$

↑ electric field $E = 2|E|(1, \pm i, 0)e^{i\omega t}$

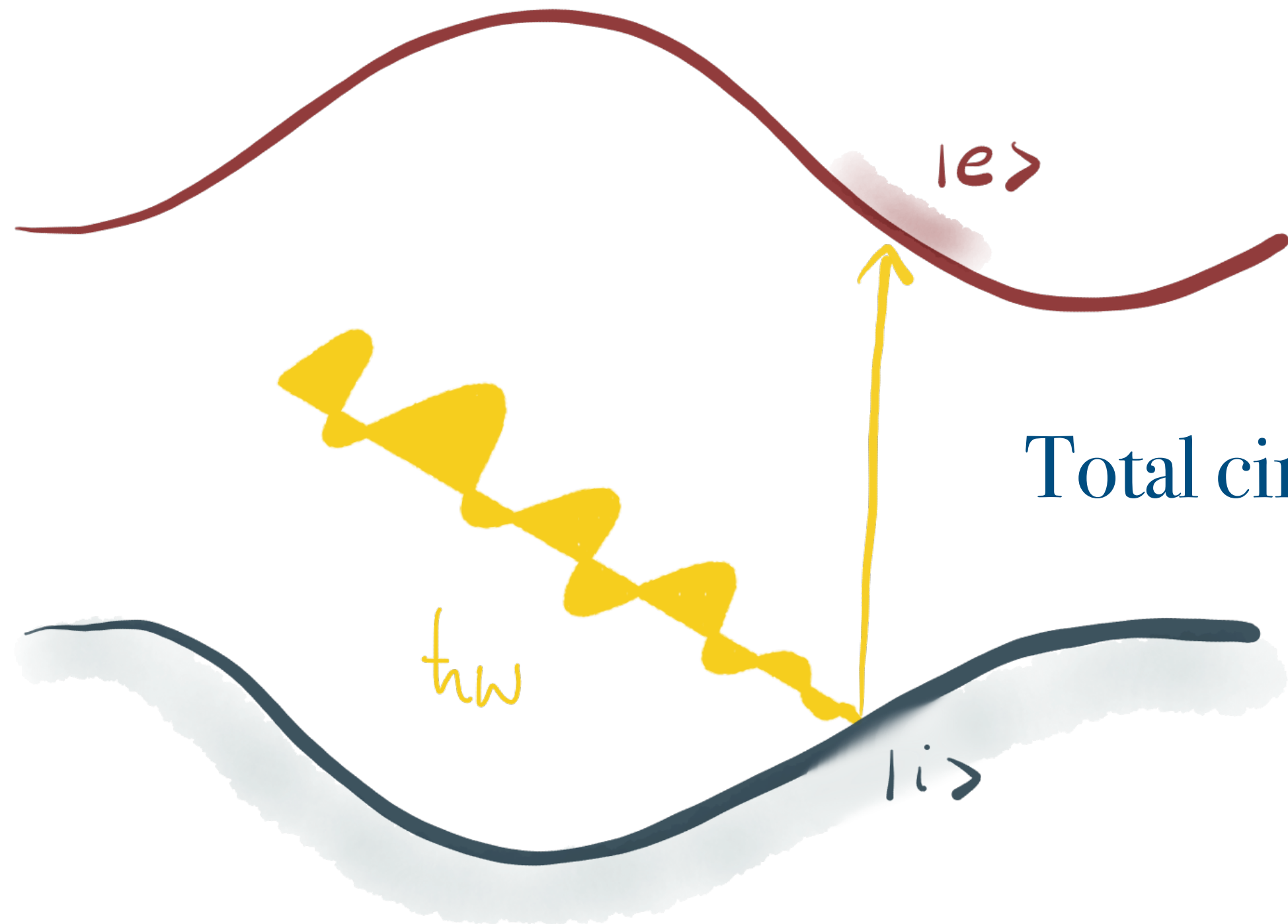


Total circular dichroism measures the DC Hall conductivity

Absorbed power $\frac{P}{A} = \text{Re} \langle J_i^* E_i \rangle = \text{Re} [\sigma_{ij}^* E_i^* E_j] = 4|E|^2 (\text{Re}[\sigma_{xx}(\omega)] \pm \text{Im}[\sigma_{xy}(\omega)])$

\uparrow current $J_i = \sigma_{ij} E_j$

\uparrow electric field $E = 2|E|(1, \pm i, 0)e^{i\omega t}$

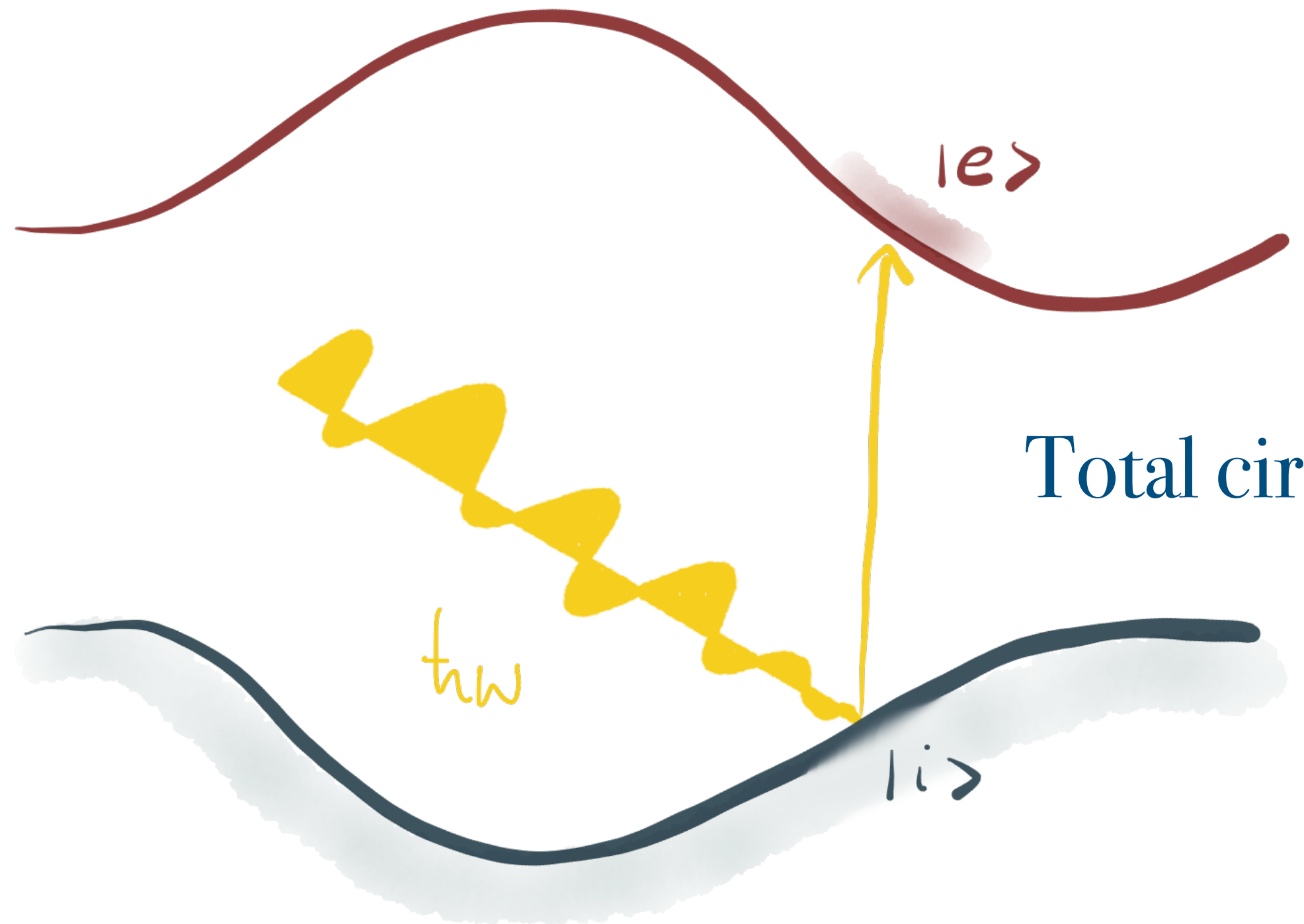


Total circular dichroism measures the DC Hall conductivity

Absorbed power $\frac{P}{A} = \text{Re} \langle J_i^* E_i \rangle = \text{Re} [\sigma_{ij}^* E_i^* E_j] = 4|E|^2 (\text{Re}[\sigma_{xx}(\omega)] \pm \text{Im}[\sigma_{xy}(\omega)])$

↑ current $J_i = \sigma_{ij} E_j$

↑ electric field $E = 2|E|(1, \pm i, 0)e^{i\omega t}$



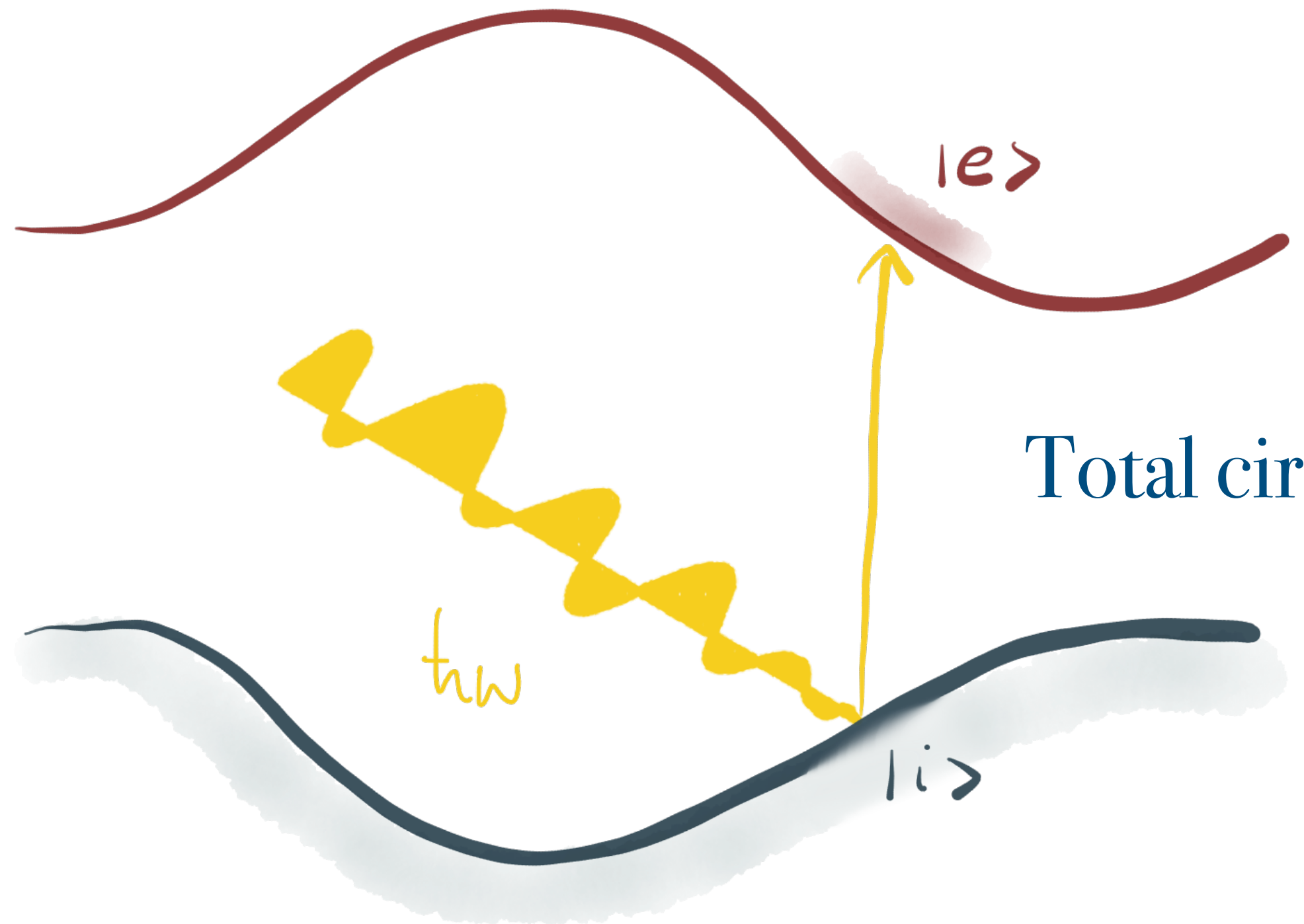
Power absorbed $P_{\pm} = \hbar\omega\Gamma_{\pm}$

Total circular dichroism measures the DC Hall conductivity

Absorbed power $\frac{P}{A} = \text{Re} \langle J_i^* E_i \rangle = \text{Re} [\sigma_{ij}^* E_i^* E_j] = 4|E|^2 (\text{Re}[\sigma_{xx}(\omega)] \pm \text{Im}[\sigma_{xy}(\omega)])$

↑ current $J_i = \sigma_{ij} E_j$

↑ electric field $E = 2|E|(1, \pm i, 0)e^{i\omega t}$



Power absorbed $P_{\pm} = \hbar\omega\Gamma_{\pm}$

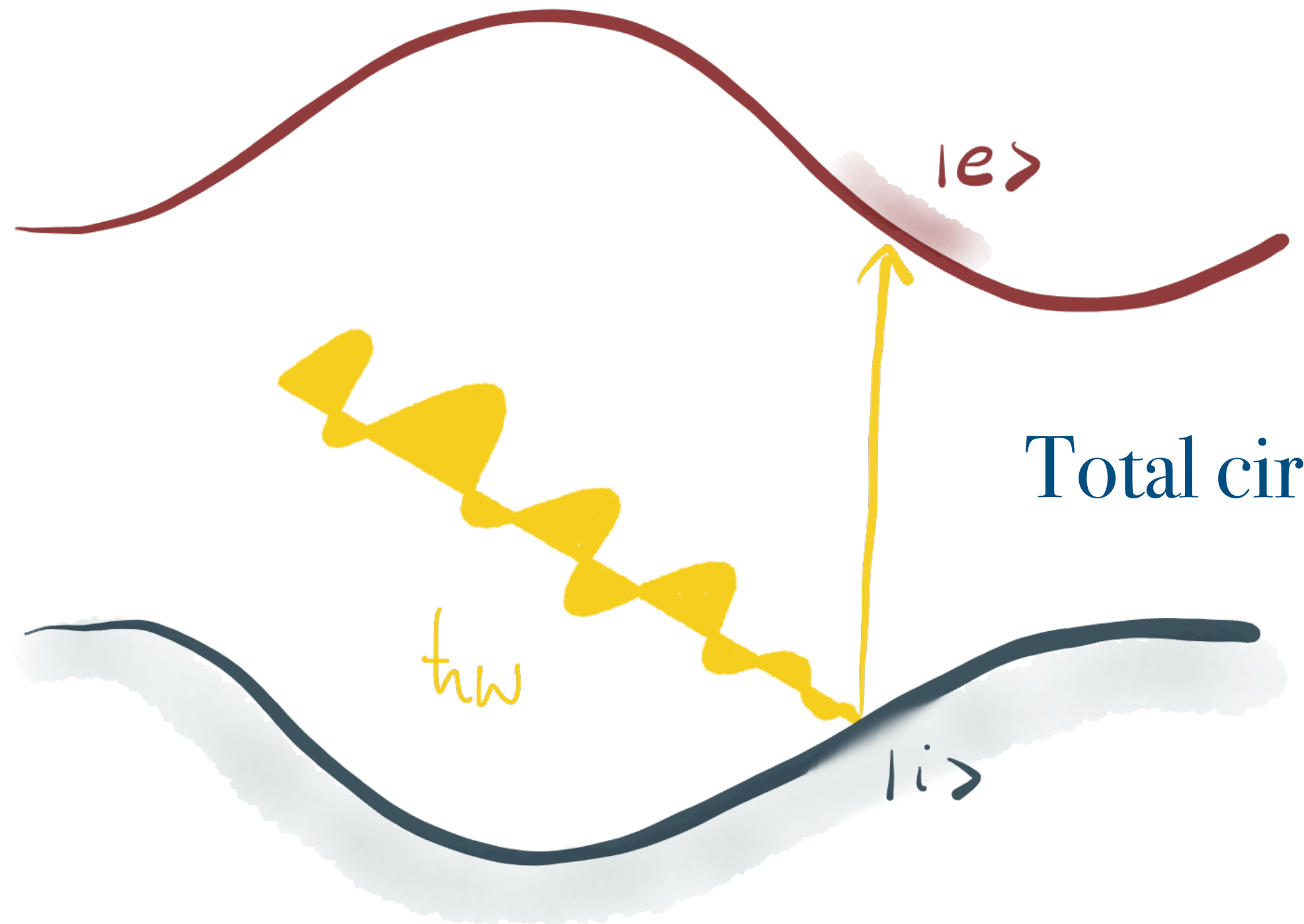
Total circular dichroism measures the DC Hall conductivity

$$\frac{\Delta\Gamma}{A} = \frac{1}{A} \int d\omega (\Gamma_+ - \Gamma_-) / 2$$

Absorbed power $\frac{P}{A} = \text{Re} \langle J_i^* E_i \rangle = \text{Re} [\sigma_{ij}^* E_i^* E_j] = 4|E|^2 (\text{Re}[\sigma_{xx}(\omega)] \pm \text{Im}[\sigma_{xy}(\omega)])$

↑ current $J_i = \sigma_{ij} E_j$

↑ electric field $E = 2|E|(1, \pm i, 0)e^{i\omega t}$



Power absorbed $P_{\pm} = \hbar\omega\Gamma_{\pm}$

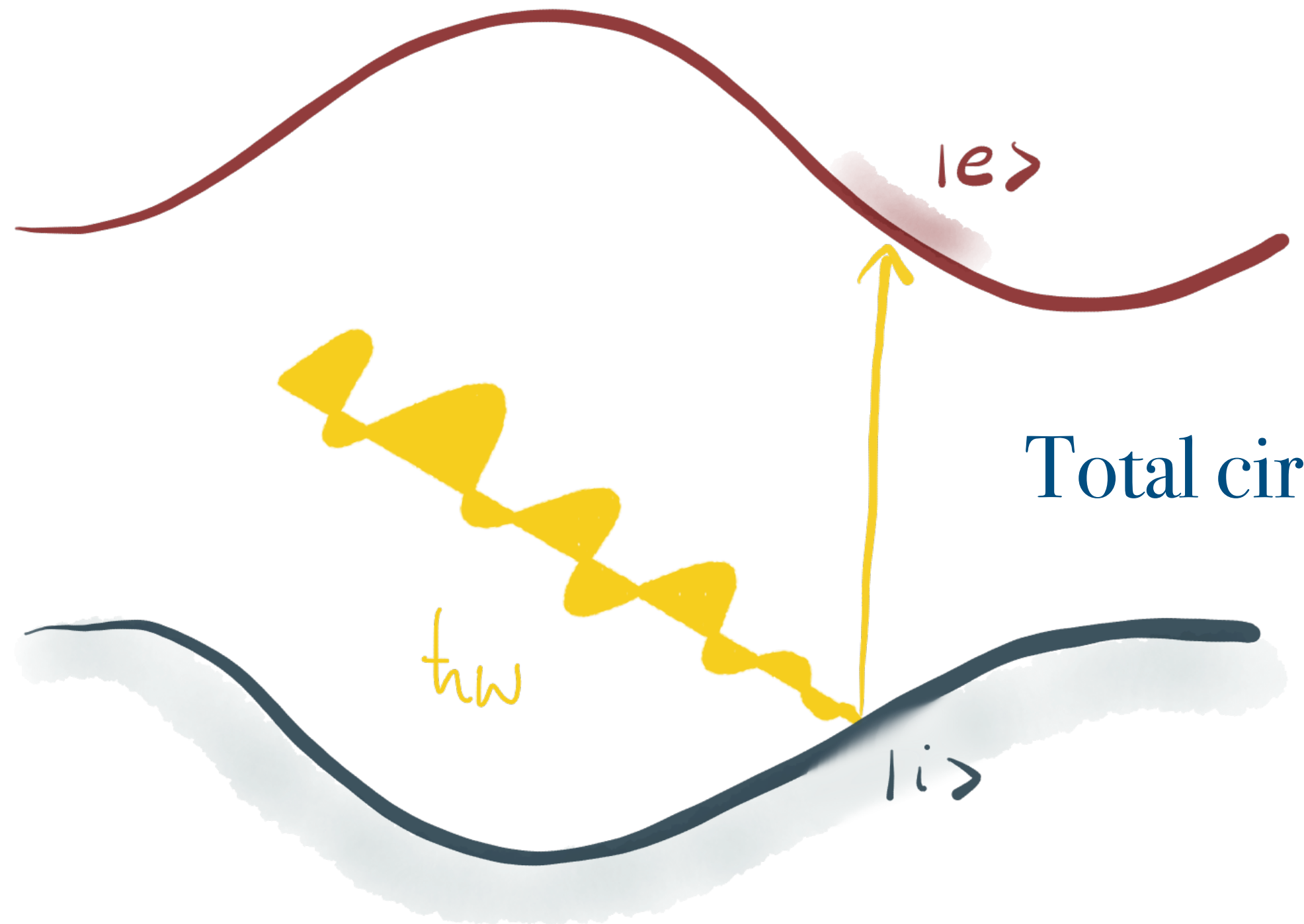
Total circular dichroism measures the DC Hall conductivity

$$\frac{\Delta\Gamma}{A} = \int d\omega \frac{4|E|^2 \text{Im} [\sigma_{xy}(\omega)]}{\hbar\omega}$$

Absorbed power $\frac{P}{A} = \text{Re} \langle J_i^* E_i \rangle = \text{Re} [\sigma_{ij}^* E_i^* E_j] = 4|E|^2 (\text{Re}[\sigma_{xx}(\omega)] \pm \text{Im}[\sigma_{xy}(\omega)])$

↑ current $J_i = \sigma_{ij} E_j$

↑ electric field $E = 2|E|(1, \pm i, 0)e^{i\omega t}$



Power absorbed $P_{\pm} = \hbar\omega\Gamma_{\pm}$

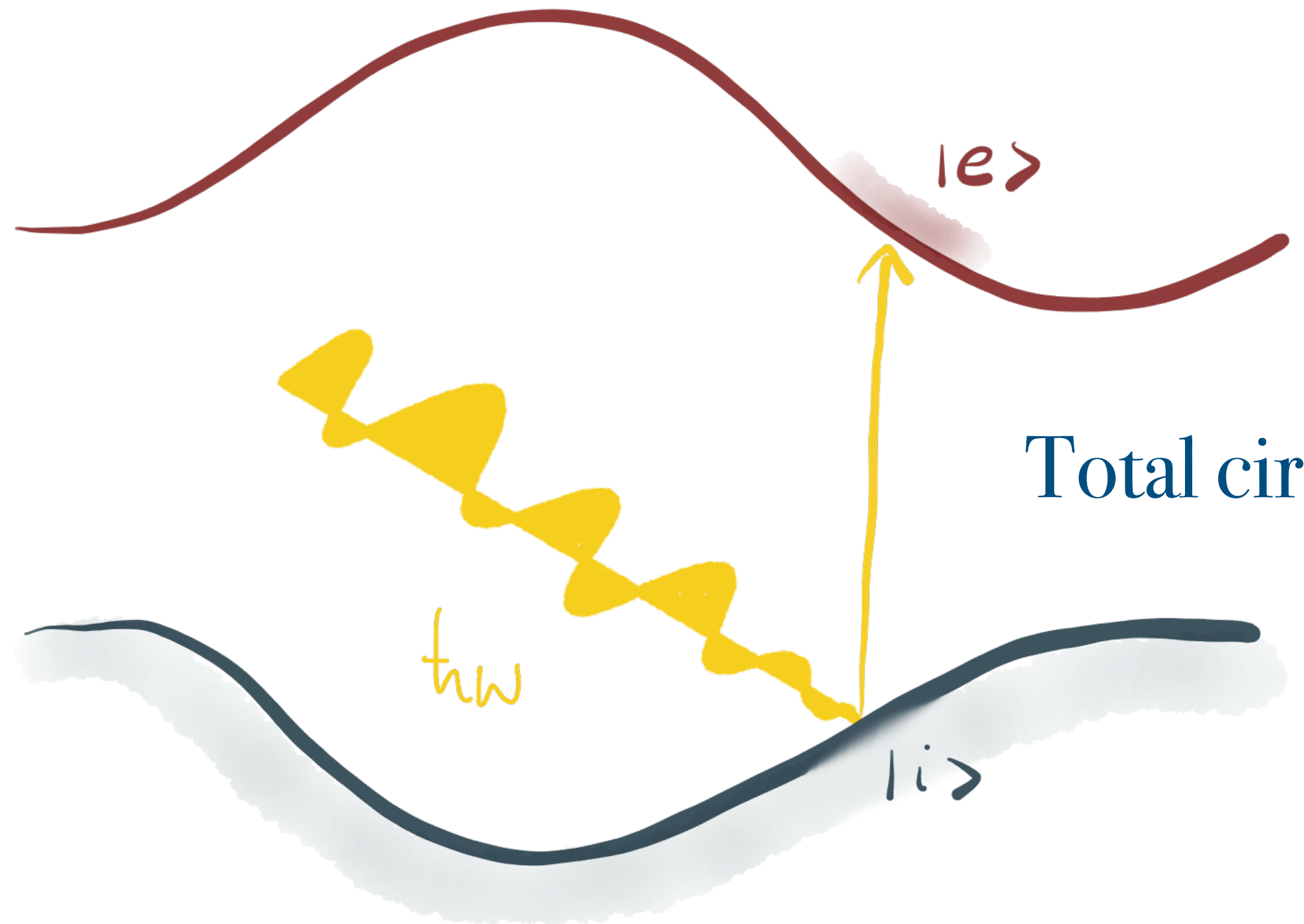
Total circular dichroism measures the DC Hall conductivity

$$\frac{\Delta\Gamma}{A} = 2\pi \text{Re}[\sigma_{xy}(\omega = 0)] \frac{E^2}{\hbar}$$

Absorbed power $\frac{P}{A} = \text{Re} \langle J_i^* E_i \rangle = \text{Re} [\sigma_{ij}^* E_i^* E_j] = 4|E|^2 (\text{Re}[\sigma_{xx}(\omega)] \pm \text{Im}[\sigma_{xy}(\omega)])$

↑ current $J_i = \sigma_{ij} E_j$

↑ electric field $E = 2|E|(1, \pm i, 0)e^{i\omega t}$



Power absorbed $P_{\pm} = \hbar\omega\Gamma_{\pm}$

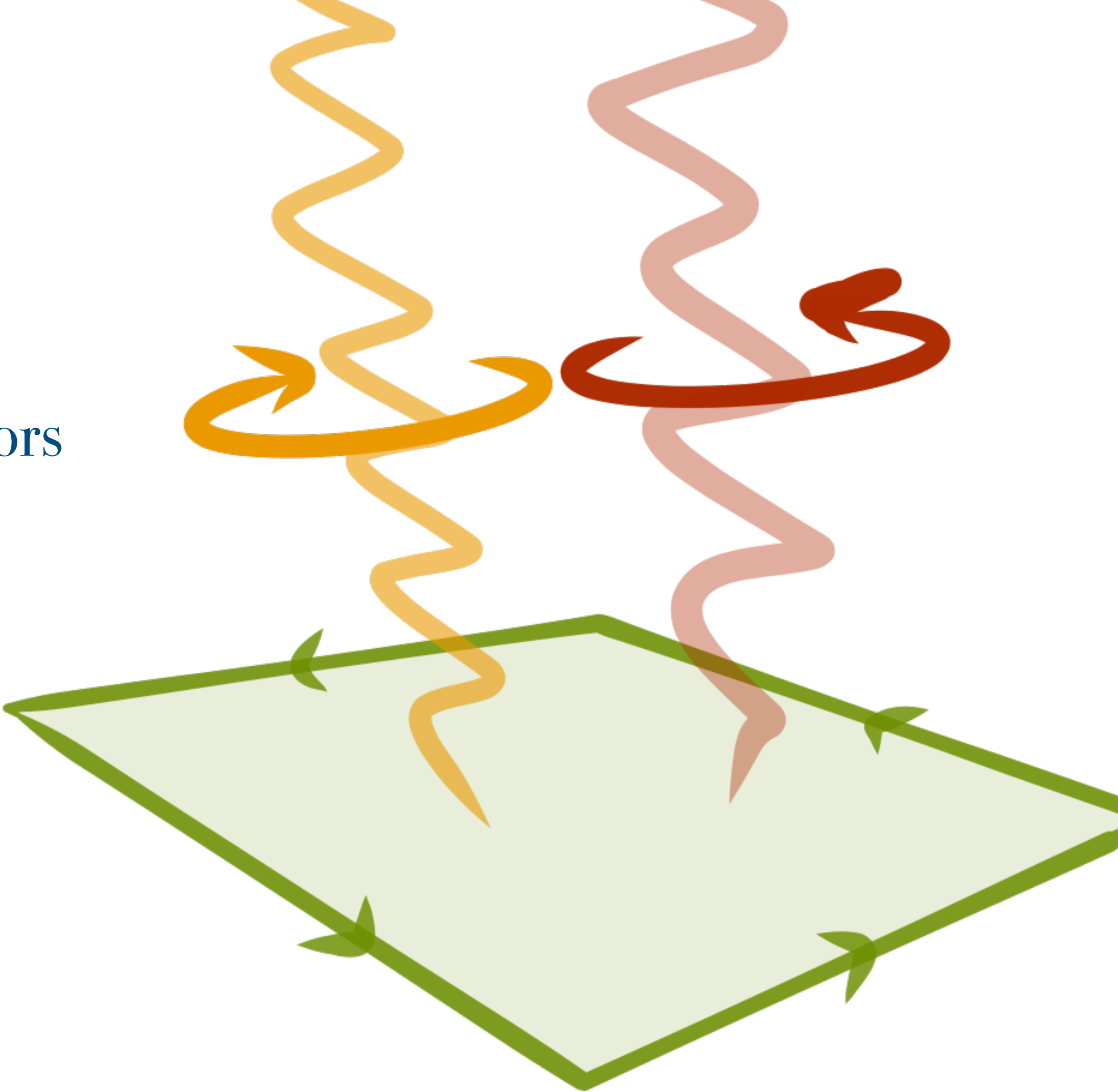
Total circular dichroism measures the DC Hall conductivity

$$\frac{\Delta\Gamma}{A} = \nu \frac{e^2 E^2}{\hbar^2}$$

↑ 2D insulator

Total circular dichroism is quantized in Chern insulators

$$\frac{\Delta\Gamma}{A} = \nu \frac{e^2 E^2}{\hbar}$$



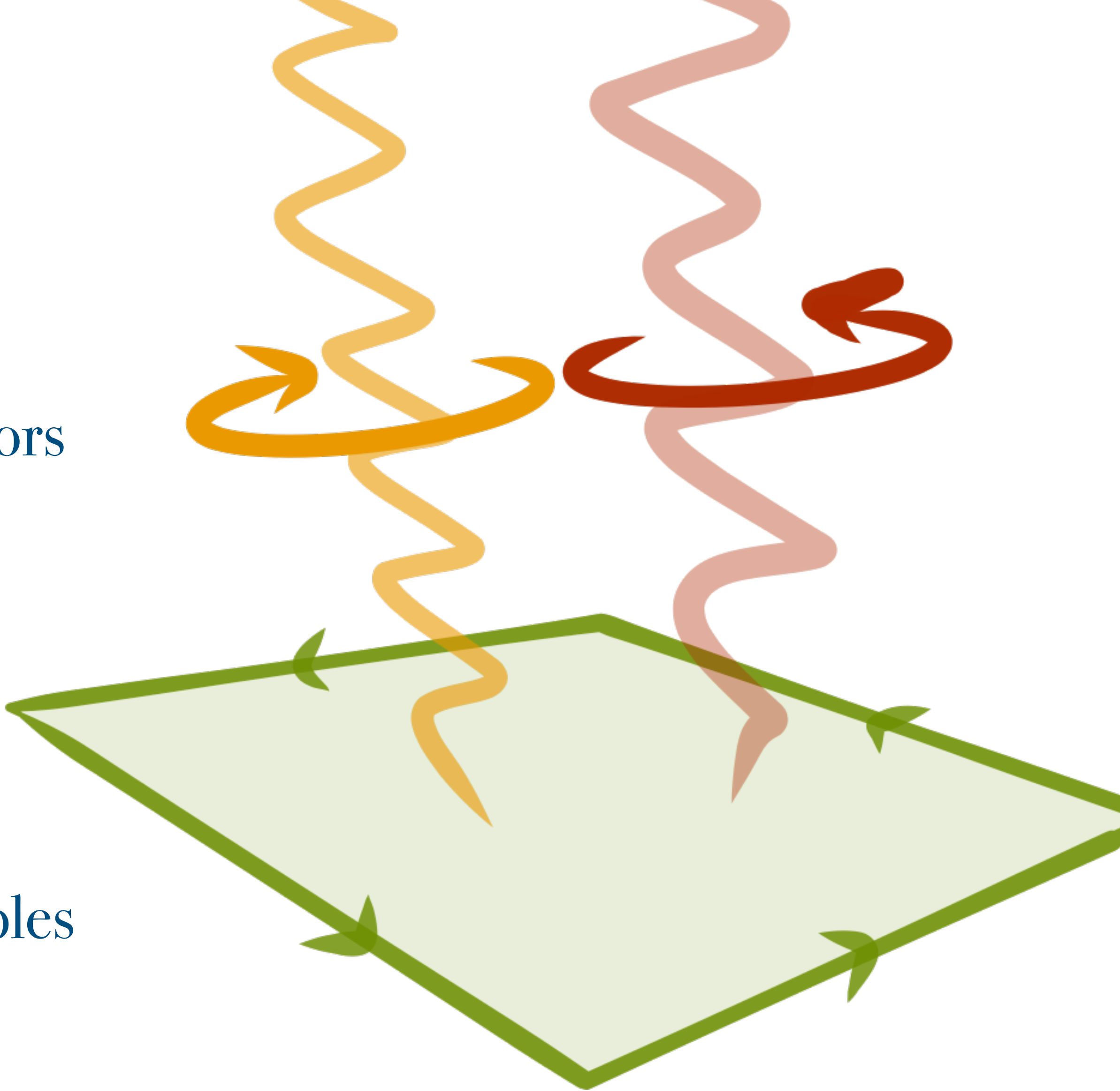
D. T. Tran, A. Dauphin, AGG, P. Zoller, N. Goldman Science Advances (2017)

L. Asteria et al Nat. Phys. (2019)

Total circular dichroism is quantized in Chern insulators

$$\frac{\Delta\Gamma}{A} = \nu \frac{e^2 E^2}{\hbar}$$

...but the total circular dichroism is zero in finite samples



D. T. Tran, A. Dauphin, AGG, P. Zoller, N. Goldman Science Advances (2017)

L. Asteria et al Nat. Phys. (2019)

the total circular dichroism is zero in finite samples (real space picture)

$$\nu = \frac{1}{A} \sum_{\mathbf{r}} C_{xy}(\mathbf{r}) = 0$$

$$C_{xy}(\mathbf{r}) = 2\pi \text{Im} \langle \mathbf{r} | [\hat{Q}\hat{x}, \hat{P}\hat{y}] | \mathbf{r} \rangle$$

Wannier basis

ground-state
projector operator

the total circular dichroism is zero in finite samples (real space picture)

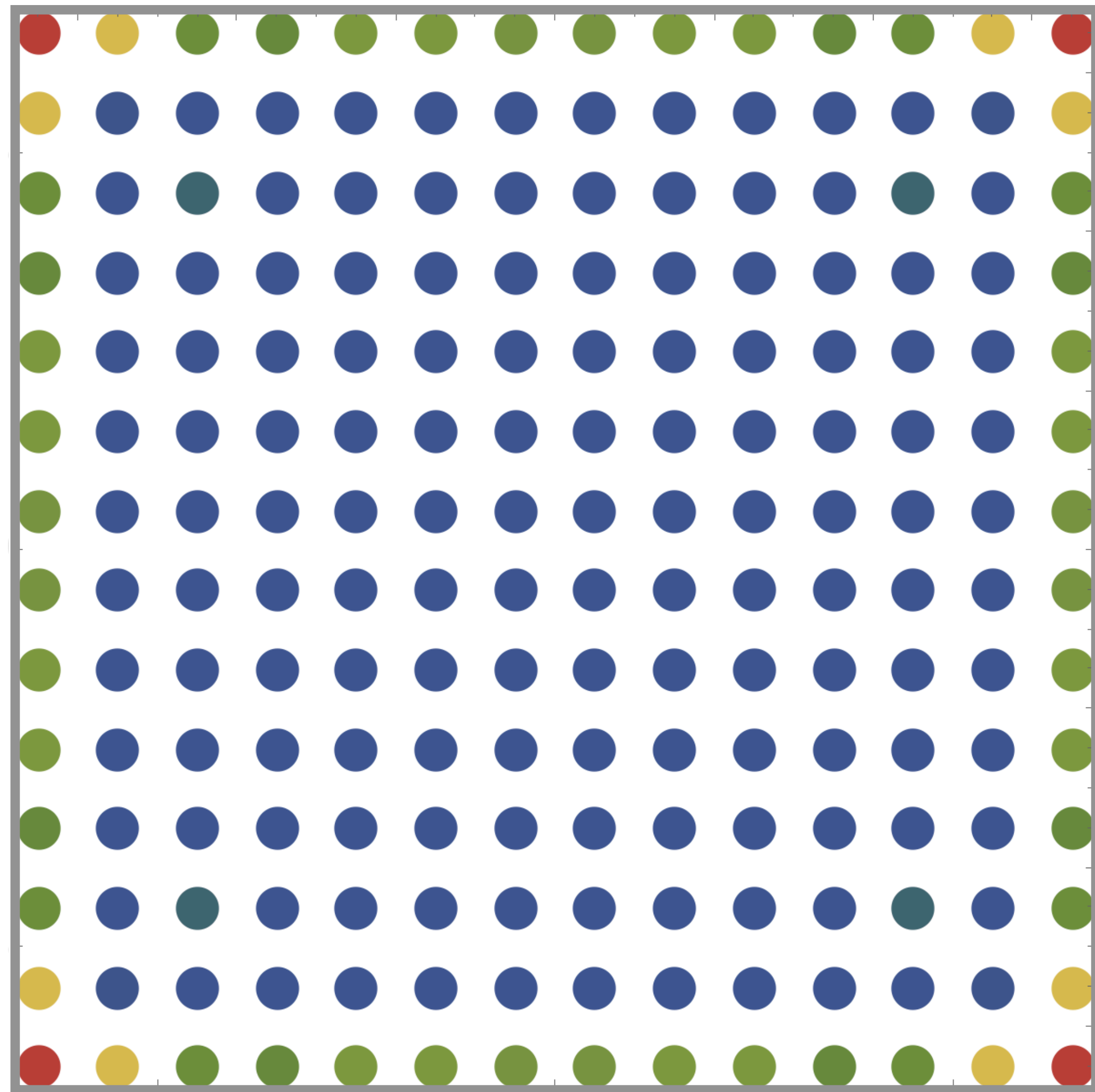
$$\nu = \frac{1}{A} \sum_{\mathbf{r}} C_{xy}(\mathbf{r}) = 0$$

$$C_{xy}(\mathbf{r}) = 2\pi \text{Im} \langle \mathbf{r} | [\hat{Q}\hat{x}, \hat{P}\hat{y}] | \mathbf{r} \rangle$$

Wannier basis

ground-state
projector operator

y/a



x/a

$C_{xy}(\mathbf{r})$

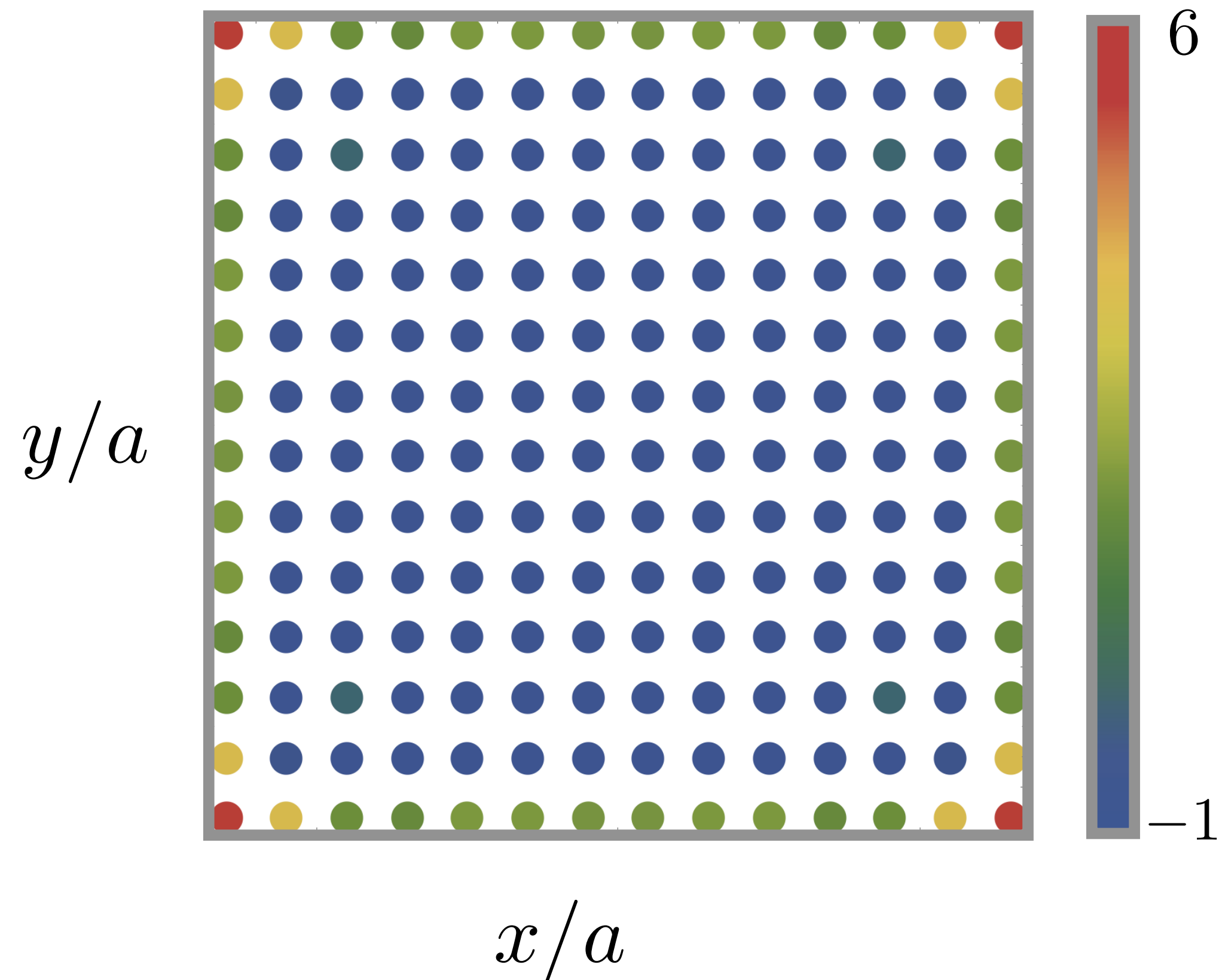
6

-1

the total circular dichroism is zero in finite samples (real and energy space picture)

Real space

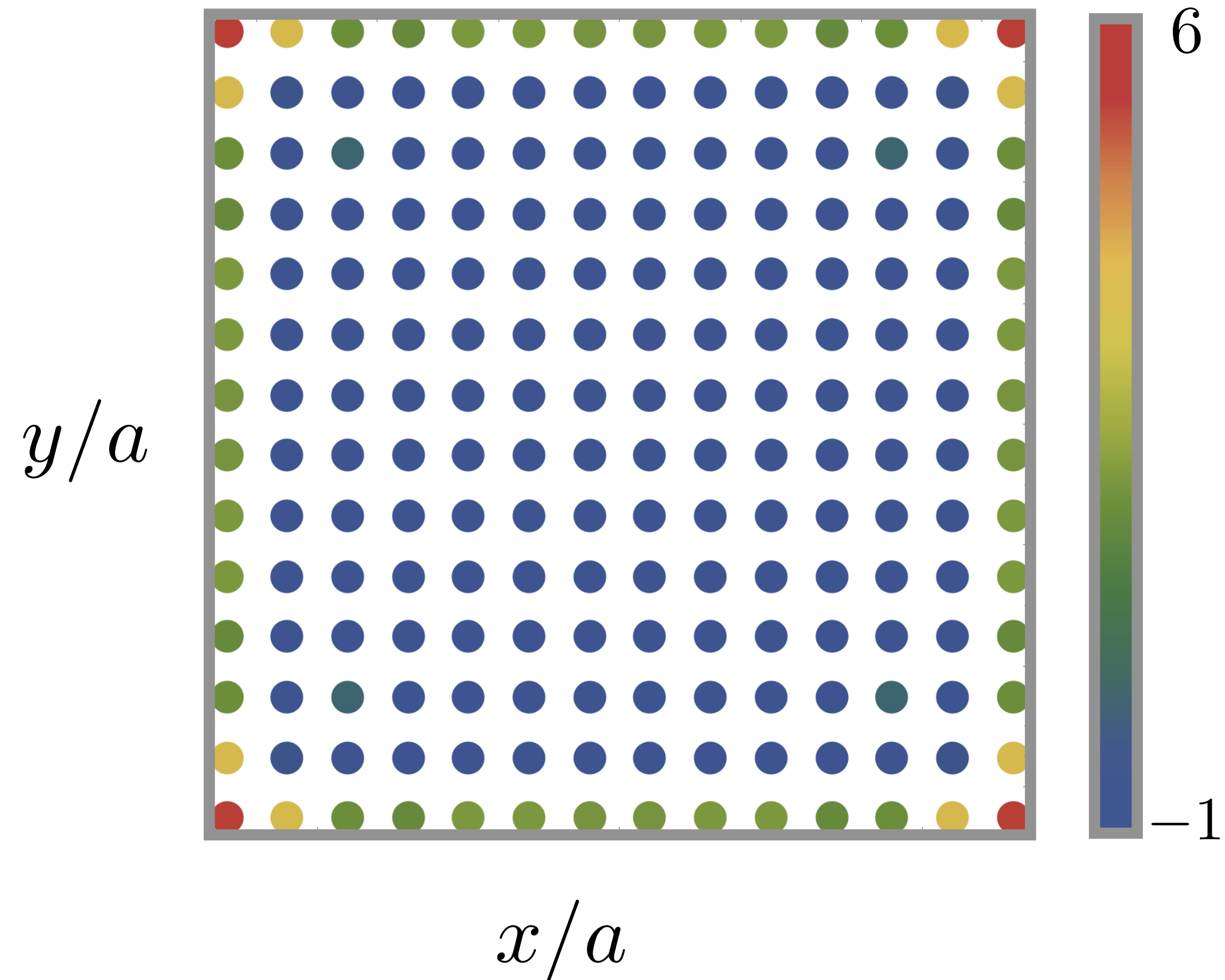
$$\Delta\Gamma = \frac{e^2 E^2}{\hbar^2} \sum_{\mathbf{r}} C_{xy}(\mathbf{r}) = 0$$



the total circular dichroism is zero in finite samples (real and energy space picture)

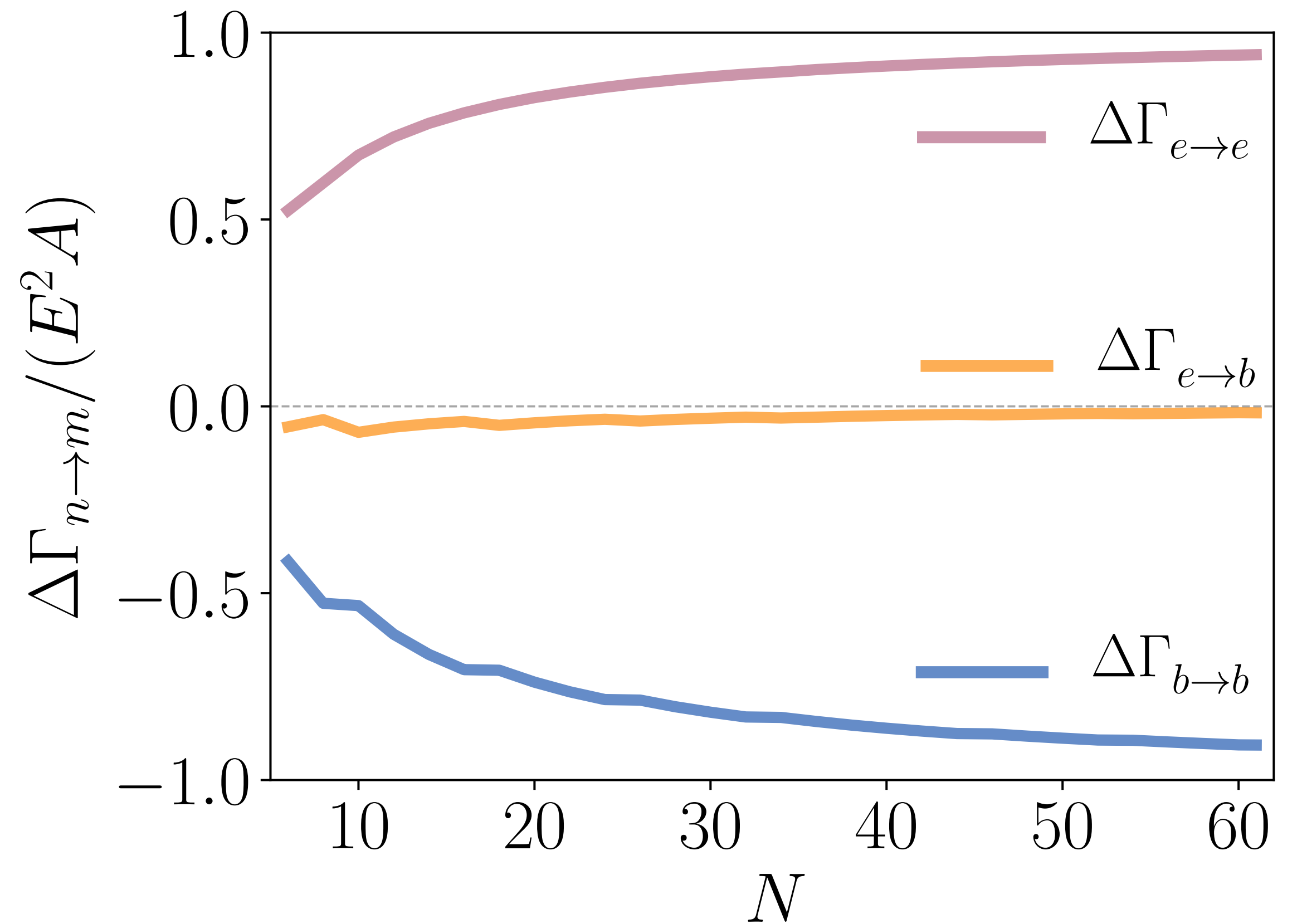
Real space

$$\Delta\Gamma = \frac{e^2 E^2}{\hbar^2} \sum_{\mathbf{r}} C_{xy}(\mathbf{r}) = 0$$



Energy space

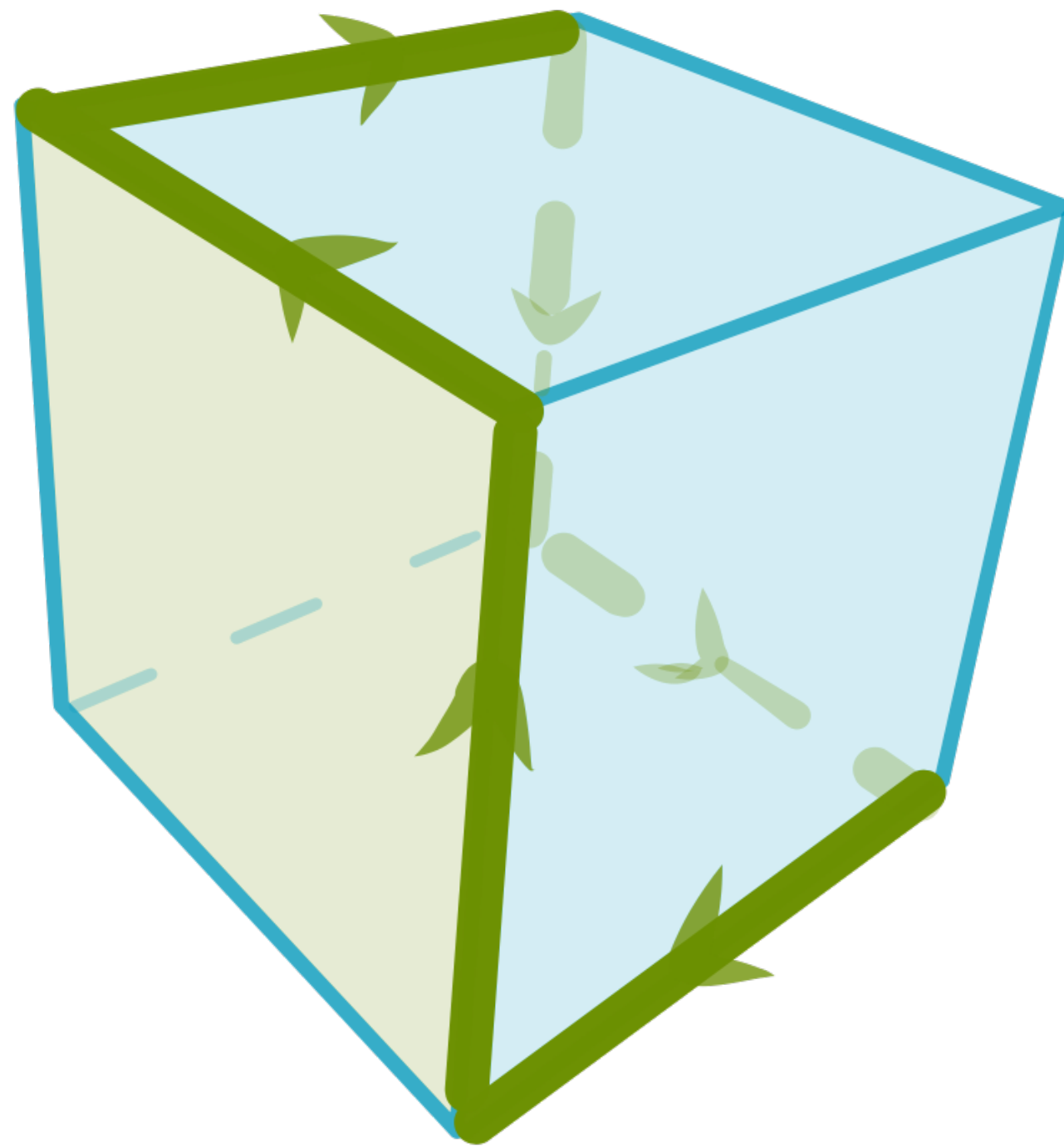
$$\Delta\Gamma = \sum_{n,m \in \{e,b\}} \Gamma_{n \rightarrow m} = 0$$



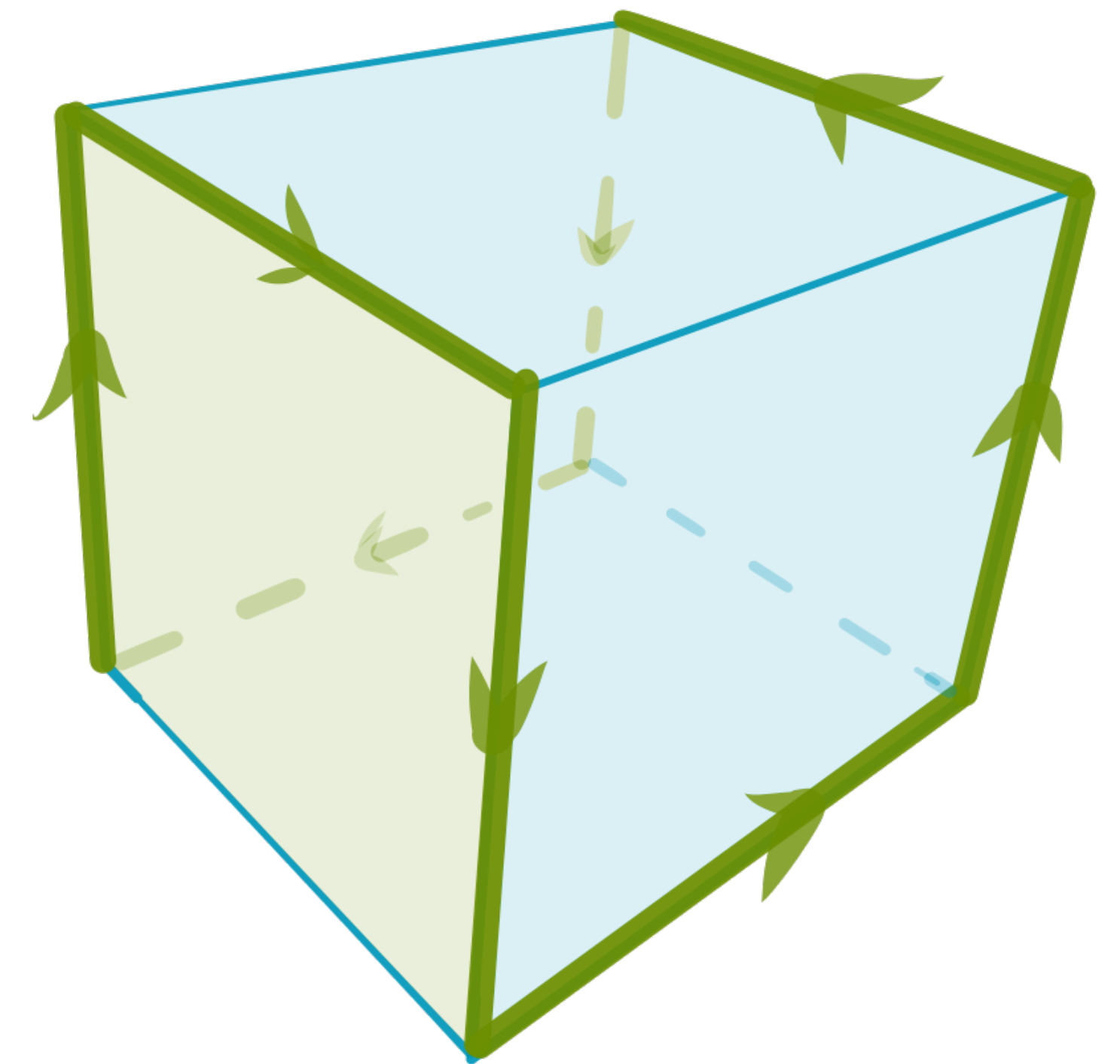
Calculated using Fermi's Golden Rule $\frac{\Gamma_{\pm}(\omega)}{2\pi E^2} = \sum_{n,m} |\langle m | (\hat{x} \pm i\hat{y}) | n \rangle|^2 \delta(E_m - E_n - \hbar\omega)$

Chiral higher order topological insulators

$$H = H_{\text{TI}} + H_{C_4^z} \tau + H_{\text{Zeeman}}$$

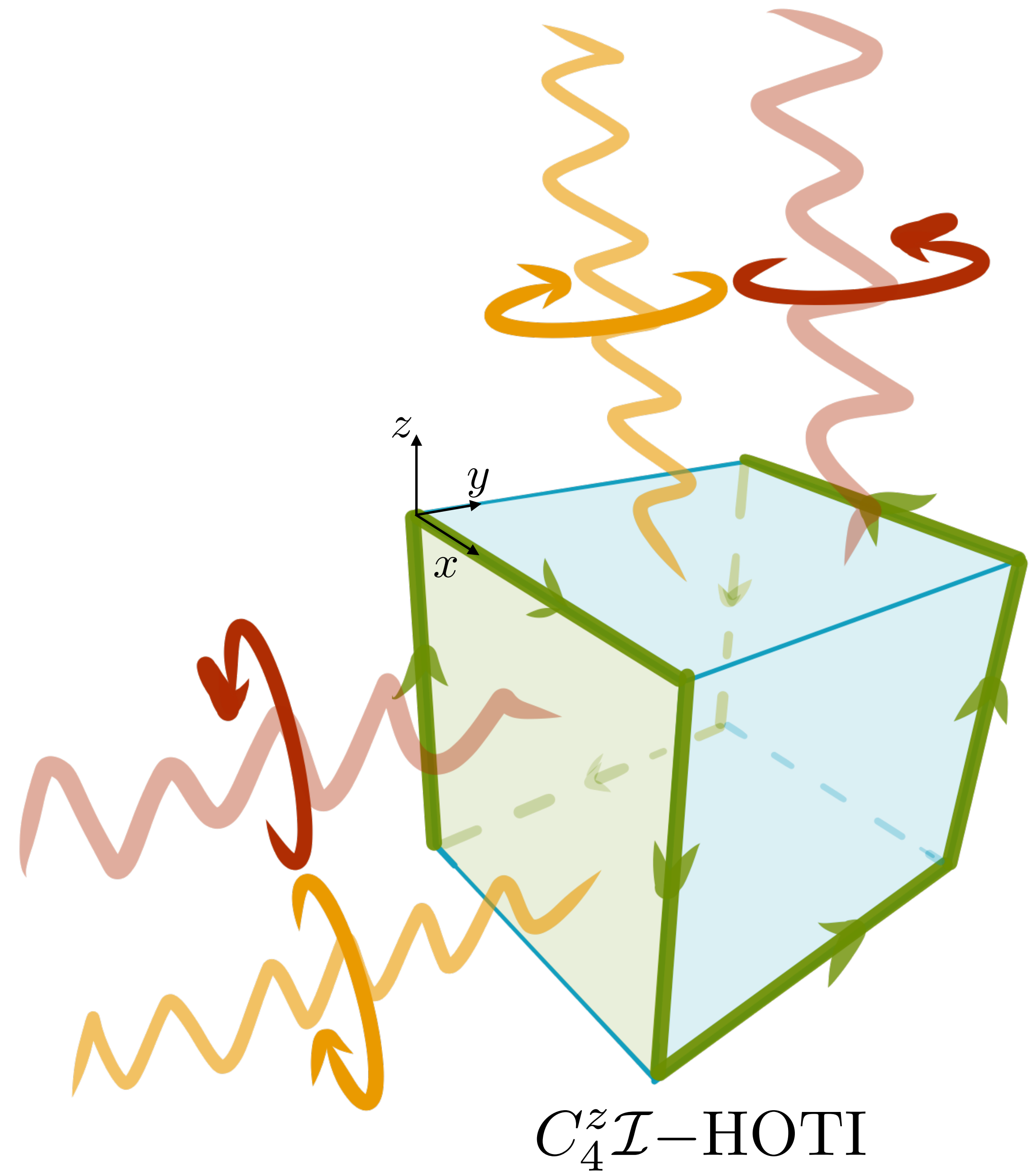
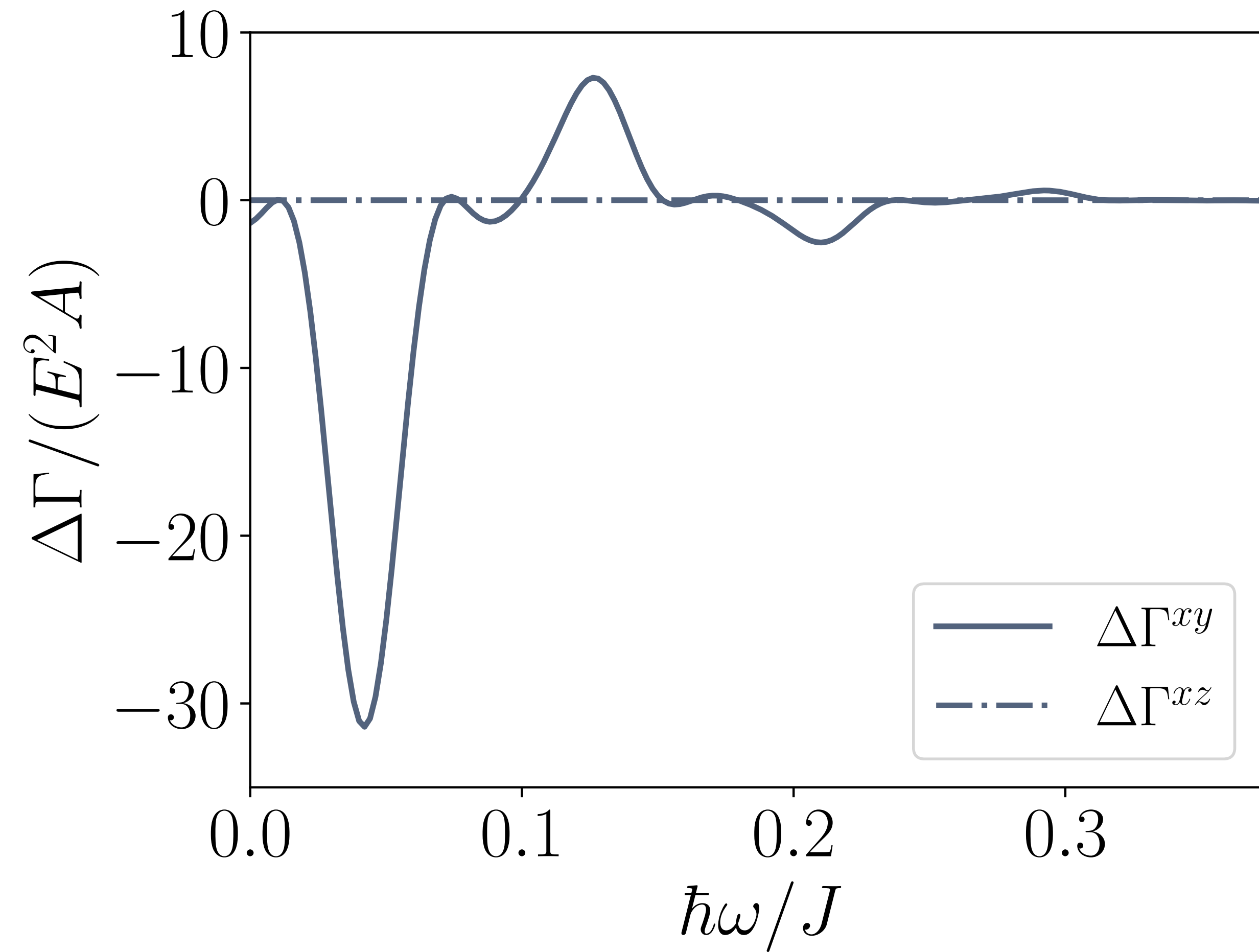


\mathcal{I} -HOTI

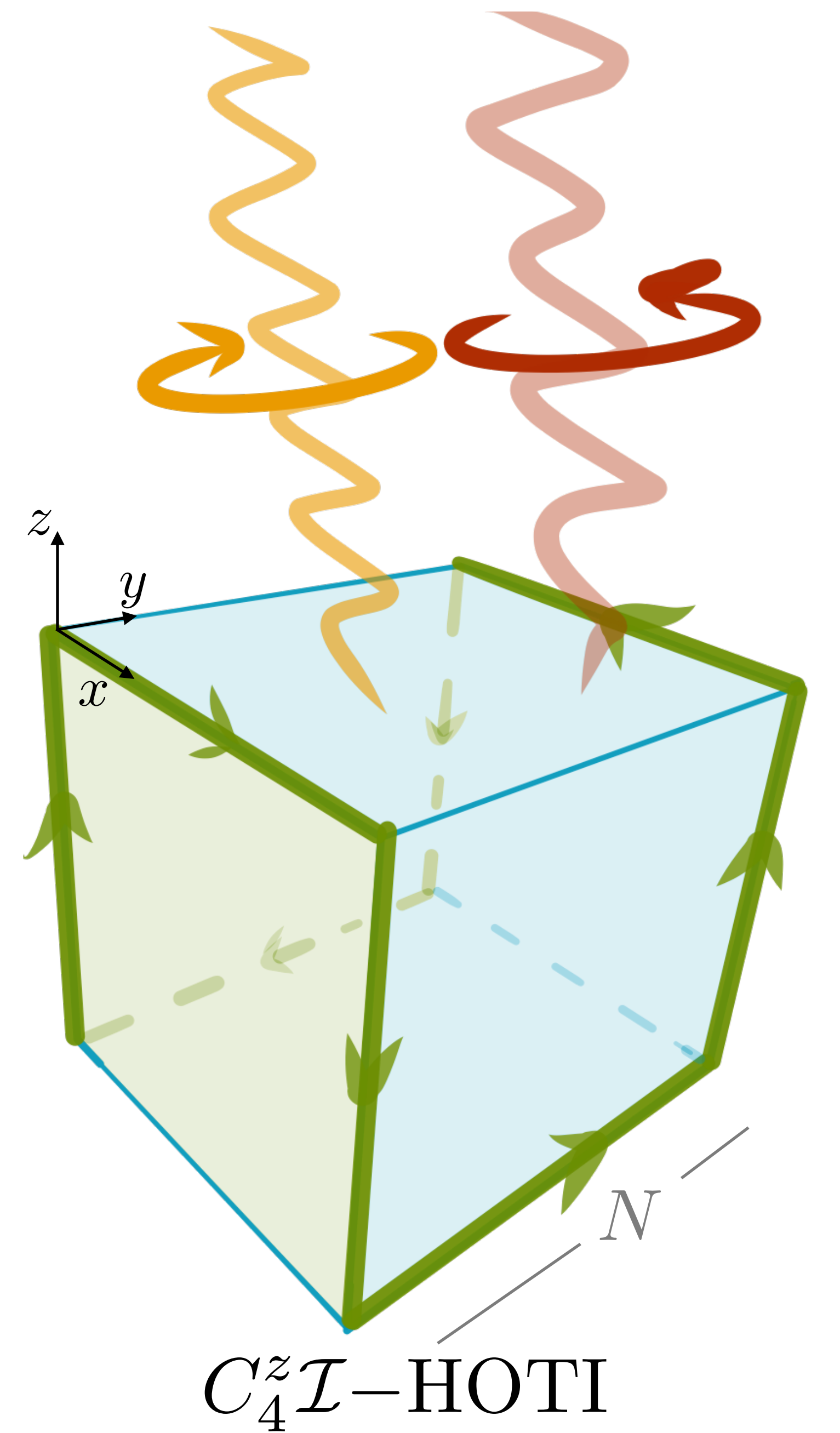
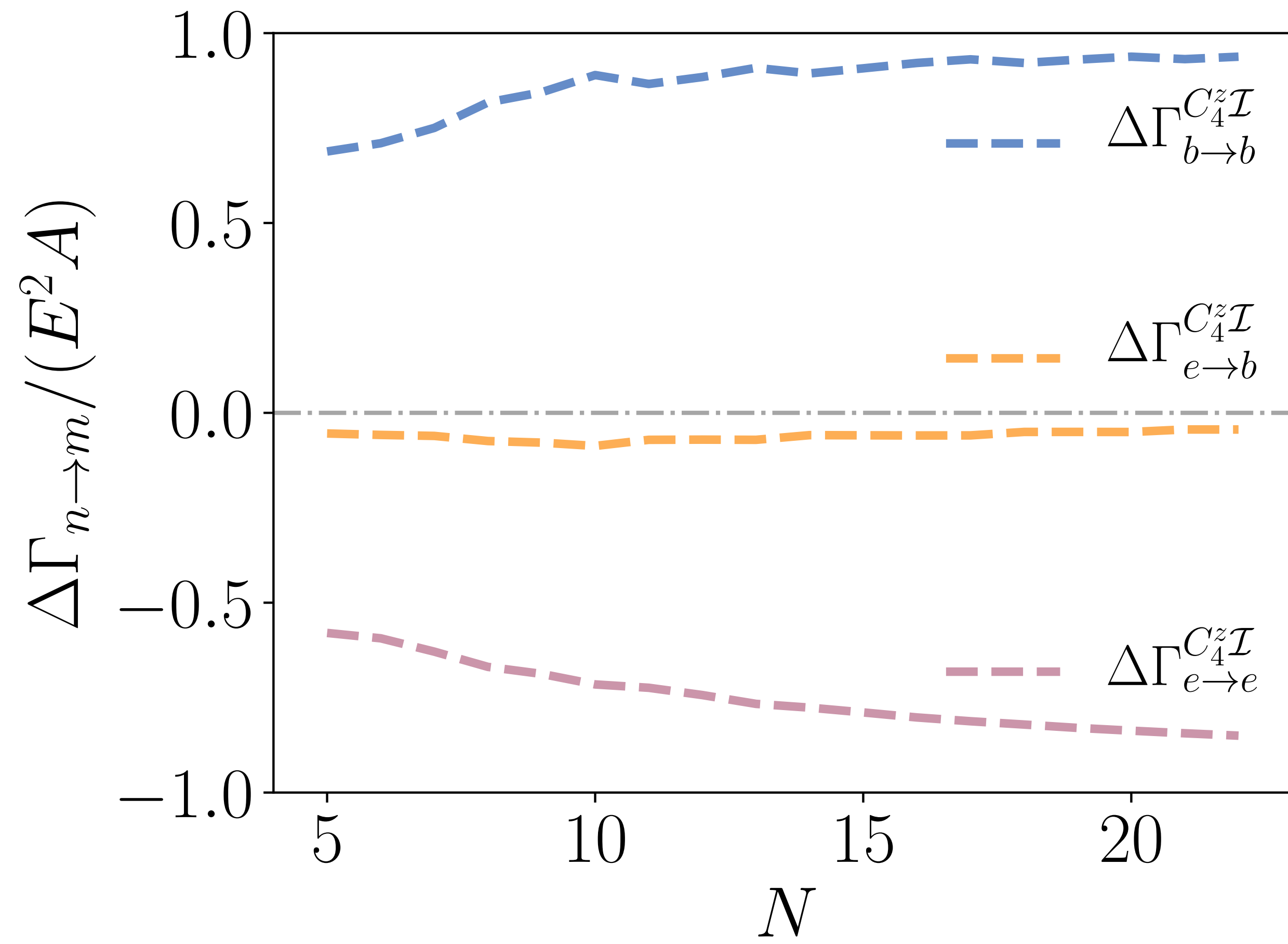


$C_4^z \mathcal{I}$ -HOTI

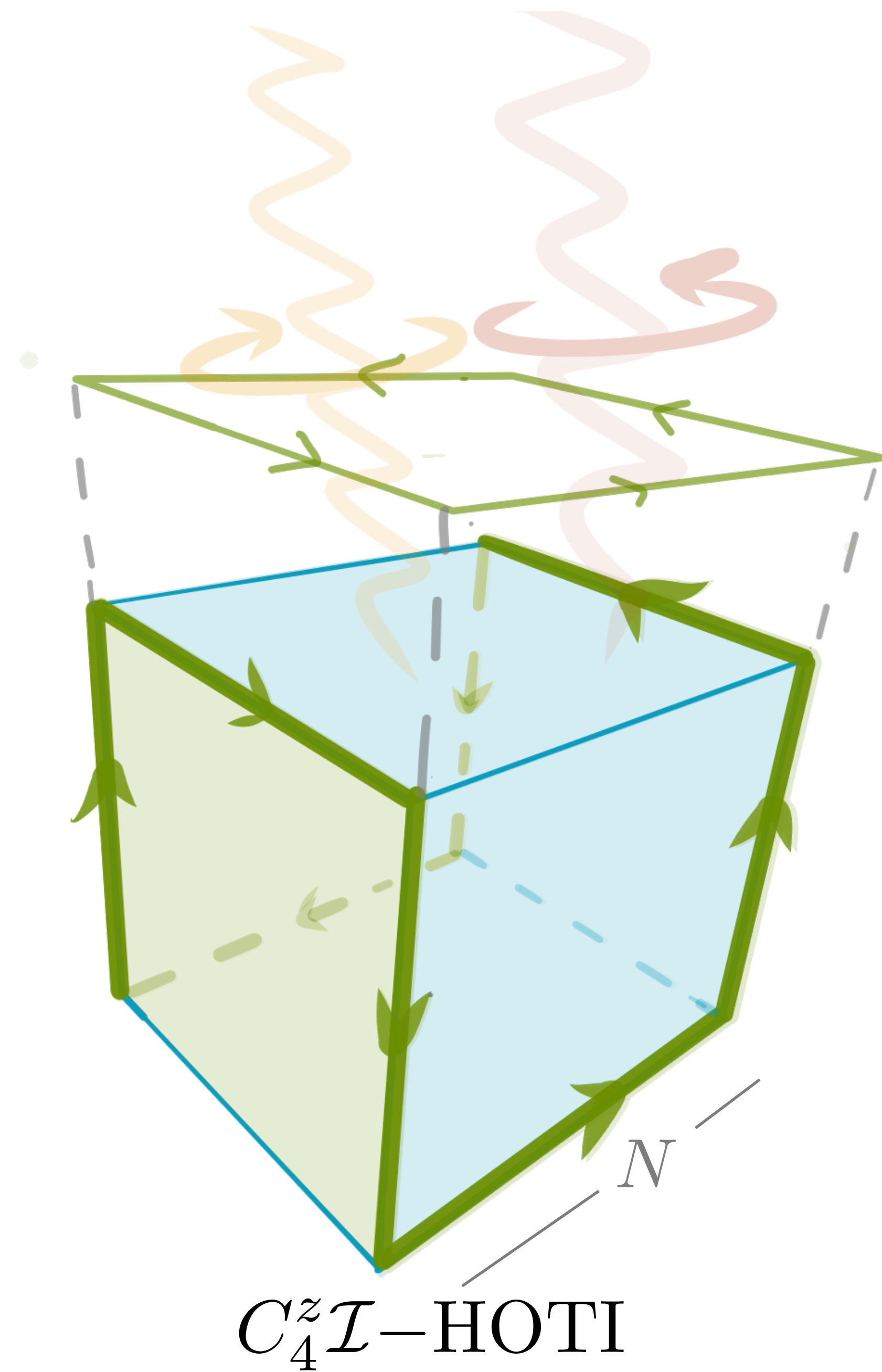
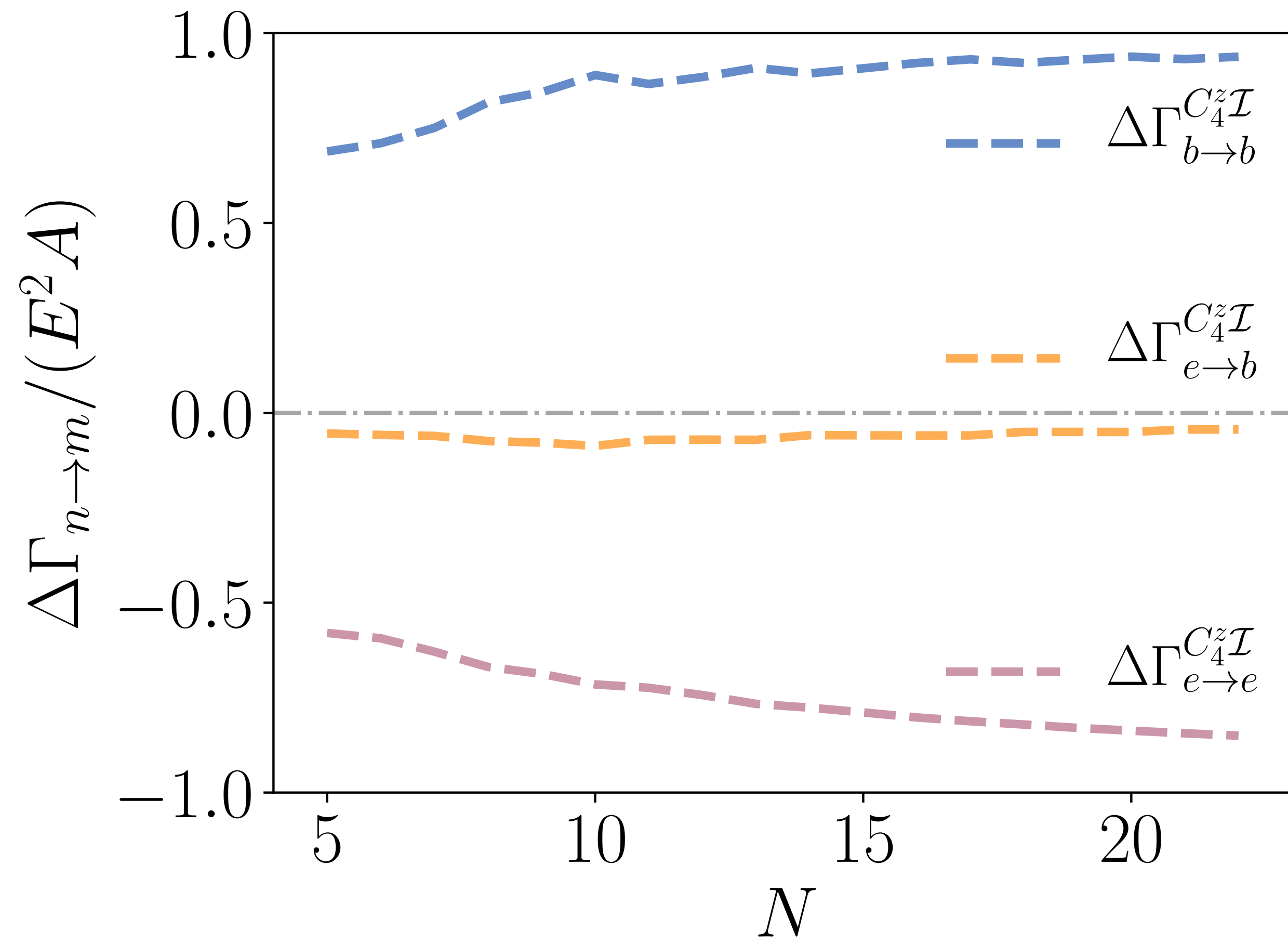
Quantized circular dichroism depends on irradiated surface



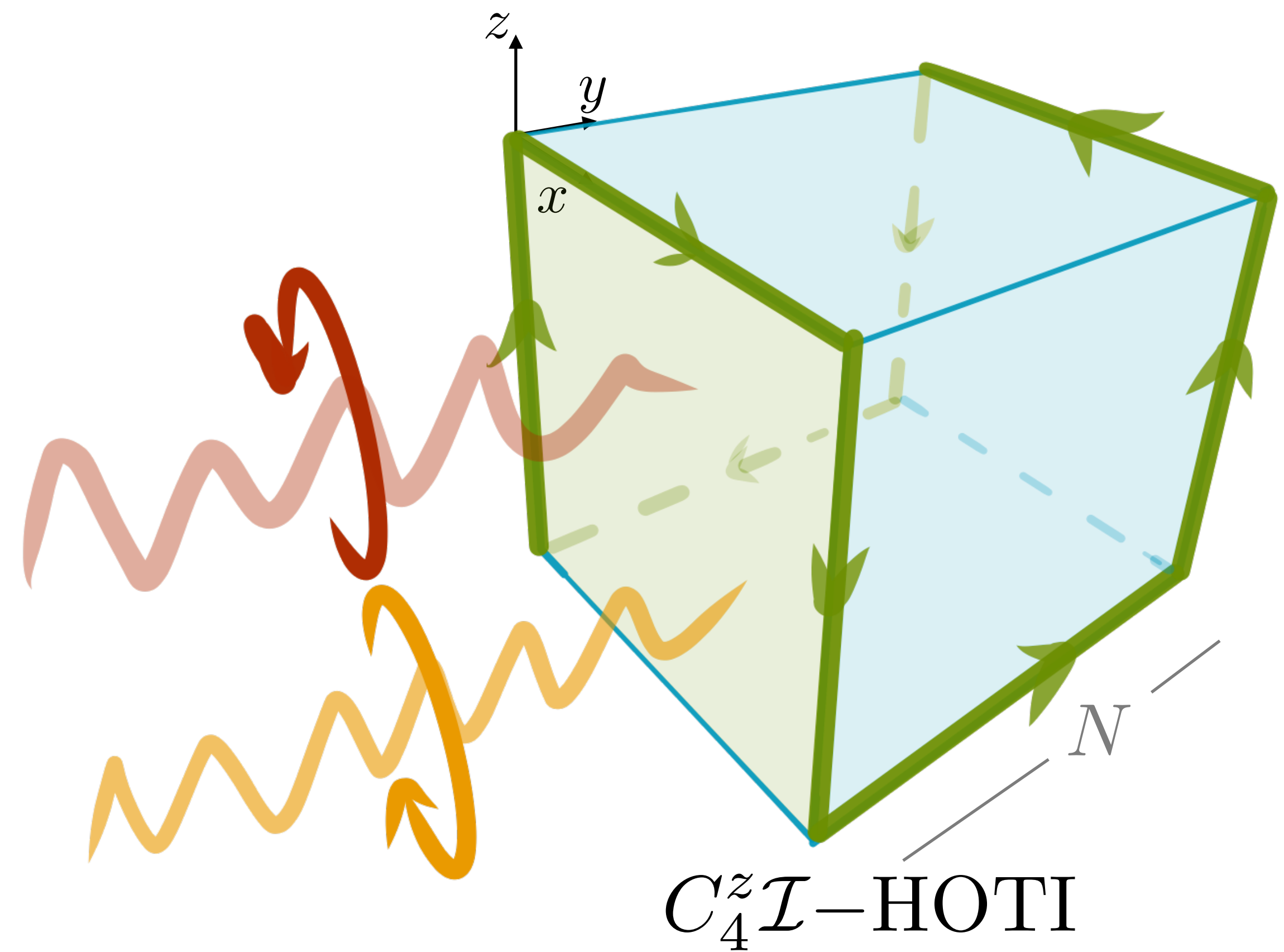
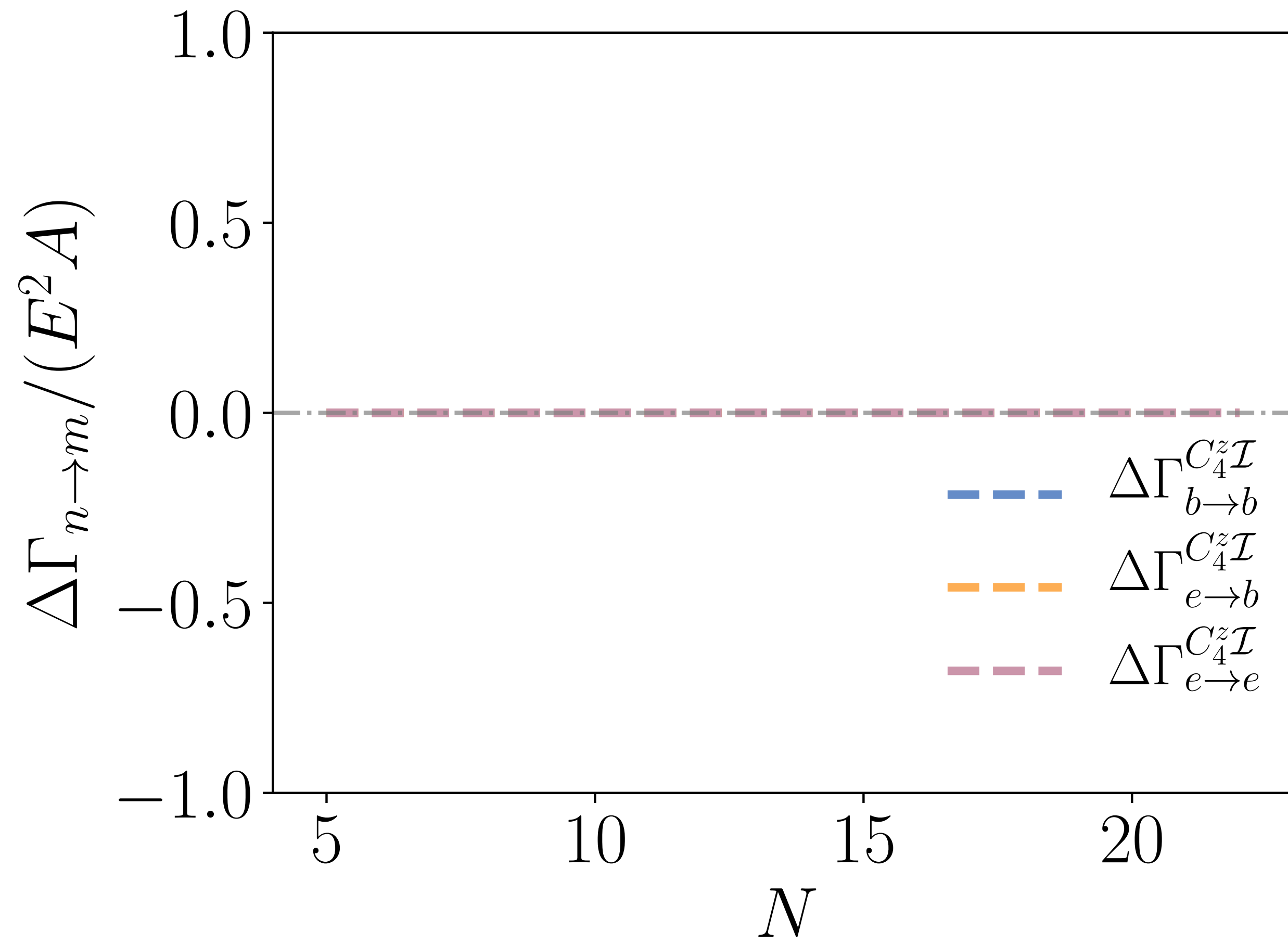
Quantized circular dichroism depends on irradiated surface



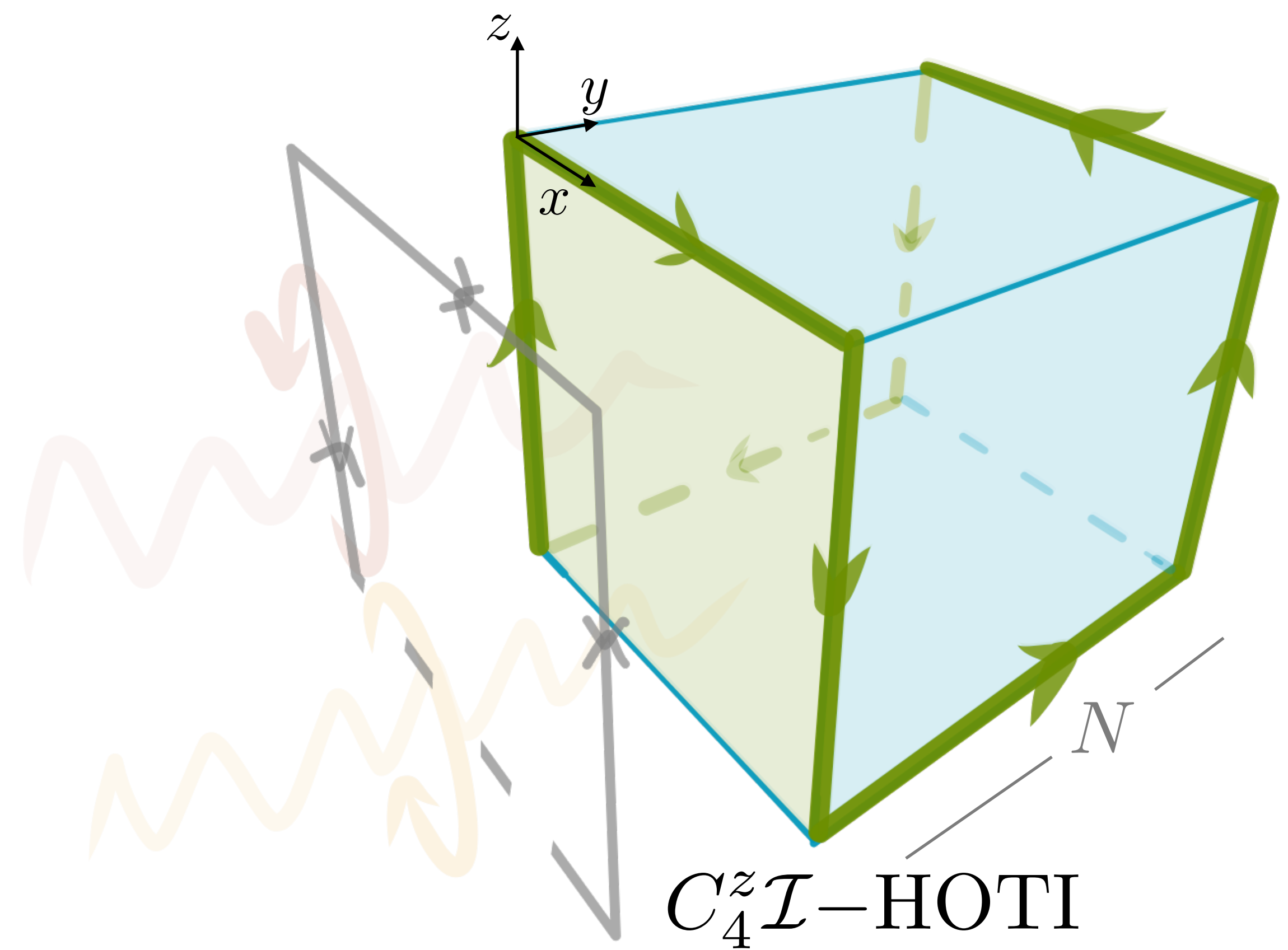
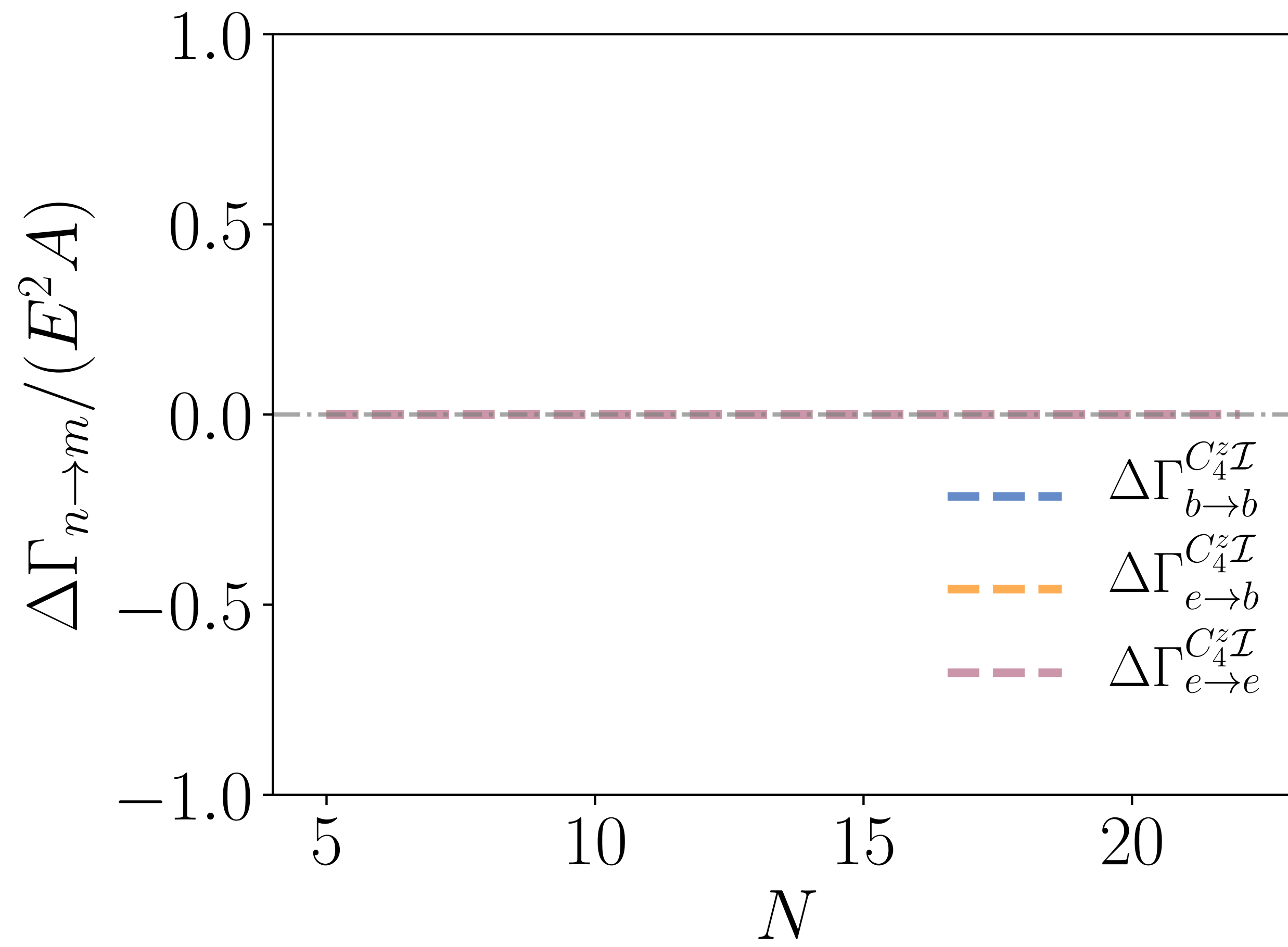
Quantized circular dichroism depends on irradiated surface



Quantized circular dichroism depends on irradiated surface



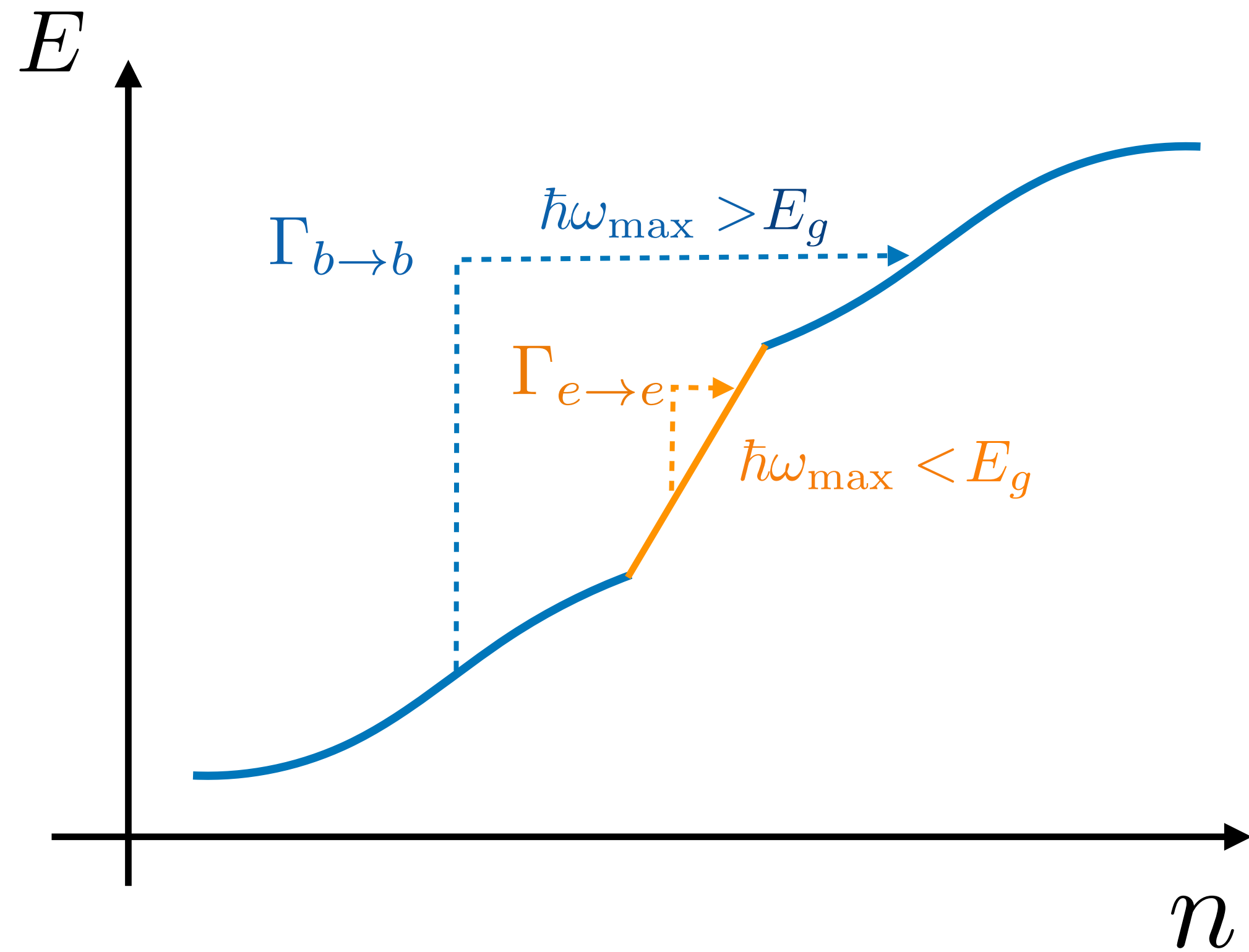
Quantized circular dichroism depends on irradiated surface



...but how can one measure quantization?

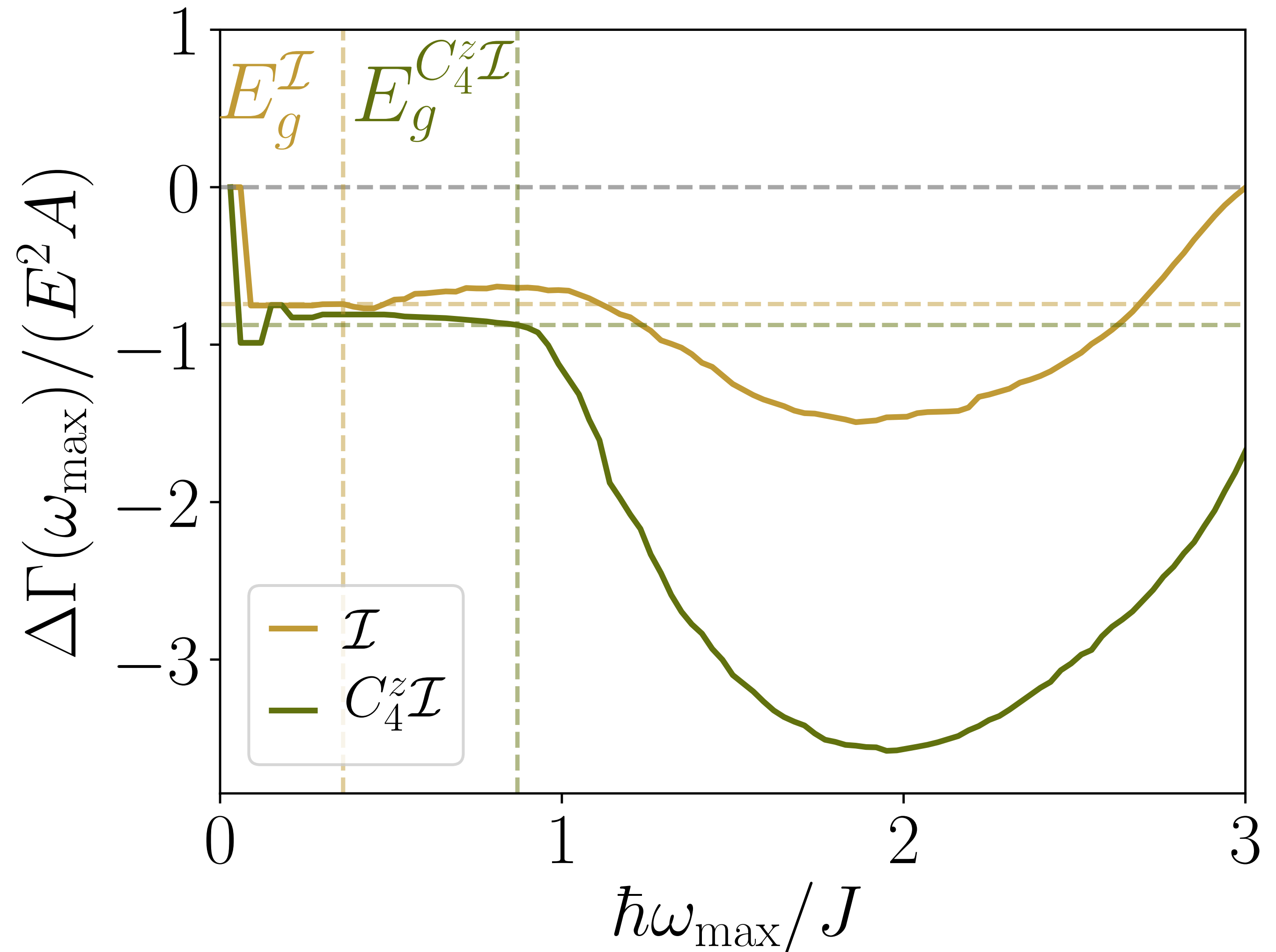
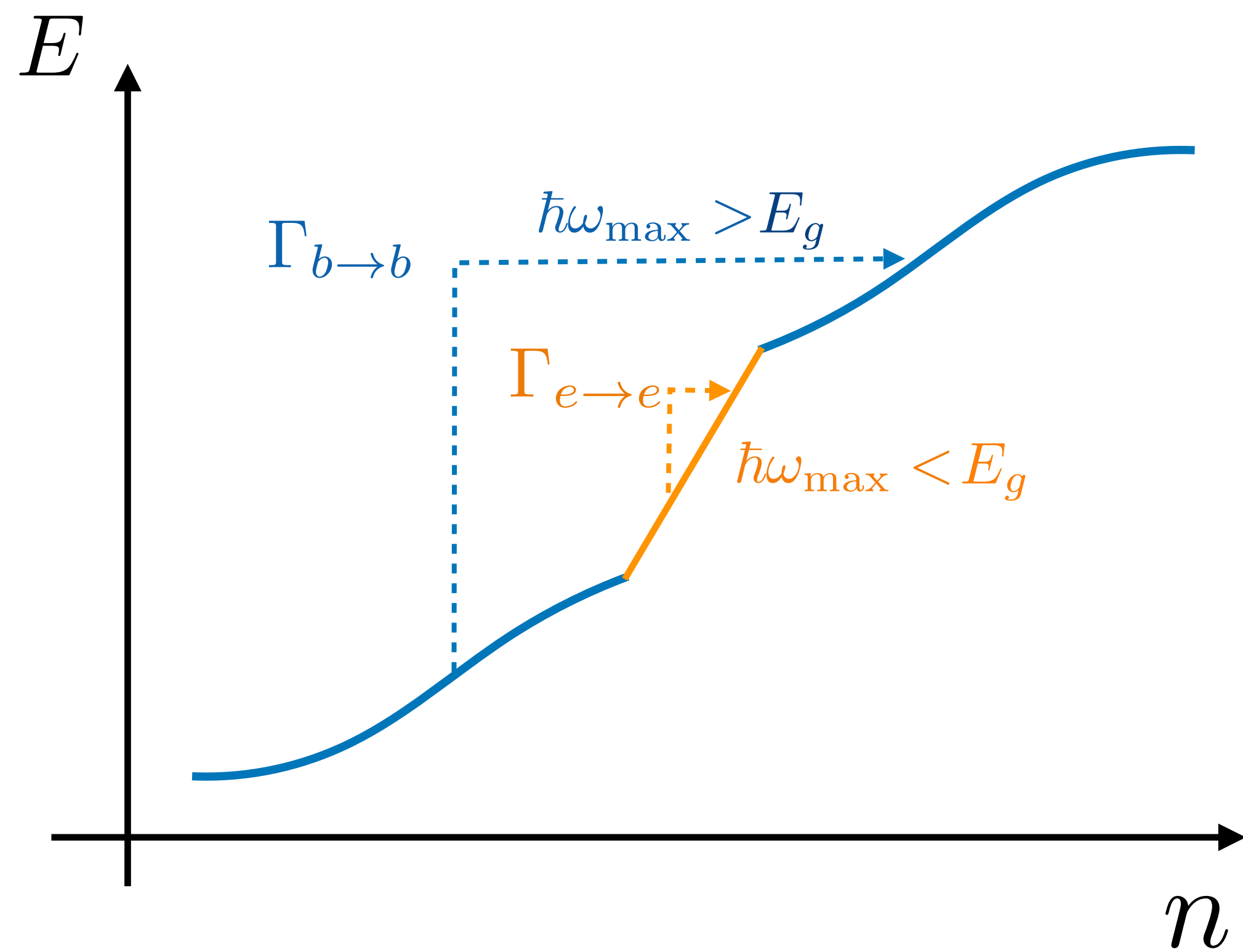
Edge state signal can be filtered out to measure quantization

$$\Delta\Gamma(\omega_{\max}) \equiv \int_0^{\omega_{\max}} d\omega (\Gamma_+(\omega) - \Gamma_-(\omega))/2.$$



Edge state signal can be filtered out to measure quantization

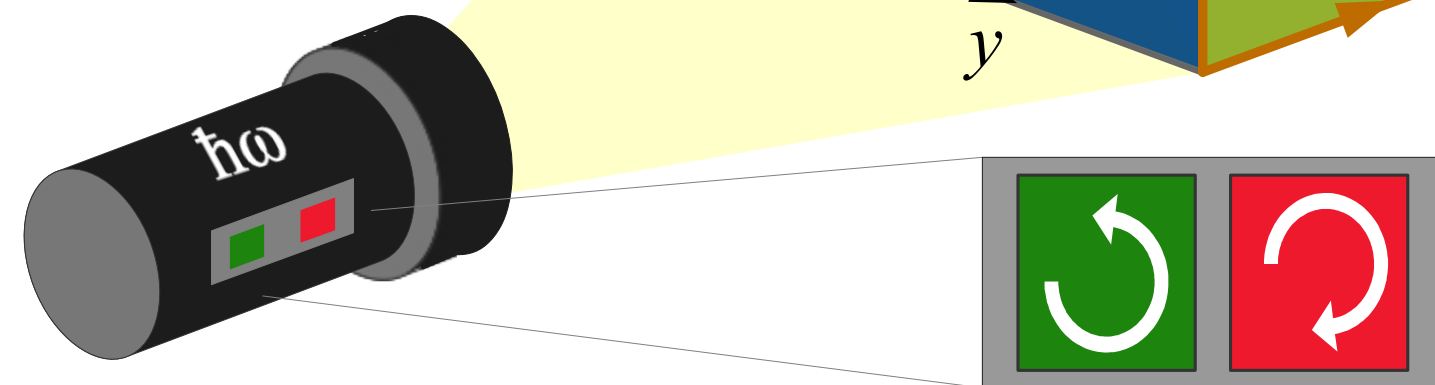
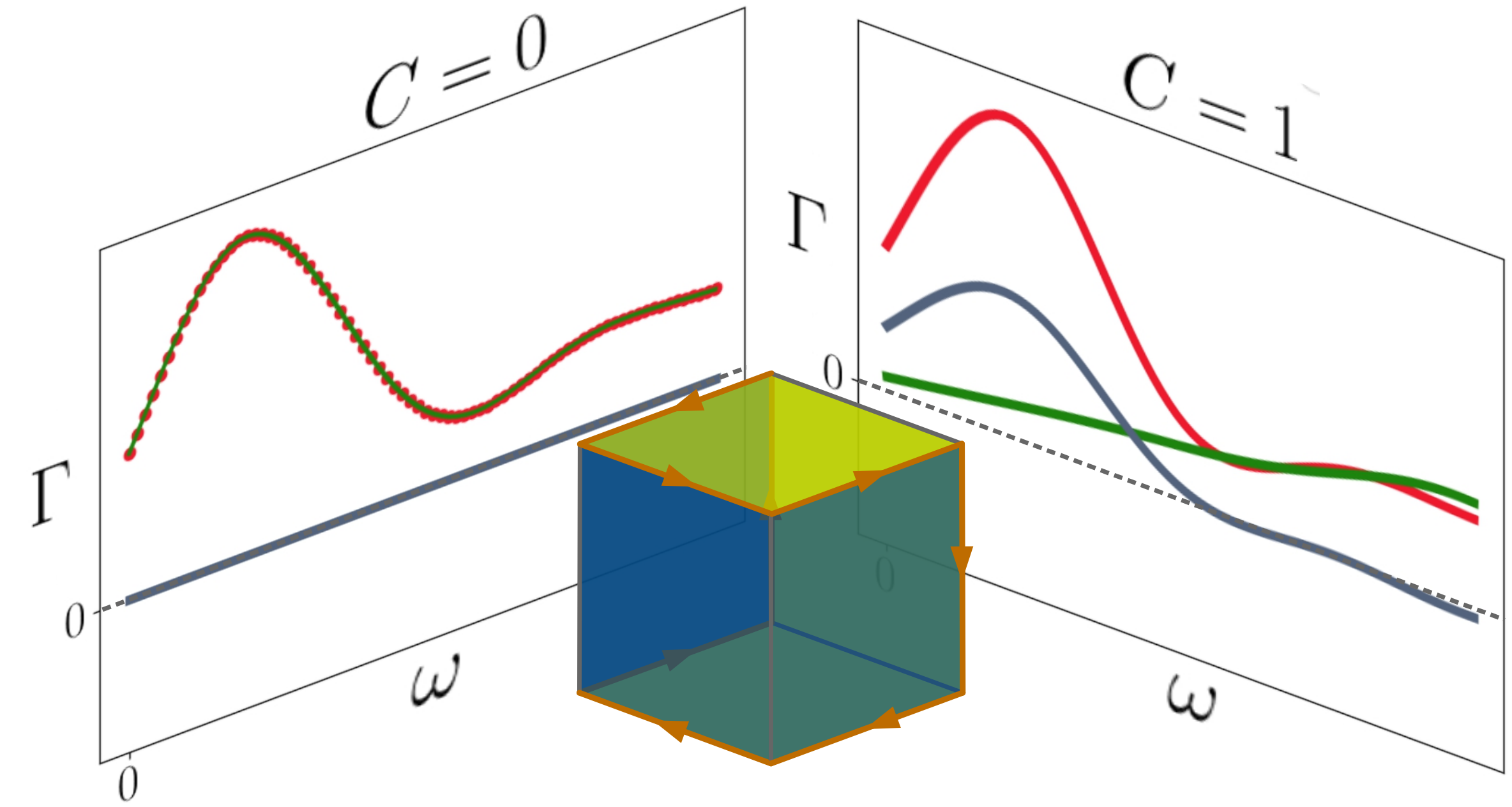
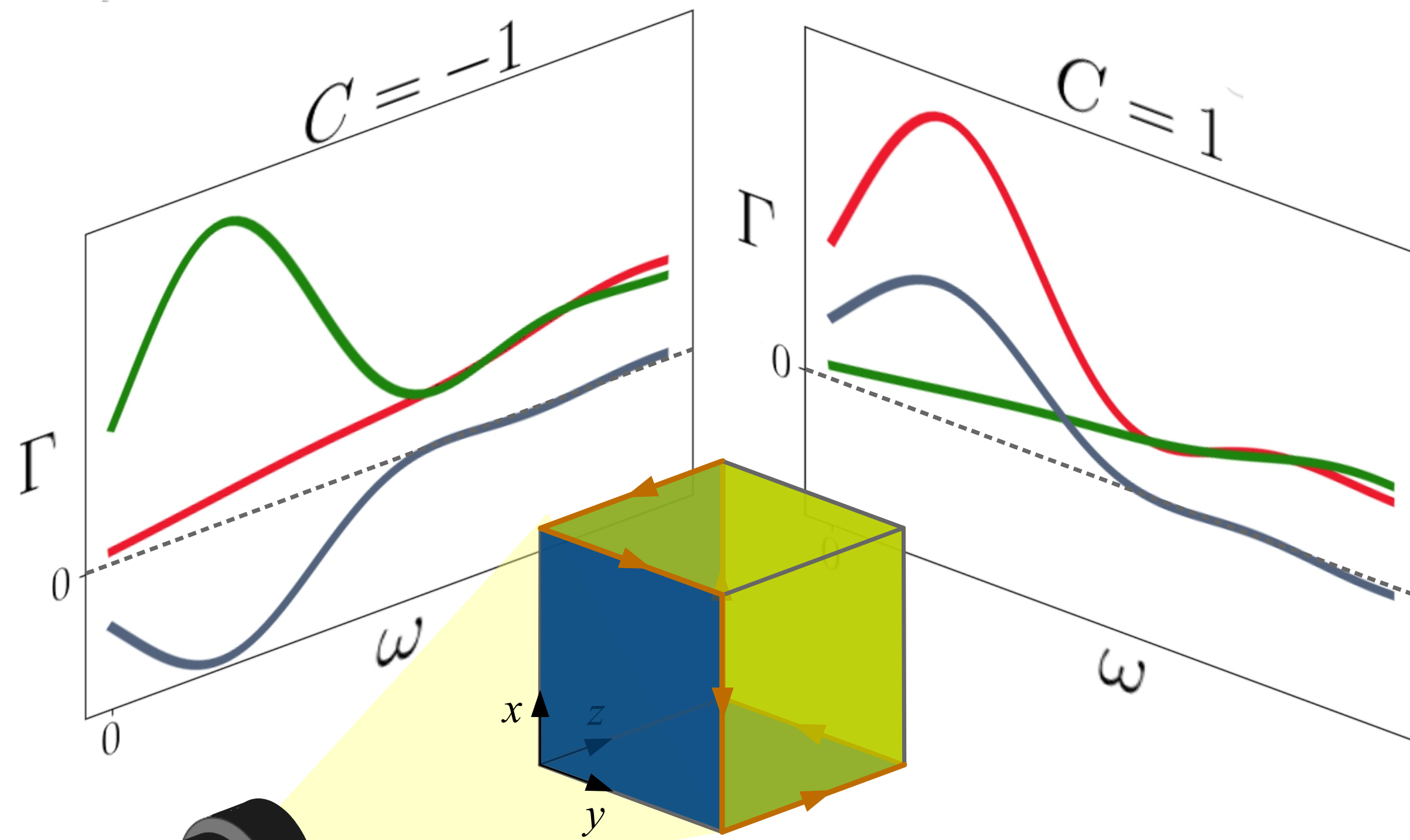
$$\Delta\Gamma(\omega_{\max}) \equiv \int_0^{\omega_{\max}} d\omega (\Gamma_+(\omega) - \Gamma_-(\omega))/2.$$



Quantized circular dichroism distinguishes chiral higher order topological insulators

\mathcal{I} -HOTI

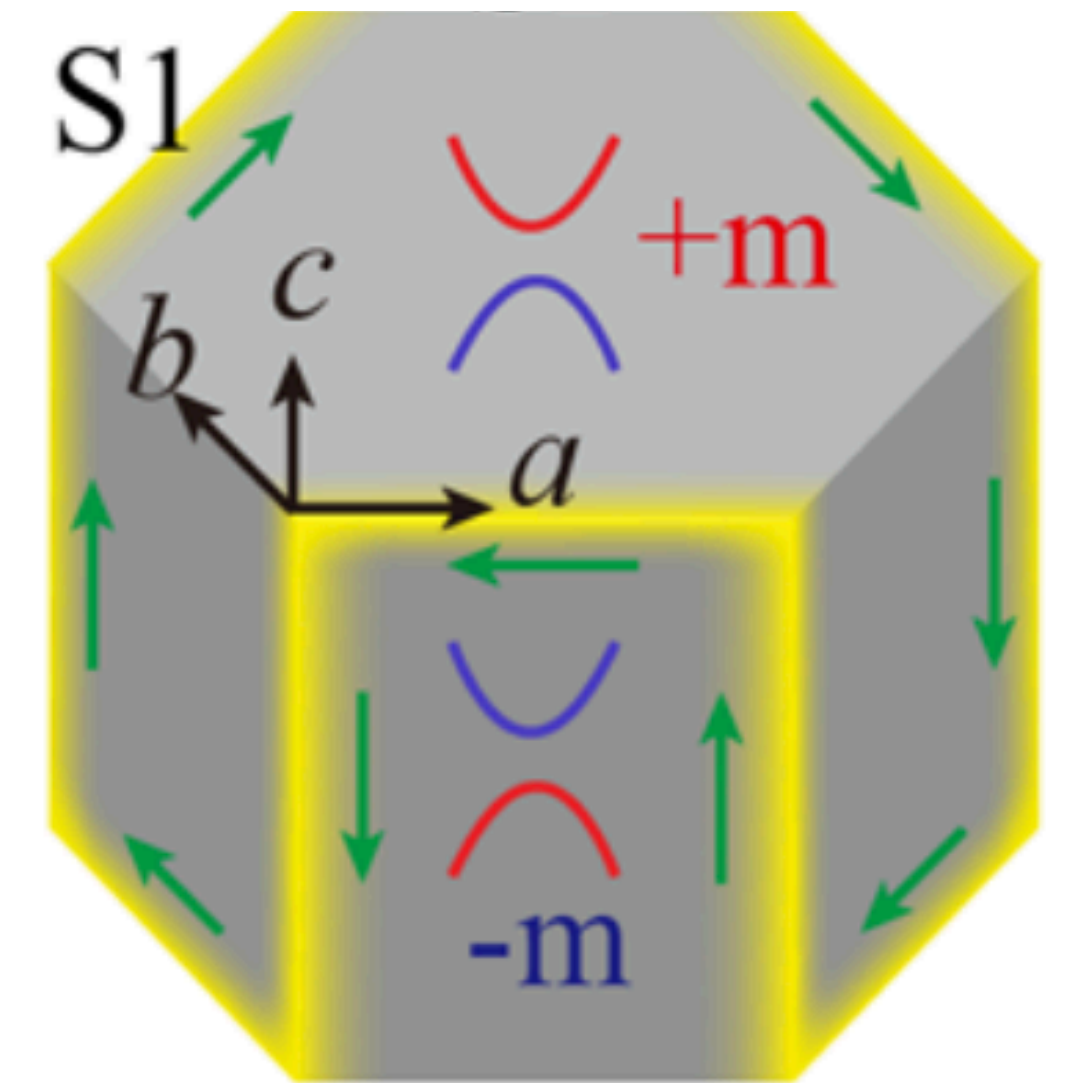
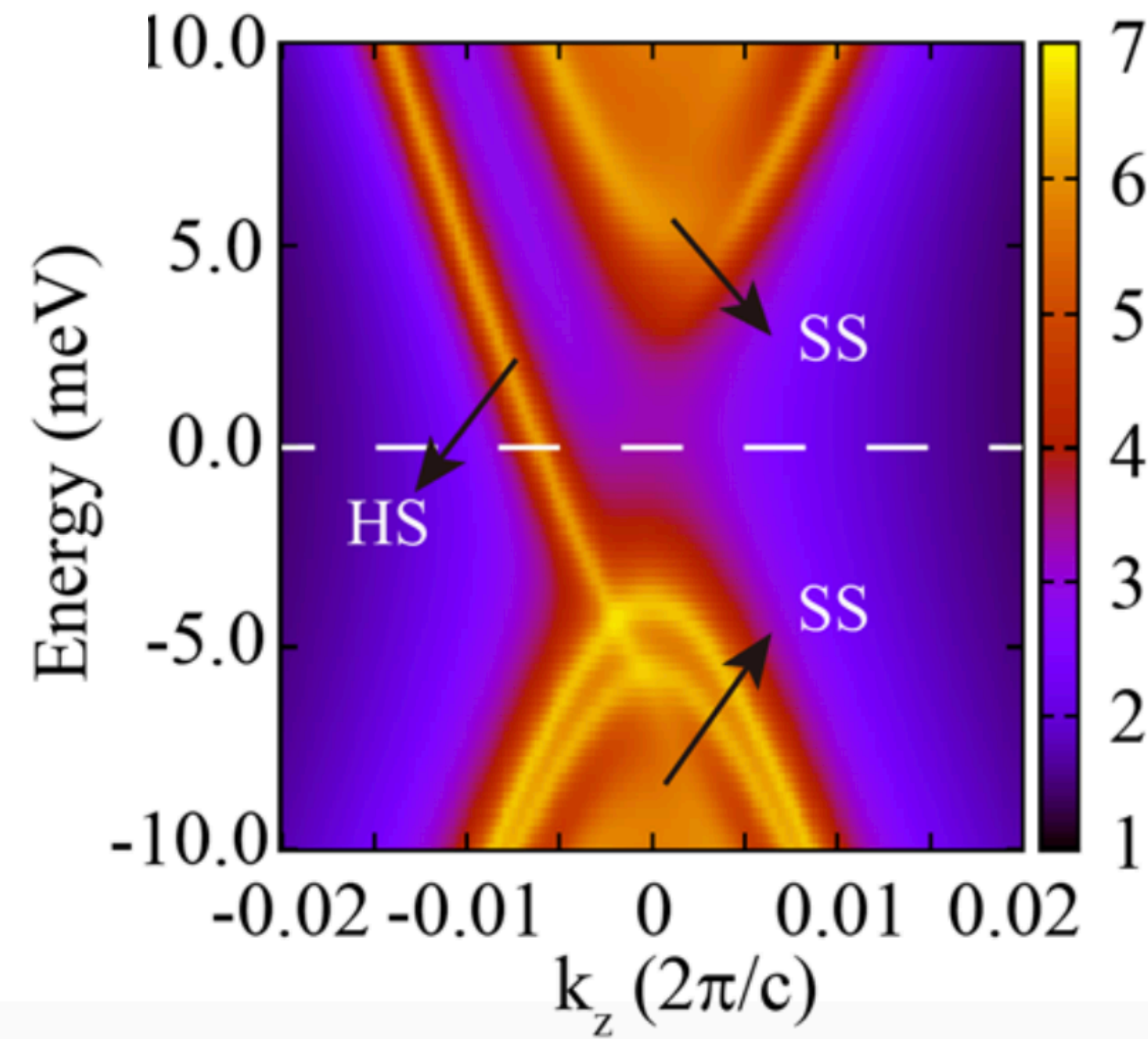
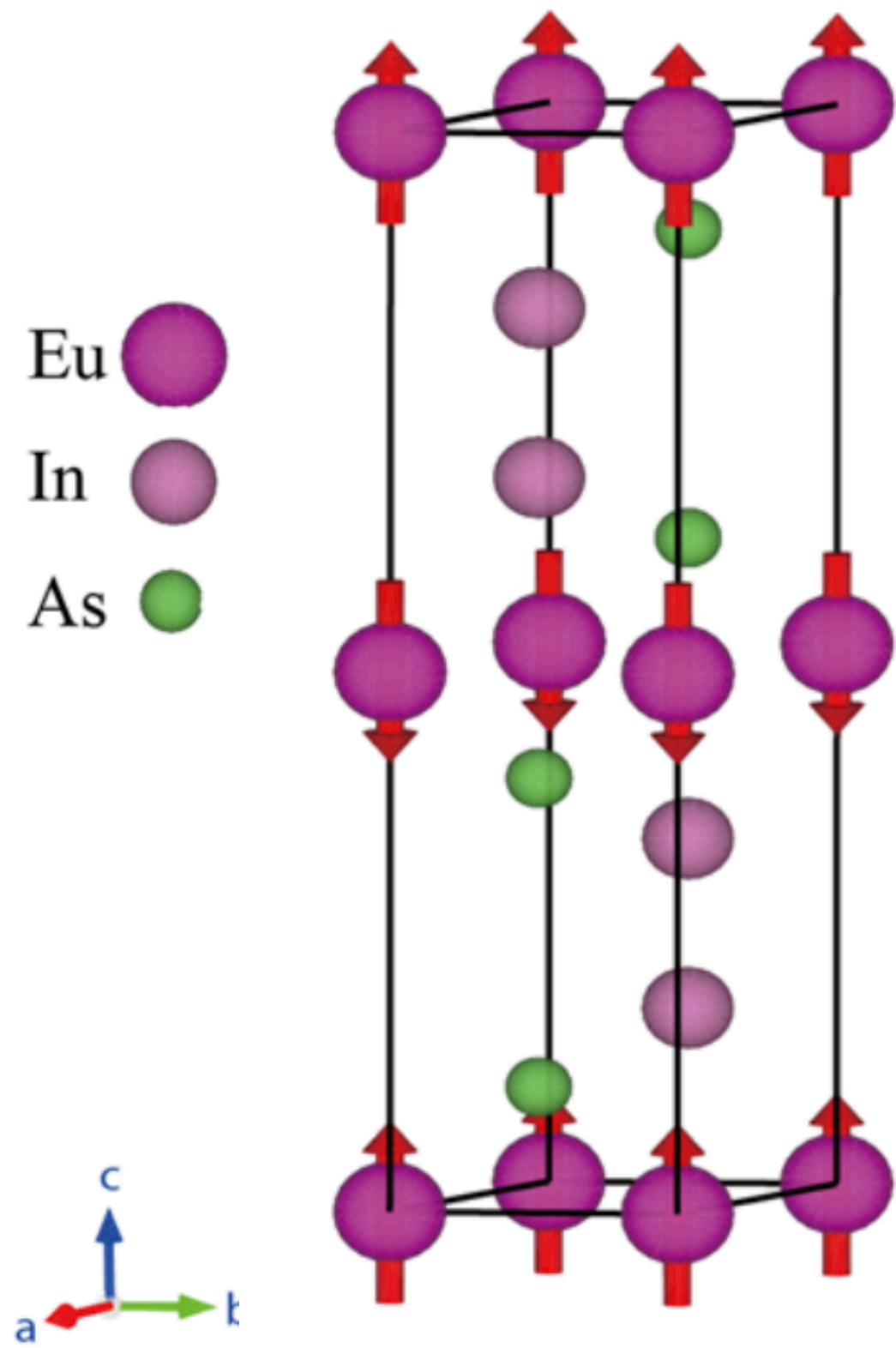
$C_4^z \mathcal{I}$ -HOTI



$$\Delta\Gamma = \frac{\Gamma_+ - \Gamma_-}{2}$$

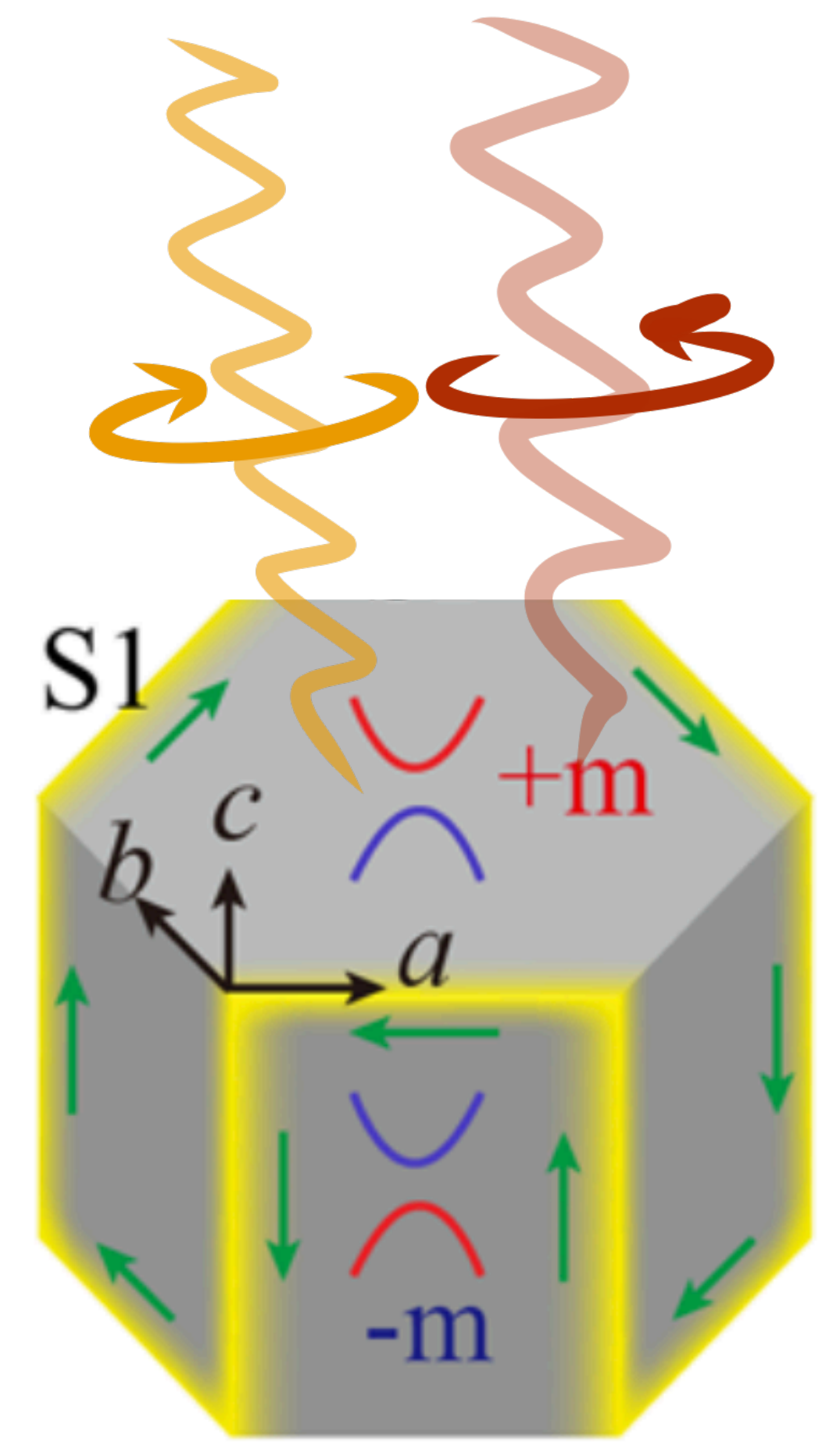
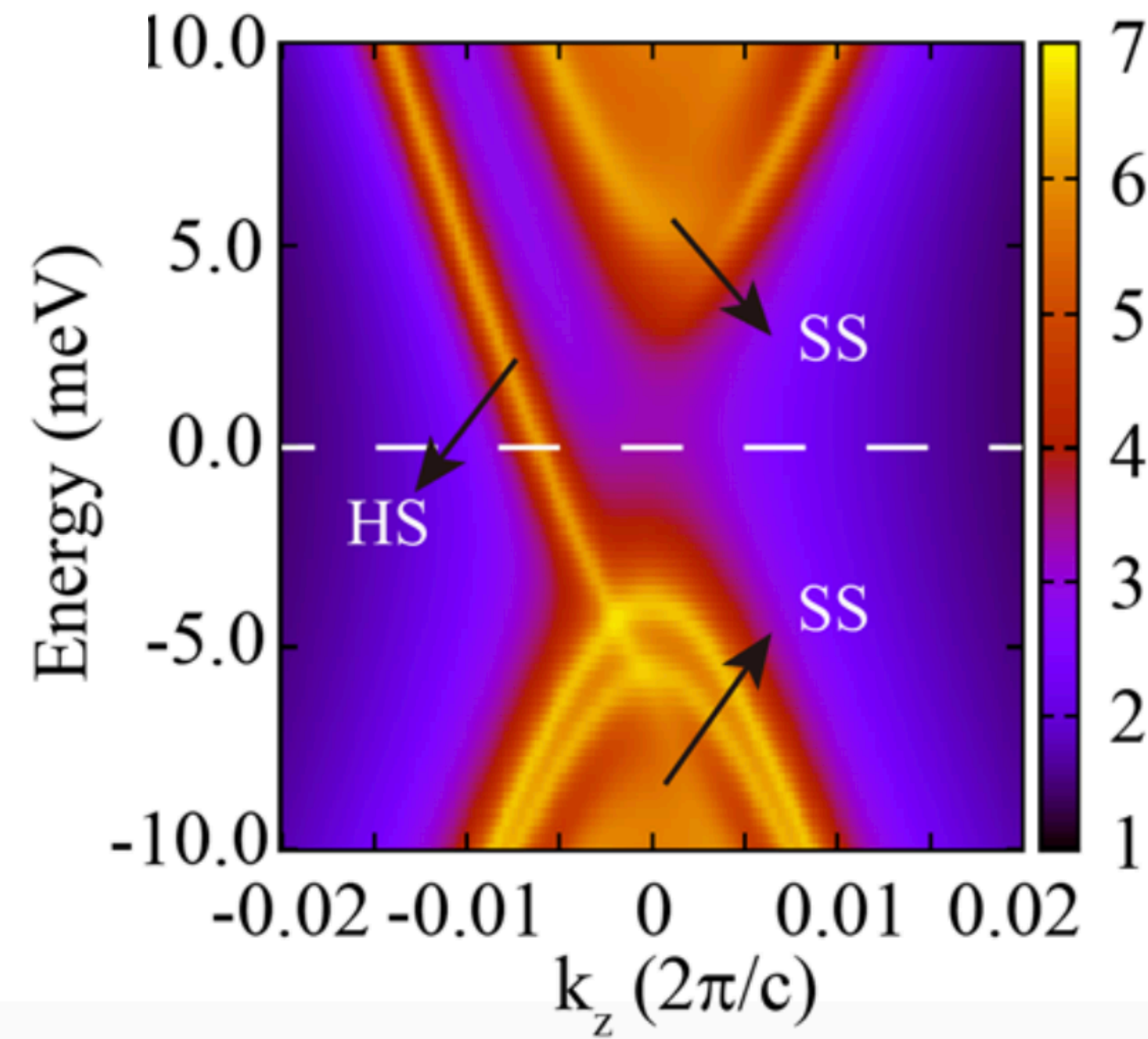
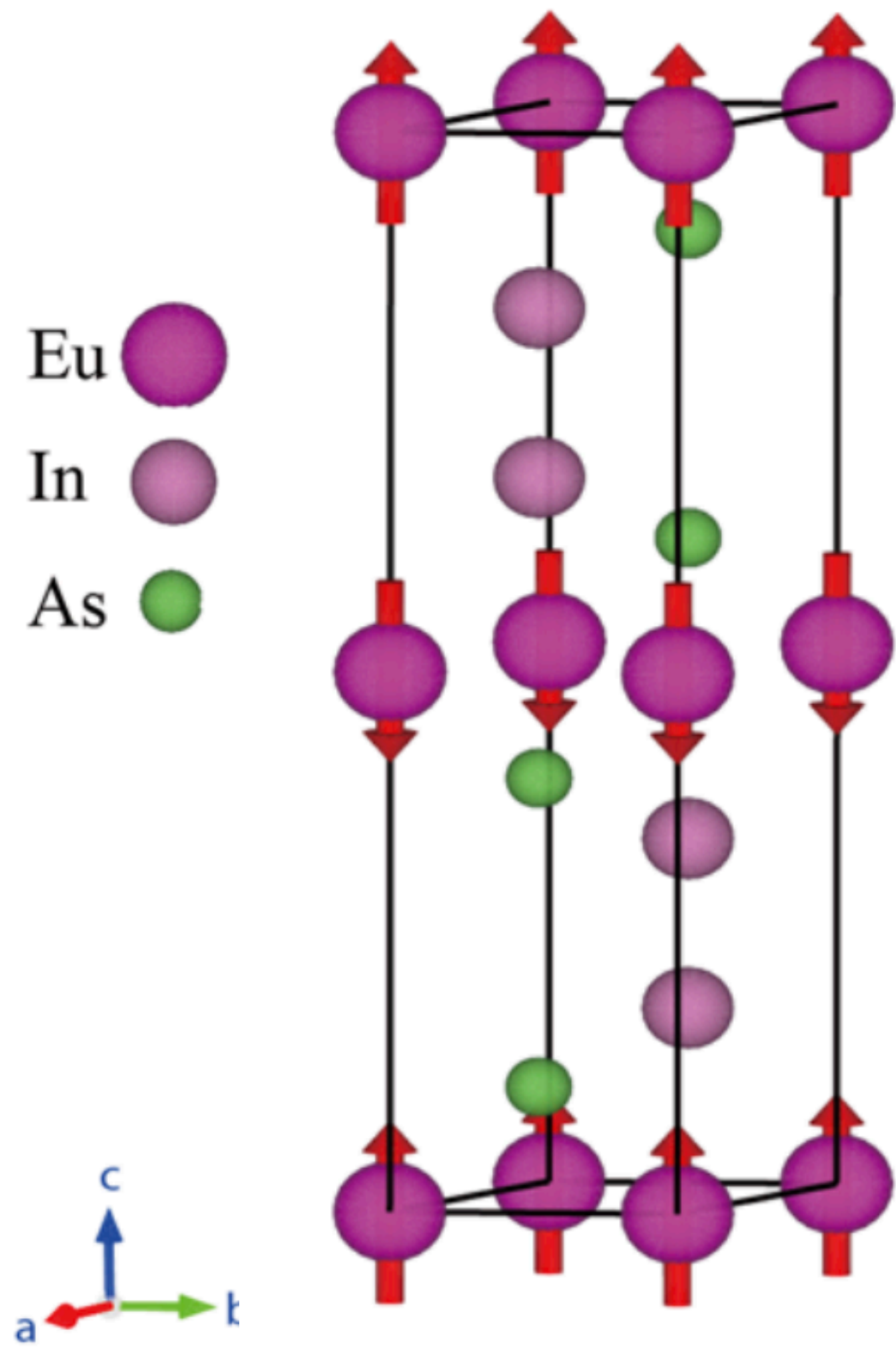
Experiments?

EuIn_2As_2



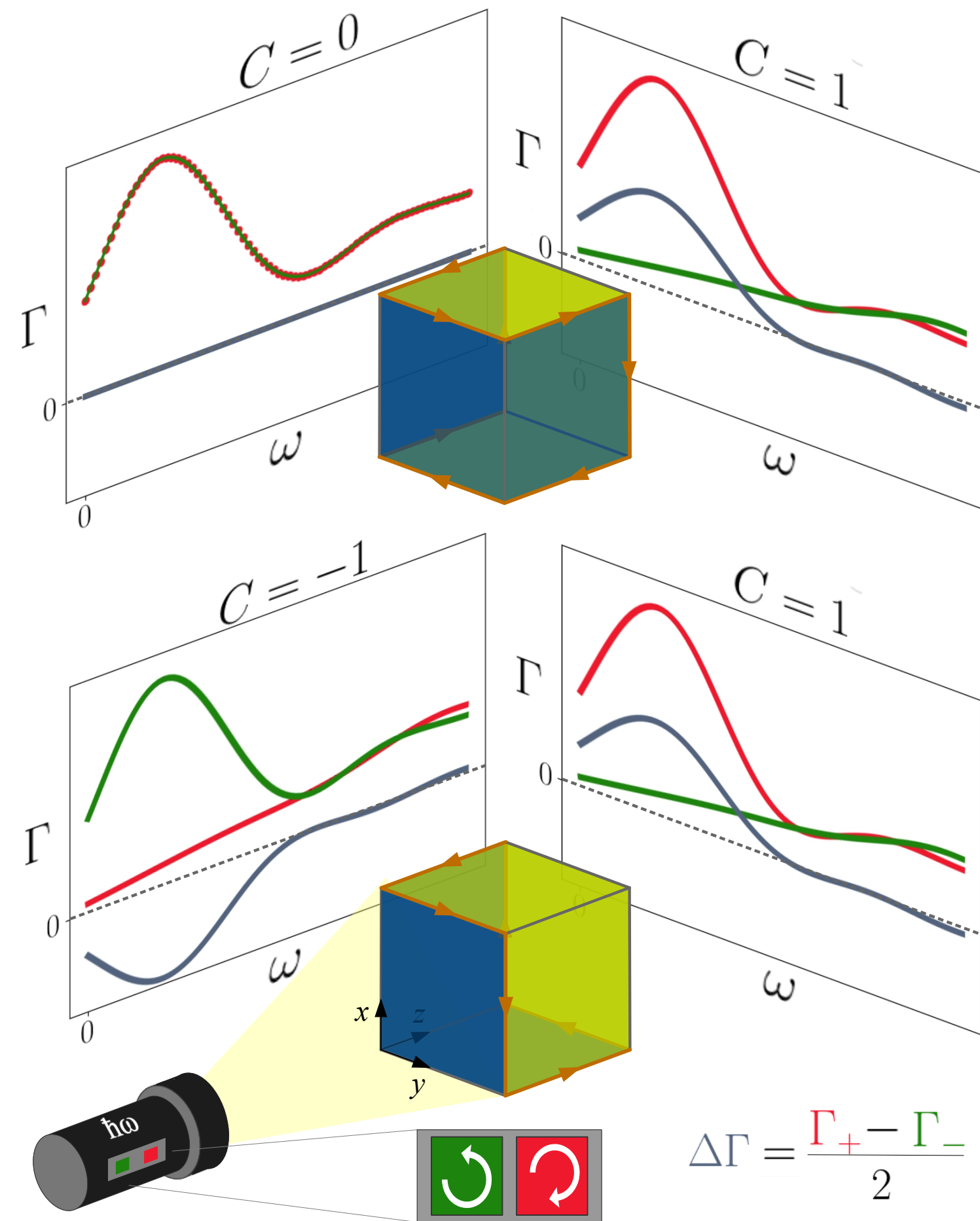
Experiments?

EuIn_2As_2

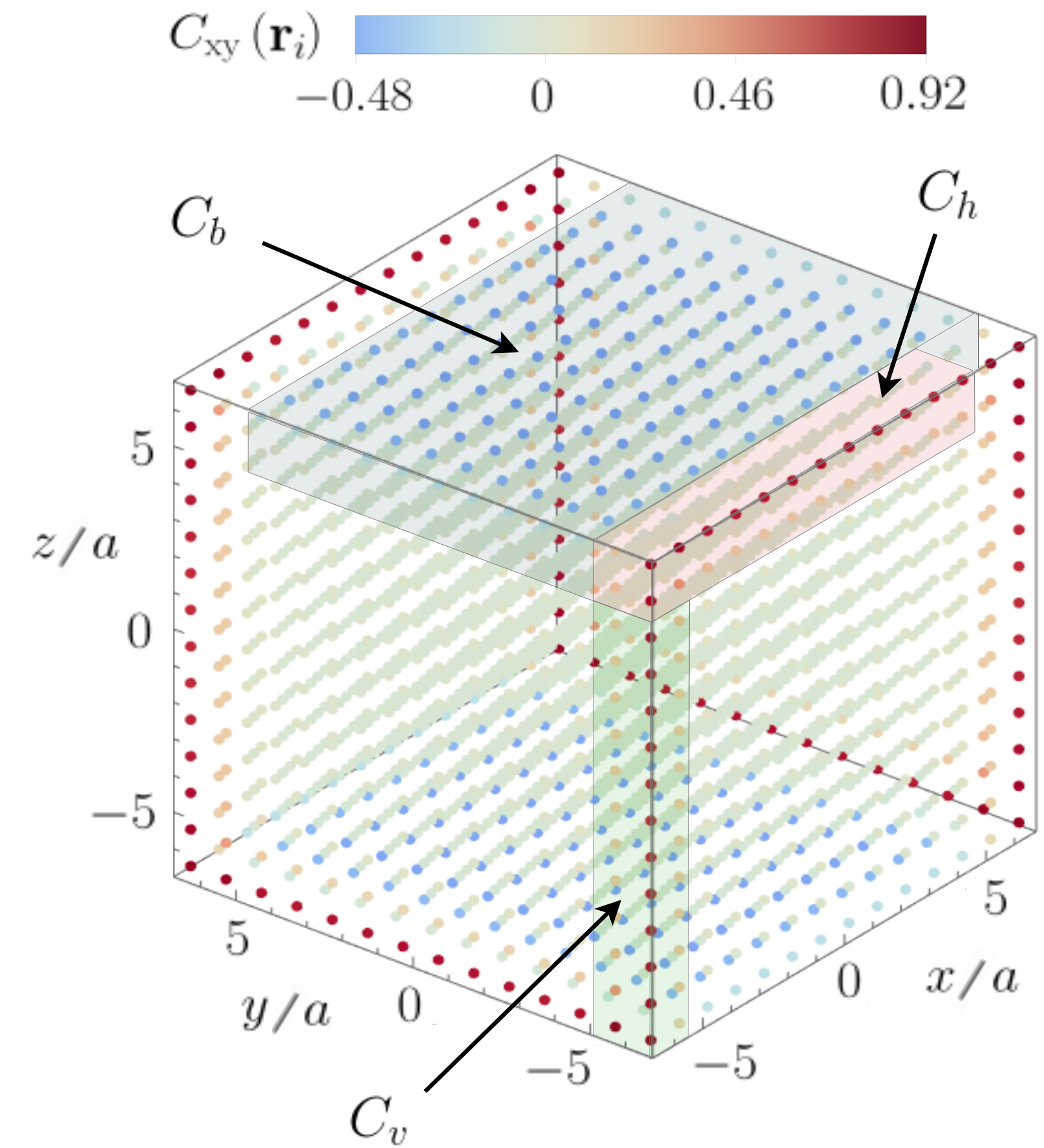


Quantization in chiral higher order topological insulators

Quantized circular dichroism distinguishes HOTIs



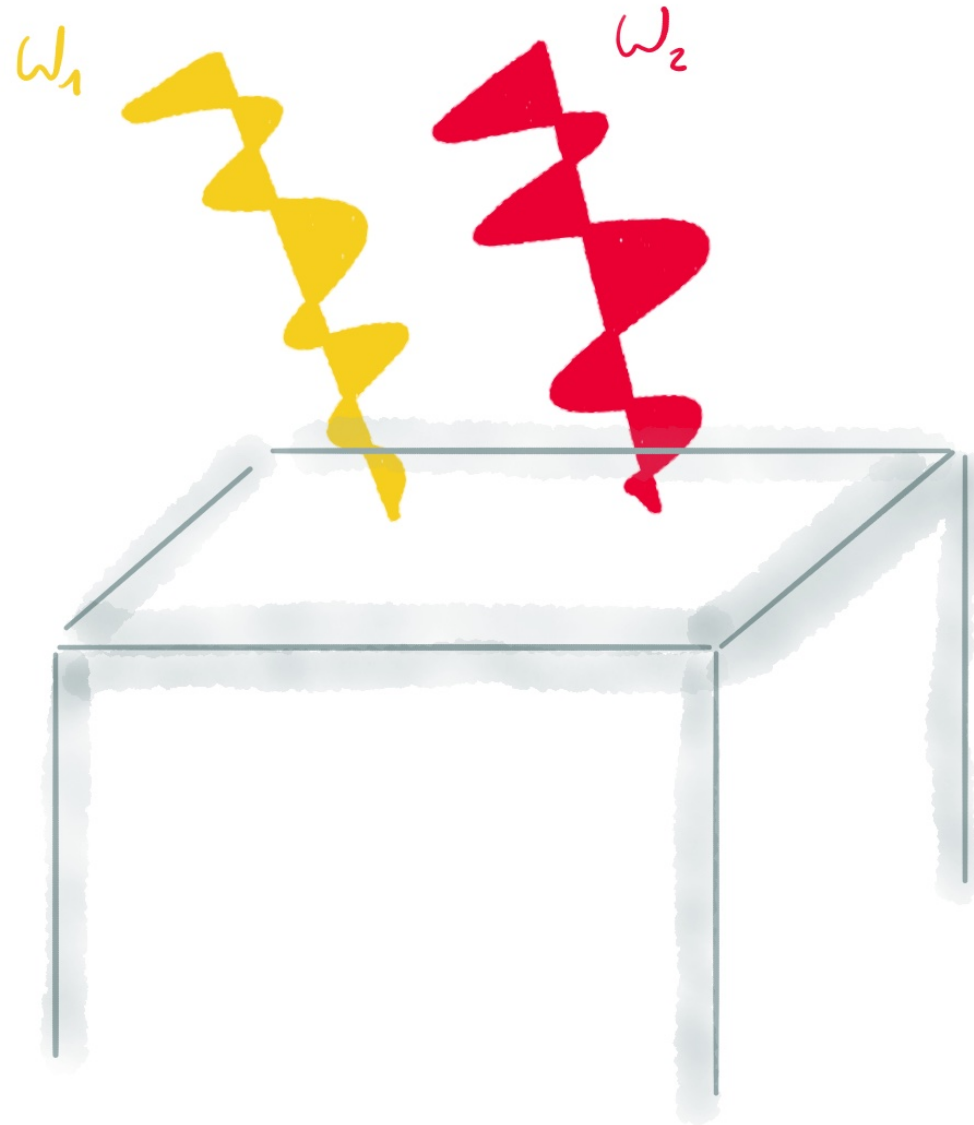
Non-universal surface average of the local Chern marker



Quantized optical responses in chiral insulators and metals

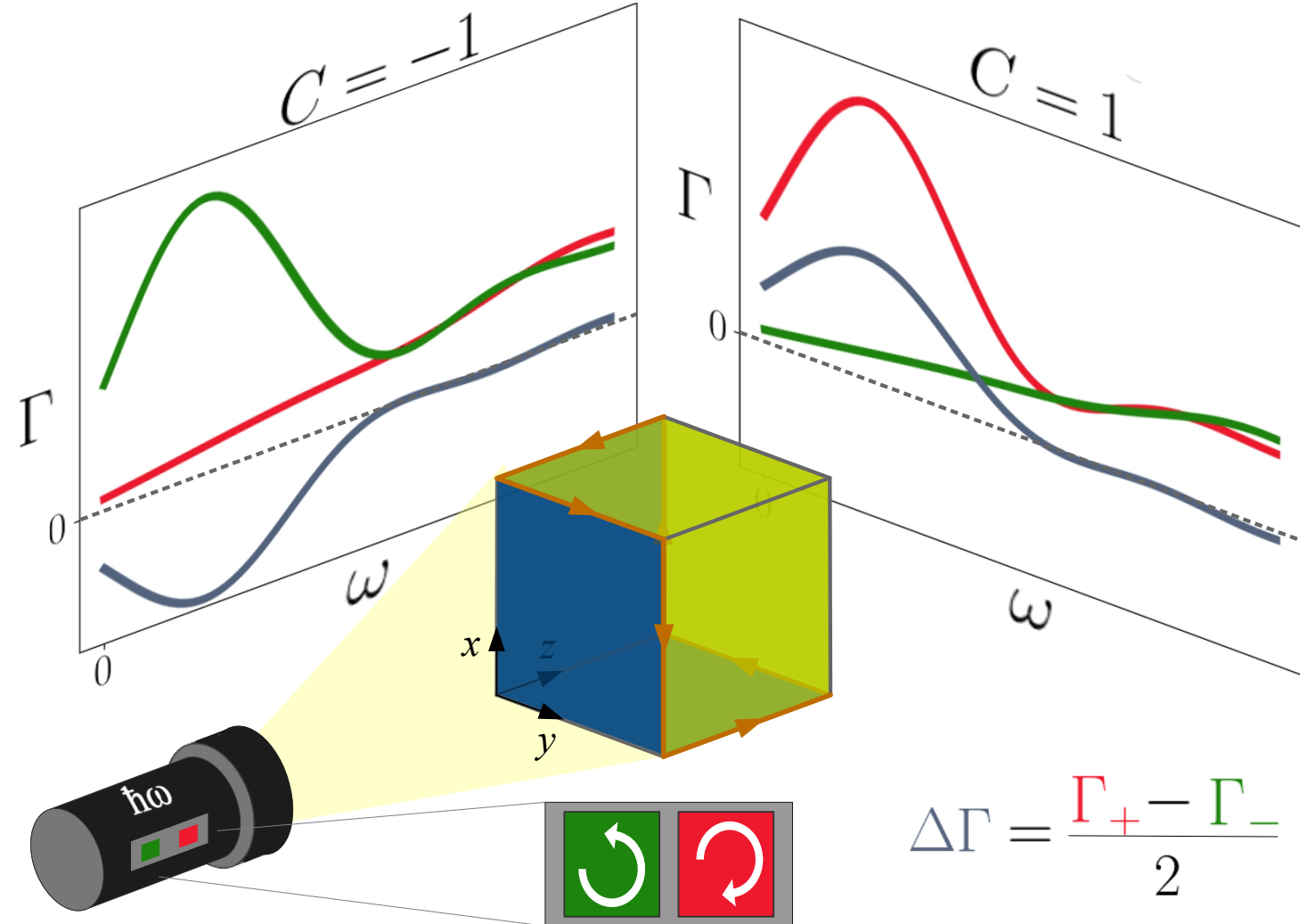
Difference frequency generation reveals quantization and a free carrier response

metallic
1907.02537.
(to appear in PRR)



insulating
1906.05863
(to appear in PRL)

Quantized circular dichroism distinguishes HOTIs

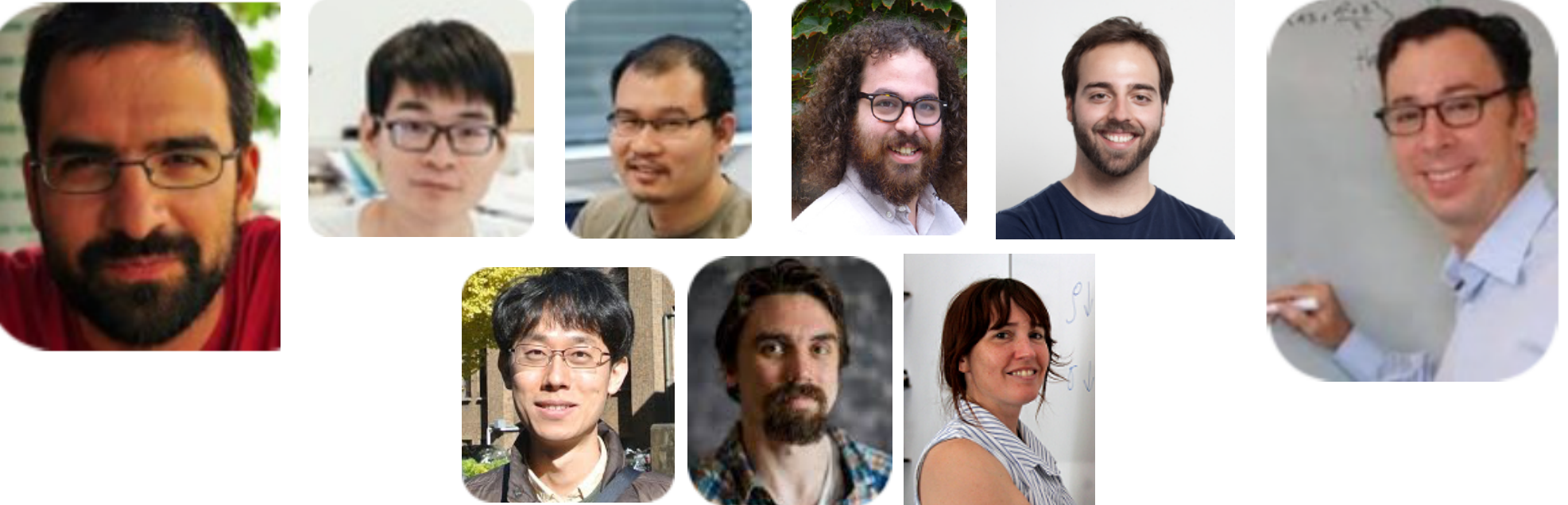


It is still worth looking for chiral Weyls to find exact quantization!

F. Flicker, F. de Juan, T. Morimoto, B. Bradlyn, M. Vergniory, AGG PRB (2018)

F. de Juan, AGG, T. Morimoto, J. E. Moore Nat. Comm (2017)

M.A. Sanchez-Martinez, F. de Juan, AGG PRB (2019)



FET-OPEN



$$\gamma_{ab} = \epsilon^{abc} \rho^{dbc}$$